

The neglected role of environmental fluctuations as modulator of stress

Dissertation



In fulfilment of the requirements for the degree “Dr. rer. nat”

of the Faculty of Mathematics and Natural Sciences

at the Christian-Albrechts-Universität zu Kiel

Submitted by

Jahangir Vajedsamiei

Kiel 2021

First referee: Prof. Dr. Martin Wahl

Second referee: Dr. Christian Pansch

Date of the oral examination: March 24, 2021

Table of Contents

Summary	7
Zusammenfassung	9
General Introduction	11
Toward understanding environmental fluctuations' impacts on marine organisms.....	11
Prediction of fluctuations' long-term effects based on performance curves	12
Biological modulation of performance curves as gaps in empirical knowledge.....	15
The study system	17
Aims, hypotheses, and findings.....	19
Chapters and contributions of authors.....	20
Chapter 1: Simultaneous recording of filtration and respiration in marine organisms in response to short-term environmental variability	22
Abstract	23
Introduction	24
Materials and Procedures	25
The Setup.....	25
General experimental design and procedure	28
Data processing through Python scripts.....	29
Dissolved-oxygen concentration calculator	30
Trial-by-trial analysis.....	30
Step 1 (filtration and feeding rates)	30
Step 2 (respiration rate)	33
Step 3 (Scope for Growth)	35
Step 4 (cumulative random effects).....	35
FOFS integrative processing.....	36
Assessment and Discussion	37
Demonstration experiment	37
Blank trials provide a performance check.....	38
Mussel trials confirm applicability.....	39
Challenges and solutions provided by FOFS and the suggested data processing	42
Limitations and potential solutions.....	43
Significance, directions and possible advancements of the method.....	43
Conclusions.....	45
Acknowledgments	45

References	46
Chapter 2: Burden or relief? Impact of cyclic thermal variability on ectotherms capable of metabolic suppression	50
Abstract.....	51
Introduction	52
Materials and methods.....	55
Long-term (5-weeks) experiment.....	55
Short-term (one-day) assay	57
Predicting long-term metabolic rates by upscaling.....	58
Relating observed impacts on growth with upscaling-predicted impacts.....	59
Results.....	59
Impacts of thermal averages and daily fluctuations on mussel growth during the long-term experiment.....	59
Metabolic performance during the short-term fluctuation assay.....	61
Upscaling-predicted impacts of fluctuations on feeding and respiration.....	61
Correlating observed and predicted impacts of thermal fluctuations	62
Discussion	63
At critically high summer thermal averages, fluctuations may be beneficial to the long-term performance of marine ectotherms.....	63
Metabolic suppression and recovery and the potential benefits and costs during daily thermal cycles	64
Upscaling from short-term thermal feeding responses may predict longer-term fluctuation impacts	65
A framework indicating how thermal fluctuations may provide a refuge for ectotherms.....	66
Perspectives and conclusion	68
Acknowledgments.....	69
References	69
Chapter 3: The higher the needs, the lower the tolerance: Extreme events may select ectotherm recruits with lower metabolic demand and heat sensitivity.....	75
Abstract.....	76
Introduction	77
Material and methods.....	79
Long-term incubations and short-term assays.....	80
Initial data processing.....	82
Hypothesis testing.....	82
Results and discussion.....	83

The future summer thermal extreme resulted in rare recruits of higher heat tolerance.....	83
Lower metabolic demand might have led to higher heat tolerance in recruited mussels	85
Shortcomings and perspectives	87
Acknowledgements.....	88
References	89
<i>General Discussion.....</i>	<i>93</i>
FOFS-like experimental methods can fill methodological gaps.....	93
Depending on the context, fluctuations can be beneficial or harmful for ectotherms	94
Ectotherms' capacity for thermal metabolic suppression and recovery defines their long-term responses to thermal fluctuations.....	95
May summer heatwaves induce warm adaptation?	97
Perspectives for future research	98
<i>References (for General Introduction and General Discussion).....</i>	<i>100</i>
<i>Supplementary Information to Chapters 1–3.....</i>	<i>109</i>
SI for Chapter 1	109
Supplementary Texts.....	110
Text S1: Temperature correction and conversion coefficients for chlorophyll data.....	110
Text S2: Criterion for selecting the 'pre- or post-trial stable data'	110
Text S3: Dampening-effect correction	111
Text S4: Temperature sensitivity of the planktonic food	112
Text S5: Mytilus filtration and respiration based on published literature	113
References:	113
Supplementary Figures.....	114
Supplementary Tables.....	121
Supplementary Python scripts.....	123
Script S1: 'Dissolved_oxygen_calculator.py'	123
Script S2: 'FOFS_trial-by-trial_processing.py'	127
Script S3: 'FOFS_integrative_processing.py'	151
SI for Chapter 2	160
Supporting Tables.....	161
Supporting figures.....	163
Supporting R and Python scripts.....	169
Script S1	169
Script S2	170
Script S3	171
Script S4	173

Script S5	178
SI for Chapter 3	183
Supplementary figures	184
Supplementary Tables	186
Supplementary Python and R scripts	188
Script S1	188
Script S2	189
<i>Acknowledgement</i>	190
<i>Declaration</i>	191

Summary

Ongoing changes in ocean climate (e.g., warming trends) are accompanied by increases in frequency and intensity of extreme weather events (e.g., heatwaves), particularly in shallow-water habitats. Traditionally, empirical studies intending to project the ecological impacts of environmental variability have focused on species or community responses to shifts in average conditions (trends), extracted from days to weeks-long experiments under static treatment conditions. Henceforth, some studies have applied nonlinear averaging on performance curves established under static treatments and predicted (based on *Jensen's Inequality*) that fluctuations might significantly modulate the responses to environmental trends (e.g., daily cycles). However, as species might express cumulative stress responses under continuous critical exposures, the performance curves based on static experimental conditions commonly show a concave drop over the beyond-optimal interval of the environmental factors in focus. Accordingly, nonlinear averaging usually predicted fluctuations' adverse effects, neglecting the role of acclimation, stress recovery, and evolutionary adaptation. Instead, some other studies have empirically found that alternative (positive) fluctuation effects on time-integrated performance might also be relevant. Most of these studies highlighted the need to incorporate environmental fluctuations into experimental designs but did not go beyond the observed patterns' mere description. This thesis provides a general introduction to the above issues and then tries to move forward by investigating (i) the environmental fluctuations' long-term impacts on fitness-related traits (e.g., growth) at beyond-optimal average conditions, (ii) the role of fluctuation-mediated metabolic suppression and recovery, and (iii) how these relations may be modulated by warm adaptation forces (acclimation and selection). Such practice and its required method development are optimized by focusing on cyclic (daily) temperature fluctuations, i.e., one of the most common and ecologically important environmental forces, and an ecosystem engineer, the mytilid mussel *Mytilus* spp., from the Western Baltic Sea.

The first Chapter describes the Fluorometer and Oximeter equipped Flow-through Setup (FOFS), the experimental design, and data processing protocols for recording metabolic performance (feeding and aerobic respiration) of benthic filter-feeders in response to fine-tuned environmental variability. The FOFS method's functionality is successfully demonstrated through recording mussels' responses during short-term (one-day) thermal fluctuation cycles. In the following research, FOFS is used in short-term assays to evaluate mussels' capacity to suppress and recover their metabolic performance over successive phases of stressful and benign temperatures.

Chapter 2 presents a combination of a long-term (5 weeks) experiment, a short-term (one-day) FOFS assay, and an associated upscaling framework (nonlinear averaging). The results show that (i) daily high-amplitude thermal cycles improved mussel growth when fluctuations were imposed around an extreme average condition representative of end-of-century heatwaves. In contrast, (ii) the thermal cycles negatively affected mussel growth at a less extreme average, representing today's peak summer temperatures in the region. Furthermore, (iii) nonlinear averaging of the short-term (non-acclimated) thermal feeding responses could well predict fluctuation impacts observed on growth rates from the long-term experiment. Merging these findings with physiological and mathematical principles, I propose a simple prediction framework based on various possible time-dependent changes in thermal metabolic performance. The framework explains how fluctuations, mediating metabolic suppression and

recovery, can be beneficial or detrimental to ectotherm's long-term performance, depending on the fluctuations' average and amplitude.

Chapter 3 then tests whether and how intensified summer thermal regimes would result in higher heat tolerance in individuals' daily thermal metabolic suppression and recovery. Mussels were grown from juveniles (transplanted mussels) or larval recruits (recruited mussels) under current versus warmed (end-of-century extreme) summer regimes in a near-natural mesocosm setting. Then, mussels' feeding and aerobic respiration rates were assessed in response to a mild temperature for six hours (baseline performances) followed by two 24 h fluctuation cycles in mild to critical temperature range. The results show that the warmer history negatively impacted transplanted mussels' four-month growth rates while not leading to changes in the baseline and the daily pattern of metabolic performances. The recruitment was substantially (96.5 %) less in the future (+ 4 °C) compared to the current summer thermal regime. These potentially selected recruits were more capable of recovering their feeding and respiration rates in benign phases of daily temperature fluctuations and expressed lower baseline respiration rates (metabolic demand). These findings support the hypotheses that (i) extremely warm events may select for rare heat-tolerant individuals of marine ectotherms at their very early life-history stages, (ii) lower metabolic demand is a mechanism for such heat tolerance, and (iii) the capacity to acquire such tolerance through acclimation is minor.

Overall, this research highlights the significance of studying the metabolic performance of ectothermic species at timescales relevant to natural fluctuations to advance our understanding of climate change impacts on aquatic systems. Whether selection-induced shifts in stress tolerance can lead to ectotherms' evolutionary adaptation to ocean warming is an essential research subject of future studies.

Zusammenfassung

Stattfindende Veränderungen des Ozeanklimas (z.B. Erwärmung) werden, insbesondere in Flachwasserlebensräumen, von einer Zunahme der Häufigkeit und Intensität extremer Wetterereignisse (z.B. Hitzewellen) begleitet. Empirische Studien, dessen Ziel es ist die Auswirkungen von Umweltschwankungen vorherzusagen, haben sich traditionell auf die Reaktionen von Arten oder Gemeinschaften auf Verschiebungen unter konstanten Bedingungen (sogenannten Tendenzen) konzentriert. Diese Daten wurden aus oft tage- bis wochenlangen Experimenten unter statischen Behandlungsbedingungen gewonnen. Kürzlich haben Studien die *nichtlineare Mittelung* ('Jensen's Inequality' = Ungleichung) auf Temperatur-Leistungskurven angewendet, welche unter statischen Behandlungen erstellt wurden. Die Vorhersagen zeigten, dass die Reaktionen auf Umwelttendenzen durch die Schwankungen (z.B. Tageszyklen) moduliert werden können. Da jedoch viele Arten unter kontinuierlich kritischen Stressbedingungen kumulative Stressreaktionen ausdrücken können, zeigen deren resultierende Leistungskurven üblicherweise einen konkaven Abfall über das nicht-optimale Intervall des jeweiligen Umweltfaktors. Dementsprechend prognostizierte die *nichtlineare Mittelung* normalerweise die nachteiligen Auswirkungen von Umweltschwankungen, wobei die Rolle von Akklimatisierung, Erholung von Stress, sowie der evolutionären Anpassung vernachlässigt wurde. Weitere Langzeitstudien haben gezeigt, dass auch alternative (positive) Schwankungseffekte auftreten könnten. Sie betonten die Notwendigkeit, Umweltschwankungen in zukünftige Experimente einzubeziehen, konnten jedoch nicht über die bloße Beschreibung der beobachteten Muster hinausgehen. In dieser Arbeit werden zunächst allgemein die oben genannten Themen, die Vorhersagemethoden und ihre jeweiligen Annahmen vorgestellt. In den drei Hauptkapiteln untersuchte ich zusammen mit meinen Koautoren die Auswirkungen zyklischer Temperaturschwankungen, einer der ökologisch wichtigsten Umweltparameter, auf einen wechselwarmen Ökosystemingenieur, die Muschel *Mytilus* spp., aus der Westlichen Ostsee. Ich testete prinzipienbasierte (mechanistische) Hypothesen, um zu erklären inwieweit sich kurzfristige Wetterbedingungen, z. B. täglich bis wöchentliche thermische Schwankungen, auf marine Wechselwarme Tiere auswirken, insbesondere bei stressigen Durchschnittsbedingungen wie extremen Sommern oder längeren Hitzewellen.

Im ersten Kapitel beschreibe ich den mit Floreszenz- und Sauerstoffsonden ausgestattete Experimentieraufbau, das sogenannte, 'Fluorometer and Oximeter equipped Flow-through Setup' (FOFS), das experimentelle Design und die Datenverarbeitungsprotokolle zur Aufzeichnung der Stoffwechselleistung, einschließlich der Fütterungs- und aeroben Atmungsraten von bodenlebenden Filtrierer als Reaktion auf eine genau abgestimmte Umgebungsvariabilität. Ich demonstriere erfolgreich die Funktionalität der FOFS-Methode, indem ich die Reaktionen der Muscheln während kurzfristiger (eintägiger) thermischer Schwankungszyklen aufzeichne. In den folgenden Kapiteln wende ich die FOFS-Methode in Kurzzeitversuchen an, um die Fähigkeit von Muscheln zu testen, ihre Stoffwechselleistung in aufeinanderfolgenden Phasen anstrengender und entlasteter Temperaturen zu unterdrücken und wiederherzustellen. In Kapitel 2 wende ich eine Kombination aus der kurzfristigen (eintägigen) FOFS-Methode und einem längerfristigen (5-wöchigen) Experiment, sowie dem dazugehörigen Upscaling-Approach (*nichtlineare Mittelung*) an. Ich zeige, dass tägliche thermische Schwankungen mit hoher Amplitude das Muschelwachstum verbessern, wenn Schwankungen

um einen extremen Durchschnittswert appliziert wurden, der für Hitzewellen zum Ende des Jahrhunderts repräsentativ ist. Im Gegensatz dazu wirkten sich die thermischen Schwankungen negativ auf das Muschelwachstum in einem weniger extremen Durchschnittswert aus, was heutigen Maximaltemperaturen in der Region im Sommer entspricht. Diese Ergebnisse legen nahe, dass Schwankungen das Wachstum nur bei kritisch hohen Durchschnittstemperaturen verbessern. Darüber hinaus weise ich darauf hin, dass eine *nichtlineare Mittelung* der kurzfristigen (nicht akklimatisierten) thermischen Fraßreaktionen (die FOFS-Methode) die aus dem Langzeitexperiment beobachteten Schwankungsauswirkungen auf die Wachstumsraten gut vorhersagen konnte. Indem ich meine Ergebnisse mit physiologischen und mathematischen Prinzipien zusammenführe, schlage ich ein einfaches Konzept vor, welches auf verschiedenen möglichen und zeitabhängigen Veränderungen der thermischen Stoffwechselleistung basiert. Das Konzept erklärt, wie Schwankungen eines Umweltparameters, der die Unterdrückung und Erholung des Stoffwechsels vermittelt, je nach Mittelwert und Amplitude der Schwankungen für die Langzeitleistung des wechselwarmen Organismus von Vorteil oder nachteilig sein können. In Kapitel 3 teste ich, ob (und wie) Akklimatisation oder gezielte Selektion durch extreme sommerliche Temperaturen zu Individuen mit höherer Hitzetoleranz bei ihrer täglichen Unterdrückung und Erholung des thermischen Stoffwechsels führen kann. In einer viermonatigen Inkubation wurden Muscheln unter Verwendung eines nahezu natürlichen Mesokosmen-Systems aktuellen und erwärmten (extremen) Sommertemperaturen, prognostiziert für das am Ende des Jahrhunderts, ausgesetzt. Ich konnte keinen signifikanten Einfluss der vorhergehenden Temperatur in der Fütterungs- oder Atmungsleistung von transplantierten Muscheln finden. Jedoch war die Besiedlung der Mesokosmen in erwärmten Bedingungen wesentlich (96,5%) geringer als unter Kontrollbedingungen. Im Vergleich dazu waren die potenziell selektierten Muscheln (neu gesiedelt) in der Lage, ihre Fütterungs- und Atmungsraten in den Entspannungsphasen täglicher Temperaturschwankungen besser wiederherzustellen, und zeigten in der Phase vor der Schwankung niedrigere Atmungsraten. Die Ergebnisse unterstützen die Hypothesen, dass (i) extrem warme Temperaturereignisse seltene hitzetolerante Individuen mariner Wechselwarmer in ihren sehr frühen Lebensstadien selektieren können und (ii) ein geringerer Stoffwechselbedarf ein Mechanismus für eine solche höhere Hitzetoleranz sein kann.

Im Allgemeinen unterstreicht diese Forschung die Bedeutung der Untersuchung der Stoffwechselleistung von Wechselwarmen-Arten in natürlich relevanten Zeiträumen, um unser Verständnis zu den Auswirkungen des Klimawandels auf aquatische Systeme zu verbessern. Eine weitere Bewertung der hier getesteten Hypothesen und die Frage, ob gerichtete Selektion Erhöhungen der mittleren Stresstoleranz von Populationen zu ihrer evolutionären Anpassung an die Erwärmung der Ozeane führen können, sind wesentliche Forschungsthemen zukünftiger Studien.

General Introduction

Toward understanding environmental fluctuations' impacts on marine organisms

The setting in which marine species and populations assemble and evolve is characterized by external traits, including physicochemical (or environmental) characteristics such as seawater temperature, salinity, oxygen, pH, and nutrients, and biological factors such as predation, competition, or parasitism. These external traits commonly fluctuate over space and time, with higher frequency and amplitude in shallow regions (Boyd et al., 2016) compared to more stable deep-sea habitats (Goocii and Schopf, 1972). Theoretically, a long-term time series of an external factor collected in a particular locality can be composed of a decadal or centennial trend, systematic (multi-)decadal to daily fluctuations, and stochastic fluctuations of different durations (minutes to months to decades) (Ma et al., 2020). The fluctuations can be due to climate events such as North Atlantic Oscillation, El Niño or La Niña events (Soares et al., 2014; Ma et al., 2020) or, on shorter timescales, caused by seasonal and diurnal variation in solar irradiance (Helmuth and Hofmann, 2001). Besides, up and downwelling and tidal events (Lima and Wethey, 2012; Vajedsamiei et al., 2014; Saleh et al., 2020), as well as biological activities (e.g., respiration and photosynthesis) (Saderne et al., 2013), can influence systematic and stochastic environmental variability, especially in shallow marine habitats (Wahl et al., 2016).

How environmental fluctuations shift by ongoing climate change is still mostly unknown. What is highly probable is that climate change induces unusual long-term environmental trends (e.g., warming, acidification, and deoxygenation), shifting the fluctuations' baseline conditions (Lima and Wethey, 2012). For example, due to ongoing shifts in climatological baselines, shallow-water organisms are increasingly exposed to days- to months-long supra-optimal thermal conditions (Holbrook et al., 2019). Besides, seasonal to diurnal temperature fluctuations will have warmer peaks in coastal and shallow-water regions (Wang and Dillon, 2014).

An organism's potential for performance in response to external (abiotic and biotic) variations is defined by the inherited genetic and epigenetic traits given (Devey, 2005). In theory, an organism's performance can be assumed to be an n-dimensional function of external predictor variables (Hutchinson and MacArthur, 1959; Kearney et al., 2010; Blonder, 2017). In empirical practices, however, the parsimonious functional relationships, e.g., thermal performance curves (TPCs), are commonly defined based on a particular (experimentally-simulated) scenario (Angilletta, 2006). The initial condition and variability patterns of all influential predictors,

including those manipulated and not manipulated in the experiment, characterize the specific scenario. However, this parsimony is usually at the expense of less capacity to generalize from the empirical performance curves. To date, studies intending to predict the ecological impact of climate change have focused on species or communities' responses to static environmental conditions signifying the trends (Deutsch et al., 2008). Until recently, environmental fluctuations have been mostly neglected (Jentsch et al., 2007), while they can have significant consequences for organisms' performance as suggested by theoretical frameworks (Ruel and Ayres, 1999; Martin and Huey, 2008) and empirical evidence (Niehaus et al., 2012; Kingsolver et al., 2015). Yet, advancement in this field of research demands a critical evaluation of the methods and their assumptions (Helmuth et al., 2014; Sinclair et al., 2016).

Prediction of fluctuations' long-term effects based on performance curves

Here I provide an inclusive overview of the mathematical definition of environmental fluctuation effects, considering single or multiple predictors (e.g., temperature, light, dissolved oxygen, salinity, and pH). This general framework will be tailored later in Chapter 2 to predict the long-term impacts of (daily) temperature fluctuations on a filter-feeder's metabolic performance and growth.

A (multi-dimensional) performance curve can be identified with additive (or non-additive) effects of predictors on the performance, in which the joint (compound) impacts of predictors are or are not equal to the sum of single forces alone (Gunderson et al., 2016). The mixed partial derivative of an additive performance function with two different variables is equal to zero ($\frac{\partial^2 g}{\partial x_i \partial x_j} = 0$), whereas that for a non-additive performance function is not necessarily equal to zero. The mixed partial derivative explains how performance changes induced by one predictor are altered by another predictor, for example, how temperature-induced changes in growth are altered due to the food-level variation. When the mixed partial derivative is negative (or positive), it represents antagonistic (or synergistic) effects of the predictors (Koussoroplis et al., 2017). Further, variation across predictor values may appear to be disproportional to changes in the performance due to nonlinearity in the respective predictor-performance relationship (nonlinear averaging or Jensen's Inequality, Jensen, 1906; see also Fig. S1 in Chapter 2). Indeed, when the second partial derivative of the performance curve (around a hypothetical point) with respect to a single predictor (meaning $\frac{\partial^2 g}{\partial x_i^2}$) is positive, the performance response would be accelerated. The opposite is true for negative derivatives.

One of the most commonly used clear-cut mathematical technique to explain the predictor variability effects is the *Taylor expansion of moments* in which a nonlinear function (e.g., a performance curve) is substituted by its truncated Taylor-polynomial approximation expanded around the mean value(s) of the predictor(s) (Soubra and Bastidas-Arteaga, 2014). In ecology, the moment-approximation method was initially used by (Chesson et al., 2005) to define the *Scale Transition Theory*, theoretically describing the effects of spatial variability (variance and covariance) in one or two predictors on population-level performances. The method was recently used to describe the potential effects of single predictor variability on the organism-level performance (Denny and Benedetti-Cecchi, 2012; Dowd et al., 2015). More recently, Koussoroplis et al. (2017) merged the approach with the co-limitation concept (Sperfeld et al., 2016) to explain the potential impacts of variability in two resources on organism performance. The Moment-approximation method has been increasingly applied in ecology. Equations below approximately describe the effects of real-world scenarios of multi-predictor variability on the mean and the variance of the performance (Soubra and Bastidas-Arteaga, 2014).

$$\text{Eq. 1.1. } E[g(X_1, X_2, \dots, X_n)] = g(\mu_{X_1}, \mu_{X_2}, \dots, \mu_{X_n}) + \frac{1}{2} \sum_{i=1}^n \sum_{j=1}^n \frac{\partial^2 g}{\partial X_i \partial X_j} (X_i - \mu_{X_i})(X_j - \mu_{X_j})$$

$$\text{Eq. 1.2. } \text{Var}[g(X_1, X_2, \dots, X_n)] = \sum_{i=1}^n \sum_{j=1}^n \frac{\partial g}{\partial X_i} \frac{\partial g}{\partial X_j} (X_i - \mu_{X_i})(X_j - \mu_{X_j})$$

In the first equation (Eq. 1.1) $E[g(X_1, X_2, \dots, X_n)]$ is the first moment or expectation of a performance curve with n predictors, representing the estimated average of the performance curve's outputs (e.g., the mean performance of an organism over a specific period during which the predictors were being manipulated). The first term on the right side of the equation, $g(\mu_{X_1}, \mu_{X_2}, \dots, \mu_{X_n})$, is the output of the performance curve where the performance curve's input dataset represents the mean values of the predictors. The second term indicates the variance [or covariance] in [or between] predictor(s), $(X_i - \mu_{X_i})(X_i - \mu_{X_i})$ [or $(X_i - \mu_{X_i})(X_j - \mu_{X_j})$], which can have consequences for the mean performance only if the performance curve has some nonlinearity [or non-additivity] components around the predictor's mean(s). The variance of each predictor interacts with its corresponding nonlinear term; for example, for a function of two predictors and around predictor X_1 (imagine X_1 and X_2 are the temperature and food level, respectively), it is calculated as $\frac{1}{2} \frac{\partial^2 g(\mu_{X_1}, \mu_{X_2})}{\partial X_1^2} \sigma_{X_1}^2$. At the same time, the covariance of each pair of predictors interacts with their corresponding combinatory effect (e.g., for two specific predictors X_1 and X_2 , $\frac{\partial^2 g(\mu_{X_1}, \mu_{X_2})}{\partial X_1 \partial X_2} \sigma_{X_1 X_2}$).

The second equation (Eq. 1.2) describes the second moment or variance of a performance curve, representing the main components driving the performance variance. According to that, the performance-variance is related to (i) the product of the predictor's variance and the squared slope of the performance curve (with respect to each of the predictors, e.g., for X_1 : $\left(\frac{\partial g(\mu_{X_1}, \mu_{X_2})}{\partial X_1}\right)^2 \sigma_{X_1}^2$), and (ii) summation of the product of each pair of the predictor's covariance multiplied by corresponding first partial derivatives (e.g., for X_1 and X_2 : $\left(2 \frac{\partial g}{\partial X_1} \frac{\partial g}{\partial X_2}\right) \sigma_{X_1 X_2}$). According to that, the sign and magnitude of the covariance between each pair of predictors and the respective (interacting) slopes are essential to define the variability of the performance. In marine ecosystems, the covariance between external traits commonly occurs; for example, the temperature and light level fluctuate daily. The temperature, salinity, pH, dissolved oxygen, and nutrient levels are simultaneously altered during upwelling. However, the effect of different predictor covariance scenarios for mean organismal performance and fitness has remained less investigated (also not experimentally investigated in this thesis; see Koussoroplis and Wacker, 2016). In Table 1.1, we present qualitative predictions on how the performance variance may be influenced by different predictor covariance scenarios and the interacting slopes, based on the theoretical expectations (the bivariate version of Eq. 1.2 described in the previous paragraph). For example, one can imagine the temporal variability of light and temperature, which have positive daily covariance. Such (co)variability can be associated with the broadest daily variance in an autotrophic benthic organism's performance when both external traits fluctuate in intervals with enormous similar-sign effects on the performance (where the slope of the respective performance curve is the highest with respect to both factors). This scenario is highlighted by blue in Table 1.1.

Table 1.1. Qualitative prediction of the consequences of two predictors' covariance for the performance variance based on Taylor expansion of variance of a bivariate function (eq. 1.2.). PD denotes the partial derivative. The blue-highlighted row indicates the specific scenario where the covariance is positive and the slope of the performance curve is also positive with respect to both factors; thus, larger variance in both predictors will result in larger performance variance over a specific period.

Sign of PD of predictor i	Sign of PD of predictor j	Sign of the product of PDs	Sign of the covariance	Change in performance variance
+	-	-	-	+
+	-	-	+	-
+	+	+	-	-
+	+	+	+	+
-	+	-	-	+
-	+	-	+	-
-	-	+	-	-
-	-	+	+	+

The approximation method can be applied to provide quantitative or qualitative predictions, especially useful for hypothesizing about the effects of the predictor's (co)variability in experimental climate change ecology. However, it must be noted that the approximation method is derived from Taylor (polynomial) approximation of performance curves. Therefore, its accuracy is higher when the approximated function's shape (order) agrees more with the initial performance curve in the predictors' intervals of interest. For simplicity, I presented components of third-order Taylor expansion of the mean (i.e., based on the third-order Taylor polynomial) and the first-order expansion of the variance of a general multivariate function.

Notably, the approximation method can provide an upscaled relation (see Chapter 2), decomposing predictor effects into the predictor's mean and variability effects. When the predictor's distributions (e.g., thermal regimes of a particular environment) are known, and the upscaled relation (and the decomposition) is not needed, one may prefer to predict performance under different variability scenarios (nonlinear averaging) via applying the predictor's data sets into the performance curve. One can use a bootstrapping technique (e.g., Benedetti-Cecchi, 2005), conducting numerous random samplings with replacement from predictor's (joint) distribution and using the samples as inputs to a performance curve to obtain a rich output-dataset (performance dataset) with a specific probability distribution function.

Biological modulation of performance curves as gaps in empirical knowledge

Applying the mathematical frameworks to predict environmental variability's consequences assumes that an environmental predictor's immediate effect on an organism's performance remains temporally constant. Thus, the predictions neglect the time-dependent effects, particularly the modulatory role of compensational acclimation, accumulation of stress, and evolutionary adaptation (Davenport and Davenport, 2005; Wittmann et al., 2008; Kingsolver and Woods, 2016; Sinclair et al., 2016).

Acclimation includes complex regulatory processes in response to environmental stimuli, which may preserve or recover the homeostasis and long-term performance (i.e., Beneficial Acclimation Hypothesis; Leroi et al., 1994; Huey et al., 1999). In this sense, (compensational or beneficial) acclimation is in contrast with stress response or reverse acclimation (Precht 1958; Havird et al., 2020). Acclimation may first start with functional inertia in response to external fluctuations, e.g., volume-dependent thermal inertia (Harris, 1909). Acclimation then involves processes such as the phosphagen system keeping ATP concentrations stable during exercise/hypoxia (Ellington, 2001), cyclic gene expression counter expected stress during

diurnal fluctuations may (Podrabsky and Somero, 2004), and seasonal reshuffling of cellular machinery, including membrane lipids, mitochondrial density, enzyme concentrations, and isoforms (Hofmann and Todgham, 2010). Acclimation during or after exposure to a stressful event (e.g., heatwave) may functionally prepare the organism for successive stress events (Walter et al., 2013). Accordingly, acclimation may also occur independently for static beyond-optimal conditions and fluctuating beyond-optimal conditions with the same average.

Notably, fluctuations may modulate the fitness response to a critical average condition, even when the organism does not express compensational or reverse acclimation during critical exposures. Potentially, this phenomenon may occur when fluctuations mediate alternations between phases of tolerance (with minor thermal damage) and recovery phases at milder conditions (Schulte et al., 2011; Wahl et al., 2015; also see Chapter 2). This phenomenon is mostly neglected while being quite relevant for ectotherms that evolved an elastic capacity of metabolic suppression and recovery in response to fluctuating stress regimes. In metazoans, suppression of metabolic performance commonly involves decreases in the feeding rate, followed by reductions in aerobic respiration and occasional transition to anaerobic metabolism (Sokolova and Pörtner, 2001). The metabolic suppression is often mediated through post-translational modification of existing enzymes (Falfushynska et al., 2020), followed by changes in gene expression, membrane composition, and enzyme profiles (Podrabsky and Somero, 2004). Elongation of the suppression phase at constant but critical conditions may render the organism vulnerable to stress. For example, ectotherms commonly express cumulative stress responses under continuous exposure to critical temperatures (Deutsch et al., 2008), possibly due to their inability to maintain the balance between the demand for metabolic substrates and the supply capacity (Schulte et al., 2011; see Chapter 2 and 3). Thus, TPCs established under static treatment levels commonly show a concave drop over the beyond-optimal to the critical temperature interval, resulting in predictions of thermal fluctuations' adverse impacts by nonlinear averaging (Martin and Huey, 2008; Vasseur et al., 2014; see also Fig. S1 in Chapter 2). Notably, nonlinear averaging on performance curves generated at timescales (e.g., hours) that relate to (daily) fluctuation cycles (i.e., in general, the upscaling approach; Chesson et al., 2005; Denny and Benedetti-Cecchi, 2012; Denny, 2019) may allow us to predict fluctuations' refuge effects (Chapter 2).

Yet, performance curves can also be altered through the evolutionary adaptation of populations. Microbial organisms, having short generation times and high population densities, can evolve within weeks or months due to selection on both pre-existing tolerant genotypes or *de novo* mutations (Padfield et al., 2016). However, the adaptation through beneficial genetic mutation

may not be fast enough to preserve longer-generation macro-organisms facing global changes (Somero, 2010). Instead, the directional selection of existing stress-tolerant genotypes may result in evolutionary adaptation of longer-lived species (Logan et al., 2014, 2018; Ma et al., 2014; Gilbert and Miles, 2017). Empirical evidence is needed to understand whether and how climate change-driven extreme events can enforce such directional selection (Grant et al., 2017; Al-Janabi et al., 2019).

In the context of climate change ecology, empirical investigations have, so far, mainly focused on addressing (i) whether the organism's long-term performance differs between fluctuating and constant regimes (e.g., Frieder et al., 2014; Kingsolver et al., 2015; Morón Lugo et al., 2020) and (ii) whether the performance under fluctuating regimes can be predicted based on performance curves established under static treatments (e.g., Niehaus et al., 2012; Bernhardt et al., 2018). Their findings have emphasized the need to incorporate environmental fluctuations into experimental designs. However, to date, a lack of principle-based (mechanistic) hypotheses has limited the ability to generalize from empirical findings (Gouhier and Pillai, 2019). To move forward, this thesis tries to relate the effects of environmental variability on metabolic (energy-budget) performance, particularly the fluctuations-mediated metabolic suppression and recovery, to the impacts on fitness-related traits (i.e., long-term performance such as survival, growth, and reproduction rates), and explain how these relations can be modulated due to acclimation or rapid evolutionary adaptation.

The study system

A prerequisite for such investigations is the ability to continuously record marine ectotherms' metabolic performance in response to short-term environmental fluctuations. Such an experimental approach is yet far from developed. To progress, in practice, a focus on the effect of a single environmental variable that is more controllable and ecologically highly influential would be necessary considering the time and financial constraints of a doctoral study. It is also essential to concentrate on a single species that is not only of considerable ecological value but can also be preserved and fed in a laboratory setting. Notably, necessary reliable information about the physiological functioning of the study species under static (benign) conditions should be available. Therefore, the research presented in Chapters 1, 2, and 3 mainly focuses on the impacts of cyclic (daily) temperature fluctuations on the blue mussel (*Mytilus* spp.).

Temperature is the most influential environmental predictor of ectotherms' metabolic performance (Pörtner, 2012). Daily temperature fluctuations are common in shallow marine

habitats and may modulate the impact of intensifying heatwaves on benthic communities (Safaie et al., 2018). Ocean climate warming and the associated weather changes are the most ecologically influential component of ocean climate change, particularly in shallow ecosystems, altering the biogeographical distribution of many species (Barry et al., 1995; Sagarin et al., 1999; Wethey et al., 2011).

In shallow coastal habitats of the Western Baltic Sea, our study region, seawater temperature fluctuates by 1–6 °C (at depths ca. 1 m) due to daily irradiance variation and up to 8 °C due to days to weeks-long upwelling and heatwave events (Franz et al., 2019; Pansch and Hiebenthal 2019). By the end of the 21st century, the average sea surface water temperature is projected to increase by 1.5–4 °C in the Baltic Sea (Gräwe et al., 2013; Meier et al., 2012). Baltic Sea's coastal habitats is ideal for our study not only because their past and future thermal regimes (and, in general, environmental conditions) are well characterized and projected (Lennartz et al., 2014; Reusch et al., 2018) but also as they commonly experience minor (< 10 cm) tidal shift in water levels (Medvedev et al., 2016). Thus, the effect of temperature on the Baltic Sea's benthic organisms can be experimentally assessed without considering aerial exposure as a covariate.

Our study organism is the ectothermic filter feeder *Mytilus edulis trossulus* (Stuckas et al., 2017), the dominant species complex forming the Baltic Sea's mussel beds (Larsson et al., 2017). Genus *Mytilus* has a worldwide distribution, and its various species form mussel beds in the sub- and intertidal habitats of temperate- and cold-water ecosystems (Zippay and Helmuth, 2012). Mussels' filtration activity can contribute to the cycling of nutrients and energy (Gili and Coma, 1998), regulating the load of suspended particulate organic matter and contaminants such as heavy metals (Widdows et al., 1998), and controlling the population density and community structure of micro-planktonic primary producers and pathogens in shallow marine ecosystems (Burge et al., 2016). Besides, these bivalves contribute substantially to commercially important aquaculture industries that provide food and non-food services with an annual global worth of ~ 35 billion US dollars (van der Schatte Olivier et al., 2018).

Reliable basic physiological information is available for *Mytilus* spp. Importantly, the relationships of filtration and aerobic respiration to the body size (Hamburger et al., 1983; Pleissner et al., 2013) are needed for testing the performance of a developing experimental setup. The species is also known to express remarkable suppression (and recovery) of metabolic performance, the capacity which is further investigated in this thesis.

The cryptophyte *Rhodomonas salina* (cultured at 16 °C by the Kiel Marine Organism Culture Centre at GEOMAR, KIMOCC) is applied as a live food source as its efficiency has been confirmed in several published studies (Clausen and Riisgaard, 1996; Riisgård et al., 2013; Sanders et al., 2018). Only a few published studies described the thermal biology of *R. salina* (Hammer et al., 2002; Chaloub et al., 2015; Gómez et al., 2016). Most recently, Gómez et al. (2016) successfully cultured several strains of *R. salina* at temperatures of 19–29 °C, suggesting that the species is tolerant to high seawater temperatures. Still, independent tests are needed to check the robustness of the KIMOCC-cultured *R. salina* against experimental temperature regimes (Chapter 1).

Details and relevance of the study system are also explained in the upcoming chapters.

Aims, hypotheses, and findings

The three chapters of this thesis mainly aim at providing insights on (i) how cyclic temperature fluctuations impact ectotherms' performance at critical baseline temperatures, with an emphasis on (ii) the role of metabolic suppression and recovery capacity, and finally on (iii) how this capacity may be altered by directional selection or acclimation.

Chapter 1 describes and successfully demonstrates the functionality of the Fluorometer- and Oximeter-equipped Flow-through Setup (FOFS), an empirical setup for recording benthic filter feeders' metabolic traits, including filtration and aerobic respiration activities, at an unprecedented temporal resolution under simulated dynamic environmental conditions (Chapter 1; Vajedsamiei et al., 2021). The proposed method includes the protocol for semi-automated data processing through Python scripts, making the method more understandable and adaptable for future studies. This method can be applied to (i) produce species' short-term TPCs and in (ii) side incubations to investigate how long-term exposure to different scenarios of environmental variability may affect the predictor-metabolic response relations, as conducted in the second and third chapters of this thesis.

Chapter 2 tests the hypothesis stating that short-term thermal fluctuations can be not only detrimental to organisms but, at times, also be beneficial to marine ectotherms exposed to scenarios of current to future summer heatwaves. This study supports the hypothesis by assessing the long-term daily-fluctuation impacts on *Mytilus* growth at benign to critical thermal averages. In a second step, using data collected in the short-term FOFS assay, I indicate mussels' capacity to suppress and recover feeding and aerobic respiration in response to a 24 h fluctuation in the temperature range as utilized in the longer-term experiment. Finally, the

upscaling from short-term (non-acclimated) TPCs shows that the predicted fluctuations' impacts on feeding well explain the long-term fluctuation impacts on growth. I propose a simple framework describing the context-dependent stress sensitivity of ectotherms under fluctuating versus constant stress regimes.

Chapter 3 extends the inquiry line to answer related eco-evolutionary questions: How thermal history in the form of extreme summer conditions lead to improved heat tolerance in ectotherm populations? In this chapter, I evaluate feeding and respiration rates of *Mytilus* mussels with different thermal histories in response to a mild temperature for six hours followed by two successive 24 h fluctuation cycles in the range of mild to critical temperatures. The results indicate that extremely warm summers (heatwave events) may not result in warm beneficial acclimation of mussels but may select rare individuals of higher heat-tolerance at the very early life-history stage. Besides, the data support the supposition that lower demand for metabolic substrates can be a mechanism for higher heat tolerance.

Chapters and contributions of authors

Parts of this doctoral thesis have been published or submitted as research articles:

Chapter 1: Simultaneous recording of filtration and respiration in marine organisms in response to short-term environmental variability

Authors: Jahangir Vajedsamiei, Frank Melzner, Michael Raatz, Rainer Kiko, Maral Khosravi, and Christian Pansch

History: Published in *Limnology & Oceanography: Methods*

Contributions: J.V. designed and developed the method, run the experiment, and wrote the manuscript. F.M., R.K., and C.P. verified the analytical methods. F.M. encouraged J.V. to run the blank trials and write the Oxygen-calculator script. M.R. and R.K. verified the Python scripts. M.R. verified the mathematical procedures and encouraged J.V. to add a detailed derivation of the dampening-effect correction. M.K. assisted J.V. in setting up and implementation of the experiment. All co-authors discussed the results, as well as reviewed and contributed to the final manuscript.

Chapter 2: Burden or relief? Impact of cyclic thermal variability on ectotherms capable of metabolic suppression

Authors: Jahangir Vajedsamiei, Frank Melzner, Michael Raatz, Sonia Moron, and Christian Pansch

History: Resubmitted (on Dec. 28, 2020) and under review in *Functional Ecology*

Contributions: J.V. and C.P. designed the study. J.V. developed the mechanistic framework, ran the experiments, analyzed the data, and wrote the manuscript. F.M. and C.P. verified the experimental methods. M.R. verified the mathematical procedures. S.M. assisted J.V. during the long-term experiment. All co-authors discussed the results, as well as reviewed and contributed to the final manuscript.

Chapter 3: The higher the needs, the lower the tolerance: Extreme events may select ectotherm recruits with lower metabolic demand and heat sensitivity

Authors: Jahangir Vajedsamiei, Martin Wahl, Andrea Schmidt, Maryam Yazdanpanahan, and Christian Pansch

History: Submitted (by Jan. 31. 2021) to *Frontiers in Marine Science*

Contributions: J.V., M.W., and C.P. designed the study. J.V. developed the hypotheses and performed the modelling and analyses, and wrote the manuscript. M.Y., and A.S. assisted J.V. during the experiments. All co-authors discussed the results, as well as reviewed and contributed to the final manuscript.

Chapter 1: Simultaneous recording of filtration and respiration in marine organisms in response to short-term environmental variability

Jahangir Vajedsamiei ^{1*}, Frank Melzner ¹, Michael Raatz ², Rainer Kiko ^{1,3}, Maral Khosravi ¹, Christian Pansch ^{1,4}

¹ Department of Marine Ecology, GEOMAR Helmholtz Centre for Ocean Research Kiel, Germany

² Max-Planck Institute for Evolutionary Biology, Plön, Schleswig-Holstein, Germany

³ Laboratoire d'Océanographie de Villefranche-sur-Mer, Sorbonne Université, France

⁴ Department of Environmental & Marine Biology, Åbo Akademi University, Turku, Finland

*** Corresponding author:** address: GEOMAR Helmholtz Centre for Ocean Research Kiel, Düsterbrook Weg 20, 24105 Kiel, Germany, telephone: +49 431 600 1598, e-mail: jahangir.vajedsamiei@gmail.com; jvajedsamiei@geomar.de

Author ORCIDs: JV: 0000-0002-8625-4719, FM: 0000-0002-5884-1318, MR: 0000-0002-6968-6560, RK: 0000-0002-7851-9107, MK: 0000-0001-5734-6502, CP: 0000-0001-8442-4502

Conflict of Interest: None declared.

Data accessibility statement: The data supporting the results of the demonstration experiment are archived in PANGAEA (<https://doi.org/10.1594/PANGAEA.919682>).

Abstract

Climate change imposes unusual long-term trends in environmental conditions, plus some tremendous shifts in short-term environmental variability, exerting additional stress on marine ecosystems. This paper describes an empirical method that aims to improve our understanding of the performance of benthic filter feeders experiencing changes in environmental conditions, such as temperature, on time scales of minutes to hours, especially during daily cycles or extreme events such as marine heatwaves or hypoxic upwelling. We describe the Fluorometer and Oximeter equipped Flow-through Setup (FOFS), experimental design, and methodological protocols to evaluate the flood of data, enabling researchers to monitor important energy budget traits, including filtration and respiration of benthic filter-feeders in response to fine-tuned environmental variability. FOFS allows online recording of deviations in chlorophyll and dissolved oxygen concentrations induced by the study organism. Transparent data processing through Python scripts provides the possibility to adjust procedures to needs when working in different environmental contexts (e.g., temperature versus pH, salinity, oxygen, biological cues) and with different filter-feeding species. We successfully demonstrate the functionality of the method through recording responses of Baltic Sea blue mussels (*Mytilus*) during one-day thermal cycles. This method practically provides a tool to help researchers exposing organisms to environmental variability for some weeks or months, to relate the observed long-term performance responses to short-term energy budget responses, and to explain their findings with the potential to generalize patterns. The method, therefore, allows a more detailed description of stress-response relationships and the detection of species' tolerance limits.

Keywords: ecology, energetics, fluctuations, functional traits, SFG, warming

Introduction

Benthic filter-feeders play critical roles in the cycling of nutrients and energy in numerous marine habitats (Gili and Coma 1998; Dame et al. 2001). Their filtration activity can regulate the load of suspended particulate organic matter and contaminants such as heavy metals (Widdows et al. 1998) as well as the population density and community structure of microplanktonic primary producers and pathogens in shallow waters (Burge et al. 2016). Due to their profound effect on structural heterogeneity, species diversity and functioning of ecosystems, various species of benthic filter-feeders are viewed as ecosystem engineers (Dame et al. 2001). Besides, benthic filter-feeders support commercially important aquaculture industries that provide food and non-food services with an annual global worth of ~ 35 billion US dollars (van der Schatte Olivier et al. 2018).

In shallow marine ecosystems, benthic filter-feeders can experience short-term systematic or stochastic fluctuations in ambient seawater conditions (daily to weekly cycles) due to weather events, irradiance variation, tides or wind-driven changes in water levels, upwelling and downwelling events, and changes in biological activity (Wahl et al. 2016; Boyd et al. 2016). Ongoing climate change induces long-term (annual to decadal) unusual trends in environmental conditions (e.g., warming, acidification, and deoxygenation), as well as shifts in short-term fluctuation patterns of environmental regimes (Lima and Wethey 2012), which threatens benthic taxa, including filter-feeders (Przeslawski et al. 2008). To advance our empirical understanding of organisms' performance in a changing ocean, developing experimental setups for high temporal resolution monitoring of organisms' energetics traits in dynamic environments and automated data processing is crucial. This enables a more detailed description of stress-response relationships and detection of species' tolerance limits.

The two most important energy budget traits of benthic filter-feeders, filtration (feeding) and respiration rates, can be monitored through flow-through setups (Riisgård 2001; Filgueira et al. 2006; Bayne 2017). In a closed chamber setup (including intermittent closure techniques), the filtration activity of the organism can substantially decrease or stop due to depletion of food before a significant oxygen-depletion signal (i.e., respiration) can be detected (Widdows 1976) and the physicochemical conditions can be controlled less efficiently. Importantly, during exposure to suboptimal food levels, filter-feeders usually decrease and decelerate their filtration and aerobic metabolism to conserve energy (Kittner and Riisgård 2005; Riisgård et al. 2006; Tang and Riisgård 2016). In a flow-through setup, the experimental food level can be manually or automatically maintained within the range of interest. However, so far, the application of

flow-through setups has been mostly limited to investigations on a single response (filtration or respiration) to constant treatment conditions (Riisgård 2001; Filgueira et al. 2006; Pleissner et al. 2013). Widdows (1973) measured filtration or respiration of mussels under constant temperatures based on weekly snapshot-measurements of phytoplanktonic food and dissolved oxygen concentrations in water flowing into and out of an experimental chamber using an oximeter and a Coulter counter. High-temporal resolution (continuous) recording of filtration and respiration responses in parallel was only described by Haure et al. (2003) who used a flow-through setup equipped with a laboratory fluorometer and an oximeter in a short (three hours) experiment. One limiting factor preventing more frequent use of such experimental setups in the past could have been the high cost of measurement equipment (especially the laboratory fluorometer) limiting replication of measurements. Furthermore, it is technically challenging to record the responses of filter-feeders exposed to environmental fluctuations in an air- and water-tight flow-through setup, as time, temperature, and other physical and chemical factors can confound measurements.

In this paper, we present an experimental method developed for monitoring rates of filtration and respiration in parallel as well as simplistic estimation of filter-feeders' surplus of energy available for growth (Scope for Growth, SFG), in response to short-term environmental fluctuations. We describe the design of our setup in conjunction with the protocols used for semi-automated data processing. We also implement and test the method in an experiment on the responses of blue mussels (*Mytilus spp.*) from the Baltic Sea to daily thermal fluctuation cycles. Finally, we discuss the benefits and constraints of the setup and recommend directions for future applications, such as its potential applicability to multi-factorial investigations.

Materials and Procedures

The Setup

We designed a Fluorometer- and Oximeter-equipped Flow-through Setup (FOFS) with the ability to simulate thermal regimes and to record physiological parameters of benthic filter-feeders. FOFS is schematically illustrated in Fig. 1 (see also the photographic view in Supplementary Information Fig. S1). The peristaltic pump 'Pump1' (ISMATEC MCP 12 channels, Cole-Parmer, Wertheim, Germany) creates a constant flow of seawater from a multi-parameter-controlled source tank (600 L; Kiel Indoor Benthocosms, KIBs, described in Pansch and Hiebenthal 2019) to the 'dilution tank' (250 mL). The peristaltic pump 'Pump2' (ISMATEC REGLO digital four channels, Cole-Parmer, Wertheim, Germany) produces a

steady flow of phytoplankton food suspension from the ‘food tank’ to the dilution tank. The cryptophyte *Rhodomonas salina* (cultured at 16 °C by the Kiel Marine Organism Culture Centre at GEOMAR, KIMOCC) is applied as the food source in our setup as in many other experiments with filter-feeding marine invertebrates (e.g., Clausen and Riisgård 1996; Riisgård et al. 2013; Sanders et al. 2018). Before each experiment, the food tank (~ 10 L) is filled with a high-concentration *R. salina* suspension (e.g., ~ 3×10^5 cells mL⁻¹). The food concentration in the dilution tank can be adjusted according to the needs of the study organisms by varying concentration, composition and pumping rates of Pump1 and Pump2. The resulting food suspension is pumped from the dilution tank into four separate paths (Path_C and Path_{S1-3}). Path_C represents the control path where oximetry and fluorometry are conducted in the absence of the study specimen, while Path_{S1-3} can harbor one or more specimen per unit (Figs. 1 and S1). For higher replication, the number of parallel paths can be easily increased. Along each path, the food suspension flows first into a cylindrical Plexiglas chamber (100 mL; incubation or oximetry chamber) through an inlet at its lower part of the sidewall. After filling the chamber, the suspension flows out via an outlet at the top of the incubation chamber and into a cylindrical non-transparent PVC chamber (350 mL; fluorometry chamber). Finally, the suspension discharges from the outlet located at the upper part of the fluorometry chambers. Relatively thin (here 0.80- and 2.54-mm inner diameter in Pump2- and Pump1-paths, respectively) silicon tubes in the setup reduce settling rates of the phytoplankton suspension. Plexiglas tube-compatible connectors are used as inlets and outlets of the chambers. The suspensions inside the food and dilution tanks, and incubation and fluorometry chambers are steadily mixed by laboratory magnetic stirrers (HI190M, HANNA instruments, USA; Figs. 1a, b, and S1).

Dissolved oxygen concentration is recorded via sensor spots (SP-PSt3-NAU, PreSens Precision Sensing, Regensburg, Germany; resolution ± 0.1 % O₂ at 20.9 % O₂ or ± 0.04 mg L⁻¹ at 9.1 mg L⁻¹) attached to the inner surface of the incubation chambers (Figs. 1a, b, and S1). Sensor spots are read out by an oximeter (OXY-4 mini, PreSens Precision Sensing, Regensburg, Germany) through optical fibers connected to the cylinders’ outer surface. Configuration and data logging are achieved using the corresponding software. Sensor spots are calibrated based on the two-point calibration protocol (PreSens 2017). The reference measurements were conducted in anoxic water (prepared by dissolving 10 g of sodium sulfite in 1000 mL water) and water-vapor saturated air.

Food concentration is measured using fluorometers (Cyclops 7f, Turner Designs, San Jose, USA; Application: Chlorophyll *in vivo*, blue excitation; Minimum detection limit: 0.00003 mg L⁻¹; Linear range: 0–0.5 mg L⁻¹) in dark and well-mixed conditions inside the fluorometry

chambers (Figs. 1 and S1). Fluorometers are set up, and data are recorded using the Cyclops-explorer connectors and software (Turner Designs, San Jose, USA).

The size of incubation (oximetry) chambers must be large enough to satisfy the space requirements for the species' normal activities (i.e., related to the size of study specimens). The volume of the fluorometry chamber is chosen to provide a distance of ~ 8 cm between the fluorometer's optical face and the chamber floor while the optical face and shade caps of the fluorometer are entirely submerged (Turner Designs 2020).

The source-water tank (600 L) is equipped with a control system (Profilux 3.1TeX; GHL Advanced Technology, Kaiserslautern, Germany) automating thermal simulations. A temperature profile (in .csv format) is submitted via the GHL-controller software to the ProfiLux computer, which then adjusts the source-water temperature. More parameters (pH/pCO₂, salinity, etc.) can also be manipulated in automated procedures. This type of GHL-equipped source-water tank has been successfully implemented within the Kiel Indoor and Outdoor Benthocosm systems (for more details, see Wahl et al. 2015 and Pansch and Hiebenthal 2019).

To minimize heat loss in FOFS, a water pump (EHEIM, Deizisau, Germany) generates a flux of source water (~ 2 L min⁻¹) into two water baths positioned in sequence: the first water bath (aquarium of 50×30×15 cm) holds incubation and fluorometry chambers and the second water bath (20×15×10 cm) holds the dilution tank (see Fig. 1a). Additionally, air-exposed areas of silicon tubes are covered by heat-reflective thermal blankets to conserve heat.

If the source water becomes supersaturated with air, the formation of air bubbles can disturb the oximetry and fluorometry. This can be avoided by intensive aeration of the source-tank water during the experiment.

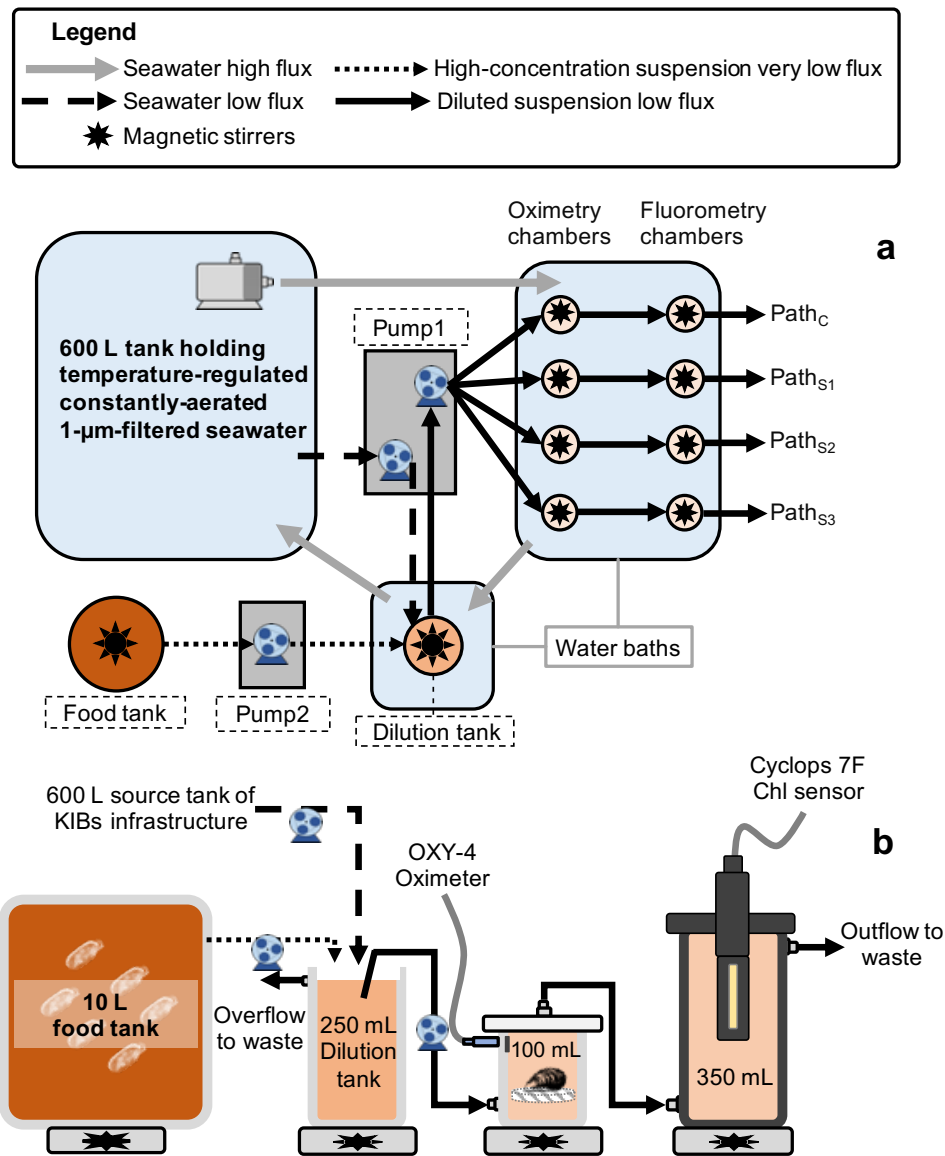


Fig. 1. Schematics of the Fluorometer- and Oximeter-equipped Flow-through Setup (FOFS). **(a)** Schematic top view indicating the flux of seawater, concentrated and diluted food suspension (depicted by the brown shading) through the setups' main components, including the source-water tank, the food tank, the dilution tank, water baths, and incubation- (Plexiglas, 100 mL) and fluorometry- (PVC, 350 mL) chambers. Path_c indicates the control path where oximetry and fluorometry are conducted without any study specimen. During a trial, filter-feeders are placed within the incubation chambers (Path_{S1-3}). **(b)** Schematic side view indicating the flux of suspension in Path_{S1}. The dissolved oxygen and chlorophyll concentrations are recorded within the incubation (oximetry) and fluorometry chambers, respectively.

General experimental design and procedure

A randomized block design can be used for experimenting with FOFS. Each experiment can involve several temporally repeated trials with similar treatments but different study specimens. Each trial has three subsequent stages, a pre-, a main-, and a post-trial (for an exemplary scheme, see Fig. 2). During pre- and post-trials, the setup runs in the absence of specimens for ~ 3 h at a constant baseline temperature until the readout of all sensors becomes and remains

stable for > 60 min (Fig. 2). Later in the data processing, we use data of each pre- and post-trial to account for the baseline dissimilarities between readouts of different sensors and to check whether measurements were affected by random factors over the corresponding main trial.

During all stages of a trial, one of the paths (i.e., Path_C) acts as the control. Accordingly, the incubation chamber located on Path_C contains only the temperature logger (EnvLogger, ElectricBlue, Vairão, Portugal) but no filter-feeder. After the pre-trial, the other incubation chambers located on Path_{Sn} are de-capped, and the study specimens are placed on plastic-mesh seats inside the chambers (Fig. 1b). The chambers are then recapped, avoiding air bubbles. At this point, the fluorometry chamber caps must be also repositioned to eliminate potentially trapped air bubbles.

After each post-trial, and before starting a new pre-trial, FOFS must be run with deionized water for ~ 20 min and the chambers' interior must be brushed thoroughly to remove remnants of the studied specimens (e.g., feces and associated microbial biota).

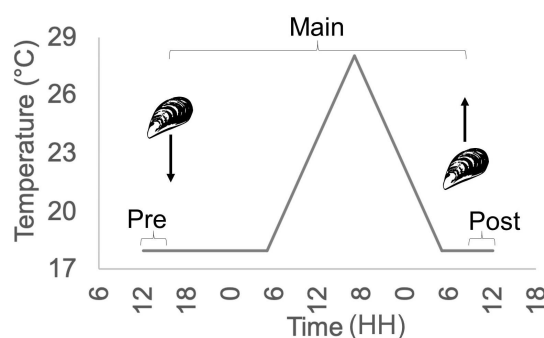


Fig. 2. An exemplary trial with a daily thermal fluctuation cycle is indicated. The main trial is preceded and followed by a pre- and post-trial period without filter-feeder, respectively. During the main trial, the organisms' response to fluctuation is recorded. The main trial can also comprise periods of a constant condition before and after the fluctuation, which allows organisms to acclimate to the ambient condition and provides insight into how consistent the responses are during exposure to a static ambient condition.

Data processing through Python scripts

Here, an overview of different steps of the data processing is provided with a focus on the techniques used to correct and convert measurements and calculate the response variables. The associated Python scripts can be found in the Supplementary Information Scripts. Notes and explanatory remarks provided throughout the scripts clarify how the steps and commands in the scripts work and how one can use and adopt them.

Dissolved-oxygen concentration calculator

‘DO_calculator.py’ (Supplementary Information Script S1) transforms the phase angle data (ϕ) collected via PreSens Pts3 sensor spots (and Oxi4-mini oximeter) to the dissolved-oxygen concentration in % air-saturation considering the temperature-sensitivity of the phase angle and Stern-Volmer constant. The % air-saturation data are then converted to $\mu\text{molO}_2 \text{ L}^{-1}$ considering ambient temperature and salinity. The ambient temperature data used in the processing are recorded by the logger placed within FOFS. The equations used in this calculator are based on the Oxi4-mini instruction manual (PreSens 2004).

Future users applying oximeters lacking the automatic temperature-correction and unit conversion can revise the script based on the specifications of their device (sensors).

Trial-by-trial analysis

FOFS_trial-by-trial_processing.py (Supplementary Information Script S2) can be applied to process raw data and generate outputs including data frames and time series plots of raw, corrected and converted versions of measurements and calculated data of the response variables for each experimental trial.

Step 1 (filtration and feeding rates)

The script reads in pre-trial series of food concentration (mV) and names them ‘pre_C_mV_Ch1’ or ‘pre_Sn_mV_Ch1’. The series are denoised (trended) using a time-windowed slider with an iterative robust location estimator such as Tukey’s biweight or Welsch estimators (Wotan module; Hippke et al. 2019). Robust estimation assigns more weight to the data points closer to the central values of the sliding window (for a detailed description of different types of estimators, refer to Hippke et al. 2019). The trended mV series suffixed by ‘_Trend’ are then corrected using the temperature correction coefficient (Supporting Information Text S1) and saved with the additional suffix ‘_TC’.

The trended- and temperature-corrected mV series are plotted to select the ‘pre-trial stable-data’. The criterion for selecting the stable-data is explained in Supplementary Information Text S2. The pre-trial stable-data of Path_c is averaged and then converted from mV to cells mL^{-1} using the conversion coefficient (Supporting Information Text S1), which will be used later as ‘the initial concentration’. Ideally, the conversion coefficient is checked at each pre-trial since

it might change slightly due to variation in the positioning of the fluorometer on the chamber and the rate of magnetic stirring.

The main trial mV series are also denoised and, then, corrected using the temperature-correction coefficient (e.g., Fig. 3b). The mV data of each sensor are then expressed as percentage of the mean value of the pre-trial stable-data of the same sensor (named ‘percent_C’ and ‘percent_Sn’ in the script). This procedure eliminates the baseline differences in the absolute value of output between the fluorometers as the output of each fluorometer is directly proportional to the chlorophyll (*R. salina*) concentration signal (Cyclops 7 User’s Manual; $R^2 > 0.985$ based on our observations). The food concentration series are finally converted from the percentage to cells mL⁻¹ (‘cell_per_ml_C’ and ‘cell_per_ml_Sn’), considering that the ‘initial cell concentration’ is 100 % (compare Fig. 3b with 3c).

In each FOFS path, the fluorometry chamber, which has a 350-mL volume due to the space requirements of the fluorometer (refer to Material and Procedures: The setup), is inevitably positioned downstream to the incubation (oximetry) chambers (Fig. 1b). The oximetry chamber contains a relatively small volume of a well-mixed solution. Any change in the respiration or filtration activities of the study specimen almost instantly alters the dissolved oxygen or food concentration in the oximetry chamber and in the inflow to the fluorometry chamber. The inflow is being mixed with the solution in the larger fluorometry chamber; therefore, any measured change in food concentration is a dampened (temporally lagged and weakened) version of a change in the inflow food concentration. The script uses a linear differential equation (Campbell and Haberman 2008; Supporting Information Text S3) to improve the estimation of rapid changes in the measured food concentration (Fig. 3c, d). These rapid changes in food concentration can occur because of filtration shutdown or recovery of the study organism. Notably, if the measured food concentration follows a consistent trend with no rapid changes, no correction is done (Supplementary Information Fig. S3).

The resulting time-series is used to calculate the filtration and feeding rates of study specimens (Fig. 3e) based on Eq. 1 and Eq. 2, respectively (modified after Larsen and Riisgård 2011).

$$\text{Eq. 1. } \text{filt}_{\text{Sn}}(\text{mL min}^{-1}) = \frac{\text{food}_C(\text{cells mL}^{-1}) - \text{food}_{\text{Sn}}(\text{cells mL}^{-1})}{\text{food}_{\text{Sn}}(\text{cells mL}^{-1})} \times \text{flow rate}(\text{mL min}^{-1})$$

$$\text{Eq. 2. } \text{feed}_{\text{Sn}}(\text{cells min}^{-1}) = \text{food}_C(\text{cells mL}^{-1}) - \text{food}_{\text{Sn}}(\text{cells mL}^{-1}) \times \text{flow rate}(\text{mL min}^{-1})$$

The final time-series of filtration and feeding rates are named ‘filt_ml_per_min_Sn’ and ‘feed_cell_per_min_Sn’ in the script.

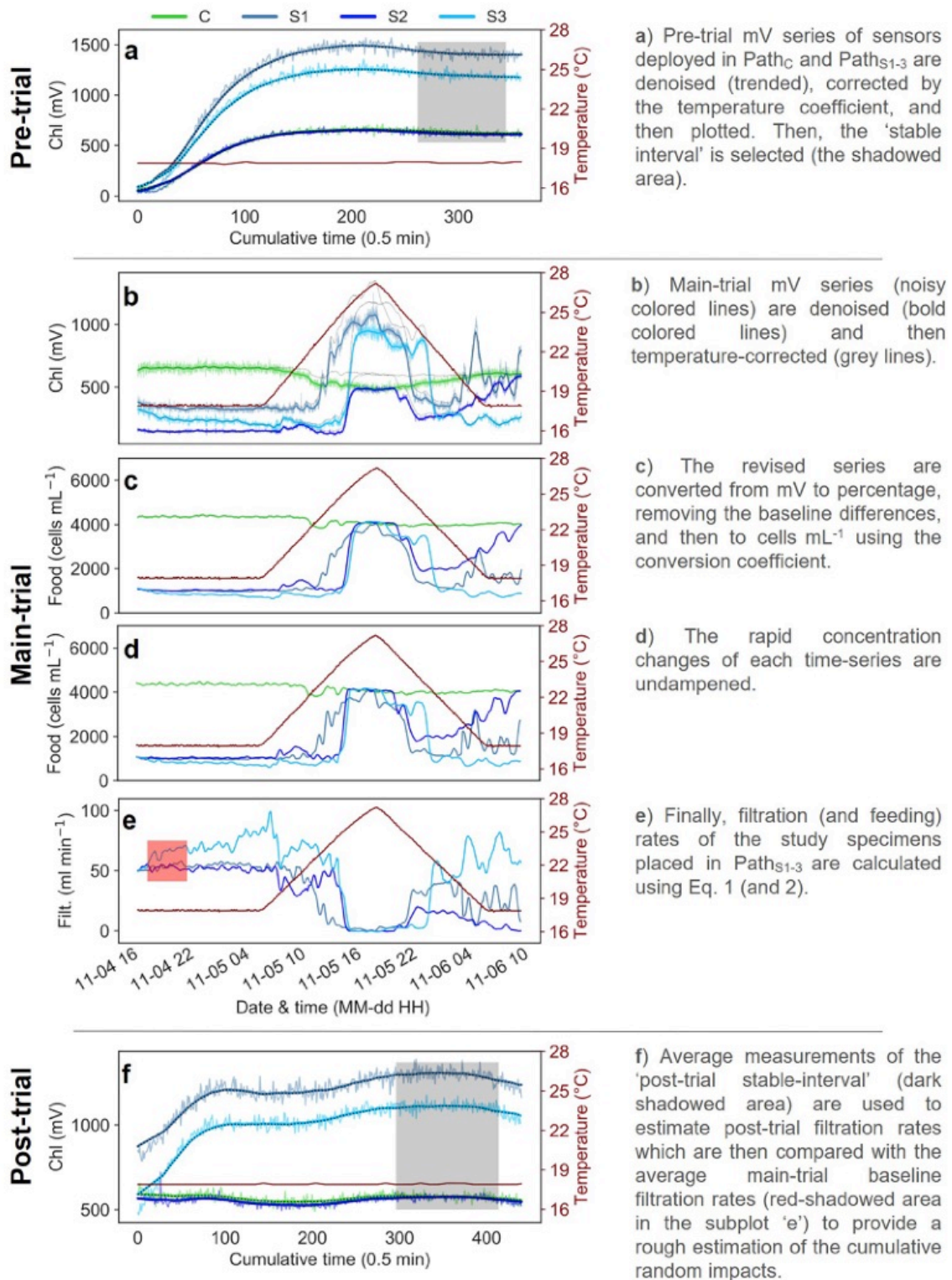


Fig. 3. Data processing flowchart with acquired time-series graphs of fluorescence intensity in mV, *Rhodomonas salina* concentration, and mussel (*Mytilus* spp.) filtration rates for an experimental trial (November 4–6, 2019) including pre- (a), main- (b–e) and post-trial (f) stages. Data from Path_C (the control path) are displayed as green lines. Data from Path_{S1-3} are displayed as shades of blue (see the legend at the top of the plot). The measurement frequency is 0.5 min (x-axis titles of pre- and post-trial subplots).

Step 2 (respiration rate)

The same techniques are used to denoise pre- and main-trial dissolved oxygen concentration (% air-saturation and $\mu\text{mol L}^{-1}$) and to define and average the 'pre-trial stable-data' (refer to *Step 1*; Fig. 4a, b).

There might be small baseline differences between the outputs of the oximeters due to imperfect sensor calibration. For example, we calibrated the sensor spots twice manually and twice using the calibration data provided in the Final Inspection Protocol for the PreSens Pts3 sensor spots. The differences between the sensors when FOFS was running in the absence of filter-feeders were comparable to the differences recorded in air (i.e., $< 1.2\%$ air saturation). The sensors' baseline outputs may be even more comparable if the sensors are calibrated in a shared calibration medium, though this is hard to conduct when the sensor spots are attached to different chambers. Nonetheless, the average pre-trial stable measurement of each sensor_{S_n} is subtracted from the counterpart value of the sensor_C, and this baseline difference is later added to the main-trial data of the sensor_{S_n} (Fig. 4c). Notably, this correction simplistically assumes that the calibration curves of sensor_{S_n} and sensor_C are nearly parallel over the experimental range of dissolved-oxygen concentration and therefore imposes cumulative errors as the measured concentration of sensor_{S_n} deviate from the pre-trial reference. For example, if the difference between measurements of sensor_{S₁} and sensor_C is $\sim 1\%$ at a real ambient concentration of 100% air saturation, after the correction the two values will depart $< 0.1\%$ per 10% decrease in the ambient concentration.

The final version of main-trial data (named 'control_ymol_per_l_C' and 'corrected_ymol_per_l_Sn' in the script) are then applied to Eq. 3 to calculate the respiration rate.

Eq. 3. $\text{resp}_{\text{Sn}}(\mu\text{molO}_2 \text{ min}^{-1}) = (\text{oxyg}_{\text{C}}(\mu\text{mol L}^{-1}) - \text{oxyg}_{\text{Sn}}(\mu\text{mol L}^{-1})) \times \text{flow rate}(\text{L min}^{-1})$

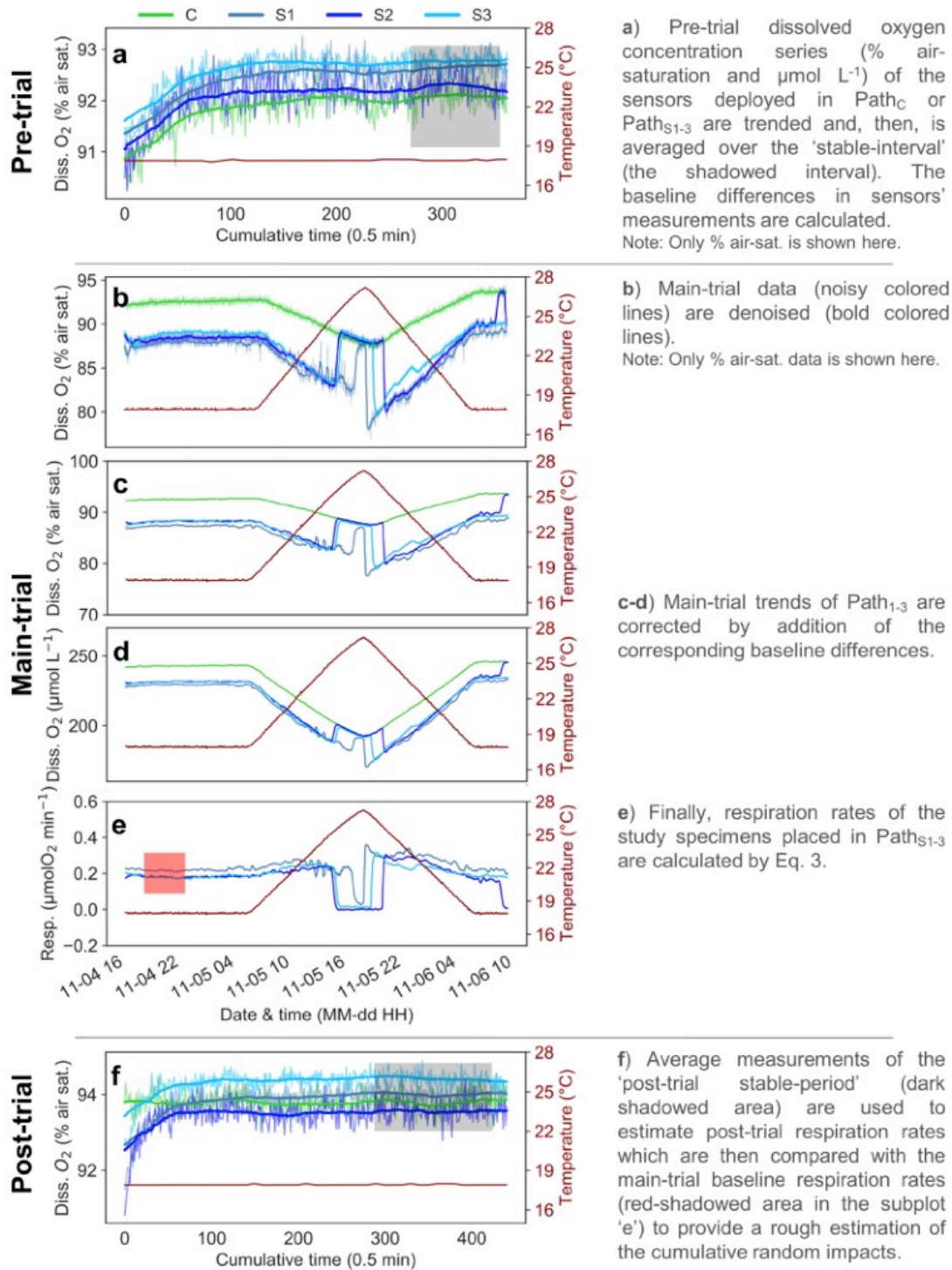


Fig. 4. Data analysis flowchart with acquired time-series graphs of the dissolved-oxygen concentration and mussel (*Mytilus* spp.) respiration rates for an experimental trial (November 4–6, 2019) including pre- (a), main- (b–e) and post-trial (f) stages. The measurement frequency is 0.5 min (x-axis titles of pre- and post-trial subplots).

Step 3 (Scope for Growth)

The principal outputs of data processing are filtration and respiration records. The script also provides a very simplistic estimation of surplus of energy available for growth based on the assimilated energy minus the respired energy (the basic definition of the Scope for Growth, SFG; Widdows 1976). The SFG can be estimated based on the experimental feeding rate (Eq. 4) or, instead, based on the feeding rate at a hypothetical food concentration (e.g., the average experimental food concentration). The hypothetical feeding rate ($\text{feed}_{\text{hyp}_{S_n}}$ in J h^{-1}) is calculated based on the filtration rate at a constant food concentration food_{hyp} in J mL^{-1} (Eq. 5). $\text{SFG}_{\text{hyp}_{S_n}}$ is then estimated based on $\text{feed}_{\text{hyp}_{S_n}}$, resp_{S_n} (i.e., the respiration rate in J h^{-1}), and the assimilation efficiency (AE) of 80 % (based on the average value reported in Widdows and Bayne 1971) through Eq. 6.

$$\text{Eq. 4. } \text{SFG}_{S_n} (\text{J h}^{-1}) = \text{feed}_{S_n} (\text{J h}^{-1}) \times \text{AE} - \text{resp}_{S_n} (\text{J h}^{-1})$$

$$\text{Eq. 5. } \text{feed}_{\text{hyp}_{S_n}} (\text{J min}^{-1}) = \text{filt}_{S_n} (\text{mL min}^{-1}) \times \text{food}_{\text{hyp}} (\text{J mL}^{-1})$$

$$\text{Eq. 6. } \text{SFG}_{\text{hyp}_{S_n}} (\text{J h}^{-1}) = \text{feed}_{\text{hyp}_{S_n}} (\text{J h}^{-1}) \times \text{AE} - \text{resp}_{S_n} (\text{J h}^{-1})$$

Conversion factors of 1.75 μJ per *R. salina* cell (Kjørboe et al. 1985) and 450 kJ per molO_2 (Widdows and Hawkins 1989) are applied.

Step 4 (cumulative random effects)

FOFS assumes that the deviations in food and dissolved-oxygen concentrations between Path_C and each Path_{S_n} are only due to the study specimens' filtration and respiration during the main trial. Therefore, it is important to check the possible contribution of random (non-filter-feeder) factors. To do so, the average of the 'post-trial stable-data' (of each sensor_{S_n}) is used to assess how close the post-trial filtration and respiration rates are to zero (refer to Figs. 3f and 4f). Post-trial responses are expected to be equal or close to zero, as this stage is conducted in the absence of study specimens. The post-trial responses are compared with the main-trial baseline filtration and respiration rates to roughly estimate the ratios of the non-filter-feeder- to filter-feeder-induced signals (i.e., the cumulative random impacts in percent; refer to Figs. 3e-f and 4e-f). Baseline filtration or respiration rate is defined in the script as the average of 180th to 480th main-trial data points, while future users may need to change the interval based on the observed responses.

It must be considered that cumulative random effects are those non-filter-feeder (confounding) effects which are still detectable after the main trial (in the post-trial stable-data), which could be due to long-lasting drifts in sensor measurements, bacterial respiration which may be boosted due to remnants of the study specimens (i.e., ammonia/feces released), settlement of the food-organism (in this case *R. salina*) and possible changes in the speed of magnetic stirrers. Future users need to also ensure that their measurements are not impacted by transient random effects (e.g. temporary electrical interventions and sensor malfunctions) through ‘blank trials’ (for an example, see Assessment and Discussion: Demonstration experiment).

FOFS integrative processing

The data frames created through the trial-by-trial processing can be integrated using ‘FOFS_integrative_processing.py’ (Supplementary Information Script S3). Importantly, a data sheet containing dry weights and shell lengths of study specimens (e.g., Supplementary Information Table S1) must be manually added to the experimental folder, before executing the script.

The script first merges post-stage data frames, including all estimated cumulative random effects (‘%_cumulative_random_effects_Sn’ in the script). Then, it concatenates main-trial data frames one by one, plus defining size-standardized rates of filtration, feeding, respiration, and SFG for the replicates. All responses are standardized to shell length and dry tissue weight as proxies for gill surface area and tissue volume (Hamburger et al. 1983; Riisgård 2001). Any change to the complete experimental data frame (‘experiment_df’), such as excluding a broken part, can be done through ‘manual imposition of changes’.

The script produces line-plots, each aggregating over replicated values of a specific variable at each time point and shows estimates of the averages with the respective 95% confidence intervals.

Finally, thermal variations in responses are described through Generalized Additive Models (pyGAM module; Servén and Brummitt 2018) using data of the whole experiment or a specific phase of it (e.g., the warming or cooling phase of a thermal fluctuation treatment). The best fit GAM is selected using a grid-search over multiple values of the regularization parameter and n-spline values seeking the lowest Generalized Cross-Validation score (for more details on GAM, refer to Wood 2017).

Assessment and Discussion

Demonstration experiment

In a few studies, flow-through setups were applied for simultaneous measurement of filtration and respiration of aquatic organisms under static experimental conditions (Widdows 1973; Haure et al. 2003). Besides, guidelines are available for the design of flow-through setups proper for measuring the filtration rate under static conditions (Filgueira et al. 2006; Larsen and Riisgård. 2011). Here, we describe the design of a Fluorometer- and Oximeter-equipped Flow-through Setup (FOFS) and provide the protocols used for semi-automated data processing through Python scripts. The method described here allows for high-resolution monitoring of filtration and respiration rates in response to dynamic environmental conditions, ultimately enabling the detection of the ecological limits of benthic filter feeders facing climate change. The methods' functionality is tested in a demonstration experiment, testing the key assumption that the deviations of processed concentrations of each specimen path ($Path_{Sn}$) from those of the control path ($Path_c$) of FOFS in time is only due to the respective filter-feeder being examined during a dynamic treatment.

In many shallow-water marine habitats (including the Baltic Sea), temperature changes at time scales of seconds, minutes or hours to days and weeks, during daily temperature cycles, heatwaves and/or upwelling events (Lima and Wetthey 2012; supplementary information in Pansch and Hiebenthal 2019). Therefore, we applied our newly developed method in six trials using daily thermal cycles.

In four trials, we exposed mussels (*Mytilus* spp. specimens from Kiel Fjord, Western Baltic Sea) to daily temperature fluctuations. Before the trials, study specimens were kept at constant 16 °C and fed once per day with *R. salina* for three weeks. The minimum and maximum temperatures experienced by the mussels in the main trials were 18 and 27.5 °C, which were reached at 5:00 and 17:00 during the day, respectively. The rate of linear change (rise and decline) was ± 0.79 °C h⁻¹. After each trial, all specimens were kept in 0.5 µm filtered seawater at room temperature (16 °C) for ~ 10 h to release feces (minimizing the effect of feces-weight on mussel dry tissue weight). Afterwards, the length of specimens was measured using a caliper and their tissue was dried at 80 °C for 30 h and weighed using an electronic balance (0.1 mg; Sartorius, Berlin, Germany). Besides, we checked that the thermal exposures do not impose substantial changes on the phytoplanktonic food (*Rhodomonas salina*) concentration (Supplementary Information Text S4 and Fig. S4).

Two blank trials, each with a pre- and a main-trial phase, were conducted to check whether processed measurements of different sensors remain comparable over the experimental time and over the temperature range in the absence of mussels. The pre-stage of the first blank trial (October 14–16, 2019) was carried out following the standard cleaning procedure. The pre-stage of the second trial (November 1–3, 2019) was initiated as a follow-up of the mussel-inclusive trial (without the cleaning) to see how remnants of the mussels (e.g., ammonia/feces released, which might have possibly affected microbial activities in the tubing and chambers) could have affected the respiration and filtration time series under the influence of temperature and time over the main trial. The minimum and maximum temperatures in our two blank trials were 18 or 20 and 28 or 29 °C, respectively.

During all demonstration trials, seawater salinity was ca. 21 PSU, and the flow rates of Pump1 and Pump2 were constantly 16 and $\sim 2 \text{ mL min}^{-1}$, respectively. The food tank was refilled with concentrated food-solution after each trial. The sensitivity of the fluorometers was set to X10, which is suitable for measuring in the range of 1 to 5 $\mu\text{g Chl L}^{-1}$, comprising the concentration range of our experiment. Readout frequencies of the fluorometers, the oximeter, and the temperature logger were set to 30 s.

All data of the demonstration experiment, including blank and mussel trials' data, are archived and accessible in Pangaea (www.pangaea.de: Vajedsamiei et al. 2020).

Blank trials provide a performance check

Trends of food or dissolved oxygen concentration were comparable between Path_{Sn} and Path_{C} over the main stage of the blank trials, supporting the main assumption that differences between Path_{Sn} and Path_{C} should only emerge from the study specimens (Supplementary Information Fig. S5). There were minor temporal decreases in food concentration (Supplementary Information Fig. S5a, c), possibly due to settlement and/or death of *R. salina* cells. As both, oxygen solubility in seawater and the rate of dissolved-oxygen removal within the FOFS tubing and chambers are temperature-dependent, oxygen content varied linearly with temperature (Supplementary Information Fig. S5b, d). Due to the constant air bubbling of the source tank, the source water remained saturated ($\sim 100 \%$) with oxygen (confirmed by a WTW dissolved oxygen concentration meter, Multi 3630 IDS, Kaiserslautern, Germany).

Calculated filtration and respiration rates stayed consistently close to zero with slight variability for both blank trials (Supplementary Information Fig. S6). The mean and standard deviation of

responses during the main stage of the two blank trials are reported in Supplementary Information Table S2.

The pre-stage of the second blank trial ('01_nov') was done as an immediate follow-up of a mussel-trial, without cleaning of the system. Its outcomes indicate that remnants of the mussels did not cause notable deviations in concentration between Path_C and each Path_{S1-3} under the influence of temperature and time over the main trial. In the second blank trial, slight (transient) irregularity in dissolved-oxygen records of Path_C caused minor transient drifts in the calculated respiration rates of Path_{S1-3} (Supplementary Information Figs. S5d and S6d), contributing almost half of the mean respiration rate (Supplementary Information Table S2). Random transient irregularities were also observed in chlorophyll data but affected data of all four paths similarly. Yet, these random drifts are minor compared to the filter-feeders' response signal (compare Supplementary Information Figs. S5 with Fig. 5). Random irregularities might be explained by voltage fluctuations during working hours when high loads of electricity are being used. Future users may need to apply an online Uninterruptible Power Supply (UPS) to stabilize the voltage.

Mussel trials confirm applicability

The mussels induced differences in food and dissolved oxygen concentrations between Path_{S1-S3} and the control (Path_C), which were used to define filtration and respiration rates (Supplementary Information Figs. S7 and S8). In one mussel trial, the specimen of Path_{S3} expressed filtration shutdown and intermittent respiration shutdowns before being exposed to the thermal fluctuation, which was different from the responses of other studied mussels (Supplementary Information Fig. S8c-d). Besides, in another mussel-trial, the resumption of respiration of the specimen of Path_{S2} resulted in unusually high respiration rates (Supplementary Information Fig. S8f), due to magnetic stirrer arrest preventing efficient mixing of the solution inside the oximetry chamber. As the size of the studied mussels was large, the release of hypoxic water trapped within the shells during the metabolic depression resulted in a decrease in oxygen concentration recorded when the medium was not mixed efficiently. Data of these two replicates were excluded from the following integrative processing.

For each replicate, the ratio of the post-trial filtration (or respiration) and the main-trial baseline filtration (or respiration) rate expressed as a fraction of 100 are provided as estimates of cumulative random effects, estimating how big the random effect is compared to the baseline response signal (Supplementary Information Table S3). A negative (or positive) effect means

that non-filter-feeder factors might have led to a higher (or lower) food or dissolved oxygen measurements by Sensor_{Sn} compared to Sensor_C during the post-trial. The values indicate how much the filtration (or respiration) might have been under- or overestimated especially for data points recorded closer to the end of the main-trial period. The absolute value of average post-trial filtration rate was 0.1 mL min⁻¹ that could be expressed as ~ 0.2 % with reference to the baseline rate. The remnants of mussels and the resulting microbial activity contributed to post-trial respiration rates, which was on average 0.016 μmolO₂ min⁻¹ (i.e., ~ 7 % of the mussels' mean baseline respiration). While the random effects cannot be corrected, their recognition can help the user to better interpret the results and decide if data of a replicate must be removed from the analysis due to large drifts.

The rates of Scope for Growth of the studied mussels, estimated based on calculated filtration rates at (hypothetical) concentrations of 1000 and 4000 cells mL⁻¹, are presented in Supplementary Information Fig. S9. It should be noted that our estimation of hypothetical SFG simplistically assumes that the respiration rate is independent of the ambient food concentration (not considering respiratory costs of the feeding at different food levels; Secor 2009). Future users can also estimate 'SFG at the experimental food regime' based on real-time feeding and respiration rates (plots not presented here). Notably, both experimental and hypothetical SFGs neglect that assimilation efficiency may vary when environmental conditions change, especially in relation to organic content of food and ingestion rate (Hawkins 1996).

Temporal variation in rates of filtration and respiration averaged over pooled replicated data of the mussel-trials are presented in Fig. 5. The mean rates of filtration decreased with warming (Fig. 5a). The maximum tolerated temperature, at which a steep drop in average filtration rate could be observed, was ~ 24 °C during the warming phase. During the subsequent cooling phase, mussels started increasing their filtration at ~ 27–28 °C, however, only to a maximum level of ~ 50 % of the initial rate (Fig. 5a). The mean respiration rate started to decline during the warming phase at ~ 24 °C, down to half of the initial values, and then started to increase again during the subsequent cooling phase at ~ 30 °C, and finally reached the initial respiration rate (Fig. 5b). Variance (inter-individual variability) was larger for the respiration-depression response than for the filtration shutdown.

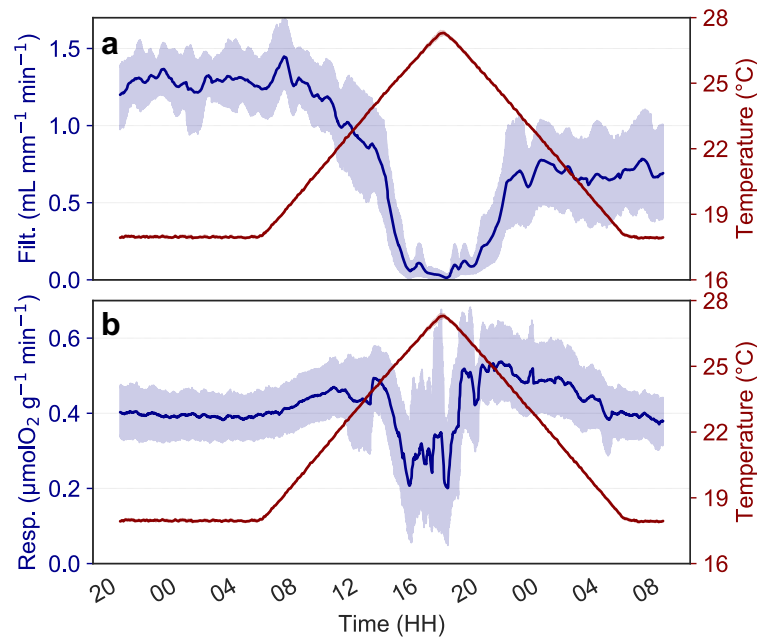


Fig. 5. Temporal variation in the length-specific filtration rate (**a**) and weight-specific respiration rate (**b**), along the daily temperature cycle. Data were pooled over multiple trials and replicates (10 replicates blocked in time) in the demonstration experiment. Replicated values were averaged at each time point, presented with 95 % confidence intervals.

The ambient food concentration and feeding rate of the study organisms over an experiment would be of interest to those investigating energetic costs of feeding or Specific Dynamic Action (refer to Secor 2009). Considering the study question and the optimal filtration rates of the study specimens, one can regulate the food-tank concentration and the pumping rates to generate any ambient food concentrations of interest. Our studied mussels were large and their filtration activity on average decreased their ambient food concentration from ~ 3800 to $800 \text{ cells mL}^{-1}$ over the period preceding the filtration shutdown (Supplementary Information Fig. S10a). Concentrations $< 1000 \text{ cells mL}^{-1}$ can be considered as marginal to suboptimal food levels for the filtration activity of *Mytilus* spp. (Riisgård et al. 2013); therefore, our studied mussels were probably food limited over that few-hour period. Mussels' respiration rates induced on maximum $\sim 10 \%$ air-saturation decrease in dissolved oxygen (Supplementary Information Fig. S10b). The outflowing water oxygen levels remained above 80 % saturation.

We compared our estimates of the baseline mean filtration and respiration rates of *Mytilus* specimens with the predictions based on previously published literature functions (Hamburger et al. 1983; Pleissner et al. 2013; more detailed description in Supplementary Information Text S5). The predicted rates of length-specific filtration and weight-specific respiration for *Mytilus* are $1.85 \text{ (mL mm}^{-1} \text{ min}^{-1})$ and $0.41 \text{ (}\mu\text{molO}_2 \text{ g}^{-1} \text{ h}^{-1})$. Our average baseline estimates were ~ 1.3

and 0.4, respectively (Fig. 5a, b), showing that our estimates are in line with expectations. Thermal variation in filtration and respiration rates in the warming and cooling phases of the mussel trials was described by Generalized Additive Models (GAMs; Fig. 6). Differences of the thermal response curves between the warming and cooling phases indicate time-dependent effects (i.e., in general, changes in the instant rate of thermal response over time due to alteration of the functional context by, for example, acclimatization, stress and damage; Kingsolver et al. 2015).

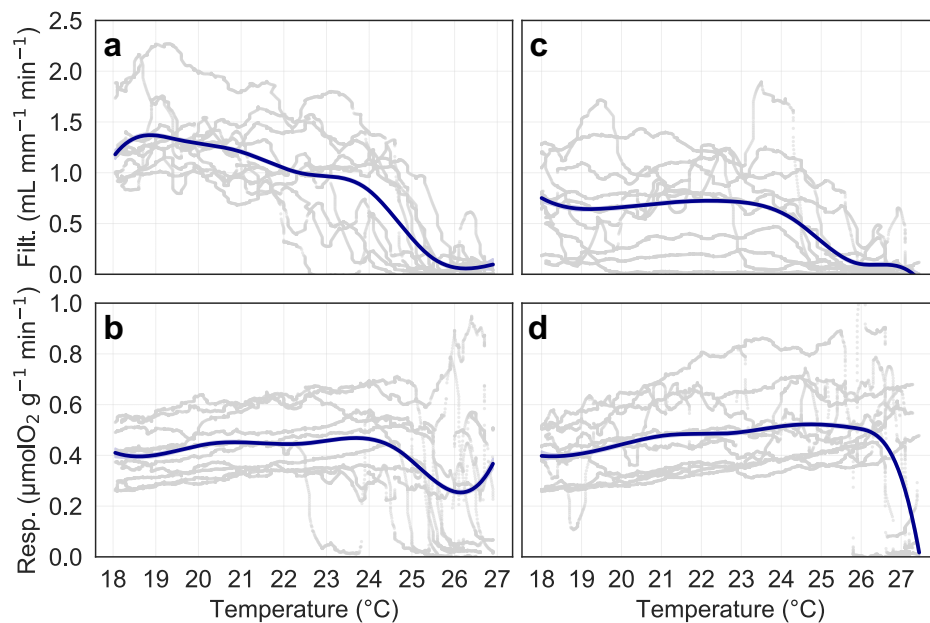


Fig. 6. Thermal response curves. Filtration and respiration rates of mussels as functions of the temperature in the warming (a–b) and cooling phases (c–d) of the mussel trials of demonstration experiment, modelled by the best-fit Generalized Additive Models (dark-blue lines). The warming and cooling phases correspond to the time intervals 5:00-17:00 and 17:00-5:00, respectively.

Challenges and solutions provided by FOFS and the suggested data processing

In FOFS, we successfully used submersible fluorometers that are more affordable and easier to handle due to their small size compared to previously applied laboratory fluorometers (Haure et al. 2003; Pleissner et al. 2013). We provide the procedure for temperature correction and unit conversion of Chlorophyll data, which was successfully tested in the demonstration experiment. The Python scripts explicitly facilitate all steps of data processing, making our method more understandable and adaptable for future studies. It applies a robust modeling technique for denoising measurements. It includes the dampening-effect correction which can be applied to data obtained through similar flow-through setups (including aquarium or mesocosm-based systems) in which the sensors are inevitably positioned in a series of chambers of different

sizes. The three-stage design of experimental trials enables estimation of cumulated random effects (as a measure of the temporal precision of measurements) soon after the end of a trial, allowing the users to exchange malfunctioning sensors in time and to better interpret the observed patterns of temporal variation in responses.

Other technical issues include the bubble formation in tubing and chambers and inherent differences between sensor readouts. These are explained and resolved in our method.

Limitations and potential solutions

Respiration rates recorded using FOFS represent the energy consumption rate by aerobic metabolism (Widdows and Hawkins 1989). To measure the rate of anaerobic metabolism, which might be especially important when filter-feeders experience phases of (thermally-induced) metabolic depression (valve closure), a direct calorimetry method would have to be applied (Guppy and Withers 1999; Regan et al. 2013; Nelson 2016). Another limitation of FOFS is the lack of automated control over the ambient food level, which can change under the influence of any filter-feeders' filtration activity throughout an experiment (e.g., thermal shutdown of filtration). By developing a feedback loop connecting Cyclops fluorometers and Pump2 through their software interfaces in the present setup, it should be possible to upgrade the setup to a system allowing automated control of ambient food concentrations.

Biofilm or bio-deposit accumulation may limit the time window of continuous recording of respiration in FOFS experiments. After our 1.5-day-long trials, the respiration from the remnants of mussels and biofilms was, on average, ca. 7 % of the mussels' mean baseline respiration (for mussels with ca. 4 cm shell length). To keep the error caused by microbial respiration minimal, especially during longer-term trials, one must stop the trial for a few minutes, for example, once a day, clean the incubation (Plexi-glass) chambers using deionized water and soft brush, and then continue the trial.

Significance, directions and possible advancements of the method

The decadal to centennial patterns of thermal changes in shallow-water marine habitats can be decomposed into (i) long-term trends, (ii) mid- and short-term (annual to daily) systematic fluctuations, and (iii) stochastic fluctuations of various durations (minutes and hours to months) (Lima and Wetthey 2012). Empirical studies recently inferred that, because of acclimatization and other time-dependent effects (e.g. physiological stress or damage), consequences of short-

term environmental fluctuations on the ecological performance might differ from mathematical predictions based on performance curves empirically-established under static treatment conditions (Niehaus et al. 2012; Kingsolver et al. 2015; Koussoroplis et al. 2017). Advancement in empirical methods is thus urgently needed to enable the description of the underlying causes of discrepancies between the predicted and observed effects of environmental fluctuations. FOFS practically provides a tool for researchers exposing organisms to environmental variability for some weeks or months, to relate the observed long-term integrated performance responses to short-term energy budget responses and explain their findings with the potential to generalize patterns. This procedure may improve the description of stress-response relationships and detection of species' tolerance limits.

The method can be used to provide more accurate data needed for parametrizing theoretical mechanistic models such as Scope-For-Growth (SFG, Winberg 1960) and Dynamic Energy Budget models (DEB, Kooijman 2010). Besides, it will allow researchers to investigate inter-individual variability in energetics responses of filter-feeders to temperature, mechanistically explaining intra-species variability in growth, reproduction, and survival (Fuentes-Santos et al. 2018).

We tested the setup to describe mussels' responses to a scenario of daily thermal fluctuations. The setup with the attributes described here can be used in more extended trials (~ 7–10 days compared to two days currently), and to investigate responses of many other filter-feeding taxa. Also, this setup might be used to explain physiological responses of organisms (from online recordings) with data retrieved in longer-term experiments (e.g. Pansch and Hiebenthal 2019; Morón Lugo et al. 2020). With minor modifications in chamber characteristics and flow-rates, the setup can be applied to studies of small- to large-sized filter-feeders, and may be extended to small communities of in- and epi-faunal suspension feeders. In that line, the setup can also be applied to test the response of systems of closely interacting species such as the filter-feeder-predator and filter-feeder-endoparasite systems to environmental variability (Stier et al. 2015). In principle, many drivers (e.g., temperature, oxygen, food, salinity, pH, and biological cues such as predator cues) can be manipulated in the setup, while respiration and filtration are constantly monitored. Therefore, we infer that the method can be adapted for multi-factorial exploration of filter-feeders' eco-physiology.

Conclusions

We described and successfully demonstrated the functionality of a method, including the experimental setup (FOFS), design, and data processing protocols, enabling researchers to monitor energy budget responses including filtration and metabolic activities of benthic filter-feeders in response to fine-tuned environmental variability. Importantly, the method can be adapted to study multi-factorial eco-physiology of shallow-water marine filter-feeders, shedding light onto species responses to environmental changes occurring within timescales of minutes or hours especially during daily cycles or extreme events such as marine heatwaves or hypoxic upwelling. This method can be applied by researchers exposing organisms to environmental variability for some weeks or months, to describe the observed integrated impacts of variability on the performance through energy budget responses to short-term environmental changes. In general, the method, therefore, allows a more mechanistic description of stress-response relationships and species' tolerance limits which are required for enhancing our understanding of filter feeders' performance responses to climate change.

Acknowledgments

The authors would like to acknowledge Ulrike Panknin for providing the *Rhodomonas* culture and technical assistance. We also thank Dakeishla Mary Diaz Morales for her comments on the final manuscript and Prof. Martin Wahl for his supports throughout this project.

This work and JV were funded through the Deutsche Forschungsgemeinschaft (DFG) project: The neglected role of environmental fluctuations as modulator of stress and driver of rapid evolution (Grant Number: PA 2643/2 / 348431475) and through GEOMAR. The project was supported by the Cluster of Excellence "The Future Ocean", funded within the framework of the Excellence Initiative by the DFG on behalf of the German federal and state governments. CP was funded by the postdoc program of the Helmholtz- Gemeinschaft Deutscher Forschungszentren and by GEOMAR. RK was supported by the collaborative research center 754 "Climate-Biogeochemistry Interactions in the Tropical Ocean" (www.sfb754.de) which was supported by the DFG. RK also acknowledges support from the Make Our Planet Great Again program of the French National Research Agency within the Programme d'Investissements d'Avenir; reference ANR-19-MPGA-0012. MK was funded through the PhD program of "studienstiftung des deutschen volkes".

References

- Bayne, B. 2017. Biology of oysters, 1st ed. Academic press.
- Boyd, P. W., C. E. Cornwall, and A. Davison. 2016. Biological responses to environmental heterogeneity under future ocean conditions. **22**: 2633–2650. doi:10.1111/gcb.13287
- Burge, C. A., C. J. Closek, C. S. Friedman, M. L. Groner, C. M. Jenkins, A. Shore-Maggio, and J. E. Welsh. 2016. The use of filter-feeders to manage disease in a changing world. *Integr. Comp. Biol.* **56**: 573–587. doi:10.1093/icb/icw048
- Campbell, S., and R. Haberman. 2008. Introduction to differential equations with dynamical systems. Princeton University Press.
- Clausen, I., and H. U. Riisgård. 1996. Growth, filtration and respiration in the mussel *Mytilus edulis*: no evidence for physiological regulation of the filter-pump to nutritional needs. *Mar. Ecol. Prog. Ser.* **141**: 37–45. doi:10.3354/meps14103
- Dame R. F., D. Bushek, and T.C. Prins. 2001. Benthic suspension feeders as determinants of ecosystem structure and function in shallow coastal waters. P. 11-37. In: K. Reise [eds.], *Ecological Comparisons of Sedimentary Shores. Ecological Studies (Analysis and Synthesis)*. Springer. doi: 10.1007/978-3-642-56557-1_2
- Filgueira, R., U. Labarta, and M. J. Fernandez-Reiriz. 2006. Flow-through chamber method for clearance rate measurements in bivalves: design and validation of individual chambers and mesocosm. *Limnol. Oceanogr. Methods* **4**: 284–292. doi:10.4319/lom.2006.4.284
- Fuentes-Santos, I., U. Labarta, and M. J. Fernández-Reiriz. 2018. Characterizing individual variability in mussel (*Mytilus galloprovincialis*) growth and testing its physiological drivers using Functional Data Analysis. *PLoS One* **13**: 1–13. doi:10.1371/journal.pone.0205981
- Gili, J. M., and R. Coma. 1998. Benthic suspension feeders: Their paramount role in littoral marine food webs. *Trends Ecol. Evol.* **13**: 316–321. doi:10.1016/S0169-5347(98)01365-2
- Guppy, M., and P. Withers. 1999. Metabolic depression in animals: Physiological perspectives and biochemical generalizations. *Biol. Rev.* **74**: 1–40. doi:10.1111/j.1469-185X.1999.tb00180.x
- Hamburger, K., F. Mohlenberg, A. Randlov, and H. U. Riisgård. 1983. Marine Size, oxygen consumption and growth in the mussel *Mytilus edulis*. *J Mar Biol* **75**: 303–306.
- Haure, J., A. Huvet, H. Palvadeau, M. Nourry, C. Penisson, J. L. Y. Martin, and P. Boudry. 2003. Feeding and respiratory time activities in the cupped oysters *Crassostrea gigas*, *Crassostrea angulata* and their hybrids. *Aquaculture* **218**: 539–551. doi:10.1016/S0044-8486(02)00493-3
- Hawkins, A. J. S., R. F. M. Smith, B. L. Bayne, and M. Héral. 1996. Novel observations underlying the fast growth of suspension-feeding shellfish in turbid environments: *Mytilus edulis*. *Mar. Ecol. Prog. Ser.* **131**: 179–190. doi:10.3354/meps131179
- Hippke, M., T. J. David, G. D. Mulders, and R. Heller. 2019. Wōtan: Comprehensive time-series detrending in Python. *Astron. J.* **158**: 143. doi:10.3847/1538-

- 3881/ab3984Kingsolver, J. G., J. K. Higgins, and K. E. Augustine. 2015. Fluctuating temperatures and ectotherm growth: distinguishing non-linear and time-dependent effects. *J. Exp. Biol.* **218**: 2218–2225. doi:10.1242/jeb.12073
- Kjørboe, T., F. Mshlenberg, and K. Hamburgefl. 1985. Bioenergetics of the planktonic copepod *Acartia tonsa*: relation between feeding, egg production and respiration, and composition of specific dynamic action. *Mar. Ecol.* **26**: 85–97.
- Kittner, C., and H. U. Riisgård. 2005. Effect of temperature on filtration rate in the mussel *Mytilus edulis*: no evidence for temperature compensation. **305**: 147–152.
- Kooijman, S. A. L. M. 2010. Dynamic energy budget theory for metabolic organization, 3rd ed. Cambridge Univ. Press. doi:10.1098/rstb.2010.0167
- Koussoroplis, A. M., S. Pincebourde, and A. Wacker. 2017. Understanding and predicting physiological performance of organisms in fluctuating and multifactorial environments. *Ecol. Monogr.* **87**: 178–197. doi:10.1002/ecm.1247
- Larsen, P. S., and H. U. Riisgård. 2011. Validation of the flow-through chamber (FTC) and steady-state (SS) methods for clearance rate measurements in filter-feeders. *Biol. Open* **1**: 6–11. doi:10.1242/bio.2011011
- Lima, F. P., and D. S. Wetthey. 2012. Three decades of high-resolution coastal sea surface temperatures reveal more than warming. *Nat. Commun.* **3**: 1–13. doi:10.1038/ncomms171
- Morón Lugo, S. C., M. Baumeister, O. M. Nour, F. Wolf, M. Stumpp, and C. Pansch. 2020. Warming and temperature variability determine the performance of two invertebrate predators. *Sci. Rep.* **10**: 1–14. doi:10.1038/s41598-020-63679-0
- Nelson, J. A. 2016. Oxygen consumption rate v. rate of energy utilization of fishes: A comparison and brief history of the two measurements. *J. Fish Biol.* **88**: 10–25. doi:10.1111/jfb.12824
- Niehaus, A. C., M. J. Angilletta, M. W. Sears, C. E. Franklin, and R. S. Wilson. 2012. Predicting the physiological performance of ectotherms in fluctuating thermal environments. *J. Exp. Biol.* **215**: 694–701. doi:10.1242/jeb.05803
- Pansch, C., and C. Hiebenthal. 2019. A new mesocosm system to study the effects of environmental variability on marine species and communities. *Limnol. Oceanogr. Methods* **17**: 145–162. doi:10.1002/lom3.10306
- Pleissner, D., K. Lundgreen, F. Luskow, and H. U. Riisgård. 2013. Fluorometer controlled apparatus designed for long-duration algal-feeding experiments and environmental effect studies with mussels. *J Mar Biol* **2013**: 401961.
- PreSens. 2004. OXY-4 4-channel Fiber-Optic Oxygen Meter: Instruction manual.
- PreSens. 2017. Oxygen Sensor Spots PSt3/PSt6: Instruction manual.
- Przeslawski, R., S. Ah Yong, M. Byrne, G. Wörheide, and P. Hutchings. 2008. Beyond corals and fish: the effects of climate change on noncoral benthic invertebrates of tropical reefs. *Glob. Chang. Biol.* **14**: 2773–2795. doi:10.1111/j.1365-2486.2008.01693

- Regan, M. D., J. M. Gosline, and J. G. Richards. 2013. A simple and affordable calorimeter for assessing the metabolic rates of fishes. *J. Exp. Biol.* **216**: 4507–4513. doi:10.1242/jeb.093500
- Riisgård, H. 2001. On measurement of filtration rate in filter-feeders - the stony road to reliable data: review and interpretation. *Mar. Ecol. Prog. Ser.* **211**: 275–291. doi:10.3354/meps211275
- Riisgård, H. U., D. Pleissner, K. Lundgreen, and P. S. Larsen. 2013. Growth of mussels *Mytilus edulis* at algal (*Rhodomonas salina*) concentrations below and above saturation levels for reduced filtration rate. *Mar. Biol. Res.* **9**: 1005–1017. doi:10.1080/17451000.2012.74254
- Riisgård, H. U., J. Lassen, and C. Kittner. 2006. Valve-gape response times in mussels (*Mytilus edulis*) - Effects of laboratory preceding-feeding conditions and *in situ* tidally induced variation in phytoplankton biomass. *J. Shellfish Res.* **25**: 901–911. doi:10.2983/0730-8000(2006)25
- Sanders, T., L. Schmittmann, J. C. Nascimento-Schulze, and F. Melzner. 2018. High calcification costs limit mussel growth at low salinity. *Front. Mar. Sci.* **5**: 1–9. doi:10.3389/fmars.2018.0035
- Secor, S. M. 2009. Specific dynamic action: A review of the postprandial metabolic response. *J. Comp. Physiol. B Biochem. Syst. Environ. Physiol.* **179**: 1–56. doi:10.1007/s00360-008-0283-7
- Servén, D., and C. Brummitt. 2018. pyGAM: Generalized Additive Models in Python. Zenodo. doi: 10.5281/zenodo.1208723
- Stier, T., J. Drent, and D. W. Thielges. 2015. Trematode infections reduce clearance rates and condition in blue mussels *Mytilus edulis*. *Mar. Ecol. Prog. Ser.* **529**: 137-144. <https://doi.org/10.3354/meps11250>
- Tang, B., and H. U. Riisgård. 2016. Physiological regulation of valve-opening degree enables mussels *Mytilus edulis* to overcome starvation periods by reducing the oxygen uptake. *Open J. Mar. Sci.* **6**: 341–352. doi: 10.4236/ojms.2016.63029.
- Turner Designs. 2020. Cyclops submersible sensors: User's manual.
- Vajedsamiei, J., F. Melzner, M. Raatz, R. Kiko, M. Khosravi, and C. Pansch. 2020. Exemplary FOFS output data of experiments on simultaneous recording of filtration and respiration in marine organisms. doi:10.1594/PANGAEA.919682
- van der Schatte Olivier, A., L. Jones, L. Le Vay, M. Christie, J. Wilson, and S. K. Malham. 2018. A global review of the ecosystem services provided by filter-feeder aquaculture. *Rev. Aquac.* **12**: 1–23. doi:10.1111/raq.12301
- Wahl, M., B. Buchholz, V. Winde, and others. 2015. A mesocosm concept for the simulation of near-natural shallow underwater climates: The Kiel Outdoor Benthocosms (KOB). *Limnol. Oceanogr. Methods* **13**: 651–663. doi:10.1002/lom3.10055
- Wahl, M., V. Saderne, and Y. Sawall. 2016. How good are we at assessing the impact of ocean acidification in coastal systems? Limitations, omissions and strengths of commonly

- used experimental approaches with special emphasis on the neglected role of fluctuations. *mar. freshw. res.* **67**: 25–36. doi:10.1071/MF14154
- Widdows, J. 1973. The effects of temperature on the metabolism and activity of *Mytilus edulis*. *Net. J. Sea. Res.* **398**: 387–398
- Widdows, J. 1976. Physiological adaptation of *Mytilus edulis* to cyclic temperatures. *J. Comp. Physiol.* **105**: 115–128. doi:10.1007/BF0069111
- Widdows, J., and A. J. S. Hawkins. 1989. Partitioning of rate of heat dissipation by *Mytilus edulis* into maintenance, feeding, and growth components. *Physiol. Zool.* **62**: 764–784.
- Widdows, J., and B. L. Bayne. 1971. Temperature acclimation of *Mytilus Edulis* with reference to its energy budget. *J. Mar. Biol. Assoc.* **51**: 827–843. doi:10.1017/S0025315400018002
- Widdows, J., M. D. Brinsley, P. N. Salkeld, and M. Elliott. 1998. Use of annular flumes to determine the influence of current velocity and filter-feeders on material flux at the sediment-water interface. *Estuaries* **21**: 552-559. doi:10.2307/135329
- Winberg, G. G. 1960. Rate of metabolism and food requirements of fishes. In F. E. J. Fry and W. E. Ricker [eds.], Translation Series No. 194. Fisheries Research Board of Canada.
- Wood, S. N. 2017. Generalized Additive Models: An Introduction with R. 2nd ed. Chapman & Hall/CRC.

Chapter 2: Burden or relief? Impact of cyclic thermal variability on ectotherms capable of metabolic suppression

Jahangir Vajedsamiei ^{1*}, Frank Melzner ¹, Michael Raatz ², Sonia Moron ³, Christian Pansch ⁴

¹ Department of Marine Ecology, GEOMAR Helmholtz Centre for Ocean Research Kiel, 24105 Kiel, Germany

² Department for Evolutionary Theory, Max-Planck Institute for Evolutionary Biology, Plön, Schleswig-Holstein, Germany

³ Département des Sciences Fondamentales, Université du Québec à Chicoutimi 555, Chicoutimi, Québec G7H 2B 1 Canada

⁴ Department of Environmental & Marine Biology, Åbo Akademi University, Turku, Finland

* **Corresponding author:** Address: GEOMAR Helmholtz Centre for Ocean Research Kiel, Hohenbergstr. 2, room no. 205, 24105 Kiel, Germany, Tel: +49 431 600-1598, e-mail: jahangir.vajedsamiei@gmail.com; jvajedsamiei@geomar.de

Co-authors' emails: FM: fmelzner@geomar.de, MR: mraatz@evolbio.mpg.de, SM: moronsonia@gmail.com, CP: cpanschh@abo.fi

Author ORCIDs: JV: 0000-0002-8625-4719, FM: 0000-0002-5884-1318, MR: 0000-0002-6968-6560; SCML: 0000-0003-1467-3516, CP: 0000-0001-8442-4502

Data accessibility statement: Given the manuscript be accepted, the data supporting the results will be archived in PANGEA or one of the following approved public repositories (Dryad, Figshare, Hal, Zenodo, Github and US federal agencies repositories) and the data DOI will be included at the end of the article.

Conflict of Interest: None declared.

Type of Paper: Letters (Primary research article) to *Functional Ecology*

Abstract

Predicting the implications of ongoing ocean climate warming demands a better understanding of how short-term weather conditions, e.g., daily to week-long thermal fluctuations, impact marine ectotherms, particularly at beyond-optimal average conditions such as during extreme summers or prolonged heatwaves. Using a globally important species, the blue mussel *Mytilus* spp., in a five-week-long experiment, we (i) compared growth performance traits under daily thermal fluctuation cycles to those measured in static temperature regimes, along a temperature gradient from benign to critical averages (18.5–26 °C). Besides, we applied a short-term assay to (ii) test for mussel's ability for active suppression and recovery of metabolic performance (feeding and aerobic respiration) in response to a one-day thermal fluctuation (16.8–30.5 °C). Using the highly-resolved assay data, we (iii) generated thermal performance curves to predict and explain the growth responses found in the long-term experiment. We found that daily high-amplitude thermal cycles (± 4 °C) improved mussel growth (shell length, dry tissue, and shell mass) when fluctuations were imposed around an extreme average condition (26 °C) representative of end-of-century heatwaves. In contrast, the thermal cycles negatively affected mussel growth at a less extreme average (23.5 °C), representing today's peak summer temperatures in the region. These results suggest that fluctuations ameliorate heat stress impacts only at critically high average temperatures. The short-term assay indicates that the study species could suppress and recover their metabolic performance when the temperature fluctuates in the range tested. Furthermore, nonlinear averaging of the short-term (non-acclimated) thermal feeding responses could well predict fluctuation impacts observed on growth rates from the long-term experiment. Our findings suggest that fluctuations that induce metabolic suppression and recovery can be beneficial or detrimental to ectotherm's long-term performance, depending on the fluctuations' baseline and amplitude. We propose a simple framework based on temporal changes in the thermal metabolic performance to explain this context-dependent stress sensitivity. Our research highlights the significance of studying metabolic performance at naturally relevant scales to advance our understanding of climate change impacts on aquatic systems.

Keywords: depression, elasticity, energy budget, *Jensen's Inequality*, plasticity, *scale transition*, Taylor expansion

Introduction

Marine environments, particularly coastal and shallow water regions, can experience short-term weather conditions, including thermal variations on timescales of minutes to days, predominantly driven by variations in irradiance, up and downwelling, and tides (Boyd *et al.* 2016; Choi *et al.* 2019). Ongoing climate change imposes decadal to centurial warming trends on marine environments (Rhein *et al.* 2013), and at the same time, affects the characteristics of shorter-term thermal fluctuations (Lima & Wethey 2012; Wang & Dillon 2014; Sun *et al.* 2018). For example, marine heatwaves are projected to become more frequent and prolonged and will be of stronger amplitude (Hobday *et al.* 2016; Holbrook *et al.* 2019). Therefore, the probability of marine organisms being exposed to beyond-optimal temperature conditions generally increases due to ocean warming (Somero 2010), and the impacts may be influenced by the pattern of short-term (daily to week-long) fluctuations around these warming trends (Jentsch *et al.* 2007; Smale *et al.* 2019).

The performance of organisms in response to temperature is usually nonlinear, commonly presented by thermal performance curves, TPCs (Angilletta 2006). The mathematics of nonlinear averaging (*Jensen's Inequality*; Jensen 1906) predicts that, compared to a non-fluctuating regime, the average response to a fluctuating thermal regime with the same average condition is higher for convex and lower for concave regions of an organism's TPC (Ruel & Ayres 1999; Fig. S1). Yet, predictions from nonlinear averaging assume that an organism's instant thermal response, as defined by its TPC, remains constant over time (i.e., lack of time-dependent effects; *sensu* Kingsolver *et al.* 2015; Sinclair *et al.* 2016). This assumption limits predicting the consequences of thermal fluctuations for marine organisms that evolved in variable habitats, such as shallow subtidal and intertidal habitats with pronounced diurnal or stochastic thermal fluctuations and aerial exposures (Helmuth *et al.* 2014). In such habitats, the capacity for active suppression and recovery of metabolic performance (Schulte *et al.* 2011) is required for species to persist.

Organisms have the potential to depress their metabolism by temporally shutting down high-energy demanding processes such as growth to avoid lethal thermodynamic stress during critical environmental conditions (Schulte *et al.* 2011). In metazoans, suppression of metabolism commonly involves decreases in the feeding rate, followed by reductions in aerobic respiration and occasional transition to anaerobic metabolism (Sokolova & Pörtner 2001). Metabolic suppression is mediated via post-translational modification of enzymes (Falfushynska *et al.* 2020), followed by changes in gene expression over time (Podrabsky &

Somero 2004). When metabolic suppression at constant but critical temperatures last for extended periods, organisms may not be able to maintain the balance between their demand for metabolic substrates and energy and the supply capacity (Schulte *et al.* 2011), rendering them vulnerable to stress (Stillman 2003). Therefore, TPCs commonly established through days- to months-long exposures of organisms to static treatment conditions usually show concave drops at the higher (beyond-optimal) end (Deutsch *et al.* 2008; Martin & Huey 2008). Thus, projecting the influence of thermal fluctuations on the long-term performance in a warming ocean, based on such TPCs, may only yield negative impacts (Paaijmans *et al.* 2013; Vasseur *et al.* 2014; Bernhardt *et al.* 2018). Yet, alternative (positive) effects may also be relevant according to some empirical observations (Bozinovic *et al.* 2011; Niehaus *et al.* 2012; Kingsolver *et al.* 2015; Kang *et al.* 2019). Potentially, alternations between phases of metabolic suppression and phases of recovery elicited by fluctuating regimes might be responsible for these observations of fluctuation-enhanced fitness (Schulte 2011; Wahl *et al.* 2015). Nonlinear averaging on TPCs generated at timescales (e.g., hours) that relate to (daily) cycles (i.e., in general, the upscaling approach; Chesson *et al.* 2005; Denny & Benedetti-Cecchi 2012; Denny 2019) may enable us to predict fluctuations' refuge effects.

Through a long-term (5-weeks) experiment on a globally important organism, the blue mussel *Mytilus* spp., this study first evaluates the hypothesis that (i) daily thermal fluctuations can be beneficial for the growth of an ectothermic organism at critical averages. In a second step, we applied a short-term (one-day) fluctuation assay testing (ii) whether the study organism can express thermal suppression and recovery of metabolic performance (feeding and aerobic respiration) in response to the fluctuation amplitude representing the thermal range experienced in the 5-week experiment. We finally (iii) evaluate whether upscaling of the short-term (non-acclimated) thermal metabolic responses by nonlinear averaging can predict the longer-term fluctuations' impacts observed in the 5-weeks experiment. The detailed workflow is presented in Fig. 1.

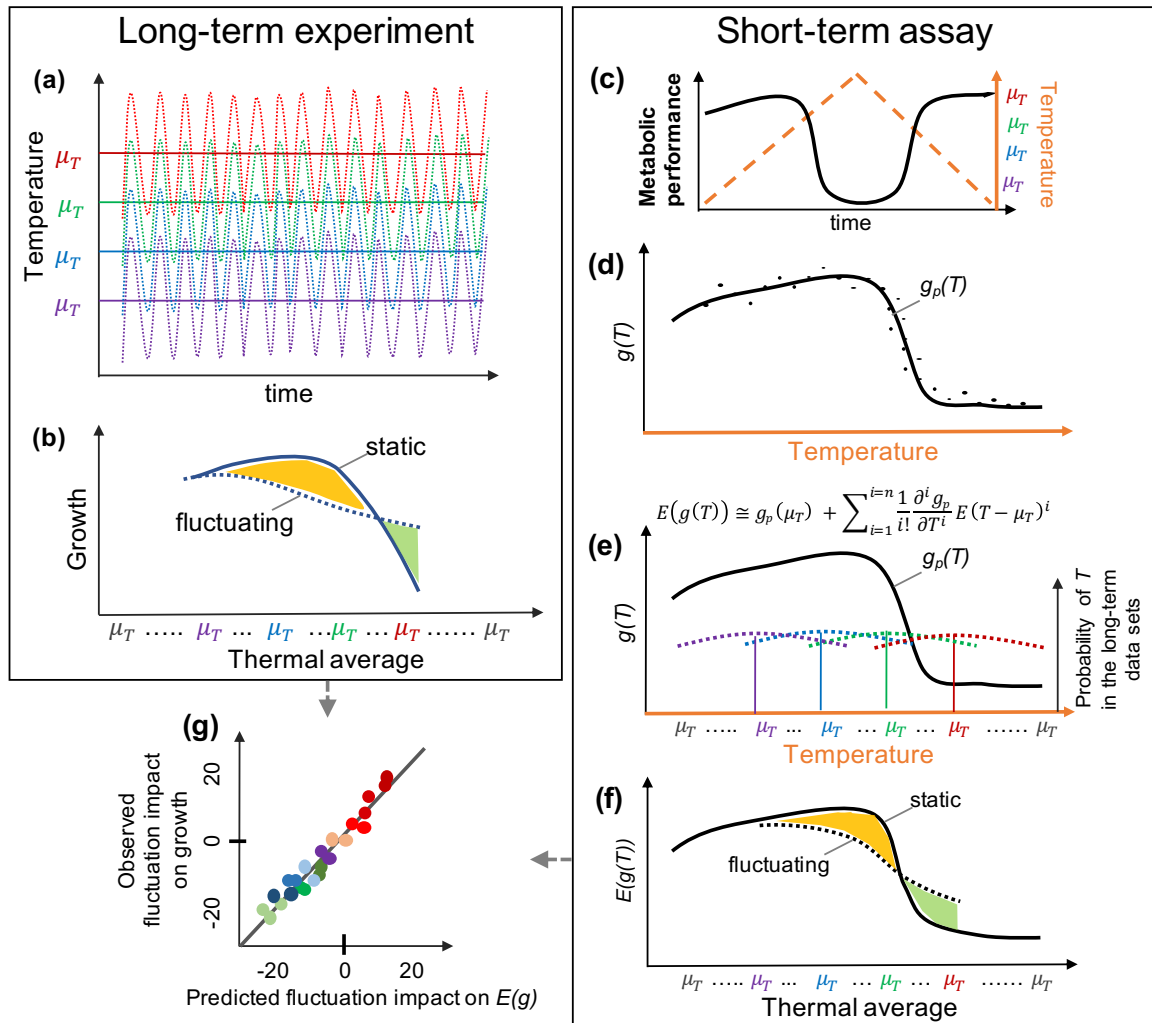


Figure 1 General sketch of the study workflow. **Long-term experiment (a and b):** (a) Time-integrated changes in growth traits, $E(G)$, are evaluated in a 5-weeks experiment. Here, the exemplary treatments include four levels of thermal averages μ_T (violet to red) potentially representing benign to critical average conditions, and two levels of fluctuations (continued and dotted lines for constant versus fluctuating regimes). (b) Thermal performance curves describing $E(G)$ as a function of μ_T are defined (solid and dotted lines represent growth under constant and fluctuating treatments, respectively). The positive and negative effects of fluctuations over μ_T are shown by green and yellow areas. **Short-term assay (c–f):** (c) The metabolic performance (feeding or respiration) $g(T)$ in response to one-day thermal cycle documents the metabolic suppression and recovery of the study organism. (d) Using data from the warming phase of the cycle, the best-fit polynomial curve explaining the thermal metabolic response, $g_p(T)$, is selected (representing a non-acclimated TPC). (e) Upscaling by taking the expectation of the Taylor expansion of $g_p(T)$ around μ_T , allows describing the long-term expected metabolic rates $E(g)$ as a function of temperature. The upscaled relation captures the effects of the thermal averages and variability of the long-term experiment (colored lines) as well as the nonlinearity of $g_p(T)$ (black curve). (f) The upscaled relation is used to generate predictions of $E(g)$ at the μ_T for constant and fluctuating scenarios of the long-term experiment (continued versus dotted black-line). Green and yellow areas indicate positive and negative fluctuation effects. (g) The correlation between the fluctuations' observed impact on $E(G)$ and the predicted impact on $E(g)$ is assessed. The color-coding in g captures thermal averages in a.

Materials and methods

Our study organism is the marine filter feeder *Mytilus edulis trossulus* (Stuckas *et al.* 2017), a keystone species complex dominating the Baltic Sea's mussel beds (Larson *et al.* 2017). The genus *Mytilus* has a worldwide distribution, and its various species are known as ecosystem engineers creating mussel beds in the sub- and intertidal habitats of temperate- and cold-water ecosystems (Seed & Suchanek 1992; Zippay & Helmuth 2012).

Long-term (5-weeks) experiment

400 *Mytilus* spp. specimens with shell-lengths of 2.5 ± 0.2 mm were collected in 0.5 m water depth from a hard-bottom area (50 m²) in Western Baltic Sea (Kiel Fjord), Kiel, Germany (54.4330891, 10.1711679) on September 22, 2018, at water temperatures of ca. 16 °C. A subsample of 30 specimens was randomly selected and frozen to present the mussel's initial size characteristics. From the remaining mussels, batches of ten randomly selected individuals (hereafter, *group*) were placed inside a rigid mesh bag (1 mm² pore size, ca. 10 cm³ volume) distributed among 36 containers (2 L). Mussels were exposed to laboratory and container conditions (at 18.5 °C) for three days. Three of the containers were placed inside each of the twelve computer-controlled Kiel Indoor Benthocosms (Pansch & Hiebenthal 2019). Mussels were exposed to the different average temperature treatments (18.5, 21.0, 23.5, and 26.0 °C) by gradual (linear) warming of 2.5 °C day⁻¹ until the target temperature was reached. Over the five next weeks, mussels experienced twelve temperature scenarios, including three daily fluctuation amplitudes ($\pm 0, 2, \text{ and } 4$ °C) around four thermal averages (18.5, 21.0, 23.5, and 26.0 °C).

Our nested experimental design is schematically described in Fig. S2 in Supporting Information (for details on the partitioning of variance in a nested design, refer to Schielzeth & Nakagawa 2013). Fluctuations were imposed as sinusoidal waves around constant averages to prevent possible confounding effects of unbalanced sequences of thermal exposures. Therefore, the treatments represent a simplified version of natural daily thermal cycles, which generally express higher stochasticity levels. The logged experimental temperatures are plotted in Fig. S3. The average temperatures applied in this study represent daily-average temperatures for the maximum climatology (18.5 °C) (Pansch *et al.* 2018), current or near-future heatwaves (21 and 23.5 °C), and a heatwave expected by the end of the 21st century during summer in the study region (26 °C) (see Gräwe *et al.* 2013). The daily fluctuation amplitudes ($\pm 0, 2, \text{ and } 4$ °C) used in this study represent conditions experienced by mussel populations at depths of 0.5–2.5 m in

the non-tidal western Baltic Sea where the daily thermal change can be 3–6 °C regularly and as high as 8 °C occasionally during the warm season (Pansch & Hiebenthal 2019; Franz *et al.* 2020). Notably, the treatment levels were likely to impose benign to critical temperatures since it was recently showed that the species could initiate suppression of metabolic performance at 23–25 °C when exposed to a 24 h fluctuation ranging from 18 to 27 °C (Vajedsamiei *et al.* 2021).

During the experiment, mussels were fed a continuous-flux of filtered (0.5 µm) seawater enriched with phytoplankton (*Rhodomonas salina*) at a flow of ca. 3.5 mL min⁻¹, from an independent source container (18 L). The positioning of the mesh bags and aeration mixing the food was kept equal between all containers and water baths. Nonetheless, mussel groups were redistributed between the three 2-L containers in each water bath every three days. The cryptophyte *R. salina* was cultured at 16 °C and Kiel Fjord salinities by the Kiel Marine Organism Culture Centre at GEOMAR, KIMOCC. The food concentration in the source and experimental containers was measured every five days using a Cell and Particle Counter (Coulter Z2, Beckman Coulter GmbH, Krefeld, Germany) for the cell concentration (cells mL⁻¹; data are presented in Fig. S4). The Coulter Counter was set to detect particles of 5–8 µm diameter, the typical *R. salina* dimensional range. Food concentrations allowing optimal filtration activity of *Mytilus* specimens (i.e., ca. 1000–7000 *R. salina* cells mL⁻¹; Riisgård *et al.* 2006) were maintained throughout the assessments.

At the end of the experiment, study specimens were kept in 0.5 µm-filtered seawater at 18.5 °C over three days to release remaining feces, so feces-weight could not affect the mussel's dry tissue-weight. Afterward, the length of specimens was measured using a caliper, and their tissue was removed from the shell and dried at 80 °C for 24 h and weighted using an electronic scale (± 0.1 mg; Sartorius, Berlin, Germany).

The response variables shell-length (mm d⁻¹), mass growth, and tissue dry weight growth (both mg d⁻¹) were calculated as the fitness-related traits (Sebens *et al.* 2018). Each study specimen's final size was subtracted from the average initial size, and the difference was divided by the experiment's duration. Averages and 95 % confidence intervals of the responses to different treatments were plotted group-wise (Fig. S5).

The significance of the main and the interactive effects for fixed factors (thermal average and fluctuation, crossed), and the effect of the random nested factor (i.e., group), were tested using Generalized Additive Mixed-effect Models (GAMM). The random (group) effects were negligible (for all three response variables, p-value > 0.3). Thus, responses to each treatment

combination were pooled over groups. The fixed-effect GAM performance was checked compared to more complex mixed-effect models based on AIC and adjusted R-squared and was found comparable. The average response was also compared between fluctuation levels (at each thermal average) using one-way ANOVA followed by post-hoc Tukey-HSD tests. Analyses were done using the packages *mgcv* and *nmle* in R (R Core Team, 2019; see Script S1).

The simplest models (fixed-effect GAMs) were fitted to data using the package *pygam* and plotted in combination with sample averages and 95 % confidence intervals in Python (Python Software Foundation; see Scripts S2 and S3).

Short-term (one-day) assay

Mytilus spp. specimens were collected from a shallow-water environment in Kiel Fjord (54.44655, 10.34551) on November 20, 2018, at water temperatures of ca. 10 °C, kept at constant 16 °C for three weeks, and fed once per day with *R. salina* (KIMOCC) before the start of the assays. The short-term assay was composed of seven temporally repeated trials. During each trial, we recorded metabolic performance (feeding and aerobic respiration rates) of three different mussel specimens in response to a one-day temperature fluctuation using our recently developed Fluorometer- and Oximeter-equipped Flow-through Setup (FOFS; Vajedsamiei *et al.* 2021). Using FOFS, we recorded mussel-induced deviations in chlorophyll and dissolved oxygen concentrations while continuous fluxes of a phytoplankton suspension maintained optimal food-levels for mussel routine metabolic functioning (Vajedsamiei *et al.* 2021). The initial data processing was done based on the protocol described in Vajedsamiei *et al.* (2021). In short, we used robust regression techniques to remove the noise from the measured time series. The chlorophyll concentration measurement was time-lagged compared to the oxygen measurement because the chlorophyll sensor was positioned after the oximeter in each flow-through path of FOFS. The time lag was corrected through linear differential modeling. Finally, the feeding (filtration) and aerobic respiration rates were calculated based on the revised time series of measured variables.

In the short-term assay, mussels with a ca. 20 mm shell length were used, allowing us to record individual-mussel responses using FOFS. In each trial, minimum and maximum temperatures experienced by the mussels were ca. 16.8 and 30.5 °C, respectively, covering the whole thermal range experienced by the specimens in the long-term thermal growth experiment. The rate of linear change over the warming and cooling phases was ± 1.17 °C h⁻¹, and the times of minimum

and maximum temperatures were reached at 5:00 and 17:00, respectively (Fig. S6 temperature axes).

The time series of each response variable (see averages with 95 % confidence intervals in Fig. S6) were split into the warming- and cooling-phase series, based on the time intervals 5:30–16:30 and 17:30–4:30, respectively, in the trials. We merged replicated series of each phase and described thermal metabolic response curves by the polynomial model $g_p(T)$ with temperature T as the predictor variable, and (ii) by GAM in Python (see Script S4). The order of the best-fit polynomial model ($i \leq 10$) was selected based on the Bayesian Information Criterion (BIC), and the best-fit GAM was chosen from 700 models using a grid-search over many multiple regularization parameters and knots (4 to 10) seeking for the lowest Generalized Cross-Validation (GCV) score (Wood 2017). The GAMs were only used to visually check the goodness of the fit of polynomials, since GAMs, in general, use the benefit of its spline basis expansion and the regularization (Wood 2017).

Predicting long-term metabolic rates by upscaling

To predict long-term-expected feeding or respiration rates $E(g)$ with the assumption of a lack of time-dependent effects (here, a lack of acclimation or stress; Fig. 1), we upscaled the polynomial curve of the short-term assay's warming phase, which represented the non-acclimated thermal feeding and respiration responses. Upscaled curves were used to predict $E(g)$ as a function of thermal average and fluctuation scenarios of the 5-weeks experiment.

Upscaled thermal metabolic response curves describing $E(g)$ as a function of thermal averages at fluctuating conditions are defined by taking the expectation of the i^{th} -order Taylor expansion of the i^{th} -order polynomial function around the predictor average (i.e., a type of *delta method for bias correction*; see Oehlert 1992; Ver Hoef 2012). The analytical procedure was done in Python (Script S4). The mathematical derivation starts with rewriting of the polynomial function, $g_p(T)$, as its Taylor Series expanded at the average temperature μ_T ,

$$\text{Equation 1 } g(T) \cong g_p(\mu_T) + \frac{\partial g_p}{\partial T}(T - \mu_T) + \frac{1}{2!} \frac{\partial^2 g_p}{\partial T^2}(T - \mu_T)^2 + \dots + \frac{1}{n!} \frac{\partial^n g_p}{\partial T^n}(T - \mu_T)^n,$$

where $\frac{\partial^i g_p}{\partial T^i}$ shows the i^{th} derivative of the original polynomial function evaluated at $T=\mu_T$. Then, the average (or expected) metabolic response as a function of the temperature, $E(g(T))$, can be estimated (Equations 2).

$$\text{Equation 2 } E(g(T)) \cong E(g_p(\mu_T)) + E\left(\frac{\partial g_p}{\partial T}(T - \mu_T)\right) + E\left(\frac{1}{2!} \frac{\partial^2 g_p}{\partial T^2}(T - \mu_T)^2\right) + \dots + E\left(\frac{1}{n!} \frac{\partial^n g_p}{\partial T^n}(T - \mu_T)^n\right)$$

The expected values of the derivatives at the average temperatures are the derivatives themselves, and they can thus be pulled out of the expected value calculation (Equation 3).

$$\text{Equation 3 } E(g(T)) \cong g_p(\mu_T) + \frac{\partial g_p}{\partial T} E(T - \mu_T) + \frac{1}{2!} \frac{\partial^2 g_p}{\partial T^2} E(T - \mu_T)^2 + \dots + \frac{1}{n!} \frac{\partial^n g_p}{\partial T^n} E(T - \mu_T)^n$$

In Equation 3, $E(t - \mu_T)^i$ represents the i^{th} central moment of the temperature probability distribution. The central moments describe the probability distribution of the temperature fluctuations applied in the long-term experiment. Generally, central moments describe the variability structure of data sets with respect to the μ_T , presenting dispersion statistics like the variance, skewness, and Kurtosis (Zwillinger & Kokoska 2000). We calculated the first ten central moments of the temperature data sets from our long-term experiment (see Script S2) and considered all existing derivatives of each polynomial function to achieve close-to-exact approximations (see Script S4).

Relating observed impacts on growth with upscaling-predicted impacts

The observed 5-weeks growth rate and the upscaling-predicted feeding and respiration rates were normalized considering their minimum and maximum values (min-max-scaled) under the constant-treatments 18.5–26 °C as 0 and 100, respectively (see Script S5). The relationship between the observed impact of fluctuations on growth and their upscaling-predicted impact on metabolic responses across thermal averages was tested based on Pearson's correlation coefficient (see Script S5). The correlation analysis was only done for the ± 4 °C treatment scenario since this fluctuation amplitude significantly impacted mussel's growth traits.

Results

Impacts of thermal averages and daily fluctuations on mussel growth during the long-term experiment

The GAMMs showed that, for all growth traits measured, the main effect of fluctuations was statistically not significant (p-values > 0.05), while the main effect of thermal average and the

interactive effect of thermal average and fluctuation were statistically significant (p -values < 0.05 ; Table S1). Besides, ANOVA and subsequent Tukey HSD tests (Table S2) indicated that the average response to temperature was significantly different (p -values < 0.05) between the two fluctuation amplitudes ± 0 and 4 °C, both at 23.5 and 26 °C thermal averages for all growth traits and between $\pm 0, 2$ and 4 °C at 26 °C for tissue growth only.

The resulting thermal performance curves, describing rates of growth traits as functions of the thermal average, differed substantially between fluctuation regimes, particularly so at ± 4 °C compared to treatments with ± 2 °C fluctuation amplitude (Fig. 2a–c; Table S1). The GAMs predicted decreases in growth traits for thermal averages between 20.5 and 25.5 °C at the highest amplitude (± 4 °C) compared to the static conditions (Fig. 2a–c). In contrast, we find that the growth increases in the fluctuating treatment compared to the static treatment at thermal averages beyond 25.5 °C (Fig. 2a–c).

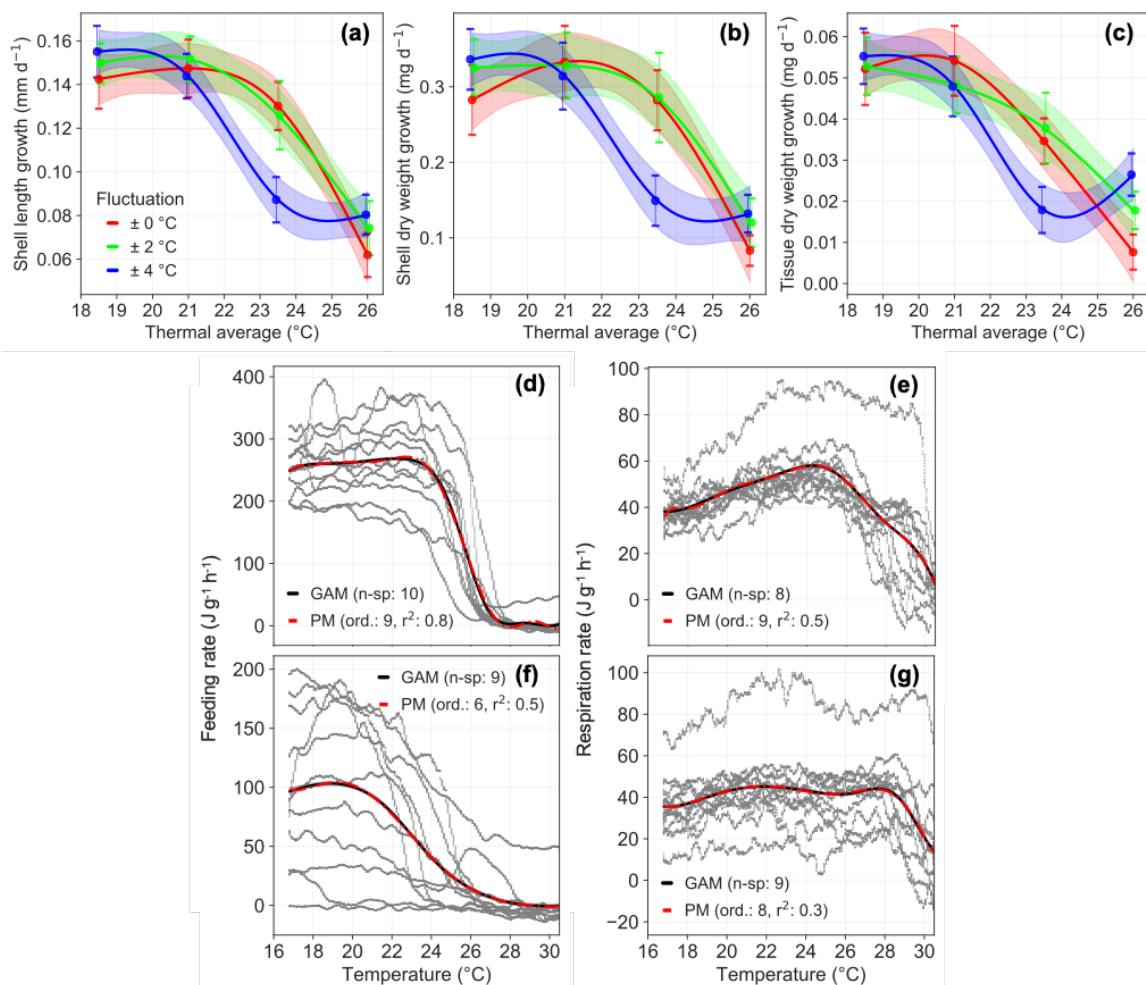


Figure 2 Thermal performance curves. (a–c) Thermal growth curves as retrieved from the long-term experiment. Generalized Additive Models (shaded areas represent 95% CIs) were fitted to data on variation in growth traits of mussel shell length (a) and shell and tissue dry weights (b and c) in 12 temperature scenarios (four average temperatures of 18.5 , 21.0 , 23.5 and 26.0 °C with 3 diurnal fluctuation amplitudes of ± 0 , 2 , and 4 °C). Sample averages with 95 % CIs are shown as dots and whiskers. (d–g) Thermal metabolic response curves as retrieved

from the short-term assay. Thermal variation in rates of metabolic processes (feeding and respiration) during the warming- (d and e) or cooling-phase (f and g) of a diurnal fluctuation were described by the best-fit polynomial function (red dashed lines, order 6 to 9) and by Generalized Additive Models (GAMs; black lines; the number of splines 8 to 10). The best-fit GAMs were used to check the goodness of the fit of Polynomials visually. Gray lines indicate experimental data (n = 11).

Metabolic performance during the short-term fluctuation assay

The best-fit polynomial functions describing thermal metabolic responses (feeding and respiration) over the warming and cooling phases of the one-day-long thermal fluctuation of the short-term assay are presented in Fig. 2d–g. In general, mussels suppressed their activities when exposed to high thermal extremes during the warming phase (Fig. 2d and e) while recovering during the subsequent cooling phase (Figs S6 and 2f and g). The average feeding rate of mussels initially only slightly increased during the warming phase (Fig. 2d). Beyond ca. 23°C, a steep decrease of the feeding rate could be observed, followed by a complete shutdown at 27 °C. During the subsequent cooling phase, mussels gradually increased feeding rates; however, only to a maximum level of ca. 40 % of the initial rate (Fig. 2f). Respiration rate increased stronger during the warming interval and decreased from ca. 25 °C onwards down to nearly zero (Fig. 2e). However, respiration increased again during the subsequent cooling phase and recovered to the initial rate (Fig. 2g).

Upscaling-predicted impacts of fluctuations on feeding and respiration

Predicted rates of feeding and respiration for a hypothetical long-term fluctuation regime with the same characteristics as our long-term experiment are presented as min-max-scaled values in Figure 3a and b (also see Fig. S7 for the responses in $J g^{-1} h^{-1}$), together with the measured shell length growth patterns obtained from our 5-week experiment (Fig. 3c, see Fig. 2a). In the treatments with daily fluctuations (± 2 and 4 °C), upscaling of the short-term performance predicts feeding and respiration rates to reach maximum values at lower average temperatures (Fig. 3a and b) compared to the constant treatment, which is similar to the pattern observed for shell length growth (Fig. 3c). At the average temperatures 21, 23.5, and 26 °C, the long-term impacts of the ± 4 °C fluctuations on feeding rates predicted from upscaling were comparable to the impact of fluctuations on the 5-week integrated length growth observed in the long-term experiment (indicated by black arrows in Fig. 3a and c). The decrease of feeding and growth for higher average temperatures is slower in the ± 4 °C treatment compared to the constant (± 0 °C) treatment and finally results in relatively higher rates of length growth and feeding at thermal averages beyond 25.5 °C. For the respiration rate, upscaling predicts decreasing effects

of fluctuations for thermal averages of 21–26 °C, with the maximum decreases at ca. 24–26 °C (Fig. 3b).

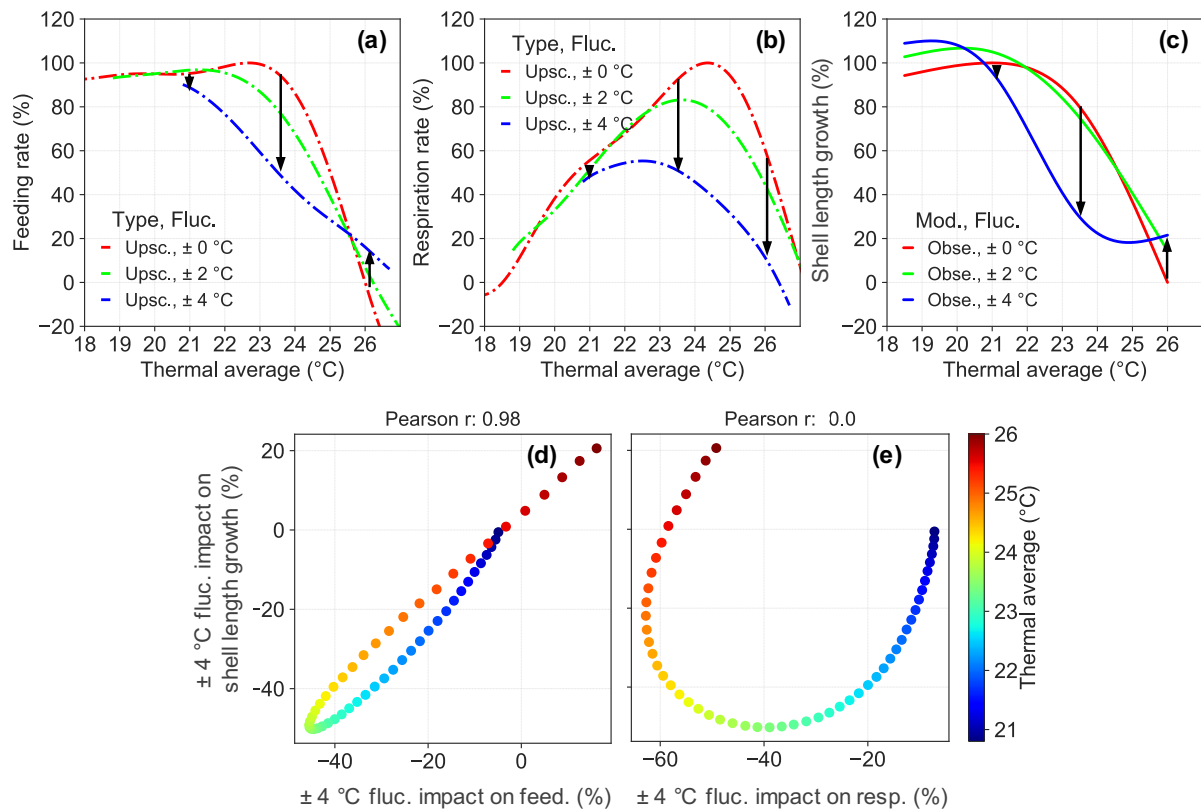


Figure 3 Effects of fluctuations on scaled metabolic rates (predicted) and growth traits (observed) at different thermal averages. (a–b) The upscaled thermal metabolic response relations obtained in the short-term assay were used to predict long-term expected rates of metabolic processes (feeding and respiration) at different average temperatures in response to the three scenarios of daily fluctuations of the long-term experiment. Predictions were min-max scaled, considering the minimum and maximum values of the constant treatment predictions. (c) Min-max scaled shell length growth from the long-term experiment (see Fig. 4a). Arrows indicate the consequences of ± 4 °C fluctuations around the average temperatures of 21, 23.5, and 26 °C. (d–e) The impact of large-amplitude (± 4 °C) fluctuations on growth as observed in the long-term experiment is correlated against the upscaling-predicted impact of fluctuations on the long-term-expected feeding and respiration rates obtained from the short-term assay.

Correlating observed and predicted impacts of thermal fluctuations

We find that for average temperatures of 21–26 °C, the impact of daily fluctuations (± 4 °C) on long-term-integrated growth rate is linearly correlated with the fluctuation impact on long-term-expected feeding rate predicted by upscaling. Pearson’s correlation coefficients for the shell length growth and the growth of shell and tissue dry weights were 0.98, 0.98, and 0.81, respectively (Figs 3d and S8). However, there were no or weak linear correlations for the respiration rate (Pearson’s correlation coefficients: 0, -0.03, and -0.46, respectively; Figs 3e and S8).

Discussion

At critically high summer thermal averages, fluctuations may be beneficial to the long-term performance of marine ectotherms

Using the blue mussel (*Mytilus* spp.) as a globally important benthic species, we provide supporting evidence to the hypothesis that short-term fluctuations can alleviate the longer-term impacts of critically high average temperatures on an ectothermic organism. In our long-term experiment, we found that, compared to colder averages, mussel growth was substantially lowered by static exposure to 26 °C, representing thermal average of end-of-century summer heatwaves (Gräwe *et al.* 2013). Large-amplitude fluctuations, however, enabled mussels to improve their growth traits at an average temperature of 26 °C, while the benefit of intermediate amplitude fluctuations was minor. In contrast, mussel growth traits were only marginally affected by the static exposure to 23.5 °C, representing conditions found during current or near-future marine heatwaves in the Western Baltic Sea (Pansch *et al.* 2018; Holbrook *et al.* 2019). At an average of 23.5 °C, large-amplitude fluctuations substantially decreased mussel growth while intermediate amplitude fluctuations had a minor effect. Therefore, in general, both average and amplitude of fluctuations were significant for long-term mussel growth, corroborating previous empirical findings for other ectotherms (Siddiqui *et al.* 1973; Bozinovic *et al.* 2011; Niehaus *et al.* 2012; Cavieres *et al.* 2018).

Shallow coastal waters of the Baltic Sea (depth ca. 0.5–2.5 m) experience minimal tidal water-level changes. Daily variation in seawater temperature can be 3–6 °C regularly and as high as 8 °C occasionally during down- and upwelling events (Pansch & Hiebenthal 2019; Franz *et al.* 2020). Even more intense fluctuations in the body temperature can be observed at the lower distribution ranges of *Mytilus* spp. along the Atlantic coast, especially where specimens experience aerial exposure during low tides (Helmuth *et al.* 2014). Therefore, in these habitats, daily fluctuations are likely influencing mussel growth and may mainly do so in a warming climate.

A large body of literature shows observed/predicted detrimental effects of thermal fluctuations on organisms' long-term performance (Paaijmans *et al.* 2013; Vasseur *et al.* 2014; Bernhardt *et al.* 2018). However, most of these studies have restricted their investigations to maximum temperatures only slightly beyond the thermal optimum, which is a necessary restriction when organisms are exposed to beyond-optimal and constant temperatures for a long time. Yet, alternative observations/projections may be equally true if organisms are subjected to more realistic fluctuating treatment conditions representative of the natural environment, allowing

the recovery at fluctuations' benign phases (Schulte 2011; Wahl *et al.* 2015), as some first empirical observations suggest (Bozinovic *et al.* 2011; Niehaus *et al.* 2012; Kingsolver *et al.* 2015; Kang *et al.* 2019).

Metabolic suppression and recovery and the potential benefits and costs during daily thermal cycles

Our studied mussels expressed suppression and recovery of feeding and respiration in response to a one-day thermal fluctuation between 16.8–30.5 °C while submerged. This daily thermal oscillation of feeding and respiration rates has not been recorded previously for any other bivalve species to the best of our knowledge. The mussels initiated feeding suppression followed by aerobic respiration suppression at about 23–25 °C. Similar thermal thresholds were recently reported for the same species exposed to a one-day fluctuation ranging from 18 to 27 °C (Vajedsamiei *et al.*, 2021). During hours-long exposures to temperatures of 10 to 20 °C, *Mytilus* respiration was shown to be more temperature-dependent (Q_{10} of 2.1–2.5; Widdows 1976) than filtration (Q_{10} of 1.25), the latter being driven mostly by the thermal change in viscosity of the surrounding solution (Kittner & Riisgård 2005). A lower thermal dependence of filtration than respiration was also evident over the temperature range of 17–23 °C applied during the warming phase of our short-term assay. This low thermal dependency of filtration might have partly helped mussels to control the ATP and oxygen demands of feeding and the associated energetic costs for digestion (i.e., typically ca. 20 % of the total mussel metabolic energy expenditure; Widdows & Hawkins 1989) when the total metabolic energy demand was rising sharply due to increasing temperature. However, above a critical temperature threshold, feeding activities might have become too costly due to limiting supply capacity. Filtration suppression poses a likely mechanism to decrease ATP and oxygen demand, enabling prolonged reserve use (Pörtner 2012; Verberk *et al.* 2016).

Mussels substantially suppressed their aerobic respiration rates, possibly to further reduce demand. Hypoxia-tolerant species, including *Mytilus* spp., can temporally shift to anaerobic metabolism and more efficient anaerobic pathways, which yields less energy but enhances their resistance against a thermodynamic collapse of cellular processes during hypoxic or hyperthermic events, especially when exposed to air in intertidal habitats (Gracey & Connor 2016). Eventually, the colder phase of the cycle in the short-term assay could have provided an opportunity to reduce the concentration of accumulated anaerobic end products (*oxygen debt*, Ellington 1983), a process potentially impossible in a static thermal scenario. In this recovery

phase, mussels expressed high respiration in parallel to a partially recovered feeding activity, with the latter being likely due to the accumulated oxygen debt's energy requirements.

Upscaling from short-term thermal feeding responses may predict longer-term fluctuation impacts

Upscaling from the short-term (non-acclimated) thermal feeding response assay well predicts the observed 5-weeks integrated impact of large-amplitude daily fluctuations on mussel growth. This significant correlation suggests that fluctuations-mediated feeding suppression and recovery could lead to declined growth at the less extreme average conditions and improved growth at the critical average condition. In contrast, short-term (non-acclimated) thermal respiration responses did not predict the long-term fluctuation impact on growth. Notably, the respiration rate was predicted to be lower in the fluctuating compared to the static regime at the average condition of 26 °C, while the observed growth rate was higher in the fluctuating regime. Considering a high energy cost of growth (i.e., ca. 32 % of the energy stored as new tissue in mussels or 34 % of the total energy used by actively ingesting mussels; Widdows & Hawkins 1989; Clarke 2020), the higher growth should have been accompanied by a higher respiration rate to satisfy the ATP demand for growth processes (e.g., cell division costs, protein biosynthesis costs). In general, short-term (unacclimated) thermal respiration responses may not accurately represent long-term-expected respiration rates at beyond-optimal temperatures due to acclimation or stress effects (Semsar-Kazerouni & Verberk 2018).

The thermal growth response curve established through 5-weeks constant exposures fairly resembled the thermal feeding response curve from the short-term assay, considering the optimal thermal thresholds and relative temperature-induced changes in two responses. Overall, these findings suggest that feeding responses to short-term thermal changes may well represent the long-term performance responses of ectotherms to various thermal fluctuation regimes, at least in the absence of time-dependent effects. Therefore, when available, these unacclimated thermal feeding responses may be more appropriate than respiration data to be used for parametrizing the temperature correction coefficient in energy-budget modelling (e.g., DEB modeling; Kooijman 2010) for ectotherms expressing remarkable metabolic suppression and recovery (Monaco & McQuaid 2018).

A framework indicating how thermal fluctuations may provide a refuge for ectotherms

In general, characteristics of thermal fluctuations, such as the rate, duration, and time of occurrence, as well as an ectotherm's functional traits, are essential factors defining how its metabolic performance may change during exposure to a constant or a fluctuating thermal regime (Terblanche *et al.* 2007; Bozinovic *et al.* 2013; Kingsolver *et al.* 2016; Semsar-Kazerouni & Verberk 2018). This wide variety of influential factors may explain why empirical studies have sometimes obtained contrasting results regarding the long-term effects of thermal fluctuations at various thermal averages or in different ecological contexts (Siddiqui *et al.* 1973; Bozinovic *et al.* 2011; Niehaus *et al.* 2012).

We propose a simple framework that may explain this context-dependency based on possible scenarios of acclimation- or stress-induced changes in an ectotherm's capacity for thermal metabolic performance. In a simple model, such plasticity would manifest as horizontal shifts of the thermal performance curve (TPC), defining the instant response to temperatures. When an individual is exposed to beyond-optimal conditions, whether constant or fluctuating, its capacity for thermal metabolic performance may remain constant or change due to acclimation or accumulation of stress (Precht 1958; Terblanche *et al.* 2007; Fischer *et al.* 2010; Kingsolver *et al.* 2016; Havird *et al.* 2020). This translates into either an unchanged TPC, a right-shifted TPC, or a left-shifted TPC, respectively (Fig. 4a–c). Our framework acknowledges the general possibility that such shifts could occur independently for static beyond-optimal conditions and fluctuating beyond-optimal conditions with the same average. Upscaling these three TPCs for beyond-optimal constant conditions predicts three long-term performance expectations (black curves in Fig. 4d–f). A similar upscaling predicts the three different performance expectations for beyond-optimal fluctuating conditions (dashed-blue curves in Fig. 4d–f). Assuming their independence, this gives rise to nine possible combinations of long-term performance responses to thermal averages under static versus fluctuating regimes (Fig. 4g–o). The correlation between thermal fluctuation effects on long-term growth and feeding rates allows us to generalize these predictions to the long-term performance responses. Note that we assume logit TPCs in this model by omitting the passive thermal dependence of (or thermodynamic effects on) metabolic rate (Schulte 2011). For simplicity, the acclimation- or stress-induced change in the performance was considered only as changes in the curve's turning points and not their maximum or slope.

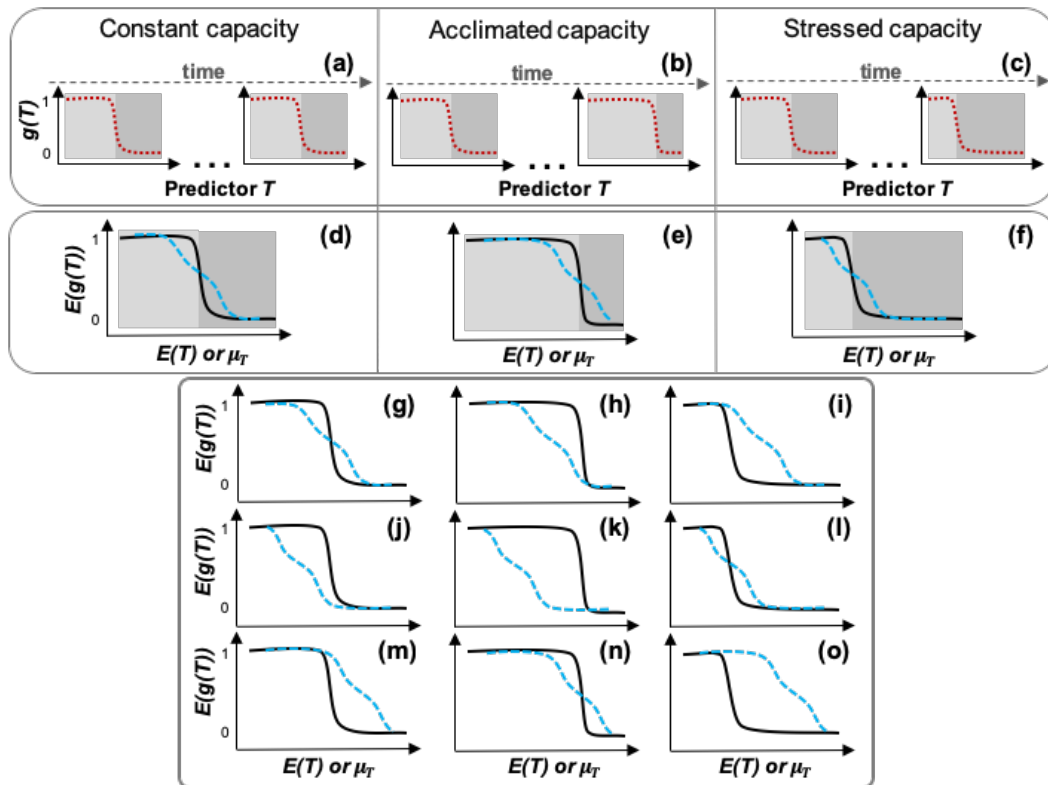


Figure 4 Mechanistic framework to understand the impact of fluctuations on ectotherms from highly fluctuating environments. (a–c, upper box) An organism’s initial capacity for thermal metabolic performance (dotted red curves in left-side subplots) can remain constant or change over time by acclimation or stress accumulation during exposure to beyond-optimal thermal conditions. These scenarios can be simply represented as unchanged thermal performance curve (TPC), a right-shifted TPC, or a left-shifted TPC, respectively (dotted red curves in right-side subplots). The grey shading separates the *Arrhenius* thermal interval (where Q_{10} effects may cause gradual changes) from the critical interval where heat-driven inactivation of metabolic performance occurs (Schoolfield *et al.* 1981). (d–f, middle box) Based on the three possible TPCs, via nonlinear averaging, we can predict three general patterns of long-term-expected metabolic responses $E(g)$ to thermal averages under constant (black curves) or fluctuating regimes (dashed blue curves). (g–o, lower box) As acclimation to constant conditions may, in theory, be independent of acclimation to fluctuating conditions, we can predict nine hypothetical combinations explaining that thermal fluctuations may be detrimental or beneficial for an ectotherm, depending on the context.

Fluctuations’ beneficial effects are predicted in six out of nine hypothetical scenarios of the framework (Fig. 4g, h, k, m–o), suggesting that the refuge effect of thermal fluctuations may indeed be a general pattern. A static exposure to extreme thermal conditions may stretch an organism’s metabolic performance up to a level that initiates stress accumulation or prevents warm acclimation. Alternatively, the counterpart fluctuating regime with the same average as the static regime may provide a refuge if the duration and intensity of beyond-optimal exposures do not negatively impact the organism’s capacity for elastic suppression and recovery of metabolic performance. In such conditions, thermal fluctuations may cause alternations between (i) phases of tolerance at high temperatures when the organism minimizes stress by matching the metabolic supply and demand at low levels, and (ii) phases of recovery at lower temperatures when the organism enhances the performance to recover from metabolic debt,

such as the oxygen debt and cellular heat damages experienced at high temperatures, and to refuel development, growth, and reproduction.

Empirical evidence suggests that the capacity for acclimation to extremely warm conditions is limited for organisms living close to their critical thermal thresholds, particularly those from highly fluctuating environments (Stillman 2003; Somero 2010; Seebacher *et al.* 2014). Our framework shows that even for these organisms that lack strong acclimation capacity, fluctuations may still be beneficial (Fig. 4g and k). Notably, with ongoing climate change, extreme events are being intensified and elongated in many coastal and shallow-water regions (Holbrook *et al.* 2019), possibly increasing the relevance of this refuge effect provided by fluctuations.

Perspectives and conclusion

Predictions based on nonlinear averaging of fluctuation impacts neglect time-dependent changes of TPCs. Therefore, these predictions can only be used as ecological null-models (Estay *et al.* 2014; Dowd *et al.* 2015; Koussoroplis *et al.* 2019). For ectotherms adapted to highly fluctuating regimes, nonlinear averaging on TPCs of feeding rate generated at timescales (e.g., hours) that relate to short-term (e.g., daily) thermal fluctuations may better predict the effect of beyond-optimal fluctuations compared to TPCs established through longer-term but static exposures.

To mechanistically explain the long-term impacts of temperature fluctuations, it is essential to shift from studies applying static treatments to those that include natural system dynamics. Our hybrid approach of long-term and short-term assessments is the first step towards the long-term recording of metabolic performance during dynamic thermal regimes.

Our study describes how temperature fluctuations inducing metabolic suppression and recovery may decrease or enhance fitness depending on the fluctuations' average and amplitude. More studies are needed to describe various realized scenarios of within- and between-generational plasticity in species' capacity for thermal metabolic suppression and recovery to better understand the ecological impacts of temperature fluctuations in a warming ocean.

Acknowledgments

The authors would like to acknowledge Claas Hiebenthal, KIMOCC, and Ulrike Panknin for providing the *Rhodomonas* culture and technical assistance.

This work and J.V. were funded through the Deutsche Forschungsgemeinschaft (DFG) project: The neglected role of environmental fluctuations as a modulator of stress and driver of rapid evolution (Grant Number: PA 2643/2/348431475) and through GEOMAR. The project was supported by the Cluster of Excellence “The Future Ocean”, funded within the framework of the Excellence Initiative by the DFG on behalf of the German federal and state governments. C.P. was funded by the postdoc program of the Helmholtz- Gemeinschaft Deutscher Forschungszentren and by GEOMAR.

References

- Angilletta, M.J. (2006). Estimating and comparing thermal performance curves. *J. Therm. Biol.*, 31, 541–545.
- Bernhardt, J.R., Sunday, J.M., Thompson, P.L. & O’Connor, M.I. (2018). Nonlinear averaging of thermal experience predicts population growth rates in a thermally variable environment. *Proc. R. Soc. B Biol. Sci.*, 285, 20181076.
- Boyd, P.W., Cornwall, C.E., Davison, A., Doney, S.C., Fourquez, M., Hurd, C.L., *et al.* (2016). Biological responses to environmental heterogeneity under future ocean conditions. *Glob. Chang. Biol.*, 22, 2633–2650.
- Bozinovic, F., Bastías, D.A., Boher, F., Clavijo-Baquet, S., Estay, S.A. & Angilletta, M.J. (2011). The Mean and Variance of Environmental Temperature Interact to Determine Physiological Tolerance and Fitness. *Physiol. Biochem. Zool.*, 84, 543–552.
- Bozinovic, F., Catalan, T.P., Estay, S.A. & Sabat, P. (2013). Acclimation to daily thermal variability drives the metabolic performance curve. *Evol. Ecol. Res.*, 15, 579–587.
- Cavieres, G., Bogdanovich, J.M., Toledo, P. & Bozinovic, F. (2018). Fluctuating thermal environments and time-dependent effects on fruit fly egg-hatching performance. *Ecol. Evol.*, 8, 7014–7021.
- Chesson, P., Donahue, M.J., Melbourne, B. & Sears, A.L. (2005). Scale transition theory for understanding mechanisms in metacommunities. In: (*Metacommunities: dynamics and ecological communities.*), {[ed(s).] [Holoyak, M., Leibold, M. A. & Holt, R. D.]} . Wiley, Chicago, Illinois, USA. pp. (279–306).
- Choi, F., Gouhier, T., Lima, F., Rilov, G., Seabra, R. & Helmuth, B. (2019). Mapping physiology: biophysical mechanisms define scales of climate change impacts. *Conserv. Physiol.*, 7, 1–18.

- Clarke, A. (2019). Energy Flow in Growth and Production. *Trends Ecol. Evol.*, 34, 502–509.
- Denny, M. (2019). Performance in a variable world: using Jensen’s inequality to scale up from individuals to populations. *Conserv. Physiol.*, 7, 1–11.
- Denny, M. & Benedetti-Cecchi, L. (2012). Scaling Up in Ecology: Mechanistic approaches. *Annu. Rev. Ecol. Evol. Syst.*, 43, 1–22.
- Deutsch, C.A., Tewksbury, J.J., Huey, R.B., Sheldon, K.S., Ghalambor, C.K., Haak, D.C., *et al.* (2008). Impacts of climate warming on terrestrial ectotherms across latitude. *Proc. Natl. Acad. Sci.*, 105, 6668–6672.
- Dowd, W.W., King, F.A. & Denny, M.W. (2015). Thermal variation, thermal extremes and the physiological performance of individuals. *J. Exp. Biol.*, 218, 1956–1967.
- Ellington, W.R. (1983). The recovery from anaerobic metabolism in invertebrates. *J. Exp. Zool.*, 228, 431–444.
- Estay, S.A., Lima, M. & Bozinovic, F. (2014). The role of temperature variability on insect performance and population dynamics in a warming world. *Oikos*, 123, 131–140.
- Falfushynska, H.I., Sokolov, E., Piontkivska, H. & Sokolova, I.M. (2020). The role of reversible protein phosphorylation in regulation of the mitochondrial electron transport system during hypoxia and reoxygenation stress in marine bivalves. *Front. Mar. Sci.*, 7, 467.
- Fischer, K., Dierks, A., Franke, K., Geister, T.L., Liszka, M., Winter, S., *et al.* (2010). Environmental effects on temperature stress resistance in the tropical butterfly *Bicyclus anynana*. *PLoS One*, 5.
- Franz, M., Lieberum, C., Bock, G. & Karez, R. (2019). Environmental parameters of shallow water habitats in the SW Baltic Sea. *Earth Syst. Sci. Data*, 11, 947–957.
- Gotelli, N. J. (2001). Research frontiers in null model analysis. *Glob. Ecol. Biogeogr.*, 10, 337–343.
- Gracey, A.Y. & Connor, K. (2016). Transcriptional and metabolomic characterization of spontaneous metabolic cycles in *Mytilus californianus* under subtidal conditions. *Mar. Genomics*, 30, 35–41.
- Gräwe, U., Friedland, R. & Burchard, H. (2013). The future of the western Baltic Sea: Two possible scenarios. *Ocean Dyn.*, 63, 901–921.
- Havird, J.C., Neuwald, J.L., Shah, A.A., Mauro, A., Marshall, C.A. & Ghalambor, C.K. (2020). Distinguishing between active plasticity due to thermal acclimation and passive plasticity due to Q10 effects: Why methodology matters. *Funct. Ecol.*, 34, 1015–1028.
- Helmuth, B., Russell, B.D., Connell, S.D., Dong, Y., Harley, C.D., Lima, F.P., *et al.* (2014). Beyond long-term averages: making biological sense of a rapidly changing world. *Clim. Chang. Responses*, 1, 6.
- Hobday, A.J., Alexander, L.V, Perkins, S.E., Smale, D.A., Straub, S.C., Oliver, E.C.J., *et al.* (2016). A hierarchical approach to defining marine heatwaves. *Prog. Oceanogr.*, 141, 227–238.

- Holbrook, N.J., Scannell, H.A., Sen Gupta, A., Benthuisen, J.A., Feng, M., Oliver, E.C.J., *et al.* (2019). A global assessment of marine heatwaves and their drivers. *Nat. Commun.*, 10, 1–13.
- Jensen, J.L. (1906). Sur les fonctions convexes et les inégalités entre les valeurs moyennes. *Acta Math.*, 30, 175–193.
- Jentsch, A., Kreyling J. & Beierkuhnlein C. (2007). A new generation of climate change experiments: events, not trends. *Front. Ecol. Environ.*, 5, 365–374.
- Kang, H.Y., Lee, Y.J., Song, W.Y., Kim, T.I., Lee, W.C., Kim, T.Y., *et al.* (2019). Physiological responses of the abalone *Haliotis discushannai* to daily and seasonal temperature variations. *Sci. Rep.*, 9, 1–13.
- Kingsolver, J.G., Higgins, J.K. & Augustine, K.E. (2015). Fluctuating temperatures and ectotherm growth: distinguishing nonlinear and time-dependent effects. *J. Exp. Biol.*, 218, 2218–2225.
- Kingsolver, J.G., MacLean, H.J., Goddin, S.B. & Augustine, K.E. (2016). Plasticity of upper thermal limits to acute and chronic temperature variation in *Manduca sexta* larvae. *J. Exp. Biol.*, 219, 1290–1294.
- Kittner, C. & Riisgård, H.U. (2005). Effect of temperature on filtration rate in the mussel *Mytilus edulis*: no evidence for temperature compensation, 305, 147–152.
- Kooijman, B. (2010). *Dynamic energy budget theory for metabolic organisation*, 3rd edn. University Press, Cambridge.
- Koussoroplis, A. M., Schälicke, S., Raatz, M., Bach, M. & Wacker, A. (2019). Feeding in the frequency domain: coarser-grained environments increase consumer sensitivity to resource variability, covariance and phase. *Ecol. Lett.* 22, 1104–1114.
- Koussoroplis, A.M., Pincebourde, S. & Wacker, A. (2017). Understanding and predicting physiological performance of organisms in fluctuating and multifactorial environments. *Ecol. Monogr.*, 87, 178–197.
- Larsson, J., Lind, E.E., Corell, H., Grahn, M., Smolarz, K. & Lönn, M. (2017). Regional genetic differentiation in the blue mussel from the Baltic Sea area. *Estuar. Coast. Shelf Sci.*, 195, 98–109.
- Lima, F.P. & Wethey, D.S. (2012). Three decades of high-resolution coastal sea surface temperatures reveal more than warming. *Nat. Commun.*, 3, 1–13.
- Martin, T.L. & Huey, R.B. (2008). Why “Suboptimal” Is Optimal: Jensen’s Inequality and Ectotherm Thermal Preferences. *Am. Nat.*, 171, E102–E118.
- Monaco, C.J. & McQuaid, C.D. (2018). Applicability of Dynamic Energy Budget (DEB) models across steep environmental gradients. *Sci. Rep.*, 8, 1–14.
- Niehaus, A.C., Angilletta, M.J., Sears, M.W., Franklin, C.E. & Wilson, R.S. (2012). Predicting the physiological performance of ectotherms in fluctuating thermal environments. *J. Exp. Biol.*, 215, 694–701.
- Oehlert, G. W. (1992). A Note on the Delta Method. *Am. Stat.*, 46, 27–29.

- Paaijmans, K.P., Heinig, R.L., Seliga, R.A., Blanford, J.I., Blanford, S., Murdock, C.C., *et al.* (2013). Temperature variation makes ectotherms more sensitive to climate change. *Glob. Chang. Biol.*, 19, 2373–2380.
- Pansch, C. & Hiebenthal, C. (2019). A new mesocosm system to study the effects of environmental variability on marine species and communities. *Limnol. Oceanogr. Methods*, 17, 145–162.
- Pansch, C., Scotti, M., Barboza, F.R., Al-Janabi, B., Brakel, J., Briski, E., *et al.* (2018). Heat waves and their significance for a temperate benthic community: A near-natural experimental approach. *Glob. Chang. Biol.*, 24, 4357–4367.
- Podrabsky, J.E. & Somero, G.N. (2004). Changes in gene expression associated with acclimation to constant temperatures and fluctuating daily temperatures in an annual killifish *Austrofundulus limnaeus*. *J. Exp. Biol.*, 207, 2237–2254.
- Pörtner H O. (2012). Integrating climate-related stressor effects on marine organisms: unifying principles linking molecule to ecosystem-level changes. *Mar. Ecol. Prog. Ser.*, 470, 273–290.
- Precht, H. (1958). Theory of temperature adaptation in cold-blooded animals. In: (*Physiological adaptation*), {[ed.] [Proser C. L.]}. American Physiological Society, Washington, DC, USA. pp. (50–78).
- Python Software Foundation. Python Language Reference, version 3.7.
- R Core Team (2019). R: A language and environment for statistical computing. R Foundation for Statistical Computing, Vienna, Austria.
- Rhein, M., Rintoul, S.R., Aoki, S., Campos, E., Chambers, D., Feely, R.A., *et al.* (2013): Observations: Ocean. In: (*Climate Change 2013: The Physical Science Basis. Contribution of Working Group I to the Fifth Assessment Report of the Intergovernmental Panel on Climate Change.*), {[ed(s)] [Stocker, T.F., Qin, D., Plattner, G.K., Tignor, M., Allen, S.K., Boschung, J., Nauels, A., Xia, Y., Bex, V. & Midgley, P.M.]}. Cambridge University Press, Cambridge, United Kingdom and New York, NY, USA.
- Riisgård, h.u., Lassen, j. & Kittner, c. (2006). Valve-gape response times in mussels (*Mytilus edulis*)—effects of laboratory preceding-feeding conditions and *in situ* tidally induced variation in phytoplankton biomass. *j. shellfish res.*, 25, 901–911.
- Ruel, J.J. & Ayres, M.P. (1999). Jensen’s inequality predicts effects of environmental variation. *Tree*, 5347, 361–366.
- Schielzeth, H. & Nakagawa, S. (2013). Nested by design: Model fitting and interpretation in a mixed model era. *Methods Ecol. Evol.*, 4, 14–24.
- Schoolfield, R. M., Sharpe, P. J. & Magnuson, C. E. (1981). Non-linear regression of biological temperature-dependent rate models based on absolute reaction-rate theory. *J. Theor. Biol.*, 88, 719–719.
- Schulte, P.M., Healy, T.M. & Fanguie, N.A. (2011). Thermal performance curves, phenotypic plasticity, and the time scales of temperature exposure. *Integr. Comp. Biol.*, 51, 691–702.

- Sebens, K.P., Sarà, G. & Carrington, E. (2018). Estimation of fitness from energetics and life-history data: An example using mussels. *Ecol. Evol.*, 8, 5279–5290.
- Seebacher, F., White, C.R. & Franklin, C.E. (2015). Physiological elasticity increases resilience of ectothermic animals to climate change. *Nat. Clim. Chang.*, 5, 61–66.
- Seed, R. & Suchanek, T. H. (1992). Population and community ecology of *Mytilus*. In: (*The mussel Mytilus: Ecology, Physiology, Genetics and Culture*), {[ed(s).] [Gosling, E.]} Elsevier Science, Amsterdam, pp. (87–169).
- Semsar-kazerouni, M. & Verberk, W.C.E.P. (2018). It's about time: Linkages between heat tolerance, thermal acclimation and metabolic rate at different temporal scales in the freshwater amphipod *Gammarus fossarum* Koch, 1836. *J. Therm. Biol.*, 75, 31–37.
- Siddiqui, W., Barlow, C., & Randolph, P. (1973). Effects of some constant and alternating temperatures on population growth of the pea aphid, *Acyrtosiphon pisum* (Homoptera: Aphididae). *Can. Entomol.*, 205, 145–156.
- Sinclair, B.J., Marshall, K.E., Sewell, M.A., Levesque, D.L., Willett, C.S., Slotsbo, S., *et al.* (2016). Can we predict ectotherm responses to climate change using thermal performance curves and body temperatures? *Ecol. Lett.*, 19, 1372–1385.
- Smale, D.A., Wernberg, T., Oliver, E.C.J., Thomsen, M., Harvey, B.P., Straub, S.C., *et al.* (2019). Marine heatwaves threaten global biodiversity and the provision of ecosystem services. *Nat. Clim. Chang.*, 9, 306–312.
- Sokolova, I.M. & Pörtner, H.O. (2003). Metabolic elasticity and critical temperatures for aerobic scope in a eurythermal marine invertebrate (*Littorina saxatilis*, Gastropoda: Littorinidae) from different latitudes. *J. Exp. Biol.*, 206, 195–207.
- Somero, G. N. (2010). The physiology of climate change: how potentials for acclimatization and genetic adaptation will determine “winners” and “losers.” *J. Exp. Biol.*, 213, 912–920.
- Stillman, J.H. (2003). Acclimation capacity underlies susceptibility to climate change. *Science*, 301, 65.
- Stuckas, H., Knöbel, L., Schade, H., Breusing, C., Hinrichsen, H.H., Bartel, M., *et al.* (2017). Combining hydrodynamic modelling with genetics: can passive larval drift shape the genetic structure of Baltic *Mytilus* populations? *Mol. Ecol.*, 26, 2765–2782.
- Sun, X., Ren, G., You, Q., Ren, Y., Xu, W., Xue, X., *et al.* (2019). Global diurnal temperature range (DTR) changes since 1901. *Clim. Dyn.*, 52, 3343–3356.
- Terblanche, J.S., Deere, J.A., Clusella-Trullas, S., Janion, C. & Chown, S.L. (2007). Critical thermal limits depend on methodological context. *Proc. R. Soc. B Biol. Sci.*, 274, 2935–2942.
- Vajedsamiei, J., Melzner, F., Raatz, M., Kiko, R., Khosravi, M. & Pansch, C. (2021) Simultaneous recording of filtration and respiration in marine organisms in response to short-term environmental variability. *Limnol. Oceanogr. Methods*.

- Vasseur, D.A., DeLong, J.P., Gilbert, B., Greig, H.S., Harley, C.D.G., McCann, K.S., *et al.* (2014). Increased temperature variation poses a greater risk to species than climate warming. *Proc. R. Soc. B Biol. Sci.*, 281, 20132612.
- Ver Hoef, J. M. (2012). Who invented the delta method? *Am. Stat.*, 66, 124–127.
- Verberk, W.C.E.P., Overgaard, J., Ern, R., Bayley, M., Wang, T., Boardman, L., *et al.* (2016). Does oxygen limit thermal tolerance in arthropods? A critical review of current evidence. *Comp. Biochem. Physiol. -Part A Mol. Integr. Physiol.*, 192, 64–78.
- Wahl, M., Buchholz, B., Winde, V., Golomb, D., Guy-Haim, T., Müller, J., *et al.* (2015). A mesocosm concept for the simulation of near-natural shallow underwater climates: The Kiel Outdoor Benthocosms (KOB). *Limnol. Oceanogr. Methods*, 13, 651–663.
- Wang, G. & Dillon, M.E. (2014). Recent geographic convergence in diurnal and annual temperature cycling flattens global thermal profiles. *Nat. Clim. Chang.*, 4, 988–992.
- Widdows, J. (1976). Physiological adaptation of *Mytilus edulis* to cyclic temperatures. *J. Comp. Physiol.*, 105, 115–128.
- Widdows, J. & Hawkins, A.J.S. (1989). Partitioning of rate of heat dissipation by *Mytilus edulis* into maintenance, feeding, and growth components. *Physiol. Zool.*, 62, 764–784.
- Wood, S. N. (2017). *Generalized Additive Models: An Introduction with R*, 2nd edn. Chapman & Hall/CRC.
- Zippay, M. L. & Helmuth, B. (2012). Effects of temperature change on mussel, *Mytilus*. *Integr. Zool.*, 7, 312–327.
- Zwillinger, D. & Kokoska, S. (2000). *CRC standard probability and statistics tables and formulae*. Chapman & Hall/CRC, Boca Raton.

Chapter 3: The higher the needs, the lower the tolerance: Extreme events may select ectotherm recruits with lower metabolic demand and heat sensitivity

Jahangir Vajedsamiei ¹, Martin Wahl ¹, Andrea Schmidt ¹, Maryam Yazdanpanahan ², Christian Pansch ³

¹ Department of Marine Ecology, GEOMAR Helmholtz Centre for Ocean Research Kiel, Germany

² Shahid Beheshti University, Tehran, Iran

³ Department of Environmental & Marine Biology, Åbo Akademi University, Turku, Finland

***Corresponding author:** address: GEOMAR Helmholtz Centre for Ocean Research Kiel, Düsternbrooker Weg 20, 24105 Kiel, Germany, telephone: +49 431 600 1598, e-mail: jahangir.vajedsamiei@gmail.com; jvajedsamiei@geomar.de

Data accessibility statement: Given the manuscript be accepted, the data supporting the results will be archived in PANGAEA the data DOI will be included at the end of the article.

Conflict of Interest: None declared.

Type of Paper: Brief research report article to *Frontiers in Marine Science*

Abstract

An adaptive trait of ectotherms living in highly fluctuating environments is the capacity to suppress and recover their metabolic performance over successive phases of stressful and benign environmental conditions. Potentially, intensified summer thermal regimes may result in individuals with lower demand for metabolic substrates mediating a higher heat tolerance in their responses to short-term (e.g., daily) thermal fluctuations. Using a globally important ectotherm, the blue mussel *Mytilus*, we evaluate this hypothesis that assumes the lower demand enables a more efficient control of thermodynamics stress caused by the mismatch between metabolic supply and demand at high critical temperatures. In a four-month incubation, mussels were grown from the juvenile stage or recruited and grown from larvae under current versus end-of-century extreme summer temperatures in a near-natural mesocosm system. Afterward, in short-term assays, mussel performance traits (feeding and respiration rates) were recorded in response to a mild temperature (20.8 °C) for six hours (baseline performance), followed by two 24 h fluctuation cycles (20.8–30.5 °C). The baseline performance represented the total supply of metabolic substrates to internal storage (except for oxygen) and the total metabolic demand, respectively, and were used for scaling the daily responses. We found no effect of thermal history on the metabolic performance of transplanted mussels. Recruitment of mussels was substantially (96.5 %) reduced in the future thermal history regime compared to the current one. Compared to recruits from the current regime, these potentially selected recruits were more capable of recovering their feeding and respiration rates in benign phases of daily temperature fluctuations and showed lower baseline respiration rates. Our findings support the hypotheses that (i) extremely warm events may select rare heat-tolerant individuals of marine ectotherms at their very early life stages, and (ii) lower metabolic demand is a mechanism for such higher heat tolerance. These propositions and whether such increases in stress tolerance can lead to rapid evolutionary adaptation of populations to ocean warming represent fruitful future research subjects.

Keywords: acclimation, climate change, energy budget, heatwave, metabolic depression, variability

Introduction

Marine ectotherms that have evolved in response to fluctuating stress regimes in environments such as shallow habitats can express remarkable suppression and recovery of metabolic performance over successive phases of critical and benign temperatures (Marshall and McQuaid, 1991). Metabolic suppression is expressed as substantial declines in feeding activities followed by partial decreases in aerobic respiration or extensive transition from aerobic to anaerobic respiration (Sokolova and Pörtner, 2001). By suppressing the rate of energy-intensive processes (e.g., feeding and growth), these organisms reduce their demand for metabolic substrates and energy (Schulte et al., 2011). Otherwise, their demands rise sharply with increasing temperature and eventually exceed the capacity to supply the required substrates from internal reserves. The supply capacity is related to the rates of resource uptake, internal reserve formation, and reserve mobilization (Kooijman, 2010), and is generally less temperature-dependent than the metabolic demand (Pörtner, 2012; Rall et al., 2012; Ritchie, 2018). The heat-induced mismatch between metabolic supply and demand can give rise to internal entropy, stress, and damage, exacerbating organismal performance over time (Pörtner, 2012; Ritchie, 2018). Therefore, metabolic suppression may allow organisms to minimize the negative impacts of critical temperatures during short-term (e.g., daily) thermal fluctuations (Vajedsamiei et al., under review).

Ongoing ocean warming increases the probability of exposure to high, beyond-optimal temperatures for marine organisms (Brewer et al., 2014). Due to this warming, periods of suppression may become longer while recovery phases may shorten, assuming no change in the temperature fluctuation amplitude and length. Enforcing metabolic suppression in response to more intense or extended periods of high critical temperatures may cause or exacerbate the supply and demand mismatch and its associated stress, limiting an organism's capacity to resume activity during the shortened recovery phases (Vajedsamiei et al., under review). Thus, it is crucial to know whether and how exposure to warming trends is associated with increased heat tolerance in the form of elevated thermal thresholds of metabolic suppression or increased capacity for recovery during thermal fluctuations.

Within- and between-generational acclimation to warmer ambient baseline regimes may increase heat tolerance in ectotherm individuals, leading to warm adaptation in some populations (Wittmann et al., 2008; Davenport and Davenport, 2005). Nonetheless, such acclimation capacity may be limited for species from highly fluctuating environments (Stillman, 2003; Somero, 2010; Seebacher et al., 2014) due to a tradeoff in favor of the capacity

for metabolic suppression and recovery (McMahon et al., 1995). Additionally, increases in heat tolerance through beneficial genetic mutation alone might not be fast enough to adapt populations to ocean warming (Somero, 2010) as suggested by the observed warming-induced extinctions and changes of biogeographical distributions of species (Barry et al., 1995; Sagarin et al., 1999; Wetthey and Woodin, 2008). Finally, emerging evidence suggests that directional selection in favor of heat-tolerant individuals may enforce a shift in a population's mean thermal performance (Logan et al., 2014, 2018; Ma et al., 2014; Gilbert and Miles, 2017). Many marine ectothermic species express their lowest heat-tolerance during the spawning, egg, and larval stages (Pörtner and Farrell, 2008; Nasrolahi et al., 2012). Therefore, in theory, directional selection may be imposed by extreme events on these sensitive life-history stages, a critical phenomenon to investigate since such extreme events are being enforced by climate change (Grant et al., 2017; Al-Janabi et al., 2019).

Whether through directional selection or acclimation, ectothermic individuals or populations may need to acquire lowered metabolic demand to decrease the risks of heat-induced supply and demand mismatch and its associated stress during critically warm phases of thermal fluctuations. This hypothesis also corroborates the *temperature compensation* (Hazel and Prosser, 1974) or *metabolic cold adaptation* (Clarke, 2003) hypotheses proposing that individuals adapted to warmer environments, compared to cold-adapted ones, usually have lower metabolic demand (represented by the respiration rate of non-stressed individuals) at similar benign temperatures. This allows individuals to optimize their metabolic performances according to their local thermal regimes (Le Lann et al., 2011).

Using blue mussels, *Mytilus* spp., an economically and ecologically important species and a system for studying metabolic suppression capability of ectotherms, this research evaluates (*i*) whether extremely warm summer conditions would select for individuals with higher heat tolerance in their daily metabolic suppression and recovery responses and (*ii*) whether such a potentially warm-adaptive shift in the metabolic responses is linked to lower metabolic demand of the individuals. In a quasi-natural flow-through benthocosm system, mussels from the western Baltic Sea (Kiel Fjord) introduced as juveniles (transplanted organisms) or as larvae (recruited organisms) were grown under the *current* (+ 0 °C) versus *future* (+ 4 °C) thermal history levels, imposed onto summer 2018 natural temperature regimes. After incubation for four months, the performance traits feeding and aerobic respiration were recorded in response to a mild temperature (20.8 °C) for six hours (baseline performance) followed by two 24 h thermal fluctuation cycles with extreme amplitudes (20.8–30.5 °C).

The hypotheses of this study were: (i) The warmer thermal history would result in individuals with higher heat tolerance as evidenced by warmer thresholds of metabolic suppression or higher recovery or both responses to daily thermal fluctuation cycles (Figure1A), and (ii) such higher heat tolerance is mediated by a lower baseline metabolic demand (Figure1B).

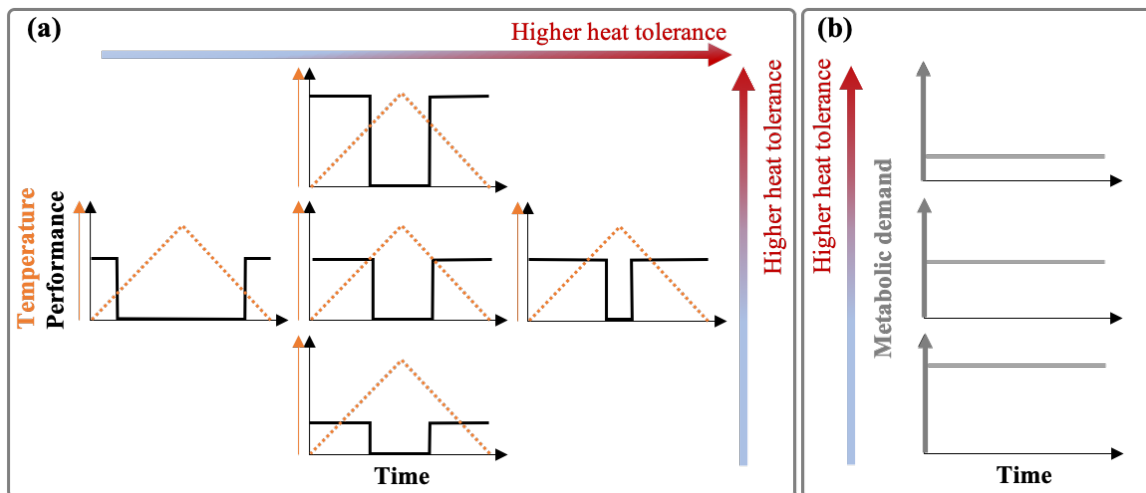


Figure 1. Hypotheses sketch. (a) Organisms selected by or acclimated to extreme summer baselines (e.g., prolonged heatwaves) can express higher heat tolerance in the form of (i) warmer thresholds of feeding and respiration suppression and recovery (a broader temperature range for optimal performance) or (ii) a higher metabolic performance (recovery) at benign phases of thermal fluctuations or both. (b) Compared to non-selected or non-acclimated individuals, the heat-tolerant organisms have lower metabolic demand (baseline performances) but with a normally high demand/supply ratio (not presented here) under a mild ambient temperature. When an organism's initial thermal performance (middle plot) is maintained over several daily fluctuation cycles, it means that the heat tolerance has not changed over time (i.e., elastic metabolic suppression and recovery in response to thermal fluctuations). However, the initial thermal performance (middle plot) can change over time due to acclimation or stress (plastic responses to fluctuations), resulting in other forms of responses. Notes: To simplify, we assumed there are no gradual thermal changes in the performance due to thermodynamics (Q_{10} effects), and the slope of fast changes in the performance is infinity leading to immediate suppression and recovery.

Material and methods

The study organism is the filter feeder *Mytilus edulis trossulus*, the species complex that forms extensive mussel beds in the Baltic Sea (Larson et al., 2017; Stuckas et al., 2017) where the tidal range is minimal (< few cm). However, ambient temperature regimes fluctuate in time due to daily irradiance variation (by 1–6 °C at depths ca. 1 m) or days- to weeks-long weather events (up to 8 °C at depths ca. 2 m) (Franz et al., 2019; Pansch and Hiebenthal 2019). By the end of the 21st century, the average sea surface water temperature is projected to increase by 1.5–4 °C in the Baltic Sea (Gräwe et al., 2013; Meier et al., 2012).

Long-term incubations and short-term assays

The long-term incubation was conducted as a part of a four-month community-level study on the effects of warming and upwelling on Baltic Sea benthic communities in summer 2018 (Wahl et al. in prep.; Pansch et al. in prep.). On May 23, 2018, juvenile mussels (7–13 mm) were collected in 0.5 m water depth from a jetty area (50 m²) in Kiel Fjord, Germany (54.4330891° N, 10.1711679° E). Batches of 40 specimens were transplanted (transplanted mussels) inside two separate baskets (3 mm² pore size and ca. 500 cm³ volume of each basket) within each 1500 L tank of the Kiel Outdoor Benthocosms (KOBs, located alongside a jetty in the Kiel Fjord; 54.330119° N, 10.149742° E; Wahl et al., 2015). Each tank received a flow-through of unfiltered Kiel Fjord seawater (ca. 8.5 L d⁻¹), which allowed near-natural abiotic (salinity, pH, oxygen, and nutrients) and biotic (bacterial load, phytoplankton, and zooplankton) conditions (Wahl et al., 2015).

In two short-term assays, we focused on measuring metabolic performance traits (filtration and respiration) for mussels from the two benthocosm tanks in which we simulated the current fjord temperature and a warmed future-expected thermal regime (hereafter, + 0 °C and + 4 °C *thermal history* levels; Figure 2A). There was only one benthocosm tank per treatment level (see the Shortcomings in the Discussion). In the Kiel Fjord, summer 2018 was an extremely warm season, involving two subsequent marine heatwaves (durations of 20 and 26 days) with maximum temperatures reaching 24–25 °C for a few days in the whole summer period (Wolf et al., 2020). The 24 °C was previously established as the high temperature threshold for initiation of mussels' metabolic suppression in response to short-term (hours-long) warming (Vajedsamiei et al., 2021; Vajedsamiei et al., under review). The + 4 °C thermal history level represented a future extreme summer regime, which will probably occur by the end of the 21st century (Gräwe et al., 2013; Meier et al., 2012). In this treatment level, the transplants had been exposed for ca. one month to temperatures above 24 °C (Figure 2A). Therefore, the two thermal history levels represent current versus future extreme summer-time thermal regimes.

We conducted lab assays for two periods. The first assay was conducted in the period from August 29 to September 10, during which filtration and respiration of 18 transplanted mussels (from + 0 °C and + 4 °C thermal history levels) were recorded in six temporally replicated (independent) trials. In each trial, filtration and respiration of three different specimens, randomly selected from the samples incubated under + 0 °C and + 4 °C levels, were recorded in response to a constant mild temperature condition (20.8 °C) followed by two 24 h thermal fluctuation cycles (Figure 2B) using a Fluorometer- and Oximeter-equipped Flow-through

Setup (FOFS; Vajedsamiei et al., 2021). In each trial, mussel-induced changes in the chlorophyll and dissolved oxygen concentrations were recorded as the difference between measurements taken from three flow-through paths containing mussels and the measurements taken from one mussel-free flow-through path. Minimum and maximum temperatures in the cycles were 20.8 and 30.5 °C, respectively, the former representing a current high (ca. the 90-percentile limit) daily thermal average in summer and the latter representing a future daily extreme (Gräwe et al., 2013; Pansch et al., 2018; Franz et al., 2019). During the performance trials, mussels were continuously fed with *Rhodomonas salina*, maintained at the concentration of their surrounding solution (Supplementary Figure 1) within the range (1000–7000 cells mL⁻¹) needed for mussel’s optimal filtration activity (Riisgard et al., 2012).

For the second assay, on September 12, 2018, we collected mussels recruited and grown on baskets located in the KOBs (recruited mussels). 480 specimens had recruited under the current thermal history level (+0 °C), while 17 were found under the +4 °C level. The recruited mussels were kept in filtered seawater at 20 °C for five days before the assay. In total, we recorded filtration and respiration rates of six batches of 5 or 6 mussels with similar shell lengths (three batches from each thermal history level) in temporally replicated trials of the same treatment, as explained earlier. Batches were randomly assigned to the repeated trials.

The size traits and assignments of replicates (individuals or batches of mussels) to trials are presented in Supplementary Table 1. Mussel dry tissue weights were measured after each assay and later used as proxies for tissue volumes (Hamburger et al., 1983; Riisgård, 2001).

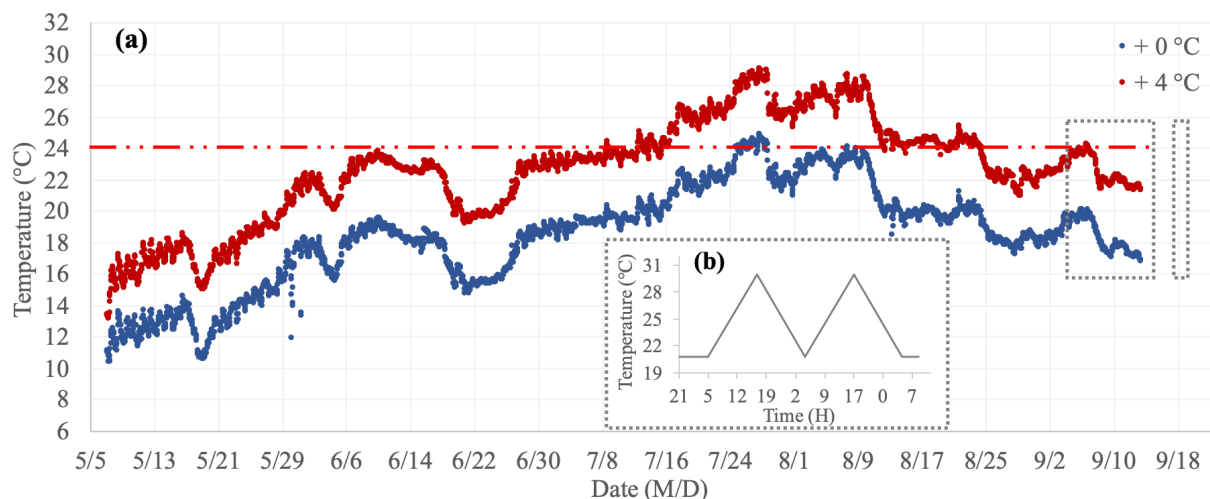


Figure 3. Temperature regimes of long-term incubation and short-term assays. (a) *Thermal history* treatment levels (+ 0 °C and + 4 °C) imposed on mussels transplanted or recruited in summer 2018 in the two mesocosm tanks of the Kiel Outdoor Benthocosms (KOBs). (b) The assay treatment included the before-fluctuation phase (when mussels were exposed to constantly 20.8 °C) and the fluctuation phase when the maximum temperature reached 30.5 °C.

Initial data processing

Data collected in each short-term assay were processed separately. Initial data processing was conducted using Python (Python Software Foundation) based on the scripts and the protocol described in Vajedsamiei et al., 2021. In short, the initial data processing had two main steps: (i) *Trial-by-trial processing* denoised the time series of dissolved oxygen and Chlorophyll (or cell) concentrations (measured in each trial) using the robust estimation technique, corrected for the effect of temperature, and converted to units of interest. The cell concentration measurement was time-lagged compared to the oxygen measurement, as the Chl sensor was positioned after the oximeter in each path of FOFS. The time lag was corrected using linear differential modeling. The revised time series of the measured variables were then applied to calculate the response variables (i.e., filtration, feeding, and respiration rates), all saved into the respective trial's output data frame. The variables' definitions, as used in the trial-by-trial processing Python script, are provided in Supplementary Script 1. (ii) *Integrative processing* scaled filtration and respiration rates for each replicate with respect to the average responses over the before-fluctuation phase and combined the revised output data frames of each assay.

Hypothesis testing

Statistical hypothesis testing was done in R (R Core Team, 2019) using the packages *mgcv*, *visreg*, and *itsadug* (Wood, 2017; van Rij et al., 2020). The testing was done for transplanted and recruited mussels separately.

To test the first hypothesis, we used Generalized Additive Mixed-effect Models (GAMMs) to explain sources of variation in the scaled filtration (potential for feeding) and respiration rates observed during the whole assay. We tested for the significance of the fixed (intercept or average) effect of *thermal history*, the smoothed effect of *time*, and the interactive effect of *thermal history* and *time*. The number of the basis functions (knots) in the GAMMs was chosen to maximize the k-index considering the tradeoff between the models' nonlinearity (degree of freedom) and the goodness of fit (Wood, 2017).

To test the second hypothesis, we used GAMMs to explain the sources of variation observed during the before fluctuation phase (at the constant temperature of 20.8°C). The potential for feeding (J h^{-1}), estimated based on the filtration rate at a constant medium food level (3000 cell mL^{-1}), and the respiration rates (J h^{-1}) were used as the response variables. The number of knots in the GAMMs was restricted to 3, limiting the smooths' maximum allowed nonlinearity. Considering all possible sources of variation in the potential for feeding, we tested for the fixed

effect of *thermal history*, the smooth effect of *dry tissue weight* (as a measure of body volume), and the smooth effect of *time* and its interactions with *thermal history*. For modeling the respiration rate, besides these factors, we also tested for the smooth effect of *real-time feeding rate* since the feeding rate could have influenced the respiration rate (due to the cost of feeding activities; Secor 2008). Therefore, in our hypothesis testing, we assumed that the smoothers explaining the responses as functions of *dry tissue weight* or *real-time feeding rate* would be relatively similar for mussels with different thermal histories.

Notably, in all GAMMs, *thermal history* was defined as an *ordered factor* to structure the model in the form of an ANOVA contrast, enabling direct comparison of the reference level smooth (+ 0 °C) with the elevated one (+ 4 °C) (van Rij et al., 2020). As measurements were longitudinal (with temporal dependency), *replicate* was defined as the random intercept factor, and the residual autocorrelation was considered by including a lag-one autoregressive term or *AR(1)* parameter in the GAMMs (Wood, 2017; van Rij et al., 2020). We also used Restricted Maximum Likelihood (REML) for the unbiased estimation of variance components (Wood et al., 2016). After the tests, we checked residuals' normality and independency through QQ and ACF plots, respectively. The general version of the R scripts can be found in Supplementary Script 2.

Results and discussion

The future summer thermal extreme resulted in rare recruits of higher heat tolerance

Over the daily cycles of our short-term assays, all transplanted and recruited mussels with different thermal histories (+ 0 °C and + 4 °C) expressed some levels of metabolic suppression and recovery (Figure 3). Their metabolic performance traits, represented by scaled rates of potential for feeding (filtration) and aerobic respiration, were depressed in response to the temperature exceeding a specific threshold range (24–26 °C) during the warming phases. The responses recovered to some extent at subsequent exposures to less extreme temperatures (recovery phases).

For recruited mussels, the variation of both metabolic traits was significantly explained by thermal history, as both the intercept (*future – current*) and the smooth term (*s(time):future*) were very significant (p-values < 0.0001; Supplementary Table 2). Indeed, recruited mussels from the warmer regime (+ 4 °C), compared to the recruits from the colder regime (+ 0 °C), were better able to restore their respiration and feeding rates during recovery phases to before-

fluctuation levels (Figure 3A, B, E, F). The thermal thresholds of respiration suppression and recovery were relatively comparable between these two groups of recruited mussels (Figure 3B), and so was the threshold of feeding suppression (Figure 3A). However, the thermal threshold of feeding recoveries was lower for recruited mussels from + 4 °C compared to the recruits from + 0 °C (Figure 3A).

Recruitment under the + 4 °C regime was reduced by ca. 96.5 % of what was found in the current regime (+ 0 °C) (see Material and Methods). Jointly, these findings propose that high selective pressure imposed by the intensified (> 24 °C) thermal regime on mussels at very early life stages might have resulted in a selection for increased heat tolerance (the capability for metabolic recovery). Most marine ectotherms at the spawning, embryo, and larval stages have the narrowest thermal tolerance window and are most vulnerable to thermal extremes (Pörtner and Farrell, 2008; Nasrolahi et al., 2012).

Instead, for transplanted mussels, thermal history's effects were not significant, both in terms of the intercept (*future – current*) and the smooth (*s(time):future*) (p-values > 0.26; Supplementary Table 2). Mussels with different thermal histories on average showed very similar metabolic depression or recovery patterns (Figure 3C, D, G, H). Additionally, the feeding recovery of these mussels weakened over the short-term assay, probably in response to the critical temperatures. These patterns generally suggest that the studied species have a limited capacity to improve their metabolic performance under critical temperatures through physiological acclimation. Accordingly, at + 4 °C, growth rates of mussels' shell length, dry shell weight, and dry tissue weight over the summer were ca. 80, 60, and 40 %, respectively, of that found under + 0 °C (Supplementary Table 3). All these findings corroborate previous empirical evidence, suggesting that marine organisms from shallow habitats with pronounced thermal fluctuations generally have a limited capacity to acclimate to warm extreme conditions (Stillman, 2003; Somero, 2010; Seebacher et al., 2014).

Metabolic suppression and recovery, mediated by thermal fluctuations, may allow eurytherms such as mussels to improve their fitness, which may be instead detrimental under constant regimes (Vajedsamiei et al., under review). Such refuge effects are more relevant to organisms as ongoing ocean climate warming generally increases the probability of beyond-optimal temperature exposures. Our findings are partly in line with emerging evidence, proposing that extreme events may result in a directional selection of heat-tolerant individuals, which can potentially lead to increases in the populations' mean heat tolerance over generations (Logan et al., 2014, 2018; Ma et al., 2014; Gilbert and Miles, 2017). Yet, selection by one environmental

factor may cause cross-tolerance or increased sensitivity to other environmental factors (Al-Janabi et al., 2019). Such selective forces may substantially decrease the recruitment success and population size in time, raising the risks of extinction due to decreased population size and genetic variation (Grant et al., 2017).

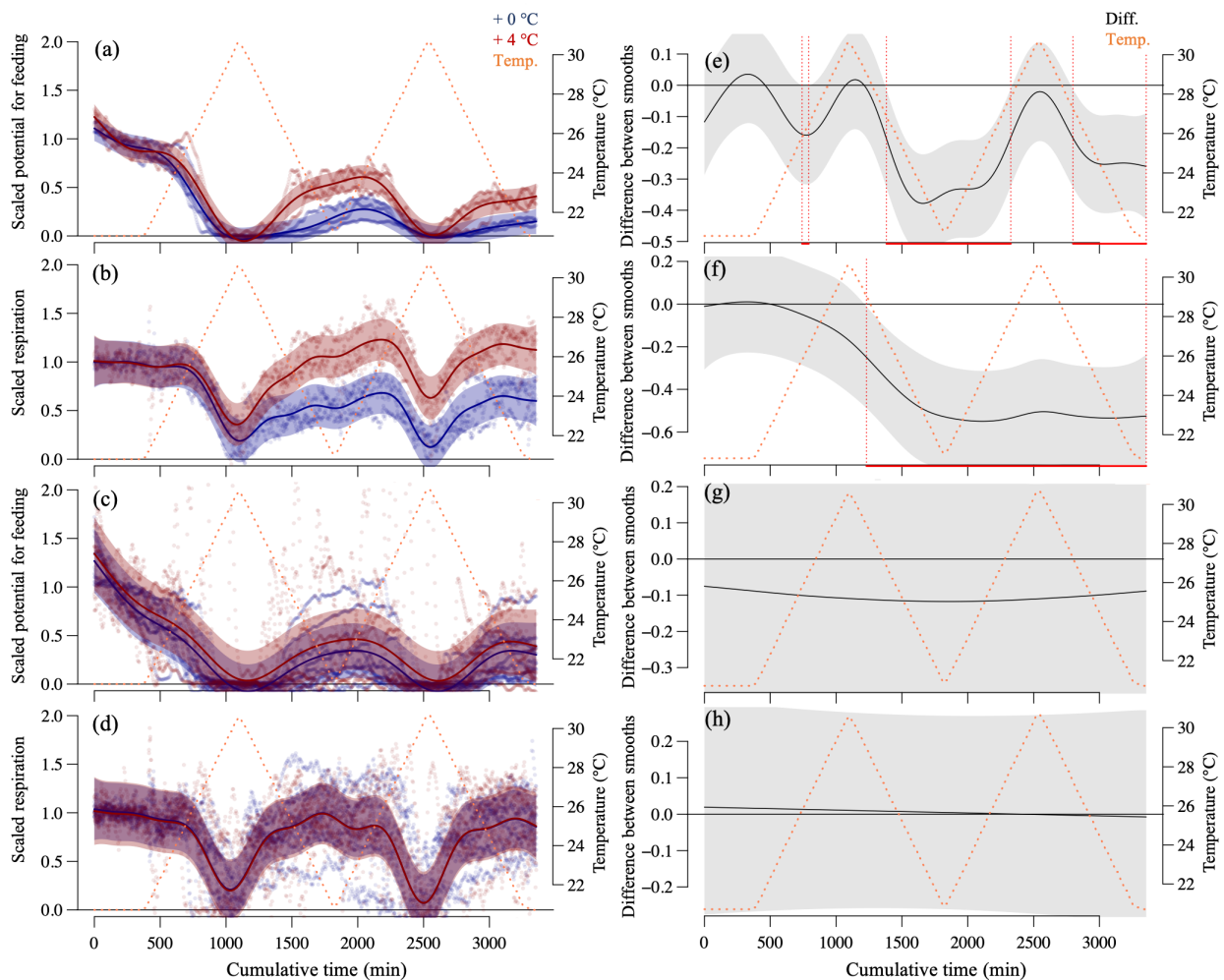


Figure 3. Mussel responses in the short-term assays. Generalized Additive Mixed-effect Models (GAMMs) of the scaled potential for feeding and respiration rates of recruited (a–b) and transplanted (c–d) mussels over diurnal thermal fluctuation cycles. The specimens experienced a *thermal history* of + 0 °C and + 4 °C imposed onto summer 2018 ambient conditions. Responses of single transplanted mussels and the recruited mussels, in groups of 5–6 specimens as a replicate, were assessed using the Fluorometer- and Oximeter-equipped Flow-through Setup (FOFS; Vajedsamiei et al., 2021). Each replicated time series was normalized concerning the average responses over the before-fluctuation phase. Respective post-hoc curve comparison plots are presented on the right (e–h) in which the predictions of the treated-level smoother (+ 4 °C) are subtracted from the reference level smoother (+ 0 °C). Red lines denote the intervals of significant differences between smoothers.

Lower metabolic demand might have led to higher heat tolerance in recruited mussels

In the before-fluctuation phase, recruited mussels from + 4 °C showed, on average, significantly lower respiration and potential for feeding (Figure 4A and B), as the intercepts (*future – current*) of the models were very significant (p -values < 0.0001; Supplementary Table 4). Instead,

transplanted mussels from + 4 °C expressed slightly lower potential for feeding and respiration rates than transplanted mussels from + 0 °C (Figure 4C and D; p-values > 0.21; Supplementary Table 4). The ratio of respired energy to energy uptake from feeding (fed energy) can be calculated using the parametric coefficients' "Estimate" values (intercept or averages) presented in Supplementary Table 4. The ratios were nearly identical, on average 0.17 versus 0.19 (J h⁻¹), for the recruited mussels from the + 0 °C versus + 4 °C, respectively. This pattern suggests that the lower metabolic demand (represented by the aerobic respiration) in recruits of the + 4 °C regime was coupled with the lower supply-to-reserve rate. The latter process is mainly represented by the potential for feeding but can include all processes involved in uptake and transport of metabolic substrates and energy into appropriate internal storage reservoirs (Kooijman, 2010). In contrast, the respired energy to fed energy ratios were on average 0.29 versus 0.36 (J h⁻¹) for transplanted mussels from the + 0 °C versus + 4 °C, respectively, suggesting that the heat-treated transplants were more at the risk of heat-induced mismatch of metabolic supply and demand.

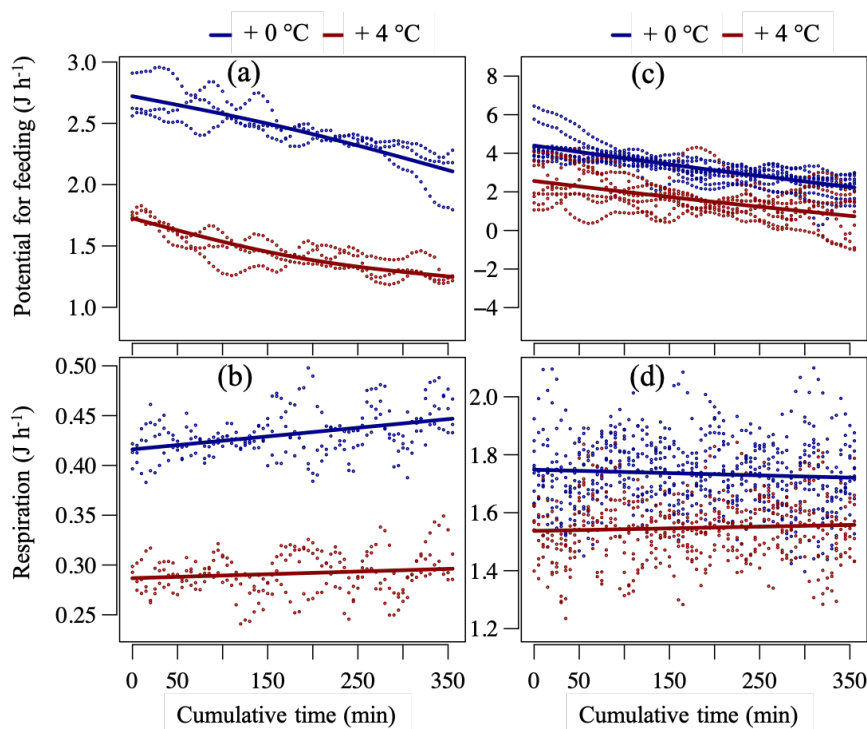


Figure 4. Mussel baseline performance at constantly 20.8 °C in the short-term assay. Potential-for-feeding and respiration rates of recruited (a and b) and transplanted (c and d) mussels at an ambient food concentration ca. 3000 cells mL⁻¹ during the before-fluctuation phase of the short-term assay. The plots are Generalized Additive Mixed-effect Model (GAMM) outputs after setting the median tissue dry weight (and a median feeding rate for predicting the respiration) and a specific replicate level. The dots represent partial residual for each model. For recruited mussels, the fixed effects of thermal history on both responses were significant (p-values < 0.001, adjusted-R² > 0.95), while for transplanted mussels, the effect was only significant for the potential for feeding (p-value = 0.03 and 0.39, and adjusted-R² = 0.97 and 0.94, for feeding and respiration, respectively). For tests on the significance of smooth and random effects, see Table 2.

These findings suggest that recruits of marine ectotherms with lower metabolic demand (but enough supply rate) may have higher heat tolerance regarding their metabolic responses to transient critical exposures during short-term thermal fluctuations. The link between lower metabolic demand and higher heat tolerance can be explained through a heat-induced limitation in marine ectotherms' capacity to supply their demand for metabolic substrates and energy, as discussed in the following.

For individuals of a marine ectotherm population (at a specific life-stage and the whole organism level), thermal dependency (denoted by Q_{10}) is usually higher for the metabolic demand than for the feeding (Rall et al., 2012). Besides, oxygen supply capacity can also become limited at high temperatures (Pörtner, 2012; Verberk et al., 2016). At the cellular level, Q_{10} may also be higher for metabolic product formation (or demand) as compared to substrate diffusion and transport processes (or supply) (Ritchie, 2018). For a growing juvenile mussel, for example, a temperature-induced rise in feeding rate (Q_{10} ca. 1.5; Kittner and Riisgård, 2005) may be enough to compensate for a relatively higher increase of energy demand (Q_{10} 2–3; Widdows, 1976; Vajedsamiei et al., under review) only if the food resource is sufficiently nutritious. However, after a specific temperature threshold or period of exposure is exceeded, the feeding activities may become too costly, as they usually consume a large portion (ca. 20 %) of the whole metabolic expenditure (Widdows and Hawkins, 1989; Secor, 2009). When organisms restrict their supply-to-reserve rate due to the high costs, the supply-from-reserve will become time-limited, meaning that the organisms may become more and more in debt, specifically regarding metabolic substrates and energy. Therefore, in theory, and as our findings suggest, more heat-tolerant ectothermic individuals compared to less tolerant ones would tend to have lower metabolic demand to better control metabolic supply and demand mismatch. The associated debt and stress of such a mismatch would be directly linked to an organism's basic levels of metabolic demand.

Shortcomings and perspectives

Our short-term assays were conducted as post-incubations to a community-level 4-month long incubation experiment, the results of which are mainly reported in two associated papers (Pansch et al., in prep; Wahl et al. in prep; but see also: Materials and Methods). The sample size and the level of between-replicate dependency were not ideal in our short-term assays. The number of recruited mussels in the end-of-century treatment level was only 17; therefore, just three replicated time series could be measured for three batches of 5–6 recruited mussels.

Additionally, since replicate mussels shared one benthocosm tank during the summer, we could not exclude (or account for) the confounding effects of between-replicate dependency in the modeling. Nonetheless, some factors could have lowered the dependency of replicate mussels, including the potential difference in their genetics, the large size of the tanks, and the high seawater exchange rate (see the Material and Methods). Notably, the growth and recruitment data collected in the two treatment levels (+ 0 °C and + 4 °C) fitted well into thermal performance curves which were created using the whole dataset from all six thermal history levels (+ 0 °C to + 5 °C) of the 4-months long incubation (See Supplementary Figure 2), inferring that the mussels under the + 4 °C regime were mainly impacted by the temperature and no other confounding factors.

Nevertheless, more investigations are needed to support the two general propositions: (i) Extreme seasons (events) select for ectothermic early-stage individuals with more heat-tolerant metabolic performance and (ii) such heat tolerance is due to the lowered metabolic demand enabling these organisms to more efficiently control the mismatch between metabolic supply and demand at high temperatures. In a second step, we must understand if the directional selection of less metabolically demanding recruits can lead to rapid evolutionary warm adaptation of populations of ectothermic benthic metazoans, as recently shown for a microbial alga (Padfield et al., 2016). Such elevated heat resistance may not result in population persistence in response to future warming when it involves a substantial decrease in new cohorts' abundance and genetic diversity.

Acknowledgements

The authors would like to acknowledge Claas Hiebenthal, KIMOCC, and Ulrike Panknin for providing the *Rhodomonas* culture and technical assistance.

This work and J.V. were funded through the Deutsche Forschungsgemeinschaft (DFG) project: The neglected role of environmental fluctuations as a modulator of stress and driver of rapid evolution (Grant Number: PA 2643/2/348431475) and through GEOMAR. The project was also supported by the Cluster of Excellence “The Future Ocean”, funded within the framework of the Excellence Initiative by the DFG on behalf of the German federal and state governments. C.P. was funded by the postdoc program of the Helmholtz- Gemeinschaft Deutscher Forschungszentren and by GEOMAR.

References

- Al-Janabi, B., Wahl, M., Karsten, U., Graiff, A., and Kruse, I. (2019). Sensitivities to global change drivers may correlate positively or negatively in a foundational marine macroalga. *Sci. Rep.* 9, 14653. doi:10.1038/s41598-019-51099-8.
- Barry, J. P., Baxter, C. H., Sagarin, R. D., and Gilman, S. E. (1995). Climate-related, long-term faunal changes in a California rocky intertidal community. *Science* (80-.). 267, 672–675. doi:10.1126/science.267.5198.672.
- Breheny, P., and Burchett, W. (2017). Visualization of Regression Models Using visreg. *The R Journal.* 9(2), 56–71.
- Brewer, P. G., Fabry, V. J., Hilmi, K., Jung, S., Poloczanska, E., and Sundby, S. (2014). Chapter 30. The Ocean. *Clim. Chang. 2014 Impacts, Adapt. Vulnerability. Contrib. Work. Gr. II to Fifth Assess. Rep. Intergov. Panel Clim. Chang.*, 1–138. Available at: http://ipcc-wg2.gov/AR5/images/uploads/WGIIAR5-Chap30_FGDall.pdf.
- Clarke, A. (2003). Costs and consequences of evolutionary temperature adaptation. *Trends Ecol. Evol.* 18, 573–581. doi:<https://doi.org/10.1016/j.tree.2003.08.007>.
- Davenport, J., and Davenport, J. L. (2005). Effects of shore height, wave exposure and geographical distance on thermal niche width of intertidal fauna. *Mar. Ecol. Prog. Ser.* 292, 41–50. doi:10.3354/meps292041.
- Franz, M., Lieberum, C., Bock, G., and Karez, R. (2019). Environmental parameters of shallow water habitats in the SW Baltic Sea. *Earth Syst. Sci. Data* 11, 947–957. doi:10.5194/essd-11-947-2019.
- Gilbert, A. L., and Miles, D. B. (2017). Natural selection on thermal preference, critical thermal maxima and locomotor performance. *Proc. R. Soc. B Biol. Sci.* 284. doi:10.1098/rspb.2017.0536.
- Grant, P. R., Rosemary Grant, B., Huey, R. B., Johnson, M. T. J., Knoll, A. H., and Schmitt, J. (2017). Evolution caused by extreme events. *Philos. Trans. R. Soc. B Biol. Sci.* 372, 5–8. doi:10.1098/rstb.2016.0146.
- Gräwe, U., Friedland, R., and Burchard, H. (2013). The future of the western Baltic Sea: Two possible scenarios. *Ocean Dyn.* 63, 901–921. doi:10.1007/s10236-013-0634-0.
- Hamburger, K., Møhlenberg, F., Randløv, A., and Riisgård, H. U. (1983). Size, oxygen consumption and growth in the mussel *Mytilus edulis*. *Mar. Biol.* 75, 303–306. doi:10.1007/BF00406016.
- Hazel, J. R., and Prosser, C. L. (1974). Molecular mechanisms of temperature compensation in poikilotherms. *Physiol. Rev.* 54, 620–677. doi:10.1152/physrev.1974.54.3.620.
- Kittner, C., and Riisgård, H. U. (2005). Effect of temperature on filtration rate in the mussel *Mytilus edulis*: no evidence for temperature compensation. 305, 147–152.
- Kooijman, S. a. L. M. (2010). *Dynamic energy budget theory for metabolic organisation.* Cambridge Univ. Press. Cambridge, UK. doi:10.1098/rstb.2010.0167.

- Le Lann, C., Wardziak, T., van Baaren, J., and van Alphen, J. J. M. (2011). Thermal plasticity of metabolic rates linked to life-history traits and foraging behaviour in a parasitic wasp. *Funct. Ecol.* 25, 641–651. doi:10.1111/j.1365-2435.2010.01813.x.
- Logan, C. A., Dunne, J. P., Eakin, C. M., and Donner, S. D. (2014). Incorporating adaptive responses into future projections of coral bleaching. *Glob. Chang. Biol.* 20, 125–139. doi:10.1111/gcb.12390.
- Logan, M. L., Curlis, J. D., Gilbert, A. L., Miles, D. B., Chung, A. K., McGlothlin, J. W., et al. (2018). Thermal physiology and thermoregulatory behaviour exhibit low heritability despite genetic divergence between lizard populations. *Proc. R. Soc. B Biol. Sci.* 285. doi:10.1098/rspb.2018.0697.
- Ma, F. Z., Lü, Z. C., Wang, R., and Wan, F. H. (2014). Heritability and evolutionary potential in thermal tolerance traits in the invasive Mediterranean cryptic species of *Bemisia tabaci* (Hemiptera: Aleyrodidae). *PLoS One* 9, 1–7. doi:10.1371/journal.pone.0103279.
- Marshall, D. J., and McQuaid, C. D. (1991). Metabolic rate depression in a marine pulmonate snail: pre-adaptation for a terrestrial existence? *Oecologia* 88, 274–276. doi:10.1007/BF00320822.
- McMahon, R. F., Russell-Hunter, W. D., and Aldridge, D. W. (1995). Lack of metabolic temperature compensation in the intertidal gastropods, *Littorina saxatilis* (Olivi) and *L. obtusata* (L.). *Hydrobiologia* 309, 89–100. doi:10.1007/BF00014475.
- Meier, H. E. M., Eilola, K., Gustafsson, B. G., Kuznetsov, I., Neumann, T., and Savchuk, O. P. (2012). Uncertainty assessment of projected ecological quality indicators in future climate. *Oceanography* 112.
- Nasrolahi, A., Pansch, C., Lenz, M., and Wahl, M. (2012). Being young in a changing world: how temperature and salinity changes interactively modify the performance of larval stages of the barnacle *Amphibalanus improvisus*. *Mar. Biol.* 159, 331–340. doi:10.1007/s00227-011-1811-7.
- Pansch, C., Scotti, M., Barboza, F. R., Al-Janabi, B., Brakel, J., Briski, E., et al. (2018). Heat waves and their significance for a temperate benthic community: A near-natural experimental approach. *Glob. Chang. Biol.* 24, 4357–4367. doi:10.1111/gcb.14282.
- Pörtner, H. (2012). Integrating climate-related stressor effects on marine organisms: unifying principles linking molecule to ecosystem-level changes. 470, 273–290. doi:10.3354/meps10123.
- Pörtner, H. O., and Farrell, A. P. (2008). Physiology and Climate Change. *Science* (80-.). 322, 690 LP – 692. doi:10.1126/science.1163156.
- Riisgård, H. (2001). On measurement of filtration rate in bivalves-the stony road to reliable data: review and interpretation. *Mar. Ecol. Prog. Ser.* 211, 275–291. doi:10.3354/meps211275.
- Ritchie, M. E. (2018). Reaction and diffusion thermodynamics explain optimal temperatures of biochemical reactions. *Sci. Rep.* 8, 1–10. doi:10.1038/s41598-018-28833-9.

- Sagarin, R. D., Barry, J. P., Gilman, S. E., and Baxter, C. H. (1999). Climate-Related Change in an Intertidal Community over Short and Long Time Scales. *Ecol. Monogr.* 69, 465–490. doi:10.2307/2657226.
- Schulte, P. M., Healy, T. M., and Fangué, N. A. (2011). Thermal performance curves, phenotypic plasticity, and the time scales of temperature exposure. *Integr. Comp. Biol.* 51, 691–702. doi:10.1093/icb/icr097.
- Secor, S. M. (2009). Specific dynamic action: A review of the postprandial metabolic response. *J. Comp. Physiol. B Biochem. Syst. Environ. Physiol.* 179, 1–56. doi:10.1007/s00360-008-0283-7.
- Seebacher, F., White, C. R., and Franklin, C. E. (2014). Physiological plasticity increases resilience of ectothermic animals to climate change. 1–6. doi:10.1038/NCLIMATE2457.
- Sokolova, I. M., and Pörtner, H. O. (2001). Physiological adaptations to high intertidal life involve improved water conservation abilities and metabolic rate depression in *Littorina saxatilis*. *Mar. Ecol. Prog. Ser.* 224, 171–186. doi:10.3354/meps224171.
- Somero, G. N. (2010). The physiology of climate change: how potentials for acclimatization and genetic adaptation will determine “winners” and “losers.” *J. Exp. Biol.* 213, 912–920. doi:10.1242/jeb.037473.
- Stillman, J. H. (2003). Acclimation capacity underlies susceptibility to climate change. *Science* 301, 65. doi:10.1126/science.1083073.
- Vajedsamiei, J., Melzner, F., Raatz, M., Kiko, R., Khosravi, M., and Pansch, C. (2021). Simultaneous recording of filtration and respiration in marine organisms in response to short-term environmental variability. *Limnol. Oceanogr. Methods* n/a. doi:https://doi.org/10.1002/lom3.10414.
- van Rij, J., Wieling, M., Baayen, R., van Rijn, H. (2020). itsadug: Interpreting Time Series and Autocorrelated Data Using GAMMs. R package version 2.4.
- Verberk, W. C. E. P., Overgaard, J., Ern, R., Bayley, M., Wang, T., Boardman, L., et al. (2016). Does oxygen limit thermal tolerance in arthropods? A critical review of current evidence. *Comp. Biochem. Physiol. -Part A Mol. Integr. Physiol.* 192, 64–78. doi:10.1016/j.cbpa.2015.10.020.
- Wahl, M., Buchholz, B., Winde, V., Golomb, D., Guy-Haim, T., Müller, J., et al. (2015). A mesocosm concept for the simulation of near-natural shallow underwater climates: The Kiel Outdoor Benthocosms (KOB). *Limnol. Oceanogr. Methods* 13, 651–663. doi:10.1002/lom3.10055.
- Wetthey, D. S., and Woodin, S. a. (2008). Ecological hindcasting of biogeographic responses to climate change in the European intertidal zone. *Hydrobiologia* 606, 139–151. doi:10.1007/s10750-008-9338-8.
- Widdows, J. (1976). Physiological adaptation of *Mytilus edulis* to cyclic temperatures. *J. Comp. Physiol. B* 105, 115–128. doi:10.1007/BF00691115.

- Widdows, J., and Hawkins, A. J. S. (1989). Partitioning of rate of heat dissipation by *Mytilus edulis* into maintenance, feeding, and growth components. *Physiol. Zool.* 62, 764–784. doi:10.1086/physzool.62.3.30157926.
- Wittmann, A. C., Schröer, M., Bock, C., Steeger, H. U., Paul, R. J., and Pörtner, H. O. (2008). Indicators of oxygen- and capacity-limited thermal tolerance in the lugworm *Arenicola marina*. *Clim. Res.* 37, 227–240. doi:10.3354/cr00763.
- Wolf, F., Bumke, K., Wahl, S., Nevoigt, F., Hecht, U., Hiebenthal, C., et al. (2020). High resolution water temperature data between January 1997 and December 2018 at the GEOMAR pier surface. doi:10.1594/PANGAEA.919186.
- Wood, S. N., Pya, N., and Säfken, B. (2016). Smoothing Parameter and Model Selection for General Smooth Models. *J. Am. Stat. Assoc.* 111, 1548–1563. doi:10.1080/01621459.2016.1180986.
- Wood, S. N. (2017). *Generalized Additive Models: An Introduction with R*, 2nd edn. Chapman & Hall/CRC.

General Discussion

The empirical findings presented in Chapter 2 and 3 generally imply that:

- (i) Short-term (daily) thermal fluctuations mediating oscillations in metabolic performance (suppressions and recoveries) of an ectotherm (Chapters 1–3) can lead to its lower or higher time-integrated performance (fitness) compared to the response under a static exposure to the fluctuations' average temperature (Chapter 2).
- (ii) The fluctuations can provide refuge to an ectotherm at critical average temperatures, i.e., the temperatures at which the organism's metabolic performance is suppressed (Chapter 2).
- (iii) The ectotherms with remarkable capacity for metabolic suppression may have low capacities for compensational acclimation to critically high temperatures within day-to-months-long exposures (Chapters 2 and 3).
- (iv) Extremely-warm events may select for heat-tolerant ectothermic individuals at their very early life-history stages (Chapter 3).
- (v) The higher heat tolerance in metabolic suppression and recovery of an ectotherm can be mediated through lower metabolic demand (Chapter 3).

The experimental studies were enabled through the Fluorometer- and Oximeter-equipped Flow-through Setup (FOFS) and associated data processing protocols (Vajedsamiei et al., 2021).

FOFS-like experimental methods can fill methodological gaps

FOFS integrated method allows monitoring of filter-feeders' metabolic performance (feeding and aerobic respiration) in response to environmental variations at temporal resolutions relevant to natural systems. The approach addresses several critical considerations for users and prospective developers of continuous biomonitoring systems from benchtop to mesocosm setups. These issues particularly involve (i) the confounding effect of environmental variability on sensor measurements, (ii) the time series noise removal or trending using robust regression techniques, (iii) the random drift estimation, and (iv) the lag-time estimation and correction based on linear differential modeling. Besides, FOFS Python scripts provide semi-automatic and adaptable data processing.

The FOFS approach was successfully used to record the thermal metabolic performance of the study species, *Mytilus* spp., in short-term assays and as complements to longer-term

incubations. Using this approach, I could relate the observed effects of daily fluctuations on mussel growth to their capacity for thermal suppression and recovery of feeding and respiration (Chapter 2; Vajedsamiei et al., under review), and explain whether and how a thermal history of extremely warm summer conditions may alter heat tolerance of a mussel population (Chapter 3; Vajedsamiei et al., submitted).

Depending on the context, fluctuations can be beneficial or harmful for ectotherms

Results of the 5-weeks long experiment show that daily thermal fluctuations can be negative or positive for mussel growth depending on the fluctuations' average and amplitude (Chapter 2). (i) At the less-extreme average condition (23.5 °C), the large-amplitude fluctuations (± 4 °C) significantly decreased mussel growth while the impact of the intermediate-amplitude fluctuations (± 2 °C) was not significant. In contrast, (ii) at the more extreme thermal average (26 °C), the ± 4 °C fluctuations improved the growth, and the ± 2 °C also benefited mussels. Still, the latter effect was only significant in terms of mussels' tissue growth, i.e., one of three measured response traits.

Our experimental thermal averages corresponded to current and future-expected scenarios in the Western Baltic Sea, as specified based on published literature in the method section of Chapter 2. According to a more recent analysis, in this location, a 22-year (1997–2018) thermal mean and the upper 90th-percentile thermal threshold at a depth of 1.5 m reached ca. 18.5 and 22 °C, respectively (Wolf et al., 2020). In summer 2018, the daily mean temperature was > 22 °C (max. 24 °C) for 13 days (Wolf et al., 2020). Therefore, our moderately-warm and extremely-warm average treatment levels (23.5 and 26 °C, respectively) represented the average temperatures for a current to near-future and an end-of-century marine heatwave (Meier et al., 2012; Gräwe et al., 2013). In the Kiel Fjord, daily thermal variation in temperature can rarely be as high as 8 °C (± 4 °C), while a 5 °C daily variation is expected in coastal habitats with depths < 1 m during summers (Franz et al., 2019; Hennigs 2020). While ± 4 °C amplitude is considered an extreme scenario, the peak temperature of 30 °C, which was shortly experienced in such daily cycles, may be experienced regularly in summer by Baltic shallow-water organisms as we approach the year 2100. Therefore, as the findings suggest, in the Baltic Sea shallow-water habitats where organisms are usually submerged due to minor tidal changes in water levels, the *Mytilus* performance is probably modulated by the daily thermal cycles during current or near-future summers. In other marine shallow-water regions, especially in

areas where species experience aerial exposure during low tides, the modulatory impacts of daily thermal cycles on the growth may be even more substantial (Helmuth et al., 2014).

Literature findings regarding observed or predicted long-term effects of cyclic temperature fluctuations on ectotherms' performance are partly contradicting. Thermal treatments of most studies predicting or observing fluctuations' detrimental impacts (Paaijmans et al., 2013; Vasseur et al., 2014; Bernhardt et al., 2018) were limited in range as the specimens could not have withstood the constant exposure to critically high temperatures for extended durations (e.g., weeks). Alternatively, some studies have been able to witness positive effects of fluctuations when specimens were subjected to fluctuating versus static regimes of similar critical average conditions (Bozinovic et al., 2011; Niehaus et al., 2012; Kingsolver et al., 2015; Kang et al., 2019). Possibly, the organisms benefited from fluctuations' benign phases (Schulte 2011; Wahl et al. 2015).

Ectotherms' capacity for thermal metabolic suppression and recovery defines their long-term responses to thermal fluctuations

Using FOFS, I demonstrated the study species' ability to suppress and recover its feeding and aerobic respiration in response to daily fluctuations in the thermal range utilized in our 5-weeks long experiment. As introduced in Chapter 2, temperature fluctuations' refuge effects could be predicted through nonlinear averaging on thermal performance curves (TPCs) generated at very short timescales (e.g., hours) relating to (daily) thermal cycles. Through upscaling from the non-acclimated TPCs of feeding performance, we indicated that feeding rates could be higher at the fluctuating compared to the static regime (both with the same critical average temperature). This prediction suggests that an elastic suppression and recovery of metabolic performance (with no compensational acclimation or stress effects) during thermal fluctuations would elevate the long-term performance (growth) at critical average temperatures. In addition, I found a strong linear correlation between the fluctuations' upscaled impacts on feeding (predicted) and their 5-weeks impacts on growth (observed). These findings are also a critical notice for energy budget modeling of ectotherms evolved in response to highly fluctuating environments: non-acclimated TPCs of feeding are more appropriate than respiration TPCs for parametrizing the temperature correction coefficient in growth-projecting models (such as Dynamic Energy Budget models; Kooijman, 2010; Monaco and McQuaid, 2018).

As indicated in Chapter 2, investigations focusing on thermal metabolic performance and how it changes in time may provide a broader understanding of how ectotherm populations respond

to thermal fluctuations of today and in the future. The combination of the long- and short-term approaches and the associated upscaling framework went beyond the mere description of observed patterns as done in numerous previous studies addressing the influence of fluctuations on organism responses with less explanatory power (Bozinovic et al., 2011; Niehaus et al., 2012; Paaijmans et al., 2013; Vasseur et al., 2014; Kingsolver et al., 2015; Bernhardt et al., 2018). Nevertheless, conducting longer-term recordings of metabolic performance in response to thermal fluctuations can provide direct evidence on the implications of compensational acclimation or stress, an essential advancement to this field of research.

The hypothesis set (framework) presented in Chapter 2, central to all questions raised and answered in this thesis, simply integrates my findings with physiological and mathematical principles from the literature and explains possible outcomes of such compensational or reverse acclimations to beyond-optimal conditions, corroborating the experimental findings sometimes contradicting each other. I explained the fluctuations' beneficial effects in more detail as these were predicted in six out of nine hypothetical scenarios of the framework. In short, a fluctuating regime with the same average temperature as a stressful static regime may provide a refuge when the duration and intensity of critical exposures during fluctuations do not negatively impact the ectotherm's capacity for metabolic suppression and recovery. In the Discussion of Chapter 2, it is further explained that such refuge effects are relevant for eurythermal ectotherms from highly fluctuating environments as they commonly lack a capacity for warm compensational acclimation (Stillman, 2003; Seebacher et al., 2014), possibly due to a trade-off favoring the ability to actively control metabolic performance (McMahon et al., 1995). Thus, thermal fluctuations' refuge effects may be vital for these ectotherms as climate change induces intensification and elongation of extremely warm events in many coastal and shallow-water regions (Holbrook et al., 2019).

Scenarios of temporal changes in thermal metabolic performance are also presented in the hypotheses set of Chapter 3. Here, the null and alternative hypotheses were predicted based on time-dependent changes not only in the thermal thresholds of metabolic suppression and recovery but also in the absolute values of metabolic performance at benign (recovery) phases. The assumptions of both hypothesis sets are still simplistic. In reality, for example, adaptation to warmer regimes may also change the slope of gradual temperature-induced changes in metabolic performance. Nonetheless, such principle-based hypotheses sets are still crucial to improve the capacity for generalization from empirical studies. Acknowledging that all biological systems have some capacity for elastic metabolic performance in response to environmental variation, the frameworks presented here may be generalized to other systems.

Notably, the hypothesis sets can be modified with the aim to explain the organismal performance in response to different external drivers (e.g., the dissolved oxygen concentration or salinity) or the co-variabilities (see the General Introduction).

May summer heatwaves induce warm adaptation?

As expected, based on literature findings and the results from Chapter 2, we found that the transplanted mussels incubated under the intensified summer regime had a minor capacity for warm compensational acclimation (as evidenced by the warming-induced decline of growth; Chapter 3; Vajedsamiei et al. submitted). Nevertheless, this thesis provides support for the hypotheses jointly proposing that extremely warm seasons (events) may select ectotherm recruits with lower baseline demand for metabolic substrates, the capacity mediating their higher heat tolerance in response to cyclic thermal fluctuations. Compared to the recruited mussels grown under the less-extreme summer regime (current), the recruited mussels from the extremely warm summer regime (future) had (i) lower metabolic demand at constant exposure to a mild temperature and (ii) were afterward more capable of recovering their metabolic performance (filtration and respiration) at benign phases of the two successive 24 h thermal FOFS fluctuations.

In line with the *metabolic cold adaptation* or the *temperature compensation hypothesis* (Hazel and Prosser, 1974; Clarke, 2003; Le Lann et al., 2011), it is argued in Chapter 3 that more heat-tolerant ectothermic individuals, compared to less tolerant ones, would tend to have lower metabolic demands allowing them to better control metabolic supply and demand mismatch occurring at high beyond-optimal temperatures. The energetic debt, stress, and damages associated with such a mismatch would be directly linked to an organism's basic levels of metabolic demand.

Notably, the findings do not strictly mean that the selection of heat-tolerant individuals at very early life-history stages will lead to populations adapted to ocean warming, as suggested by some recent studies (Logan et al., 2014; Ma et al., 2014; Gilbert and Miles, 2017). In contrast, we observed a 96.5 percent decline in mussel recruitment success and ca. 30 percent decrease in transplanted mussels' growth rate due to the warmed summer regime. Such selective forces may substantially reduce the abundance, performance, and genetic diversity of populations and, therefore, decrease populations' persistence in response to future extreme events (Grant et al., 2017; Klerks et al., 2019). Besides, selecting individuals highly tolerant to one environmental factor (regime) may cause cross-tolerance or increased sensitivity against other environmental

factors (Al-Janabi et al., 2019), making inference and generalization from empirical findings even more complicated. Nevertheless, insights about possible mechanisms of fast warm adaptation in ectotherm metazoans may enable such generalization and advance the science of artificial selection (Carabaño et al., 2019; Ding et al., 2020).

Perspectives for future research

This thesis emphasizes the importance of investigating marine ectotherms' thermal metabolic performance in response to environmental variations within naturally-relevant timescales. While the studies focused on the feeding and aerobic respiration rates of mussels, future studies can be more inclusive and record other response variables such as the excretion rate and assimilation efficiency for a variety of model heterotrophs or photosynthesis rates for autotrophs.

Collecting such data in side-incubations or longer-term assays can provide valuable insights on how the capacity for thermal metabolic suppression and recovery is altered by acclimation. Further evaluation of mechanistic hypotheses such as the one tested here (based on the role of metabolic demand) helps us to generalize from empirical findings to the real-world significance of acclimation and selection in fast warm adaptation of ectothermic metazoan populations. More specifically, such studies need to test the following hypotheses:

- (i) Inter-individual variability in metabolic demand is related to the spatial or temporal variability in thermal tolerance.
- (ii) Natural selection by extreme events favors individuals having lower metabolic demands.
- (iii) Inter-individual variability in metabolic demand (and its thermal sensitivity) is significantly linked to inter-individual variability in the capacity for warm compensational acclimation.
- (iv) Warm acclimation of individuals will result in lower metabolic demands.

Success in relating metabolic demand variability to the organisms' capacity for warm acclimation and rapid evolutionary adaptation would enable us to improve the predictions regarding global climate change impacts on ecosystems. Particularly, the roles of other environmental forces such as deoxygenation, acidification, and (de)salination as well as biological forces such as predation and parasitism can be also explained in terms of their

impacts on the metabolic demand which itself may mediate the capacity for metabolic suppression and recovery.

References (for General Introduction and General Discussion)

- Al-Janabi, B., Wahl, M., Karsten, U., Graiff, A., and Kruse, I. (2019). Sensitivities to global change drivers may correlate positively or negatively in a foundational marine macroalga. *Sci. Rep.* 9, 14653. doi:10.1038/s41598-019-51099-8.
- Angilletta, M. J. (2006). Estimating and comparing thermal performance curves. *J. Therm. Biol.* 31, 541–545. doi:10.1016/j.jtherbio.2006.06.002.
- Barry, J. P., Baxter, C. H., Sagarin, R. D., and Gilman, S. E. (1995). Climate-related, long-term faunal changes in a California rocky intertidal community. *Science* (80-.). 267, 672–675. doi:10.1126/science.267.5198.672.
- Benedetti-Cecchi, L. (2005). Unanticipated impacts of spatial variance of biodiversity on plant productivity. *Ecol. Lett.* 8, 791–799. doi:10.1111/j.1461-0248.2005.00780.x.
- Bernhardt, J. R., Sunday, J. M., Thompson, P. L., and O'Connor, M. I. (2018). Nonlinear averaging of thermal experience predicts population growth rates in a thermally variable environment. *Proc. R. Soc. B Biol. Sci.* 285, 20181076. doi:10.1098/rspb.2018.1076.
- Boyd, P. W., Cornwall, C. E., Davison, A., Doney, S. C., Fourquez, M., Hurd, C. L., et al. (2016). Biological responses to environmental heterogeneity under future ocean conditions. *Glob. Chang. Biol.* 22, 2633–2650. doi:10.1111/gcb.13287.
- Bozinovic, F., Bastías, D. A., Boher, F., Clavijo-Baquet, S., Estay, S. A., and Angilletta, M. J. (2011). The mean and variance of environmental temperature interact to determine physiological tolerance and fitness. *Physiol. Biochem. Zool.* 84, 543–552. doi:10.1086/662551.
- Brewer, P. G., Fabry, V. J., Hilmi, K., Jung, S., Poloczanska, E., and Sundby, S. (2014). Chapter 30. The Ocean. *Clim. Chang. 2014 Impacts, Adapt. Vulnerability. Contrib. Work. Gr. II to Fifth Assess. Rep. Intergov. Panel Clim. Chang.*, 1–138. Available at: http://ipcc-wg2.gov/AR5/images/uploads/WGIIAR5-Chap30_FGDall.pdf.
- Burge, C. A., Closek, C. J., Friedman, C. S., Groner, M. L., Jenkins, C. M., Shore-Maggio, A., et al. (2016). The use of filter-feeders to manage disease in a changing world. *Integr. Comp. Biol.* 56, 573–587. doi:10.1093/icb/icw048.
- Carabaño, M. J., Ramón, M., Menéndez-Buxadera, A., Molina, A., and Díaz, C. (2019). Selecting for heat tolerance. *Anim. Front.* 9, 62–68. doi:10.1093/af/vfy033.
- Chaloub, R. M., Motta, N. M. S., de Araujo, S. P., de Aguiar, P. F., and da Silva, A. F. (2015). Combined effects of irradiance, temperature and nitrate concentration on phycoerythrin content in the microalga *Rhodomonas sp.* (cryptophyceae). *Algal Res.* 8, 89–94. doi:10.1016/j.algal.2015.01.008.
- Chesson, P., Donahue, M. J., Melbourne, B., and Sears, A. L. W. (2003). Chapter 6: Scale Transition Theory for understanding mechanisms in metacommunities. *Transition*, 1–29.
- Clarke, A. (2003). Costs and consequences of evolutionary temperature adaptation. *Trends Ecol. Evol.* 18, 573–581. doi:https://doi.org/10.1016/j.tree.2003.08.007.

- Clausen, I., and Riisgaard, H. U. (1996). Growth, filtration and respiration in the mussel *Mytilus edulis*: no evidence for physiological regulation of the filter-pump to nutritional needs. *Mar. Ecol. Prog. Ser.* 141, 37–45. doi:10.3354/meps141037.
- Davenport, J., and Davenport, J. L. (2005). Effects of shore height, wave exposure and geographical distance on thermal niche width of intertidal fauna. *Mar. Ecol. Prog. Ser.* 292, 41–50. doi:10.3354/meps292041.
- Denny, M. (2019). Performance in a variable world: using Jensen's inequality to scale up from individuals to populations. *Conserv. Physiol.* 7. doi:10.1093/conphys/coz053.
- Denny, M., and Benedetti-Cecchi, L. (2012). Scaling Up in Ecology: Mechanistic Approaches. *Annu. Rev. Ecol. Evol. Syst.* 43, 1–22. doi:10.1146/annurev-ecolsys-102710-145103.
- Deutsch, C. A., Tewksbury, J. J., Huey, R. B., Sheldon, K. S., Ghalambor, C. K., Haak, D. C., et al. (2008). Impacts of climate warming on terrestrial ectotherms across latitude. *Proc. Natl. Acad. Sci.* 105, 6668–6672. doi:10.1073/pnas.0709472105.
- Devey, D. (2005). Ecological genetics: design, analysis and application. Lowe A, Harris S, Ashton P. 2004. Oxford: Blackwell Publishing. 344 pp. *Ann. Bot.* 95, 705. doi:10.1093/aob/mci073.
- Ding, F., Li, A., Cong, R., Wang, X., Wang, W., Que, H., et al. (2020). The phenotypic and the genetic response to the extreme high temperature provides new insight into thermal tolerance for the pacific oyster *Crassostrea gigas*. *Front. Mar. Sci.* 7, 399.
- Dowd, W. W., King, F. A., and Denny, M. W. (2015). Thermal variation, thermal extremes and the physiological performance of individuals. *J. Exp. Biol.* 218, 1956–1967. doi:10.1242/jeb.114926.
- Ellington, W. R. (2001). Evolution and Physiological Roles of Phosphagen Systems. *Annu. Rev. Physiol.* 63, 289–325. doi:10.1146/annurev.physiol.63.1.289.
- Falfushynska, H. I., Sokolov, E., Piontkivska, H., and Sokolova, I. M. (2020). The role of reversible protein phosphorylation in regulation of the mitochondrial electron transport system during hypoxia and reoxygenation stress in marine bivalves. *Front. Mar. Sci.* 7, 467.
- Franz, M., Lieberum, C., Bock, G., and Karez, R. (2019). Environmental parameters of shallow water habitats in the SW Baltic Sea. *Earth Syst. Sci. Data* 11, 947–957. doi:10.5194/essd-11-947-2019.
- Frieder, C. A., Gonzalez, J. P., and Bockmon, E. E. (2014). Can variable pH and low oxygen moderate ocean acidification outcomes for mussel larvae? 754–764. doi:10.1111/gcb.12485.
- Gilbert, A. L., and Miles, D. B. (2017). Natural selection on thermal preference, critical thermal maxima and locomotor performance. *Proc. R. Soc. B Biol. Sci.* 284. doi:10.1098/rspb.2017.0536.
- Gili, J. M., and Coma, R. (1998). Benthic suspension feeders: Their paramount role in littoral marine food webs. *Trends Ecol. Evol.* 13, 316–321. doi:10.1016/S0169-5347(98)01365-2.

- Gómez, P. I., Palacios, Y., Arredondo-Vega, B. O., Guevara, M., and Saéz, K. (2016). Comparison of growth and biochemical parameters of two strains of *Rhodomonas salina* (Cryptophyceae) cultivated under different combinations of irradiance, temperature, and nutrients. *J. Appl. Phycol.* 28, 2651–2660. doi:10.1007/s10811-016-0835-2.
- Goocii, J. L., and Schopf, T. J. M. (1972). Genetic variability in the deep sea: relation to environmental variability. *Evolution (N. Y.)*. 26, 545–552. doi:10.1111/j.1558-5646.1972.tb01962.x.
- Gouhier, T. C., and Pillai, P. (2019). Commentary: Nonlinear averaging of thermal experience predicts population growth rates in a thermally variable environment. *Front. Ecol. Evol.* 7. doi:10.3389/fevo.2019.00236.
- Grant, P. R., Rosemary Grant, B., Huey, R. B., Johnson, M. T. J., Knoll, A. H., and Schmitt, J. (2017). Evolution caused by extreme events. *Philos. Trans. R. Soc. B Biol. Sci.* 372, 5–8. doi:10.1098/rstb.2016.0146.
- Gräwe, U., Friedland, R., and Burchard, H. (2013a). The future of the western Baltic Sea: Two possible scenarios. *Ocean Dyn.* 63, 901–921. doi:10.1007/s10236-013-0634-0.
- Gräwe, U., Friedland, R., and Burchard, H. (2013b). The future of the western Baltic Sea: Two possible scenarios. *Ocean Dyn.* 63, 901–921. doi:10.1007/s10236-013-0634-0.
- Gunderson, A. R., Armstrong, E. J., and Stillman, J. H. (2016). Multiple stressors in a changing world: the need for an improved perspective on physiological responses to the dynamic marine environment. *Ann. Rev. Mar. Sci.* 8, 357–378. doi:10.1146/annurev-marine-122414-033953.
- Hamburger, K., Møhlenberg, F., Randløv, A., and Riisgård, H. U. (1983). Size, oxygen consumption and growth in the mussel *Mytilus edulis*. *Mar. Biol.* 75, 303–306. doi:10.1007/BF00406016.
- Hammer, A., Schumann, R., and Schubert, H. (2002). Light and temperature acclimation of *Rhodomonas salina*: photosynthetic performance. 29, 287–296. Available at: www.int-res.com.
- Harris, F. (1909). The Functional Inertia of Living Matter. *J. Am. Med. Assoc.* LII, 503–504. doi:10.1001/jama.1909.02540320075024.
- Havird, J. C., Neuwald, J. L., Shah, A. A., Mauro, A., Marshall, C. A., and Ghalambor, C. K. (2020). Distinguishing between active plasticity due to thermal acclimation and passive plasticity due to *Q10* effects: Why methodology matters. *Funct. Ecol.* 34, 1015–1028. doi:10.1111/1365-2435.13534.
- Hazel, J. R., and Prosser, C. L. (1974). Molecular mechanisms of temperature compensation in poikilotherms. *Physiol. Rev.* 54, 620–677. doi:10.1152/physrev.1974.54.3.620.
- Helmuth, B., Russell, B. D., Connell, S. D., Dong, Y., Harley, C. D., Lima, F. P., et al. (2014). Beyond long-term averages: making biological sense of a rapidly changing world. *Clim. Chang. Responses* 1, 6. doi:10.1186/s40665-014-0006-0.
- Helmuth, B. S. T., and Hofmann, G. E. (2001). Microhabitats, thermal heterogeneity, and patterns of physiological stress in the rocky intertidal zone. *Biol. Bull.* 201, 374–384.

- Hofmann, G. E., and Todgham, A. E. (2010). Living in the Now: Physiological Mechanisms to Tolerate a Rapidly Changing Environment. *Annu. Rev. Physiol.* 72, 127–145. doi:10.1146/annurev-physiol-021909-135900.
- Holbrook, N. J., Scannell, H. A., Sen Gupta, A., Benthuisen, J. A., Feng, M., Oliver, E. C. J., et al. (2019). A global assessment of marine heatwaves and their drivers. *Nat. Commun.* 10, 1–13. doi:10.1038/s41467-019-10206-z.
- Huey, R. B., Berrigan, D., Gilchrist, G. W., and Herron, J. O. N. C. (1999). Testing the adaptive significance of acclimation: A strong inference approach. *Am. Zool.* 39, 323–336. doi:10.1093/icb/39.2.323.
- Vajedsamiei, J., Abolfazl, S., Ali, M., Shirvani, A., and Hasan, S. (2014). Specific Thermal Regime and Coral Bleaching Pattern in Hengam Island, the Eastern Persian Gulf. *J. Persian Gulf* 5, 15–25.
- Jensen, J. L. W. V (1906). Sur les fonctions convexes et les inégalités entre les valeurs moyennes. *Acta Math.* 30, 175–193. doi:10.1007/BF02418571.
- Jentsch, A., Kreyling J., and B. C. (2007). A new generation of climate change experiments : events , not trends. *Front. Ecol. Environ.*
- Kang, H. Y., Lee, Y. J., Song, W. Y., Kim, T. I., Lee, W. C., Kim, T. Y., et al. (2019). Physiological responses of the abalone *Haliotis discus hannai* to daily and seasonal temperature variations. *Sci. Rep.* 9, 1–13. doi:10.1038/s41598-019-44526-3.
- Kearney, M., Simpson, S. J., Raubenheimer, D., and Helmuth, B. (2010). Modelling the ecological niche from functional traits. *Philos. Trans. R. Soc. B Biol. Sci.* 365, 3469–3483. doi:10.1098/rstb.2010.0034.
- Kingsolver, J. G., Higgins, J. K., and Augustine, K. E. (2015). Fluctuating temperatures and ectotherm growth: distinguishing non-linear and time-dependent effects. *J. Exp. Biol.* 218, 2218–2225. doi:10.1242/jeb.120733.
- Kingsolver, J. G., and Woods, H. A. (2016). Beyond Thermal Performance Curves: Modeling time-dependent effects of thermal stress on ectotherm growth rates. *Am. Nat.* 187, 283–294. doi:10.1086/684786.
- Kittner, C., and Riisgård, H. U. (2005). Effect of temperature on filtration rate in the mussel *Mytilus edulis*: No evidence for temperature compensation. 305, 147–152.
- Klerks, P. L., Athrey, G. N., and Leberg, P. L. (2019). Response to selection for increased heat tolerance in a small fish species, with the response decreased by a population bottleneck. *Front. Ecol. Evol.* 7, 270.
- Kooijman, S. a. L. M. (2010). Dynamic energy budget theory for metabolic organisation. *Cambridge Univ. Press. Cambridge, UK.* doi:10.1098/rstb.2010.0167.
- Koussoroplis, A. M., Pincebourde, S., and Wacker, A. (2017). Understanding and predicting physiological performance of organisms in fluctuating and multifactorial environments. *Ecol. Monogr.* 87, 178–197. doi:10.1002/ecm.1247.
- Koussoroplis, A. M., and Wacker, A. (2016). Covariance modulates the effect of joint temperature and food variance on ectotherm life-history traits. *Ecol. Lett.* 19, 143–152.

doi:10.1111/ele.12546.

- Larsson, J., Lind, E. E., Corell, H., Grahn, M., Smolarz, K., and Lönn, M. (2017). Regional genetic differentiation in the blue mussel from the Baltic Sea area. *Estuar. Coast. Shelf Sci.* 195, 98–109. doi:10.1016/j.ecss.2016.06.016.
- Le Lann, C., Wardziak, T., van Baaren, J., and van Alphen, J. J. M. (2011). Thermal plasticity of metabolic rates linked to life-history traits and foraging behaviour in a parasitic wasp. *Funct. Ecol.* 25, 641–651. doi:10.1111/j.1365-2435.2010.01813.x.
- Lennartz, S. T., Lehmann, A., Herrford, J., Malien, F., Hansen, H. P., Biester, H., et al. (2014). Long-term trends at the Boknis Eck time series station (Baltic Sea), 1957-2013: Does climate change counteract the decline in eutrophication? *Biogeosciences* 11, 6323–6339. doi:10.5194/bg-11-6323-2014.
- Leroi, A. M., Bennett, A. F., and Lenski, R. E. (1994). Temperature acclimation and competitive fitness: an experimental test of the beneficial acclimation assumption. *Proc. Natl. Acad. Sci.* 91, 1917 LP – 1921. doi:10.1073/pnas.91.5.1917.
- Lima, F. P., and Wethey, D. S. (2012). Three decades of high-resolution coastal sea surface temperatures reveal more than warming. *Nat. Commun.* 3, 1–13. doi:10.1038/ncomms1713.
- Logan, C. A., Dunne, J. P., Eakin, C. M., and Donner, S. D. (2014a). Incorporating adaptive responses into future projections of coral bleaching. *Glob. Chang. Biol.* 20, 125–139. doi:10.1111/gcb.12390.
- Logan, C. A., Dunne, J. P., Eakin, C. M., and Donner, S. D. (2014b). Incorporating adaptive responses into future projections of coral bleaching. *Glob. Chang. Biol.* 20, 125–139. doi:10.1111/gcb.12390.
- Logan, M. L., Curlis, J. D., Gilbert, A. L., Miles, D. B., Chung, A. K., McGlothlin, J. W., et al. (2018). Thermal physiology and thermoregulatory behaviour exhibit low heritability despite genetic divergence between lizard populations. *Proc. R. Soc. B Biol. Sci.* 285. doi:10.1098/rspb.2018.0697.
- Ma, F. Z., Lü, Z. C., Wang, R., and Wan, F. H. (2014). Heritability and evolutionary potential in thermal tolerance traits in the invasive Mediterranean cryptic species of *Bemisia tabaci* (Hemiptera: Aleyrodidae). *PLoS One* 9, 1–7. doi:10.1371/journal.pone.0103279.
- Ma, S., Tian, Y., Li, J., Yu, H., Cheng, J., Sun, P., et al. (2020). Climate variability patterns and their ecological effects on ecosystems in the Northwestern North Pacific. *Front. Mar. Sci.* 7, 752.
- Marshall, D. J., and McQuaid, C. D. (1991). Metabolic rate depression in a marine pulmonate snail: pre-adaptation for a terrestrial existence? *Oecologia* 88, 274–276. doi:10.1007/BF00320822.
- Martin, T. L., and Huey, R. B. (2008). Why “Suboptimal” Is Optimal: Jensen’s Inequality and Ectotherm Thermal Preferences. *Am. Nat.* 171, E102–E118. doi:10.1086/527502.
- McMahon, R. F., Russell-Hunter, W. D., and Aldridge, D. W. (1995). Lack of metabolic temperature compensation in the intertidal gastropods, *Littorina saxatilis* (Olivi) and *L. obtusata* (L.). *Hydrobiologia* 309, 89–100. doi:10.1007/BF00014475.

- Medvedev, I. P., Rabinovich, A. B., and Kulikov, E. A. (2016). Tides in Three Enclosed Basins: The Baltic, Black, and Caspian Seas. *Front. Mar. Sci.* 3, 46.
- Meier, H. E. M., Eilola, K., Gustafsson, B. G., Kuznetsov, I., Neumann, T., and Savchuk, O. P. (2012). Uncertainty assessment of projected ecological quality indicators in future climate. *Oceanography* 112.
- Monaco, C. J., and McQuaid, C. D. (2018). Applicability of Dynamic Energy Budget (DEB) models across steep environmental gradients. *Sci. Rep.* 8, 1–14. doi:10.1038/s41598-018-34786-w.
- Morón Lugo, S. C., Baumeister, M., Nour, O. M., Wolf, F., Stumpp, M., and Pansch, C. (2020). Warming and temperature variability determine the performance of two invertebrate predators. *Sci. Rep.* 10, 1–14. doi:10.1038/s41598-020-63679-0.
- Nasrolahi, A., Pansch, C., Lenz, M., and Wahl, M. (2012). Being young in a changing world: how temperature and salinity changes interactively modify the performance of larval stages of the barnacle *Amphibalanus improvisus*. *Mar. Biol.* 159, 331–340. doi:10.1007/s00227-011-1811-7.
- Niehaus, A. C., Angilletta, M. J., Sears, M. W., Franklin, C. E., and Wilson, R. S. (2012). Predicting the physiological performance of ectotherms in fluctuating thermal environments. *J. Exp. Biol.* 215, 694–701. doi:10.1242/jeb.058032.
- Paaijmans, K. P., Heinig, R. L., Seliga, R. A., Blanford, J. I., Blanford, S., Murdock, C. C., et al. (2013). Temperature variation makes ectotherms more sensitive to climate change. *Glob. Chang. Biol.* 19, 2373–2380. doi:10.1111/gcb.12240.
- Padfield, D., Yvon-Durocher, G., Buckling, A., Jennings, S., and Yvon-Durocher, G. (2016). Rapid evolution of metabolic traits explains thermal adaptation in phytoplankton. *Ecol. Lett.* 19, 133–142. doi:10.1111/ele.12545.
- Pansch, C., Scotti, M., Barboza, F. R., Al-Janabi, B., Brakel, J., Briski, E., et al. (2018). Heat waves and their significance for a temperate benthic community: A near-natural experimental approach. *Glob. Chang. Biol.* 24, 4357–4367. doi:10.1111/gcb.14282.
- Pleissner, D., Lundgreen, K., Luskow, F., and Riisgård, H. U. (2013). Fluorometer Controlled Apparatus designed for long-duration algal-feeding experiments and environmental effect studies with mussels. *J. Mar. Biol.* 2013, 1–12. doi:10.1155/2013/401961.
- Podrabsky, J. E., and Somero, G. N. (2004). Changes in gene expression associated with acclimation to constant temperatures and fluctuating daily temperatures in an annual killifish *Austrofundulus limnaeus*. *J. Exp. Biol.* 207, 2237–2254. doi:10.1242/jeb.01016.
- Pörtner, H. (2012). Integrating climate-related stressor effects on marine organisms: unifying principles linking molecule to ecosystem-level changes. 470, 273–290. doi:10.3354/meps10123.
- Pörtner, H. O., and Farrell, A. P. (2008). Physiology and Climate Change. *Science* (80-.). 322, 690 LP – 692. doi:10.1126/science.1163156.
- Reusch, T. B. H., Dierking, J., Andersson, H. C., Bonsdorff, E., Carstensen, J., Casini, M., et al. (2018). The Baltic Sea as a time machine for the future coastal ocean. *Sci. Adv.* 4, eaar8195. doi:10.1126/sciadv.aar8195.

- Riisgård, H. (2001). On measurement of filtration rate in bivalves—the stony road to reliable data: review and interpretation. *Mar. Ecol. Prog. Ser.* 211, 275–291. doi:10.3354/meps211275.
- Riisgård, H. U., Luskow, F., Pleissner, D., Lundgreen, K., and López, M. Á. P. (2013). Effect of salinity on filtration rates of mussels *Mytilus edulis* with special emphasis on dwarfed mussels from the low-saline Central Baltic Sea. *Helgol. Mar. Res.* 67, 591–598. doi:10.1007/s10152-013-0347-2.
- Ritchie, M. E. (2018). Reaction and diffusion thermodynamics explain optimal temperatures of biochemical reactions. *Sci. Rep.* 8, 1–10. doi:10.1038/s41598-018-28833-9.
- Ruel, J. J., and Ayres, M. P. (1999). Jensen's Inequality predicts effects of environmental variation. *Tree* 5347, 361–366. doi:10.1016/S0169-5347(99)01664-X.
- Saderne, V., Fietzek, P., and Herman, P. M. J. (2013). Extreme variations of pCO₂ and pH in a Macrophyte Meadow of the Baltic Sea in summer: Evidence of the effect of photosynthesis and local upwelling. *PLoS One* 8, e62689.
- Safaie, A., Silbiger, N. J., McClanahan, T. R., Pawlak, G., Barshis, D. J., Hench, J. L., et al. (2018). High frequency temperature variability reduces the risk of coral bleaching. *Nat. Commun.* 9, 1–12. doi:10.1038/s41467-018-04074-2.
- Sagarin, R. D., Barry, J. P., Gilman, S. E., and Baxter, C. H. (1999). Climate-related change in an intertidal community over short and long time scales. *Ecol. Monogr.* 69, 465–490. doi:10.2307/2657226.
- Saleh, A., Vajedsamiei, J., Amini-Yekta, F., Seyed Hashtroudi, M., Chen, C. T. A., and Fumani, N. S. (2020). The carbonate system on the coral patches and rocky intertidal habitats of the northern Persian Gulf: Implications for ocean acidification studies. *Mar. Pollut. Bull.* 151, 110834. doi:10.1016/j.marpolbul.2019.110834.
- Sanders, T., Schmittmann, L., Nascimento-Schulze, J. C., and Melzner, F. (2018). High calcification costs limit mussel growth at low salinity. *Front. Mar. Sci.* 5, 1–9. doi:10.3389/fmars.2018.00352.
- Schulte, P. M., Healy, T. M., and Fangué, N. A. (2011a). Thermal performance curves, phenotypic plasticity, and the time scales of temperature exposure. *Integr. Comp. Biol.* 51, 691–702. doi:10.1093/icb/icr097.
- Schulte, P. M., Healy, T. M., and Fangué, N. A. (2011b). Thermal Performance Curves , Phenotypic Plasticity , and the Time Scales of Temperature Exposure. 1–12. doi:10.1093/icb/icr097.
- Secor, S. M. (2009). Specific dynamic action: A review of the postprandial metabolic response. *J. Comp. Physiol. B Biochem. Syst. Environ. Physiol.* 179, 1–56. doi:10.1007/s00360-008-0283-7.
- Seebacher, F., White, C. R., and Franklin, C. E. (2014). Physiological plasticity increases resilience of ectothermic animals to climate change. 1–6. doi:10.1038/NCLIMATE2457.
- Sinclair, B. J., Marshall, K. E., Sewell, M. A., Levesque, D. L., Willett, C. S., Slotsbo, S., et al. (2016). Can we predict ectotherm responses to climate change using thermal performance curves and body temperatures? *Ecol. Lett.* 19, 1372–1385.

doi:10.1111/ele.12686.

- Soares, H. C., Gherardi, D. F. M., Pezzi, L. P., Kayano, M. T., and Paes, E. T. (2014). Patterns of interannual climate variability in large marine ecosystems. *J. Mar. Syst.* 134, 57–68. doi:<https://doi.org/10.1016/j.jmarsys.2014.03.004>.
- Sokolova, I. M., and Pörtner, H. O. (2001). Physiological adaptations to high intertidal life involve improved water conservation abilities and metabolic rate depression in littorina saxatilis. *Mar. Ecol. Prog. Ser.* 224, 171–186. doi:10.3354/meps224171.
- Somero, G. N. (2010). The physiology of climate change: how potentials for acclimatization and genetic adaptation will determine “winners” and “losers.” *J. Exp. Biol.* 213, 912–920. doi:10.1242/jeb.037473.
- Sperfeld, E., Raubenheimer, D., and Wacker, A. (2016). Bridging factorial and gradient concepts of resource co-limitation: Towards a general framework applied to consumers. *Ecol. Lett.* 19, 201–215. doi:10.1111/ele.12554.
- Stillman, J. H. (2003). Acclimation capacity underlies susceptibility to climate change. *Science* 301, 65. doi:10.1126/science.1083073.
- Stuckas, H., Knöbel, L., Schade, H., Breusing, C., Hinrichsen, H. H., Bartel, M., et al. (2017). Combining hydrodynamic modelling with genetics: can passive larval drift shape the genetic structure of Baltic *Mytilus* populations? *Mol. Ecol.* 26, 2765–2782. doi:10.1111/mec.14075.
- Vajedsamiei, J., Saleh, A., Mehdinia, A., Shirvani, A., and Sharifi, H. (2014). Specific thermal regime and coral bleaching pattern in Hengam Island, eastern Persian Gulf. *J. the Persian Gulf.* 1–16.
- Vajedsamiei, J., Melzner, F., Raatz, M., Kiko, R., Khosravi, M., and Pansch, C. (2021). Simultaneous recording of filtration and respiration in marine organisms in response to short-term environmental variability. *Limnol. Oceanogr. Methods* n/a. doi:<https://doi.org/10.1002/lom3.10414>.
- van der Schatte Olivier, A., Jones, L., Vay, L. Le, Christie, M., Wilson, J., and Malham, S. K. (2018). A global review of the ecosystem services provided by bivalve aquaculture. *Rev. Aquac.*, 1–23. doi:10.1111/raq.12301.
- Vasseur, D. A., DeLong, J. P., Gilbert, B., Greig, H. S., Harley, C. D. G., McCann, K. S., et al. (2014). Increased temperature variation poses a greater risk to species than climate warming. *Proc. R. Soc. B Biol. Sci.* 281. doi:10.1098/rspb.2013.2612.
- Verberk, W. C. E. P., Overgaard, J., Ern, R., Bayley, M., Wang, T., Boardman, L., et al. (2016). Does oxygen limit thermal tolerance in arthropods? A critical review of current evidence. *Comp. Biochem. Physiol. -Part A Mol. Integr. Physiol.* 192, 64–78. doi:10.1016/j.cbpa.2015.10.020.
- Wahl, M., Buchholz, B., Winde, V., Golomb, D., Guy-Haim, T., Müller, J., et al. (2015). A mesocosm concept for the simulation of near-natural shallow underwater climates: The Kiel Outdoor Benthocosms (KOB). *Limnol. Oceanogr. Methods* 13, 651–663. doi:10.1002/lom3.10055.

- Wahl, M., Saderne, V., and Sawall, Y. (2016). How good are we at assessing the impact of ocean acidification in coastal systems? Limitations, omissions and strengths of commonly used experimental approaches with special emphasis on the neglected role of fluctuations. *Mar. Freshw. Res.* 67, 25–36. doi:10.1071/MF14154.
- Walter, J., Jentsch, A., Beierkuhnlein, C., and Kreyling, J. (2013). Ecological stress memory and cross stress tolerance in plants in the face of climate extremes. *Environ. Exp. Bot.* 94, 3–8. doi:https://doi.org/10.1016/j.envexpbot.2012.02.009.
- Wang, G., and Dillon, M. E. (2014). Recent geographic convergence in diurnal and annual temperature cycling flattens global thermal profiles. *Nat. Clim. Chang.* 4, 988–992. doi:10.1038/nclimate2378.
- Wethey, D. S., and Woodin, S. a. (2008). Ecological hindcasting of biogeographic responses to climate change in the European intertidal zone. *Hydrobiologia* 606, 139–151. doi:10.1007/s10750-008-9338-8.
- Wethey, D. S., Woodin, S. A., Hilbish, T. J., Jones, S. J., Lima, F. P., and Brannock, P. M. (2011). Response of intertidal populations to climate: Effects of extreme events versus long term change. *J. Exp. Mar. Bio. Ecol.* 400, 132–144. doi:10.1016/j.jembe.2011.02.008.
- Widdows, J. (1976). Physiological adaptation of *Mytilus edulis* to cyclic temperatures. *J. Comp. Physiol. B* 105, 115–128. doi:10.1007/BF00691115.
- Widdows, J., Brinsley, M. D., Salkeld, P. N., and Elliott, M. (1998). Use of annular flumes to determine the influence of current velocity and bivalves on material flux at the sediment-water interface. *Estuaries* 21, 552. doi:10.2307/1353294.
- Widdows, J., and Hawkins, A. J. S. (1989). Partitioning of rate of heat dissipation by *Mytilus edulis* into maintenance, feeding, and growth components. *Physiol. Zool.* 62, 764–784. doi:10.1086/physzool.62.3.30157926.
- Wittmann, A. C., Schröer, M., Bock, C., Steeger, H. U., Paul, R. J., and Pörtner, H. O. (2008). Indicators of oxygen- and capacity-limited thermal tolerance in the lugworm *Arenicola marina*. *Clim. Res.* 37, 227–240. doi:10.3354/cr00763.
- Wolf, F., Bumke, K., Wahl, S., Nevoigt, F., Hecht, U., Hiebenthal, C., et al. (2020). High resolution water temperature data between January 1997 and December 2018 at the GEOMAR pier surface. doi:10.1594/PANGAEA.919186.
- Zippay, M. L., and Helmuth, B. (2012). Effects of temperature change on mussel, *Mytilus*. *Integr. Zool.* 7, 312–327. doi:10.1111/j.1749-4877.2012.00310.x.

Supplementary Information to Chapters 1–3

SI for Chapter 1 “Simultaneous recording of filtration and respiration in marine organisms in response to short-term environmental variability”

Contents:

Supplementary Texts

Supplementary Figures

Supplementary Tables

Supplementary Python scripts

Supplementary Texts

Text S1: Temperature correction and conversion coefficients for chlorophyll data

Food concentrations food_M are measured as chlorophyll fluorescence intensity in units of mV using the fluorimeters. Fluorescence, however, decreases linearly with temperature (Turner Designs 2020). Thus, we must correct the food concentrations (food_M in mV) that are measured at different temperatures (T_M in °C) during the trials using a temperature correction coefficient (c) that gives the relative change in fluorescence intensity per °C deviation from the reference temperature (T_R).

$$\text{Eq. S1 } \text{food}_{MTC} = \frac{\text{food}_M}{1 - c \times (T_M - T_R)}$$

c is estimated by conducting fluorometry at different temperatures when the fluorometry chamber is filled with the standard solution (RWT 400 ppb, Turner Design, San Jose, USA). For our system, we obtained $c = 0.022$ per °C deviations from the reference temperature of 18 °C (Fig. S2).

The reference temperature is the temperature at which also the food concentration conversion-coefficient χ in units of cells mL⁻¹ per mV is defined. Different fluorimeters show absolutely different but proportionally equal responses to a concentration change. As the inflow to all paths is identical, it is enough to define χ only for the fluorometer deployed in Path_C. Samples can be taken from the final outflow of Path_C when FOFS is running in the absence of mussels at the reference temperature. The samples were then immediately analyzed for the cell concentration (cells mL⁻¹) using a Cell and Particle Counter (Coulter Z2, Beckman Coulter GmbH, Krefeld, Germany; set to detect particles of the expected *R. salina* dimensional range 5–8 µm diameter). The ratio of cells mL⁻¹/mV is then used as the conversion coefficient χ . We obtained $\chi = \frac{2438}{366} \cong 6.7$, based on the samples taken from the outflow of Path_C at the end of the pre-trial (October 16, 2019).

Text S2: Criterion for selecting the ‘pre- or post-trial stable data’

In the Script S2 (FOFS_trial_by_trial_processing.py), pre- and post-trial stable data are chosen and used, respectively, to correct the baseline variations between sensors’ measurements and estimate the random confounding drifts. As time passes in a pre- or a post-trial, the actual concentration of food (or dissolved oxygen) becomes more comparable between suspensions in different fluorometry (or oximetry) chambers, given there is the baseline discrepancies between the sensor measurements. The stable data interval is when the actual concentration of food (or dissolved oxygen) is comparable between the fluorometry (or oximetry) chambers.

We calculate the ‘lag-time’ which is a system parameter that describes how quickly the initial difference of food (or oxygen) concentration between the dilution tank’s suspension being pumped into a path and the suspension flowing out of the fluorometry (or oximetry) chamber is removed during a pre- or a post-trial. The ‘lag-time’ (t_{lag}) is described as

$$\text{Eq. S2. } t_{\text{lag}} = \frac{-\ln \frac{C_{\text{in}} - C_{\text{out}_{t_0+t_{\text{lag}}}}}{C_{\text{in}} - C_{\text{out}_{t_0}}}}{\frac{F}{V_i}},$$

where C_{in} and C_{out} are the food (or dissolved oxygen) concentrations of the inflow to a path and outflow of the fluorometry (or oximetry) chamber, respectively, t_0 is the time of the start of the pre- or post-trial, F is the flow rate and V_i is the integrated volume of the chambers positioned downstream to the respective fluorometer (or dissolved-oxygen sensor). For example, in our FOFS, V_i is $350 + 100 = 450$ mL for each fluorometer and 100 mL for each oximeter. Applying the V_i values, $F = 16$ mL min^{-1} , and the ratio $\frac{C_{in} - C_{out_t}}{C_{in} - C_{out_{t_0}}} = 0.01$ into Eq. S2, we estimate the time needed for the removal of 99 % of the initial difference, $t_{lag99\%} \cong 130$ and 29 min, for the real food and oxygen concentrations, respectively. The lower limit of the stable data interval must be chosen to be $> t_{99\%}$. Eq. S2 is a version of Eq. S6 (derived in Text S3) solved for the time, but with different definitions of the concentration and volume variables.

Text S3: Dampening-effect correction

One way to decrease the dampening effect is to choose and apply a higher experimental flow rate, but this is not always possible as the flow rate is reversely related to the magnitude of the respiration signal (that is usually small).

The script (FOFS_trial_by_trial_processing.py) applies a linear differential modelling to correct for the dampening of rapid changes in the measured food concentrations and thus achieve a better estimation of the food concentration in the oximetry chamber. Here we explain the procedure enabling to correct for the dampening of rapid concentration changes caused by the study organisms' filtration shutdown or recovery.

We assume that the concentration of the inflow into the fluorometry chamber ($food_{In}$) is altered by a rapid change in the filtration activity at time t_0 . Afterwards, $food_{In}$ stays constant at least for a short duration ($food_{in_{t_0}} \cong food_{in_t}$). Then, we describe the dynamic system as a linear differential equation (Campbell and Haberman 2008):

$$\text{Eq. S3. } \frac{dx}{dt} + \frac{F}{V} x = food_{in} F,$$

where x is the number of cells in the fluorometry chamber at the time t , F is the flow rate, and V is the volume of the fluorometry chamber. Therefore, the first term in Eq. S2 represents the change of the food concentration in the fluorometry chamber following the rapid change in the oximetry chamber, the second term gives the outflow from the fluorometry chamber and the right-hand side is the inflow into the fluorometry chamber. The solution to this linear differential equation is

$$\text{Eq. S4. } x_t = \frac{food_{in} F}{\frac{F}{V}} + a e^{-Ft/V} = food_{in} V + a e^{-Ft/V},$$

where a is a constant defined by the initial conditions x_{t_0} . Diving both sides of Eq. S4 by V results in

$$\text{Eq. S5. } food_{M_t} = food_{in} + \frac{a}{V} e^{-Ft/V},$$

where food_{M_t} is the fluorometrically-measured concentration at time t (which is dampened compared to food_{in}) and, by choosing $t_0 = 0$, $\frac{a}{V}$ is the initial concentration difference ($\text{food}_{M_{t_0}} - \text{food}_{in}$). Thus, Eq. S5 can be rewritten as

$$\text{Eq. S6. } \frac{\text{food}_{M_t} - \text{food}_{in}}{\text{food}_{M_{t_0}} - \text{food}_{in}} = e^{-\frac{Ft}{V}}.$$

Since $\frac{\text{food}_{M_t} - \text{food}_{in}}{\text{food}_{M_{t_0}} - \text{food}_{in}} = \frac{\text{food}_{M_t} - \text{food}_{M_{t_0}}}{\text{food}_{M_{t_0}} - \text{food}_{in}} + 1$, Eq. S6 can be rewritten as

$$\text{Eq. S7. } \text{food}_{M_{t_0}} - \text{food}_{in} = \left(\text{food}_{M_t} - \text{food}_{M_{t_0}} \right) \frac{1}{e^{-\frac{Ft}{V}} - 1},$$

and

$$\text{Eq. S8. } \text{food}_{in} = \text{food}_{M_{t_0}} + \left(\text{food}_{M_t} - \text{food}_{M_{t_0}} \right) \frac{1}{1 - e^{-\frac{Ft}{V}}},$$

which allows to estimate the food concentration in the oximetry chamber food_{in} at t_0 from the measured food concentrations at t_0 and some later time point t .

If we now assume the time span between these two time points to be Δt , and that food_{in} stays constant for at least Δt then we can correct the inflow food concentration for every time point t during the treatment using the measured concentration from that time point and from a later time point.

$$\text{Eq. S9. } \text{food}_{in_t} = \text{food}_{M_t} + \left(\text{food}_{M_{t+\Delta t}} - \text{food}_{M_t} \right) \frac{1}{1 - e^{-\frac{F\Delta t}{V}}}.$$

Eq. S9 is used in the script to achieve the dampening correction and obtain the dampening-corrected food-concentration food_{in_t} (in cells mL^{-1}) at time t . The work flow goes as follows: (i) each data series (`cells_per_ml_C` or `cells_per_ml_Sn`) is differenced using a sliding time-window of differencing (length of the window Δt is specified in the 'Variables definition' section of the script), (ii) the difference between each two measured food-concentrations ($\text{food}_{M_{t+\Delta t}} - \text{food}_{M_t}$) is corrected by the dampening-effect correction-coefficient $\frac{1}{1 - e^{-\frac{F\Delta t}{V}}}$ (specified in the 'Variables definition' section), (iii) the corrected difference is added back to the data point, food_{M_t} . The volume of the fluorometry chamber (350 mL in our FOFS) and the flow rate are also defined in the 'Variables definition' section of the script.

Text S4: Temperature sensitivity of the planktonic food

During a FOFS trial, the phytoplanktonic food is exposed to the treatment only for a short period of time from their injection into the dilution tank until their release into the final outflow of the setup. Yet, it must be checked that the exposure does not impose substantial changes on the cells' concentration.

We assessed the concentration of *Rhodomonas salina* applied as the food in our FOFS in the four final outflows and the food-tank suspension hourly, during a temperature ramp on October 15, 2019 when FOFS was run in the absence of filter-feeders. The concentrations were stable

in time (Fig. S3), suggesting that the short-term thermal exposures as occurring in our FOFS imposes no substantial impact on the concentration and integrity of *R. salina* cells.

Text S5: Mytilus filtration and respiration based on published literature

In addition to our main assessment, here we compare our estimates of the average baseline filtration and respiration rates of *Mytilus* (over the initial period of the mussel trials of the demonstration experiment) with related published literature values. It is worth to notice that all differences between the systems studied by us versus others can create a discrepancy between our observations and the predictions. This comparison is thus aimed solely to indicate that the absolute values of our estimates are in line with expectations.

The following published-studies describe filtration and respiration rates of *Mytilus edulis* at optimal conditions as functions of body-size variables. Pleissner et al. (2013) described the filtration rate (F in mL min^{-1}) using a flow-through setup as a function of the shell length (L in mm); $F = 0.0024 \times L^{2.01} \times \left(\frac{1000}{60}\right)$. Hamburger et al. (1983) described the respiration rate (R in $\mu\text{molO}_2 \text{ h}^{-1}$) in the presence of flagellate foods *Isochrysis galbana* and *Monochrysis lutheri* using a closed chamber setup as a function of tissue dry weight (W in g); $R = 0.475 \times W^{0.663} \times \left(\frac{44.6596}{60}\right)$.

When we apply the size characteristics of our studied mussels (mean shell length 45 mm and mean dry tissue weight 0.63 g) into these equations, the predicted rates of length-specific filtration and weight-specific respiration are $1.85 \text{ mL mm}^{-1} \text{ min}^{-1}$ and $0.41 \mu\text{molO}_2 \text{ g}^{-1} \text{ h}^{-1}$ from these equations. Our experimentally determined average estimates are $1.3 \text{ mL mm}^{-1} \text{ min}^{-1}$ and $0.4 \mu\text{mol O}_2 \text{ g}^{-1} \text{ h}^{-1}$, respectively (Fig. 5a, c).

References:

- Campbell, S., and R. Haberman. 2008. Introduction to differential equations with dynamical systems. Princeton University Press.
- Hamburger, K., F. Mohlenberg, A. Randlov, and H. U. Riisgård. 1983. Marine Size, oxygen consumption and growth in the mussel *Mytilus edulis*. *J Mar Biol* **75**: 303–306.
- Pleissner, D., K. Lundgreen, F. Luskow, and H. U. Riisgård. 2013. Fluorometer controlled apparatus designed for long-duration algal-feeding experiments and environmental effect studies with mussels. *J Mar Biol* **2013**: 401961.
- Turner Designs. 2020. Cyclops submersible sensors: User's manual.

Supplementary Figures

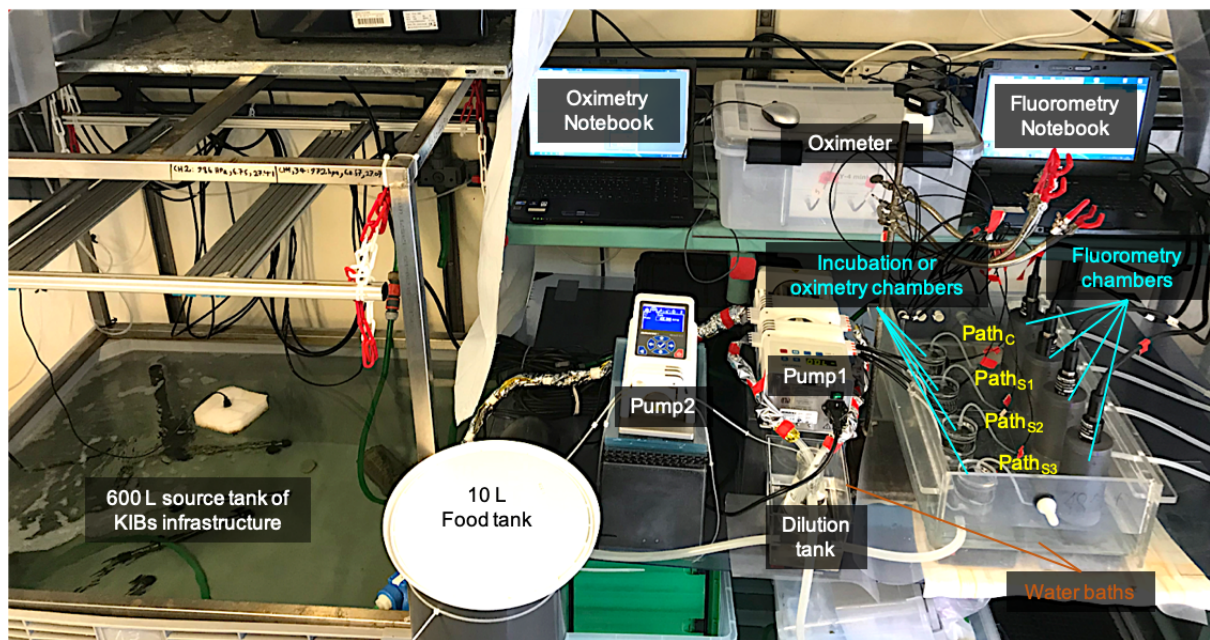


Fig. S1. Photographic view of the Fluorometer- and Oximeter-equipped flow-through setup (FOFS). Path_c stands for the control path in which the oximetry and fluorometry are conducted in the absence of any study specimen (from the incubation or oximetry chamber) over all stages (pre-, main-, and post-trial), while within Path_{s_n} the oximetry and fluorometry are conducted in the presence of specimens during the main trial. For details on water flows see also Fig. 1 in the paper.

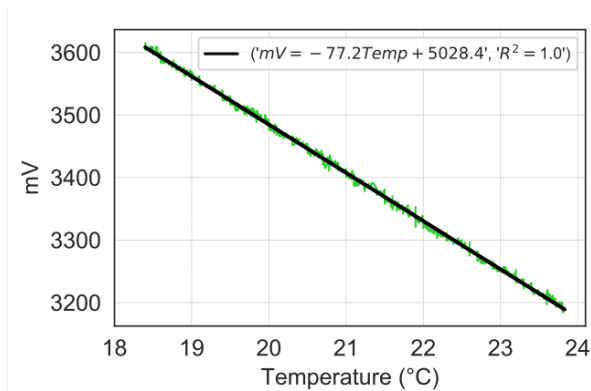


Fig. S2. Illustration of the linear thermal dependence of fluorescence. Data (mV and °C) were logged through the Cyclops 7f fluorometer and a temperature logger deployed in the fluorometry chamber filled with the standard solution when the temperature was ramped between 06:00-15:00 (on October 19, 2019).

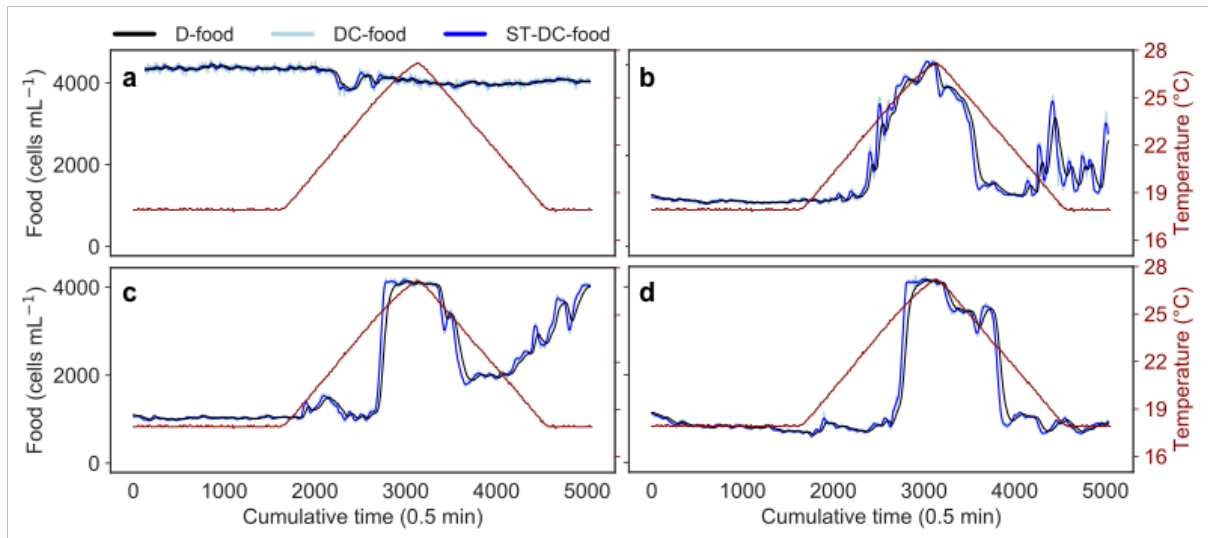


Fig. S3. Illustration of the dampening-effect correction. Dampened (D-food), dampening-corrected (DC-food), and secondary-trended dampening-corrected (ST-DC-food) food concentrations in response to a wide temperature range ($\sim 18\text{--}27.5\text{ }^{\circ}\text{C}$) from one mussel-trial conducted in November 4. Data of the fluorometers deployed in the control path Path_c (a) and the specimen paths Paths₁₋₃ holding *Mytilus* (b–d) of FOFS.

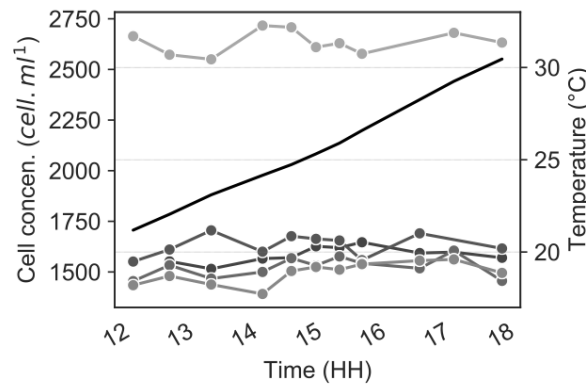


Fig. S4. Consistency of the concentration of phytoplanktonic food, *Rhodomonas salina*, in response to high temperatures used in our FOFS. Cell concentrations in samples taken every 30 min from the food tank (samples were diluted 1 to 50 mL; lightest grey) and final outflows of the four paths (other shades) when FOFS was run in the absence of study specimens. The black line indicates the ramp in the temperature from 20 to 27 $^{\circ}\text{C}$. The food tank was kept constant at 16 $^{\circ}\text{C}$.

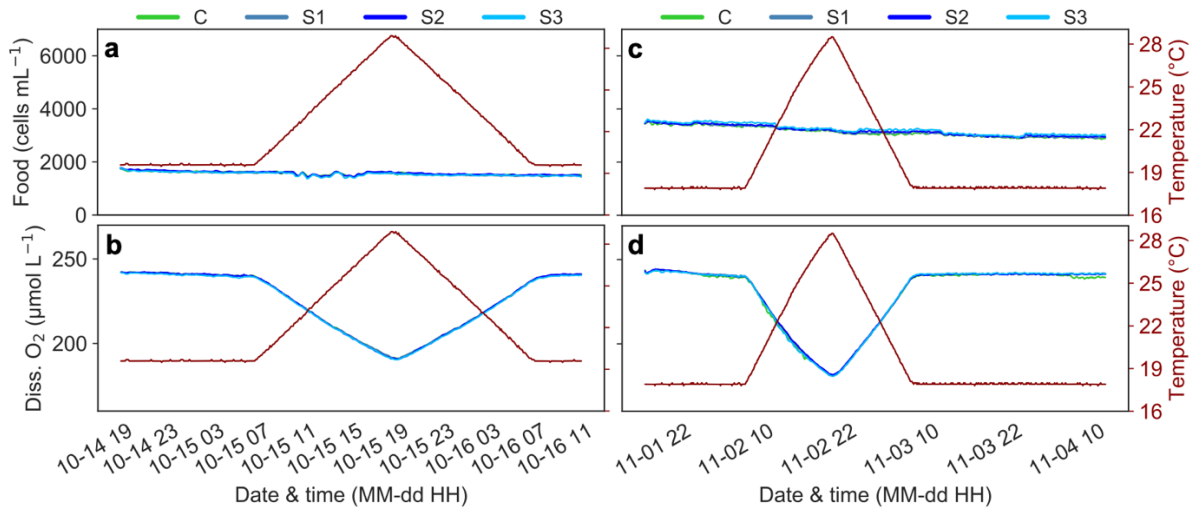


Fig. S5. Blank-trial runs to verify the method functionality. Food (a and c) and dissolved-oxygen (b and d) concentrations in the control path (Path_C) and the specimen paths (Path_{S1-3}) during the main stage of the blank trials conducted in the absence of study specimens using FOFS. The blank trials were carried out once following the standard cleaning procedure (a–b) and another time as a follow-up of a mussel-trial with no prior cleaning (c–d) in response to a wide temperature range (18–28.5 °C). Food and dissolved-oxygen concentrations are outputs of the data processing explained in Materials and Procedures in this paper.

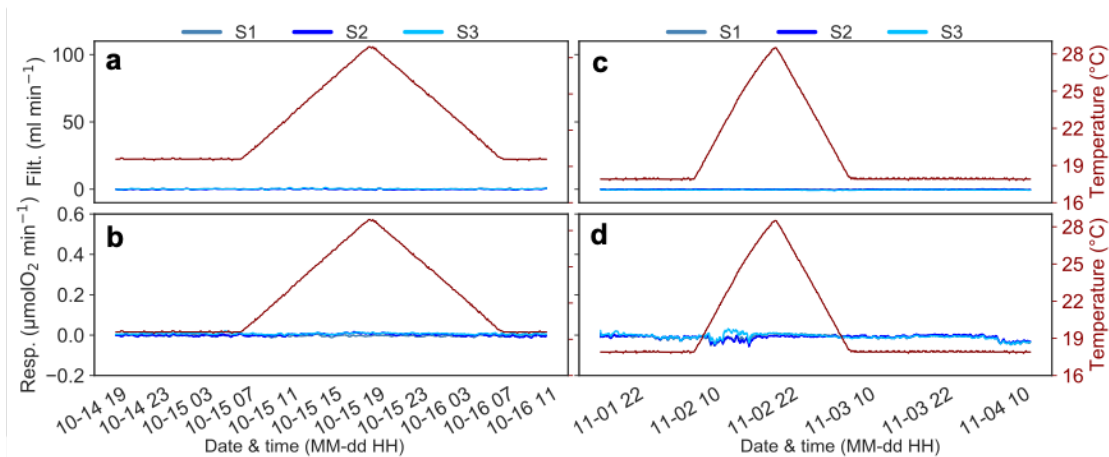


Fig. S6. Blank-trial runs to verify the method functionality. Estimates of filtration and respiration rates based on data collected in the absence of mussels from the incubation chambers of Path_{S1-3} during the main-stage of two blank trials of the demonstration experiment. The blank trials were carried out once following the standard cleaning procedure (a–b) and another time as a follow-up of a mussel-trial with no prior cleaning (c–d) in response to a wide temperature range (18–28.5 °C).

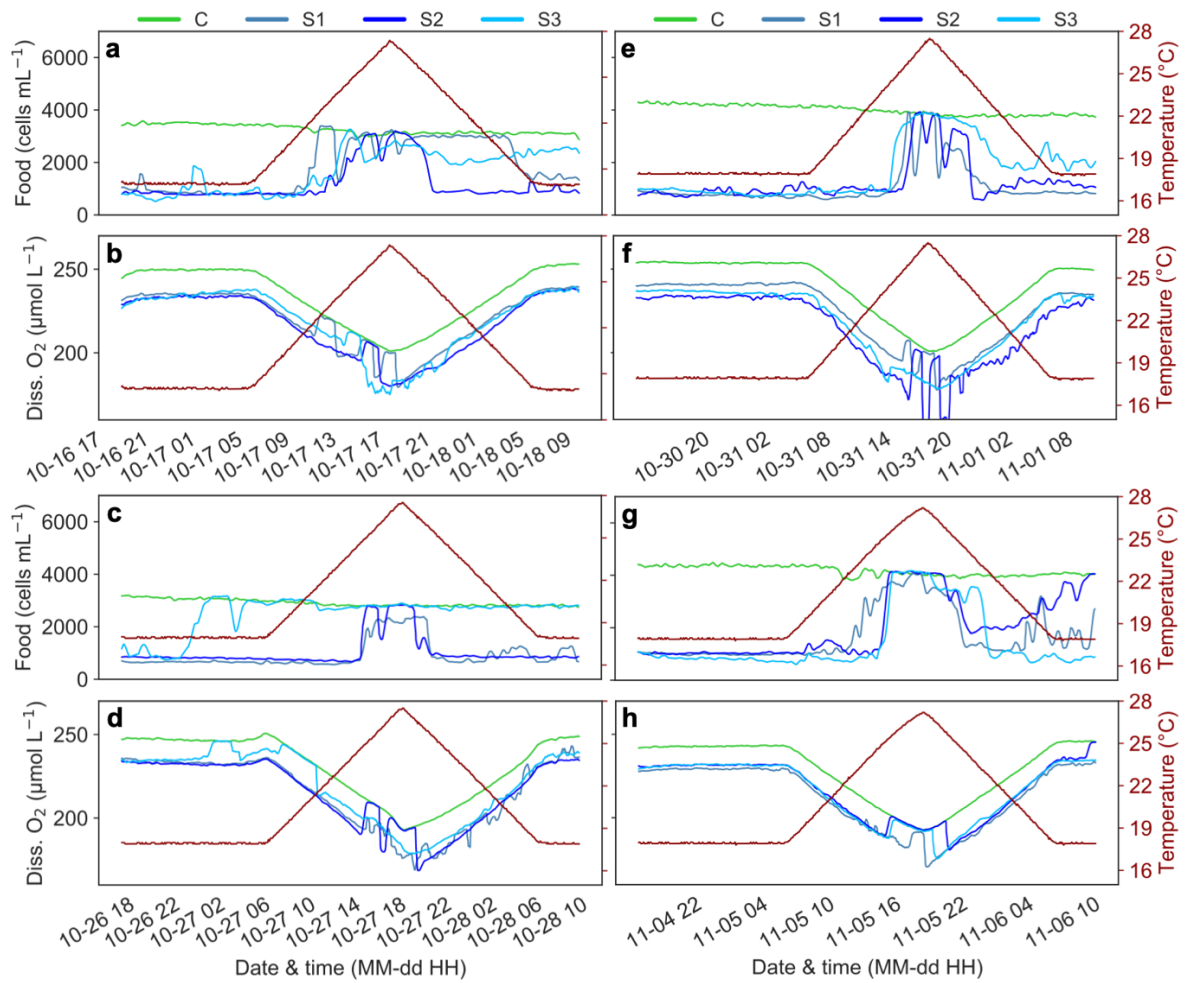


Fig. S7. Mussel-trial runs to verify the method functionality. Food (a, c, e, and g) and dissolved-oxygen concentrations (b, d, f, and h) in the control path (Path_c that had no mussel) and the specimen paths (Path_{s1-3} that contained the study *Mytilus* mussels) during the main stage of the four mussel trials using the FOFS. Food and dissolved-oxygen concentrations are processed as explained in Materials and Procedures in this paper.

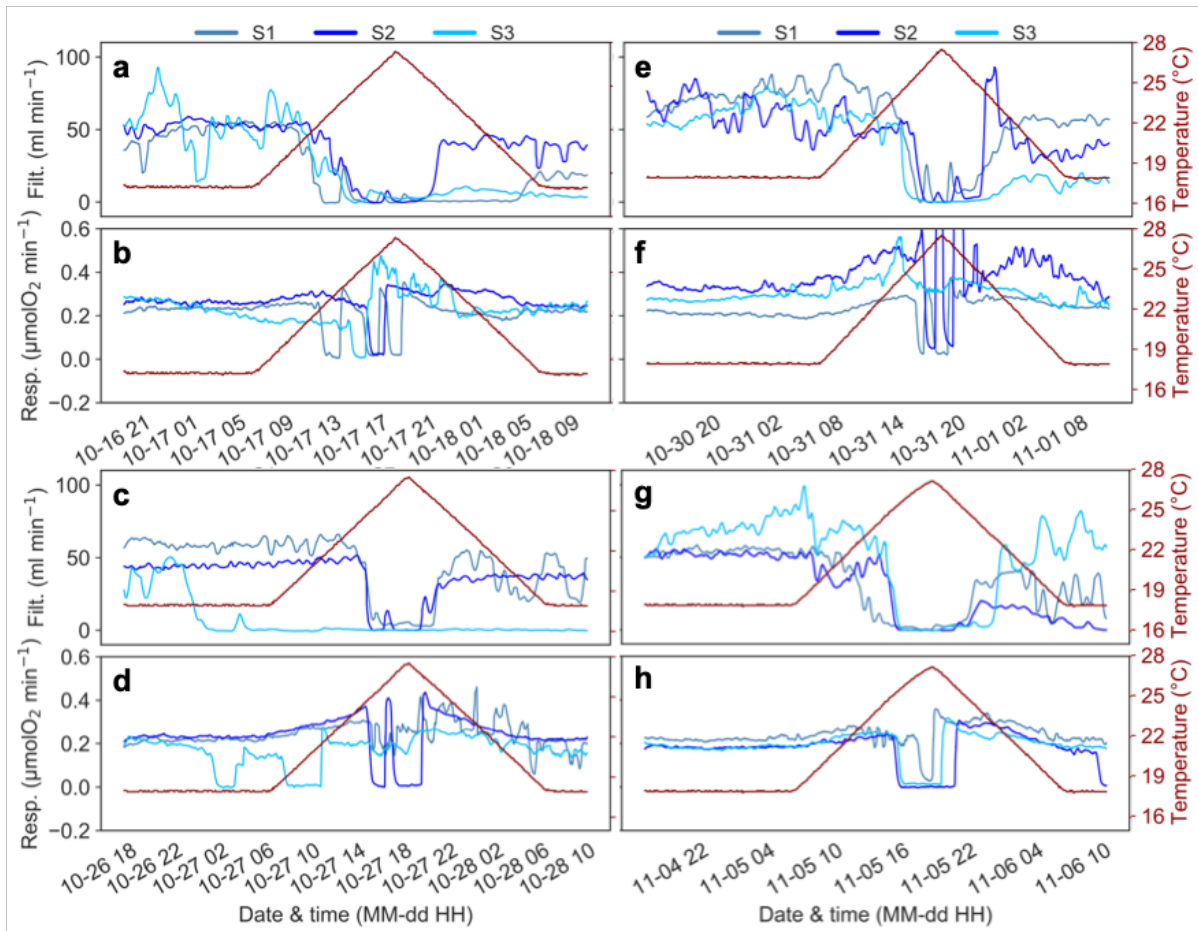


Fig. S8. Mussel-trial runs to verify the method functionality. Filtration (a, c, e, and g) and respiration rates (b, d, f, and h) of *Mytilus* mussels placed in the incubation chambers of Path_{S1-3} of FOFS during the main-stage of the four mussel trials of the demonstration experiment. Filtration and respiration rates are outputs of the data processing explained in Materials and Procedures in this paper.

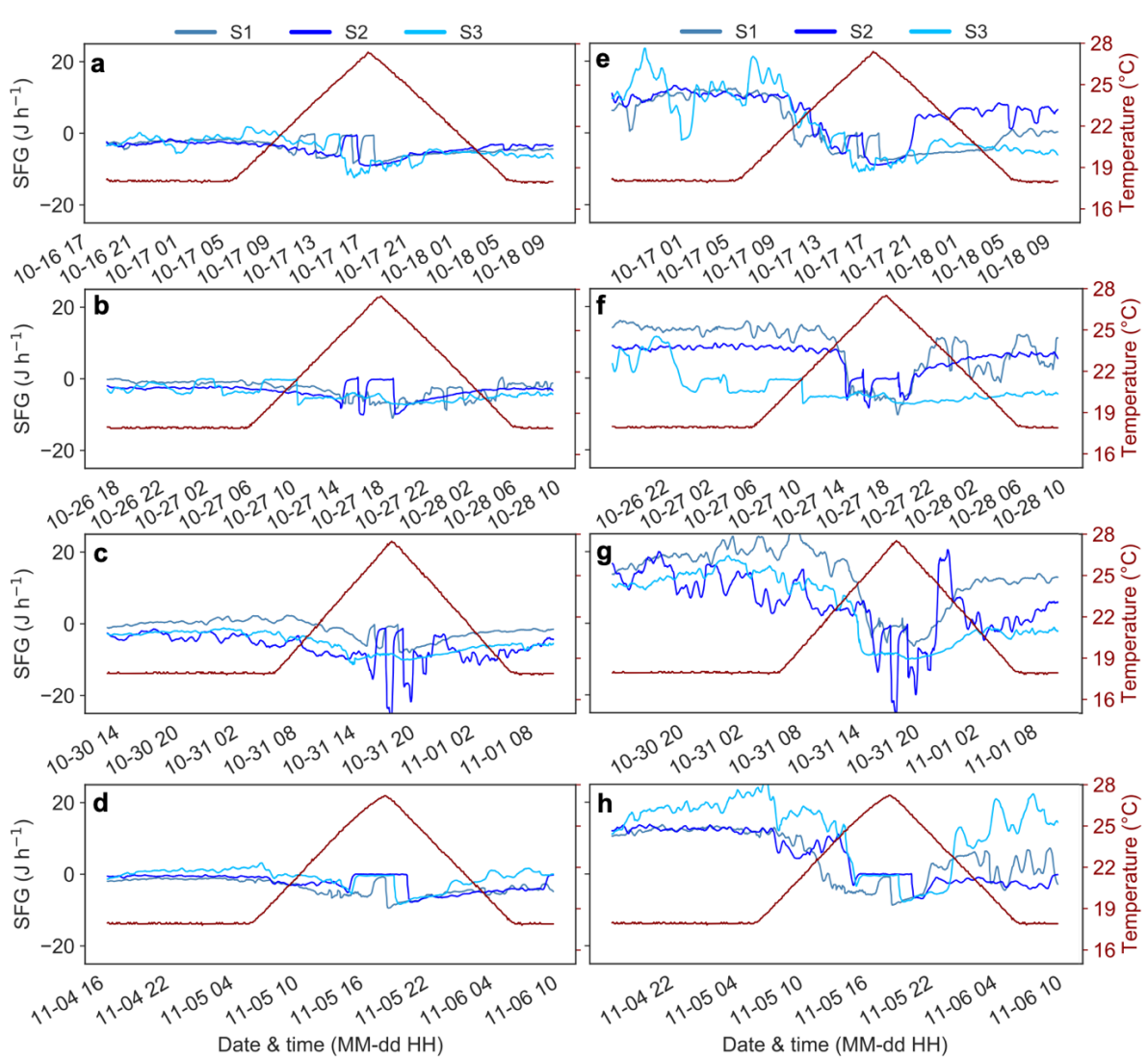


Fig. S9. Estimated Scope for Growth (SFG) at hypothetical *Rhodomonas* concentrations of 1000 (a–d) and 4000 cells (e–h) for *Mytilus* mussels placed in Path_{S1-3} during the main stage of the mussel trials. It should be noted that our estimation of SFG, based on the calculated filtration and respiration rates, simplistically assumes that the rate of energy respiration is independent of the ambient food concentration, not considering respiratory costs of the feeding at different food levels.

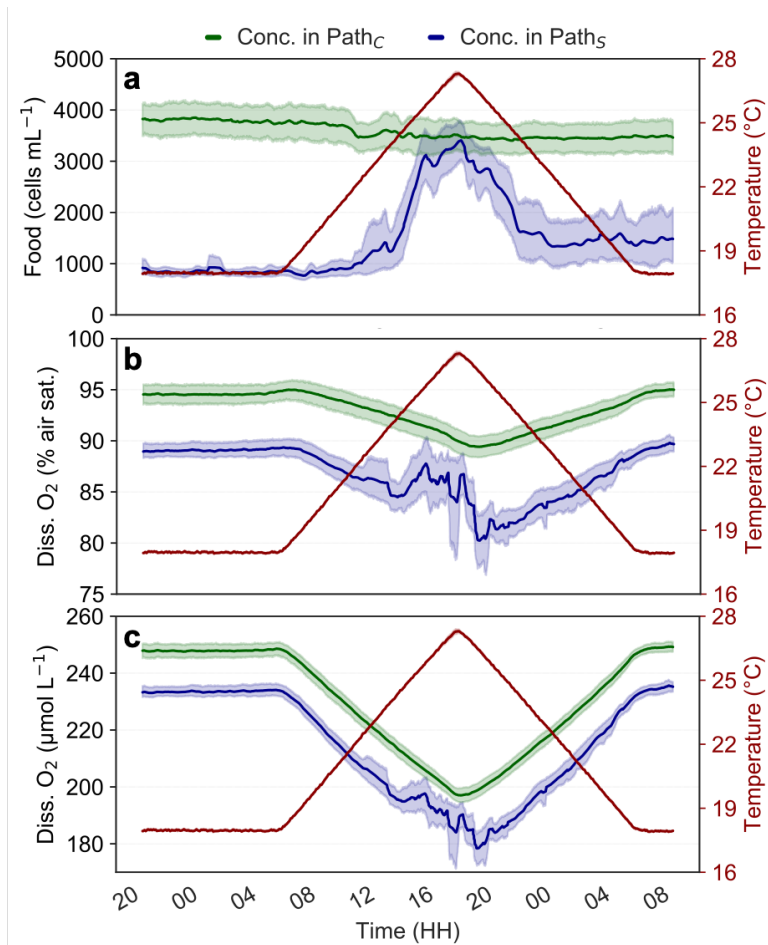


Fig. S10. Mussel-trial runs to verify the method functionality. Processed food (a) and dissolved-oxygen concentrations (b and c) in the Path_C (a) and Path_{S1-3} (holding mussel, *Mytilus*, specimens), along the applied daily temperature cycle (red lines). The replicated values (collected in the four mussel-trials) were averaged at each time point, presented with 95% confidence intervals.

Supplementary Tables

Table S1. The data sheet containing the dry-weights ('w' in g) and shell-lengths ('l' in mm) of the mussels placed in the incubation chambers of Path_{S1-3} during four mussel-trials of the demonstration experiment. Future users must manually add a data sheet (size_traits.xlsx) with the same format to the experimental folder, which will later be used by the script 'FOFS_integrative_processing.py' to define size-standardized filtration, feeding, respiration, and SFG rates for each replicate.

trial_name	S1_l	S2_l	S3_l	S1_w	S2_w	S3_w
16_oct	41.40	41.60	44.40	0.58	0.49	0.51
26_oct	44.17	47.55	44.56	0.55	0.82	0.46
30_oct	42.03	49.21	51.39	0.57	0.75	0.84
04_nov	49.41	42.47	45.85	0.82	0.34	0.70

Table S2. Blank-trial responses. The mean and standard deviation (SD) of filtration and respiration rates over the main stage of the two blank trials, calculated based on concentration data collected in Path_C and Path_{S1-3} of FOFS in the absence of study specimens (refer to Figs. S5 and S6). The values in the brackets indicate the statistics after the removal of the estimates which were impacted by the transient irregularity in dissolved-oxygen measurements of Path_C (Figs. S5d and S6d).

Trial name	Statistics	Filtration rate (mL min ⁻¹)			Respiration rate (μmolO ₂ min ⁻¹)		
		Path _{S1}	Path _{S2}	Path _{S3}	Path _{S1}	Path _{S2}	Path _{S3}
'14_oct'	Mean	0.193	-0.150	0.231	-0.002	0.001	0.007
	SD	0.247	0.242	0.269	0.004	0.005	0.003
'01_nov'	Mean	-0.066	-0.202	-0.476	-0.010 [-0.006]	-0.010 [-0.005]	-0.007 [-0.005]
	SD	0.156	0.165	0.202	0.012 [0.007]	0.011 [0.005]	0.013 [-0.008]

Table S3. Post-trial estimates of filtration and respiration rates were expected to be equal or close to zero, as the stage was conducted in the absence of study mussels. The post-trial estimates are compared with the baseline rates of main-trial filtration and respiration to roughly estimate the ratios of the non-filter-feeder- to filter-feeder-induced signals (i.e., the cumulative random impacts in percent; also refer to Figs. 3e-f and 4e-f in the paper). Baseline main-trial filtration or respiration rate were defined as the average of 180th to 480th main-trial data points. Estimates of cumulated random effects on filtration and respiration rates of the studied mussels categorized based on the respective trial and specimen Path. Values with an asterisk were not used in the calculation of the mean and SD.

Filtration rate						
	Post-trial rate (mL min⁻¹)			Cumulated random effect (%)		
Trial name	Paths₁	Paths₂	Paths₃	Paths₁	Paths₂	Paths₃
16_oct	-0.223	0.359	0.058	-0.570	0.731	0.079
26_oct	-0.319	0.012	-0.422	-0.519	0.028	-1.194
30_oct	-0.131	-0.115	0.063	-0.202	-0.175	0.118
04_nov	-0.155	-0.233	-0.217	-0.296	-0.440	-0.341
Mean	-0.207	0.006	-0.129	-0.396	0.036	-0.335
SD	0.084	0.256	0.235	0.176	0.501	0.610
Respiration rate						
	Post-trial rate (μmolO₂ min⁻¹)			Cumulated random effect (%)		
Trial name	Paths₁	Paths₂	Paths₃	Paths₁	Paths₂	Paths₃
16_oct	0.024	0.027	0.014	10.280	9.797	5.045
26_oct	-0.024*	0.013	0.016	-10.840*	5.672	7.493
30_oct	0.015	0.011	0.023	6.749	3.211	8.221
04_nov	0.014	0.018	0.002	6.499	9.667	1.014
Mean	0.018	0.017	0.014	7.843	7.087	5.443
SD	0.006	0.007	0.009	2.115	3.216	3.250

Supplementary Python scripts

The following Python scripts can be used to process data produced in FOFS experiments (e.g., the data produced in our demonstration experiment, including blank and mussel trial data, published in PANGAEA [<https://doi.org/10.1594/PANGAEA.919682>]).

Script S1: 'Dissolved_oxygen_calculator.py'

```
#!/usr/bin/env python3
# -*- coding: utf-8 -*-
"""
Created on Fri Oct 25 10:47:23 2019

@author: Jahangir Vajedsamiei (last test date: August 26, 2020)
This script can be applied for calculating temperature-corrected DO
(in percent air saturation and micromole per liter) using
the phase angle data (phi) collected via PreSens Pts3 sensor spots
(and Oxi4-mini oximeter) and independently-logged temperature data.
The equations applied in the DO calculator were published by
PreSens (Users' Manual).
"""

# The modules used in this script
import os
import math
from glob import glob as glob
import pandas as pd
from sympy import solve, Symbol, sqrt
from pandas import ExcelWriter
import numpy as np
import time

# Function definitions

""" The function needed for calculation of temperature-corrected \
percent_air_saturation using the phase angle data (phi) collected via \
PreSens Pts3 sensor spots and the temperature (tempC_) recorded via \
temperature-loggers deployed independent of the oximeter."""
def oxyg_air_sat_func(phi, phi_0, Ksv_T100_, TCC_phi, TCC_Ksv, tempC_,
    temp_cal0_, temp_cal100_, m, fl_):
    A = ((math.tan(phi*math.pi/180))/
    (math.tan((phi_0+(TCC_phi*(tempC_-temp_cal0_))*math.pi/180))*
    1/m*math.pow((Ksv_T100_+(TCC_Ksv*(tempC_-temp_cal100_)), 2))
    B = ((math.tan(phi*math.pi/180))/
    (math.tan((phi_0+(TCC_phi*(tempC_-temp_cal0_))*math.pi/180))*
    (Ksv_T100_+(TCC_Ksv*(tempC_-temp_cal100_)))+
    (math.tan(phi*math.pi/180))/
    (math.tan((phi_0+(TCC_phi*(tempC_-temp_cal0_))*math.pi/180))*
    1/m*(Ksv_T100_+(TCC_Ksv*(tempC_-temp_cal100_)))-fl_*1/m*
    (Ksv_T100_+(TCC_Ksv*(tempC_-temp_cal100_))-
    (Ksv_T100_+(TCC_Ksv*(tempC_-temp_cal100_)))+
    fl_*(Ksv_T100_+(TCC_Ksv*(tempC_-temp_cal100_))))
    C = ((math.tan(phi*math.pi/180))/
    (math.tan((phi_0+(TCC_phi*(tempC_-temp_cal0_))*math.pi/180))-1)
    y = (-B+(math.sqrt((math.pow(B, 2)-4*A*C))))/(2*A)
    return(y)

""" The functions needed for converting percent_air_saturation to \
micro_mol_O2_per_liter."""
def tempK_func(x):
    K = x + 273.15
    return(K)
def chlorinity_func(x): # provide salinity
```

```

y = (sal-0.03) / 1.805
return(y)
def pwT_func(x): # provide temp in K as argument
y = math.exp(52.57 - (6690.9/x) - 4.681*math.log(x))
return(y)
def aT_func(tempK_, chlorinity_):
a = -7.424
b = 4.417 * (10**3)
c = -2.927
D = 4.238*(10**-2)
P = -1.288*(10**-1)
Q = 5.344*10
R = -4.442*(10**-2)
S_ = 7.145*(10**-4)
aT_ = (math.exp((a + (b/tempK_) + c*math.log(tempK_) + D*tempK_) -
chlorinity_*(P + (Q/tempK_) + (R*math.log(tempK_) +
(S_*tempK_)))/1000
return(aT)
# the final funtion
def oxyg_func(air_sat_, tempC_, sal_):
patm_ = 1013.0
pn_ = 1013.0
vm_ = 22.414
tempK_ = tempK_func(tempC_)
pwT_ = pwT_func(tempK_)
chl_ = chlorinity_func(sal_)
aT_ = aT_func(tempK_, chl_)
o2_ymol = ((patm_ - pwT_)/pn_)*(
air_sat_/100.)*0.2095*aT_*1000000.*(1./vm_)
return(o2_ymol)

# Function definitions end

# experimental data path definition

experiment_path = "/Users/jahangir/Desktop/FOFS_new_test_/mussel_trials"
raw_data_path = experiment_path + "/Data"

# experimental data path definition end

# Variables and constants definition

""" The sensor constants including the temperature correction-coefficients,
TCC_phi (dphi/dtemp = -0.08255) and Ksv_T100_ (dKsv/dtemp = 0.000492), m and
fl are provided by PreSens on the 'Final Inspection Protocol' and are
identical for the sensor spots of one batch."""
TCC_phi_ = -0.0803
TCC_Ksv_ = 0.000433
m_ = 29.87
fl_ = 0.808

""" Please provide the seawater salinity used in the experiment (will be \
applied as a parameter in oxyg_func)."""
sal = 21 # (ppt)

# Variables and constants definition end

#### Run script and answer the questions that will be asked on the console!!!

# make the temperature dataframe
os.chdir(raw_data_path + "/raw_data_temperature")
temp_filenames = glob("*.xlsx")
appended_data = []
for temp_filename in temp_filenames:
temp_df = pd.ExcelFile(temp_filename)
temp_df.sheet_names

```

```

[u'Sheet1']
temp_df = temp_df.parse("Sheet1")
appended_data.append(temp_df)
temp_df = pd.concat(appended_data)

# Please choose the experimental trials or a specific trial of interest!!!
trial_name_list = os.listdir(raw_data_path + "/raw_data_Oxygen")[1:]

answer = input(
    "Do you want to correct/convert DO data of a specific trail? \
    Enter y or n: ")
if answer == "y":
    trial_name = input("Enter the name of that trial (e.g., 10_Dec): ")
    while trial_name not in trial_name_list:
        trial_name = input(
            "The name is not in the trial_list. Enter the name correctly \
            (e.g., 10_Dec): ")
    trial_name_list = [trial_name]
elif answer == "n":
    print("OK. Then, the processing will include all the trials.")
else:
    while answer not in ("y", "n"):
        answer = input("Enter y or n: ")
        if answer == "y":
            trial_name_list = input(
                "Enter the name of that trial (e.g., 10_Dec): ")
        elif answer == "n":
            print("OK. Then, the processing includes all trials.")
        else:
            print("Please enter y or n.")

start = time.time()
for trial_name in trial_name_list:
    print("Started processing of the ' + trial_name +
        ' data.....'

stage_list = ['pre', 'main', 'post']
for stage in stage_list:
    if os.path.isdir(raw_data_path + "/raw_data_Oxygen/" +
        trial_name + '/' + stage):
        os.chdir(raw_data_path + "/raw_data_Oxygen/" +
            trial_name + '/' + stage)
        filelist = glob("*.txt")
        appended_data = []
        counter = 0
        for filename in filelist:
            # reading out calibration parameters included in txt files
            cal_param = pd.read_csv(
                filename, sep='delimiter', nrows=30,
                error_bad_lines=False, engine='python', names=['col'])
            phi_0_ = float(cal_param[24:25].col.str[20:25])
            phi_100 = float(cal_param[25:26].col.str[20:25])
            temp_cal0_ = float(cal_param[24:25].col.str[30:34])
            temp_cal100_ = float(cal_param[25:26].col.str[30:34])
            # calculating Ksv based on the calibration data
            Ksv_T100 = Symbol('Ksv_T100')
            A = ((math.tan(phi_100*math.pi/180))/
                (math.tan((phi_0_)*math.pi/180))*1/m_ *Ksv_T100**2)
            B = ((math.tan(phi_100*math.pi/180))/
                (math.tan((phi_0_)*math.pi/180))*
                (Ksv_T100)+(math.tan(phi_100*math.pi/180))/
                (math.tan((phi_0_)*math.pi/180))*
                1/m_*(Ksv_T100)-f1_ *1/m_*(Ksv_T100)-(Ksv_T100)+
                f1_*(Ksv_T100))
            C = ((math.tan(phi_100*math.pi/180)) /
                (math.tan((phi_0_)*math.pi/180))-1)
            equation = ((-B+sqrt((B**2)-4*A*C))/(2*A))-100
            Ksv_T100_ = solve(equation, Ksv_T100)[1]

```

```

oxyg_df = pd.read_csv(filename, encoding="ISO-8859-1", sep=";",
                      skiprows=39, skipinitialspace=True,
                      names=['Date', 'Time', 'phi_'],
                      parse_dates=[0], dayfirst=True,
                      usecols=[0, 1, 4])
oxyg_df.loc[:, 'DateTime'] = pd.to_datetime(
    oxyg_df['Date'].apply(str)+' '+oxyg_df['Time'])
oxyg_df = oxyg_df.set_index(
    pd.DatetimeIndex(oxyg_df['DateTime']))
oxyg_df = oxyg_df.resample('30s').mean()
"""
# If data collection frequency is > 30s use the following:
oxyg_df['phi_'] = oxyg_df['phi_'].apply(
    pd.to_numeric).interpolate(axis=0)
"""
oxyg_df.reset_index(inplace=True)
oxyg_temp_df = pd.merge(
    oxyg_df, temp_df, on='DateTime', how='inner')
# changes Temp_C from object to float64
oxyg_temp_df.loc[:, 'Temp_C'] = (
    oxyg_temp_df['Temp_C'].apply(pd.to_numeric,
    errors='coerce'))
# calculating temperature-corrected percent_air_sat using \
# the oxyg_air_sat_func
oxyg_temp_df.loc[:, 'percent_air_sat'] = oxyg_temp_df.apply(
    lambda row: oxyg_air_sat_func(row['phi_'], phi_0_,
    Ksv_T100_, TCC_phi_,
    TCC_Ksv_, row['Temp_C'],
    temp_cal0_,
    temp_cal100_, m_,
    fl_),
    axis=1)
# calculating dissolved oxygen concentration in micro_mol_O2
# (ymol_per_l) using the oxyg_air_sat_func
oxyg_temp_df.loc[:, 'ymol_per_l'] = oxyg_temp_df.apply(
    lambda row: oxyg_func(row['percent_air_sat'],
    row['Temp_C'], sal), axis=1)
if counter == 0:
    oxyg_temp_df = pd.DataFrame(
        oxyg_temp_df, columns=['DateTime', 'Temp_C',
        'ymol_per_l',
        'percent_air_sat'])
else:
    oxyg_temp_df = pd.DataFrame(
        oxyg_temp_df, columns=['ymol_per_l',
        'percent_air_sat'])
oxyg_temp_df.loc[:, filename[:-4] +
    '_ymol_per_l'] = oxyg_temp_df['ymol_per_l']
oxyg_temp_df.loc[:, filename[:-4] +
    '_percent_air_sat'] = oxyg_temp_df[
    'percent_air_sat']
appended_data.append(oxyg_temp_df)
counter = counter + 1
appended_data = pd.concat(appended_data, axis=1)
oxyg_temp_df = appended_data[
    ['DateTime', 'Temp_C', stage + '_C_ymol_per_l',
    stage + '_S1_ymol_per_l', stage + '_S2_ymol_per_l',
    stage + '_S3_ymol_per_l', stage + '_C_percent_air_sat',
    stage + '_S1_percent_air_sat',
    stage + '_S2_percent_air_sat',
    stage + '_S3_percent_air_sat']]

oxyg_temp_df = oxyg_temp_df.dropna()
oxyg_temp_df.reset_index(inplace=True)

writer = ExcelWriter(trial_name + '_' + stage + '.xlsx')
oxyg_temp_df.to_excel(writer, 'Sheet1')
writer.save()

```

```
end = time.time()
print(end - start)
```

Script S2: 'FOFS_trial-by-trial_processing.py'

```
#!/usr/bin/env python3
# -*- coding: utf-8 -*-
"""
```

```
@author: Jahangir Vajedsamiei (last test date: August 26, 2020)
```

NOTES:

- This interactive Script ('FOFS_trial-by-trial_processing.py') processes raw-data collected in the three stages of each trial of a FOFS experiment, creating data frames and plots of temporal variations in measured variables (raw and corrected/converted values) and responses (NOT-standardized by the length and weight of the study organisms).
- The main directory of experimental data (e.g., FOFS_test/blank_trials) must contain subdirectories termed raw_data_temperature (including °C-temperature .xlsx files), raw_data_Ch1, and raw_data_Oxygen, the two latter contain folders named after the starting dates of the trials (e.g., 10_Dec).
- Each of these folder has three subfolders named after the three stages of trial (i.e., pre, main, and post).
- Each subfolder includes data sheets of mV-Ch1 (.CSV) or %air-saturation (.xlsx, which are outputs of the DO-calculator.py) that were collected in the corresponding stage and trial.
- In the script, data collected in the control path of the setup (Path_C) are denoted by the suffix _C, and data collected in other paths (Path_Sn) have _S1, _S2, and _S3 suffices.
- Notes and explanatory remarks provided throughout the scripts clarify how one can use (and revise) the script and how the steps and commands work.
- Description of techniques used in different steps of 'FOFS trial-by-trial processing.py' can be found in the method paper.
- For each trial, outputs of this script are:
 - (i) an excel sheet containing raw-measurements, converted/corrected measurements and not-standardized responses for the processed main-trial data (e.g., 10_Dec.xlsx),
 - (ii) plots of (raw, trended, converted and corrected) data for all three stages and plots of responses (NOT-standardized by size-characteristics of the study mussels) for the processed main-trial (e.g., 10_Dec_filt_resp_temp_time.pdf), and
 - (iii) tables of descriptive statistics for the 'pre-trial stable-period' and tables of descriptive statistics for the 'post-trial stable-period' including estimated %drift of responses (statistics_Ch1_post_10_Dec.xlsx).

```
"""
# The modules used in this script
import os
from glob import glob as glob
import pandas as pd
import matplotlib.pyplot as plt
from pandas import ExcelWriter
import numpy as np
import matplotlib as mpl
import seaborn as sns
from wotan import flatten
import math
import time
```

```
answer = input(
    "Did you already revise the absolute path to the experimental folder\
    (experiment_path) and the variables. Enter y or n: ")
if answer == "n":
    print("Please push control+c, manually revise the '###experiment_path'\
    and '###variables' below, and then rerun the script.")
```

```

    print("Push control+c")
    print("Push control+c")
    time.sleep(30)
elif answer == "y":
    print("Continued...")

# Experimental data path definition

experiment_path = "/Users/jahangir/Desktop/FOFS_new_test_/musssel_trials"
raw_data_path = experiment_path + "/Data"

# Experimental data path edefinition nd

# Variables definition (please provide the variables)

flow_rate = 16 ## The flow rate of the pump1 (ml/min)
Volume = 350 # fluorometry-chamber volume in ml
fluo_data_collection_frequency = 0.5 # in min
oxygen_data_collection_frequency = 0.5 # in min

"""The robust m-estimator used for modelling the trend of time-series can \
# include 'biweight' or 'welsch' or another robust m-estimator"""
robust_estimator = 'welsch'

"""Other variables needed for calculation of the dampening_effect correction \
coefficient"""
dt = 5 # the time-window (min) for differencing of food-concentration series
diff_window = dt/fluo_data_collection_frequency

""" The coefficients for converting the food (Rhodomonas salina) concentration\
from mV_Ch1 to cells/ml. The conversion coefficient should be empirically-\
established at a specific reference-temperature for the control sensor of \
FOFS (ideally before each experiment)"""
FC_conversion_coef = 2438/366 # (cells/ml/mV)
reference_temperature = 18 # (°C)

""" Temperature-specific coefficient for Cyclops 7f fluorometers, i.e., \
the change in Chl or food concentration (in percentage) per °C deviation from \
the reference temperature."""
TS_coef = (-2.2/100)

""" The coefficients for covering the respired molO2 and ingested R. salina \
cells to energy (J), and the assimilation efficiency and the hypothetical food\
(Rhodomonas) concentrations used for estimation of SFG"""
coef_molO2_to_kJ = 450 # 450 kJ/mol O2 (Widdows and Hawkins 1989)
coef_cells_to_microJ = 1.75 # 1.75 µJ per (R. salina) cell (Kiørboe et al. 1985)
assimilation_efficiency = 0.8
food_conc = [1000, 4000]

""" plotting specifications: provide the values of interest."""
min_temp = 16
max_temp = 31
max_filt = 110 # ml/min
min_filt = -10 # ml/min
max_resp = 0.6 # micromolO2/min
min_resp = -0.2 # micromolO2/min
max_SFG = 25 # J/h
min_SFG = -25 # J/h
min_percent_air_sat = 70
max_percent_air_sat = 100
min_micromol_per_L = 160
max_micromol_per_L = 270
min_mvChl = 0
max_mvChl = 3000
min_cells_per_mL = 0
max_cells_per_mL = 7000
font_size = 14

```



```

legend_font_size = 13
fig_width = 6
fig_height = 2.5

# Variables definition end

# Dampening-effect correction-coefficient definition (do not change)

dampening_effect_CC = 1 / \
    (1-(1/(math.exp(dt*flow_rate/Volume))))

# Dampening-effect correction-coefficient definition end

# Output-path definition

if not os.path.isdir(experiment_path + "/trial_by_trial_processing_outputs"):
    os.mkdir(experiment_path + "/trial_by_trial_processing_outputs")
output_path = experiment_path + "/trial_by_trial_processing_outputs"

if not os.path.isdir(output_path + "/all_plots"):
    os.mkdir(output_path + "/all_plots")
    os.mkdir(output_path + "/all_plots/time_series")
if not os.path.isdir(output_path + "/main_trial_dfs"):
    os.mkdir(output_path + "/main_trial_dfs")
if not os.path.isdir(output_path + "/pre_stat_post_drift_tables"):
    os.mkdir(output_path + "/pre_stat_post_drift_tables")
    os.mkdir(output_path + "/pre_stat_post_drift_tables/post")
    os.mkdir(output_path + "/pre_stat_post_drift_tables/post/food")
    os.mkdir(output_path + "/pre_stat_post_drift_tables/post/oxyg")
    os.mkdir(output_path + "/pre_stat_post_drift_tables/pre")
    os.mkdir(output_path + "/pre_stat_post_drift_tables/pre/food")
    os.mkdir(output_path + "/pre_stat_post_drift_tables/pre/oxyg")

# Output-path definition end

# Make the complete experimental temperature dataframe
os.chdir(raw_data_path + "/raw_data_temperature")
temp_filenames = glob("*.xlsx")
appended_data = []
for temp_filename in temp_filenames:
    temp_df = pd.ExcelFile(temp_filename)
    temp_df.sheet_names
    [u'Sheet1']
    temp_df = temp_df.parse("Sheet1")
    appended_data.append(temp_df)
temp_df = pd.concat(appended_data)

# Input the name(s) of the trial or trials of interest to process!!!
trial_name_list = os.listdir(raw_data_path + "/raw_data_Ch1")[1:]

answer = input("Do you want to work on a specific trail? Enter y or n: ")
if answer == "y":
    trial_name = input("Enter the name of that trial (e.g., 04_nov): ")
    while trial_name not in trial_name_list:
        trial_name = input(
            "The name is not in the trial_list. Enter the name correctly\
            (e.g., 10_Dec): ")
    trial_name_list = [trial_name]
elif answer == "n":
    print("OK. Then, the processing will include all the trials.")
else:
    while answer not in ("y", "n"):
        answer = input("Enter y or n: ")
    if answer == "y":
        trial_name_list = input(
            "Enter the name of that trial (e.g., 04_nov): ")

```



```

    os.mkdir(output_path + "/all_plots/time_series/" + trial_name)
    os.chdir(output_path + "/all_plots/time_series/" + trial_name)
else:
    os.chdir(output_path + "/all_plots/time_series/" + trial_name)
# Plot
mpl.rcParams["font.size"] = font_size
sns.set_style("white")
sns.set_style("ticks", {"xtick.major.size": 8, "ytick.major.size": 8})
fig = plt.figure(figsize=(fig_width, fig_height))
ax = fig.add_subplot(111)
lns1 = ax.plot(pre_Ch1_temp_df["index"], pre_Ch1_temp_df["pre_C_mV_Ch1"],
              label='C', color='limegreen', linestyle='-', linewidth=1, alpha=0.5)
lns2 = ax.plot(pre_Ch1_temp_df["index"], pre_Ch1_temp_df["pre_S1_mV_Ch1"],
              label='S1', color='steelblue', linestyle='-', linewidth=1, alpha=0.5)
lns3 = ax.plot(pre_Ch1_temp_df["index"], pre_Ch1_temp_df["pre_S2_mV_Ch1"],
              label='S2', color='blue', linestyle='-', linewidth=1, alpha=0.5)
lns4 = ax.plot(pre_Ch1_temp_df["index"], pre_Ch1_temp_df["pre_S3_mV_Ch1"],
              label='S3', color='deepskyblue', linestyle='-', linewidth=1, alpha=0.5)
lns5 = ax.plot(pre_Ch1_temp_df["index"], pre_Ch1_temp_df["pre_C_mV_Ch1_Trend"],
              label='C', color='limegreen', linestyle='-', linewidth=2)
lns6 = ax.plot(pre_Ch1_temp_df["index"], pre_Ch1_temp_df["pre_S1_mV_Ch1_Trend"],
              label='S1', color='steelblue', linestyle='-', linewidth=2)
lns7 = ax.plot(pre_Ch1_temp_df["index"], pre_Ch1_temp_df["pre_S2_mV_Ch1_Trend"],
              label='S2', color='blue', linestyle='-', linewidth=2)
lns8 = ax.plot(pre_Ch1_temp_df["index"], pre_Ch1_temp_df["pre_S3_mV_Ch1_Trend"],
              label='S3', color='deepskyblue', linestyle='-', linewidth=2)
lns9 = ax.plot(pre_Ch1_temp_df["index"], pre_Ch1_temp_df["pre_C_mV_Ch1_Trend_TC"],
              label='C', color='black', linestyle='-', linewidth=1)
lns10 = ax.plot(pre_Ch1_temp_df["index"], pre_Ch1_temp_df["pre_S1_mV_Ch1_Trend_TC"],
              label='S1', color='black', linestyle='-', linewidth=1)
lns11 = ax.plot(pre_Ch1_temp_df["index"], pre_Ch1_temp_df["pre_S2_mV_Ch1_Trend_TC"],
              label='S2', color='black', linestyle='-', linewidth=1)
lns12 = ax.plot(pre_Ch1_temp_df["index"], pre_Ch1_temp_df["pre_S3_mV_Ch1_Trend_TC"],
              label='S3', color='black', linestyle='-', linewidth=1)
ax.set_xlabel('Cumulative time (' + str(flou_data_collection_frequency) + ' min)')
ax.set_ylabel('Ch1 (mV)')
ax1 = fig.add_subplot(111)
ax1 = ax.twinx()
lns13 = ax1.plot(pre_Ch1_temp_df["index"], pre_Ch1_temp_df["Temp_C"],
                label='Temperature', color='darkred', linestyle='-', linewidth=1)
ax1.set_yticks(np.arange(min_temp, max_temp, 3))
ax1.set_ylim(bottom=min_temp-1)
ax1.set_ylabel("Temperature (°C)")
lns = lns5+lns6+lns7+lns8
labs = [l.get_label() for l in lns]
leg = plt.legend(lns, labs, ncol=4, loc='upper center', prop={'size': legend_font_size},
                fancybox=False, frameon=False, bbox_to_anchor=(0.5, 1.2),
                framealpha=0.7)
# set the linewidth of each legend object
for legobj in leg.legendHandles:
    legobj.set_linewidth(3.0)

ax1.tick_params(axis='y', colors='darkred')
ax1.yaxis.label.set_color('darkred')
plt.savefig(trial_name + '_pre_mVCh1_raw_vs_trend_TC.pdf',
          bbox_inches='tight')
plt.show()
plt.pause(0.001)
#input("Press [enter] to continue.")

# Choose the stable interval based on the plot and the data frame presented
# in the Console
while True:
    try:
        start_stable_data = int(input(
            'Please provide start_stable_data as an integer based on the\
            plot and the data frame presented in the Console (the stable\
            data interval usually include the last (120 or less) data points: ')
        if start_stable_data < 5 or start_stable_data > \

```

```

(max(pre_Ch1_temp_df["index"]-2):
    raise ValueError
break
except ValueError:
    print("Invalid integer. The input is out of range or not an integer!")

while True:
    try:
        end_stable_data = int(input(
            'Please provide end_stable_data as an integer (based on the \
            plot and the data frame presented in the Console): ')
        if end_stable_data < start_stable_data or \
            end_stable_data > max(pre_Ch1_temp_df["index"]):
            raise ValueError
        break
    except ValueError:
        print("Invalid integer. The input is out of range or not an integer!")

# Crop the 'pre-trial stable-period'.
mask = (pre_Ch1_temp_df["index"] >= start_stable_data) & (
    pre_Ch1_temp_df["index"] <= end_stable_data)
pre_Ch1_temp_df = pre_Ch1_temp_df.loc[mask]

""" Calculate descriptive statistics for the 'pre-trial stable-period'.
the mean value of the trended and temperature-corrected mV_Ch1 data \
collected by each sensor over the 'pre-trial stable-period' will be used \
as the reference-value for converting main-trial data of the sensor to \
percent_Ch1 (later in the processing)."""
statistics_Ch1_pre = pre_Ch1_temp_df.describe()
os.chdir(output_path + "/pre_stat_post_drift_tables/pre/food")
writer = ExcelWriter('statistics_Ch1_pre_' + trial_name + '.xlsx')
statistics_Ch1_pre.to_excel(writer, 'Sheet1')
writer.save()

# Create the main_Ch1_temp_df (similar to the pre-trial procedure)
os.chdir(raw_data_path + "/raw_data_Ch1/" + trial_name + "/main")
filelist = glob("*")
appended_data = []
counter = 0
for filename in filelist:
    os.chdir(raw_data_path + "/raw_data_Ch1/" + trial_name + "/main")
    Ch1_df = pd.read_csv(filename, encoding='utf-8', sep=",",
        names=['Date', 'Time', 'Gain', filename[:-4]+'_mV_Ch1'],
        header=0, usecols=[0, 1, 2, 3])
    Ch1_df.loc[:, 'DateTime'] = pd.to_datetime(
        Ch1_df['Date'].apply(str)+' '+Ch1_df['Time'])
    Ch1_df = Ch1_df.reset_index()
    # producing the robust estimated trend
    flatten_lc1, trend_lc1 = flatten(
        Ch1_df['index'], Ch1_df[filename[:-4]+'_mV_Ch1'],
        method=robust_estimator, window_length=60, cval=5,
        return_trend=True)
    Ch1_df[filename[:-4] + '_mV_Ch1' + '_Trend'] = pd.Series(trend_lc1)
    Ch1_df = Ch1_df.set_index('DateTime').resample('30S').last()
    Ch1_df.reset_index(inplace=True)
    # merging two dataframes while keeping the overlapping ones
    Ch1_temp_df = pd.merge(Ch1_df, temp_df, on='DateTime', how='inner')
    Ch1_temp_df.loc[:, 'Temp_C'] = Ch1_temp_df['Temp_C'].apply(
        pd.to_numeric, errors='coerce') # from object to float64

# temperature compensation (TC)
Ch1_temp_df[filename[:-4] + '_mV_Ch1' + '_Trend_TC'] = (
    Ch1_temp_df[filename[:-4] + '_mV_Ch1' + '_Trend']/
    (1 + ((Ch1_temp_df['Temp_C'] - reference_temperature)*TS_coef)))

if counter == 0:
    Ch1_temp_df = pd.DataFrame(
        Ch1_temp_df, columns=['DateTime', 'Temp_C',
            filename[:-4]+'_mV_Ch1',

```

```

        filename[:-4] + '_mV_ChI' + '_Trend',
        filename[:-4] + '_mV_ChI' + '_Trend_TC'])
else:
    Chl_temp_df = pd.DataFrame(
        Chl_temp_df, columns=[filename[:-4]+'_mV_ChI',
                             filename[:-4] + '_mV_ChI' + '_Trend',
                             filename[:-4] + '_mV_ChI' + '_Trend_TC'])
    appended_data.append(Chl_temp_df)
    counter = counter + 1
Chl_temp_df_main = pd.concat(appended_data, axis=1).reset_index()

# Plot
if not os.path.isdir(output_path + "/all_plots/time_series/" + trial_name):
    os.mkdir(output_path + "/all_plots/time_series/" + trial_name)
    os.chdir(output_path + "/all_plots/time_series/" + trial_name)
else:
    os.chdir(output_path + "/all_plots/time_series/" + trial_name)
mpl.rcParams["font.size"] = font_size
sns.set_style("white")
sns.set_style("ticks", {"xtick.major.size": 8, "ytick.major.size": 8})
fig = plt.figure(figsize=(fig_width, fig_height))
ax = fig.add_subplot(111)
lns1 = ax.plot(Chl_temp_df_main["index"], Chl_temp_df_main["main_C_mV_ChI"],
              label='C', color='limegreen', linestyle='-', linewidth=0.2, alpha=0.5)
lns2 = ax.plot(Chl_temp_df_main["index"], Chl_temp_df_main["main_S1_mV_ChI"],
              label='S1', color='steelblue', linestyle='-', linewidth=0.2, alpha=0.5)
lns3 = ax.plot(Chl_temp_df_main["index"], Chl_temp_df_main["main_S2_mV_ChI"],
              label='S2', color='blue', linestyle='-', linewidth=0.2, alpha=0.5)
lns4 = ax.plot(Chl_temp_df_main["index"], Chl_temp_df_main["main_S3_mV_ChI"],
              label='S3', color='deepskyblue', linestyle='-', linewidth=0.2, alpha=0.5)
lns5 = ax.plot(Chl_temp_df_main["index"], Chl_temp_df_main["main_C_mV_ChI_Trend"],
              label='C', color='limegreen', linestyle='-', linewidth=1)
lns6 = ax.plot(Chl_temp_df_main["index"], Chl_temp_df_main["main_S1_mV_ChI_Trend"],
              label='S1', color='steelblue', linestyle='-', linewidth=1)
lns7 = ax.plot(Chl_temp_df_main["index"], Chl_temp_df_main["main_S2_mV_ChI_Trend"],
              label='S2', color='blue', linestyle='-', linewidth=1)
lns8 = ax.plot(Chl_temp_df_main["index"], Chl_temp_df_main["main_S3_mV_ChI_Trend"],
              label='S3', color='deepskyblue', linestyle='-', linewidth=1)
lns9 = ax.plot(Chl_temp_df_main["index"], Chl_temp_df_main["main_C_mV_ChI_Trend_TC"],
              label='C', color='black', linestyle='-', linewidth=0.2)
lns10 = ax.plot(Chl_temp_df_main["index"], Chl_temp_df_main["main_S1_mV_ChI_Trend_TC"],
              label='S1', color='black', linestyle='-', linewidth=0.2)
lns11 = ax.plot(Chl_temp_df_main["index"], Chl_temp_df_main["main_S2_mV_ChI_Trend_TC"],
              label='S2', color='black', linestyle='-', linewidth=0.2)
lns12 = ax.plot(Chl_temp_df_main["index"], Chl_temp_df_main["main_S3_mV_ChI_Trend_TC"],
              label='S3', color='black', linestyle='-', linewidth=0.2)
ax.set_xlabel('Cumulative time (' + str(fluo_data_collection_frequency) + ' min)')
ax.set_ylabel('ChI (mV)')
ax1 = fig.add_subplot(111)
ax1 = ax.twinx()
lns13 = ax1.plot(Chl_temp_df_main["index"], Chl_temp_df_main["Temp_C"],
                label='Temperature', color='darkred', linestyle='-',
                linewidth=1)
ax1.set_yticks(np.arange(min_temp, max_temp, 3))
ax1.set_ylim(bottom=min_temp-1)
ax1.set_ylabel("Temperature (°C)")
lns = lns5+lns6+lns7+lns8
labs = [l.get_label() for l in lns]
leg = plt.legend(lns, labs, ncol=4, loc='upper center',
                prop={'size': legend_font_size}, fancybox=False,
                frameon=False, bbox_to_anchor=(0.5, 1.2), framealpha=0.7)
# set the linewidth of each legend object
for legobj in leg.legendHandles:
    legobj.set_linewidth(3.0)
ax1.tick_params(axis='y', colors='darkred')
ax1.yaxis.label.set_color('darkred')
plt.savefig(trial_name + '_main_mVChI_raw_vs_trend_TC.pdf',
            bbox_inches='tight')

```

```
#####
```

```
food_temp_feed_filt_df = Chl_temp_df_main
```

```
''' Calculate percent_Ch1 (accounting for inherent differences in the \
absolute sensors' readouts)'''
```

```
food_temp_feed_filt_df.loc[:, 'percent_C'] = (
    (food_temp_feed_filt_df['main_C_mV_Ch1_Trend_TC']/
     statistics_Ch1_pre.at["mean", "pre_C_mV_Ch1_Trend_TC"])*100)
food_temp_feed_filt_df.loc[:, 'percent_S1'] = (
    (food_temp_feed_filt_df['main_S1_mV_Ch1_Trend_TC']/
     statistics_Ch1_pre.at["mean", "pre_S1_mV_Ch1_Trend_TC"])*100)
food_temp_feed_filt_df.loc[:, 'percent_S2'] = (
    (food_temp_feed_filt_df['main_S2_mV_Ch1_Trend_TC']/
     statistics_Ch1_pre.at["mean", "pre_S2_mV_Ch1_Trend_TC"])*100)
food_temp_feed_filt_df.loc[:, 'percent_S3'] = (
    (food_temp_feed_filt_df['main_S3_mV_Ch1_Trend_TC']/
     statistics_Ch1_pre.at["mean", "pre_S3_mV_Ch1_Trend_TC"])*100)
```

```
# to prevent an error related to D&T
```

```
food_temp_feed_filt_df = food_temp_feed_filt_df[(
    food_temp_feed_filt_df['DateTime'] > '2018-01-01']
```

```
''' Estimate the initial concentration (cells/ml) based on the mean values
over 'pre-trial stable-period' and the empirical conversion coefficient'''
```

```
initial_concentration_cells_per_ml = statistics_Ch1_pre.at[
    "mean", "pre_C_mV_Ch1_Trend_TC"]*FC_conversion_coef
```

```
''' Convert main-trial food concentration data from percentage to
cells_per_ml'''
```

```
food_temp_feed_filt_df.loc[:, 'cells_per_ml_C'] = (
    food_temp_feed_filt_df['percent_C']*
    initial_concentration_cells_per_ml)/100
food_temp_feed_filt_df.loc[:, 'cells_per_ml_S1'] = (
    food_temp_feed_filt_df['percent_S1']*
    initial_concentration_cells_per_ml)/100
food_temp_feed_filt_df.loc[:, 'cells_per_ml_S2'] = (
    food_temp_feed_filt_df['percent_S2']*
    initial_concentration_cells_per_ml)/100
food_temp_feed_filt_df.loc[:, 'cells_per_ml_S3'] = (
    food_temp_feed_filt_df['percent_S3']*
    initial_concentration_cells_per_ml)/100
```

```
### Dampening-effect correction (DC)
```

```
dampened_cols = [i for i in list(
    food_temp_feed_filt_df) if 'cells_per_ml' in i]
```

```
for i in dampened_cols:
```

```
''' The data column is differenced (diff-window specified in the \
'Variables' section). The differences are corrected applying the \
'dampening_effect_CC' (specified in the 'Variables' section). The \
corrected-differences are added back the original data column.'''
```

```
food_temp_feed_filt_df[i + '_diff_DC'] = (
    food_temp_feed_filt_df[i].diff(int(diff_window)).
    shift(- int(diff_window)).mul(dampening_effect_CC))
food_temp_feed_filt_df['DC_' + i] = food_temp_feed_filt_df[i] + \
    food_temp_feed_filt_df[i + '_diff_DC']
```

```
'''The secondary trending (ST) is needed to remove the noise \
boosted by the dampening-effect correction.'''
```

```
flatten_lc1, trend_lc1 = flatten(food_temp_feed_filt_df['index'],
    food_temp_feed_filt_df['DC_' + i],
    method=robust_estimator,
    window_length=40, cval=5,
    return_trend=True)
food_temp_feed_filt_df['ST_' + 'DC_' + i] = pd.Series(trend_lc1).fillna(0)
```

```
# Plot
```



```

os.chdir(raw_data_path + "/raw_data_Oxygen/" + trial_name + "/pre")
filename = glob("*.xlsx")
pre_oxyg_temp_df = pd.ExcelFile(filename[0])
pre_oxyg_temp_df.sheet_names
[u'Sheet1']
pre_oxyg_temp_df = pre_oxyg_temp_df.parse("Sheet1")
pre_oxyg_temp_df = pre_oxyg_temp_df.reset_index()

oxyg_cols = [i for i in list(pre_oxyg_temp_df) if 'pre_' in i]
for i in oxyg_cols:
    # producing robust time-series models using robust_estimators
    flatten_lc1, trend_lc1 = flatten(pre_oxyg_temp_df['index'], pre_oxyg_temp_df[i],
                                   method=robust_estimator, window_length=60,
                                   cval=5, return_trend=True)
    pre_oxyg_temp_df[i + '_Trend'] = pd.Series(trend_lc1)

with pd.option_context('display.max_rows', 100, 'display.max_columns', None):
    print(pre_oxyg_temp_df)

# Change the path for plot-saving
if not os.path.isdir(output_path + "/all_plots/time_series/" + trial_name):
    os.mkdir(output_path + "/all_plots/time_series/" + trial_name)
    os.chdir(output_path + "/all_plots/time_series/" + trial_name)
else:
    os.chdir(output_path + "/all_plots/time_series/" + trial_name)

""" Plot raw and trended percent_air_sat time-seies of the pre_trial for \
visuall-checking of the Trend modelling and determining 'pre-trial \
stable-period' over which variation in measurements of all sensors are \
stable (the real concentrations in different paths are comparable while \
the absolute value of records are dissimilar)."""
mpl.rcParams["font.size"] = font_size
sns.set_style("white")
sns.set_style("ticks", {"xtick.major.size": 8, "ytick.major.size": 8})
fig = plt.figure(figsize=(fig_width, fig_height))
ax = fig.add_subplot(111)
lns1 = ax.plot(pre_oxyg_temp_df["index"], pre_oxyg_temp_df["pre_C_percent_air_sat"],
              label='C', color='limegreen', linestyle='-', linewidth=1, alpha=0.5)
lns2 = ax.plot(pre_oxyg_temp_df["index"], pre_oxyg_temp_df["pre_S1_percent_air_sat"],
              label='S1', color='steelblue', linestyle='-', linewidth=1, alpha=0.5)
lns3 = ax.plot(pre_oxyg_temp_df["index"], pre_oxyg_temp_df["pre_S2_percent_air_sat"],
              label='S2', color='blue', linestyle='-', linewidth=1, alpha=0.5)
lns4 = ax.plot(pre_oxyg_temp_df["index"], pre_oxyg_temp_df["pre_S3_percent_air_sat"],
              label='S3', color='deepskyblue', linestyle='-', linewidth=1, alpha=0.5)
lns5 = ax.plot(pre_oxyg_temp_df["index"], pre_oxyg_temp_df["pre_C_percent_air_sat_Trend"],
              label='C', color='limegreen', linestyle='-', linewidth=2)
lns6 = ax.plot(pre_oxyg_temp_df["index"], pre_oxyg_temp_df["pre_S1_percent_air_sat_Trend"],
              label='S1', color='steelblue', linestyle='-', linewidth=2)
lns7 = ax.plot(pre_oxyg_temp_df["index"], pre_oxyg_temp_df["pre_S2_percent_air_sat_Trend"],
              label='S2', color='blue', linestyle='-', linewidth=2)
lns8 = ax.plot(pre_oxyg_temp_df["index"], pre_oxyg_temp_df["pre_S3_percent_air_sat_Trend"],
              label='S3', color='deepskyblue', linestyle='-', linewidth=2)
ax.set_xlabel('Cumulative time (' + str(oxyg_data_collection_frequency) + ' min)')
ax.set_ylabel('Diss. O2 (% air sat.)')
ax1 = fig.add_subplot(111)
ax1 = ax.twinx()
lns9 = ax1.plot(pre_oxyg_temp_df["index"], pre_oxyg_temp_df["Temp_C"],
              label='Temperature', color='darkred', linestyle='-', linewidth=1)
ax1.set_ylabel("Temperature (°C)")
ax1.set_yticks(np.arange(min_temp, max_temp, 3))
ax1.set_ylim(bottom=min_temp-1)
lns = lns5+lns6+lns7+lns8
labs = [l.get_label() for l in lns]
leg = plt.legend(lns, labs, ncol=4, loc='upper center', prop={'size': legend_font_size},
               fancybox=False, frameon=False, bbox_to_anchor=(0.5, 1.2),
               framealpha=0.7)
# set the linewidth of each legend object
for legobj in leg.legendHandles:
    legobj.set_linewidth(3.0)

```



```

ax1.tick_params(axis='y', colors='darkred')
ax1.yaxis.label.set_color('darkred')
plt.savefig(trial_name + '_pre_oxyg_raw_vs_trended.pdf', bbox_inches='tight')
plt.show()
plt.pause(0.001)

while True:
    try:
        start_stable_data = int(input(
            'Please provide start_stable_data as an integer based on the\
            plot and the data frame presented in the Console (the stable\
            data interval usually include the last 120 or more minutes): ')
        if start_stable_data < 0 or start_stable_data > \
            (max(pre_oxyg_temp_df["index"])-2)):
            raise ValueError
        break
    except ValueError:
        print("Invalid integer. The input is out of range or not an integer!")

while True:
    try:
        end_stable_data = int(
            input('Please provide end_stable_data as an integer: ')
        if end_stable_data < start_stable_data or end_stable_data > \
            max(pre_oxyg_temp_df["index"]):
            raise ValueError
        break
    except ValueError:
        print("Invalid integer. The input is out of range or not an integer!")

# Crop the 'pre-trial stable-period'.
mask = (pre_oxyg_temp_df["index"] >= start_stable_data) & (
    pre_oxyg_temp_df["index"] <= end_stable_data)
pre_oxyg_temp_df = pre_oxyg_temp_df.loc[mask]

"""The differences between the measurements of the sensors of Path_Sn and \
Path_C (over the pre-trial stable-period) is calculated."""
pre_oxyg_temp_df.loc[:, 'pre_C_minus_S1_percent_air_sat'] = (
    pre_oxyg_temp_df['pre_C_percent_air_sat_Trend'] -
    pre_oxyg_temp_df['pre_S1_percent_air_sat_Trend'])
pre_oxyg_temp_df.loc[:, 'pre_C_minus_S2_percent_air_sat'] = (
    pre_oxyg_temp_df['pre_C_percent_air_sat_Trend'] -
    pre_oxyg_temp_df['pre_S2_percent_air_sat_Trend'])
pre_oxyg_temp_df.loc[:, 'pre_C_minus_S3_percent_air_sat'] = (
    pre_oxyg_temp_df['pre_C_percent_air_sat_Trend'] -
    pre_oxyg_temp_df['pre_S3_percent_air_sat_Trend'])

pre_oxyg_temp_df.loc[:, 'pre_C_minus_S1_ymol_per_l_Trend'] = (
    pre_oxyg_temp_df['pre_C_ymol_per_l_Trend'] -
    pre_oxyg_temp_df['pre_S1_ymol_per_l_Trend'])
pre_oxyg_temp_df.loc[:, 'pre_C_minus_S2_ymol_per_l_Trend'] = (
    pre_oxyg_temp_df['pre_C_ymol_per_l_Trend'] -
    pre_oxyg_temp_df['pre_S2_ymol_per_l_Trend'])
pre_oxyg_temp_df.loc[:, 'pre_C_minus_S3_ymol_per_l_Trend'] = (
    pre_oxyg_temp_df['pre_C_ymol_per_l_Trend'] -
    pre_oxyg_temp_df['pre_S3_ymol_per_l_Trend'])

""" Calculate descriptive statistics of the 'pre-trial stable-data'."""
os.chdir(output_path + "/pre_stat_post_drift_tables/pre/oxyg")
statistics_oxyg_pre = pre_oxyg_temp_df.describe()
writer = ExcelWriter('statistics_oxyg_pre_' + trial_name + '.xlsx')
statistics_oxyg_pre.to_excel(writer, 'Sheet1')
writer.save()

# Create main_oxyg_temp_df
# main
os.chdir(raw_data_path + "/raw_data_Oxygen/" + trial_name + "/main")
filename = glob("*.xlsx")
main_oxyg_temp_df = pd.ExcelFile(filename[0])

```

```

main_oxyg_temp_df.sheet_names
[u'Sheet1']
main_oxyg_temp_df = main_oxyg_temp_df.parse("Sheet1")
main_oxyg_temp_df = main_oxyg_temp_df.reset_index()

oxyg_cols = [i for i in list(main_oxyg_temp_df) if 'main_' in i]
for i in oxyg_cols:
    # producing robust time-series models using robust_estimators
    flatten_lc1, trend_lc1 = flatten(main_oxyg_temp_df['index'],
                                   main_oxyg_temp_df[i],
                                   method=robust_estimator,
                                   window_length=40, cval=5,
                                   return_trend=True)
    main_oxyg_temp_df[i + '_Trend'] = pd.Series(trend_lc1)

# change the path
if not os.path.isdir(output_path + "/all_plots/time_series/" + trial_name):
    os.mkdir(output_path + "/all_plots/time_series/" + trial_name)
    os.chdir(output_path + "/all_plots/time_series/" + trial_name)
else:
    os.chdir(output_path + "/all_plots/time_series/" + trial_name)
mpl.rcParams["font.size"] = font_size
sns.set_style("white")
sns.set_style("ticks", {"xtick.major.size": 8, "ytick.major.size": 8})
fig = plt.figure(figsize=(fig_width, fig_height))
ax = fig.add_subplot(111)
lns1 = ax.plot(main_oxyg_temp_df["index"], main_oxyg_temp_df["main_C_percent_air_sat"],
              label='C', color='limegreen', linestyle='-', linewidth=0.2, alpha=0.5)
lns2 = ax.plot(main_oxyg_temp_df["index"], main_oxyg_temp_df["main_S1_percent_air_sat"],
              label='S1', color='steelblue', linestyle='-', linewidth=0.2, alpha=0.5)
lns3 = ax.plot(main_oxyg_temp_df["index"], main_oxyg_temp_df["main_S2_percent_air_sat"],
              label='S2', color='blue', linestyle='-', linewidth=0.2, alpha=0.5)
lns4 = ax.plot(main_oxyg_temp_df["index"], main_oxyg_temp_df["main_S3_percent_air_sat"],
              label='S3', color='deepskyblue', linestyle='-', linewidth=0.2, alpha=0.5)
lns5 = ax.plot(main_oxyg_temp_df["index"], main_oxyg_temp_df["main_C_percent_air_sat_Trend"],
              label='C', color='limegreen', linestyle='-', linewidth=1)
lns6 = ax.plot(main_oxyg_temp_df["index"], main_oxyg_temp_df["main_S1_percent_air_sat_Trend"],
              label='S1', color='steelblue', linestyle='-', linewidth=1)
lns7 = ax.plot(main_oxyg_temp_df["index"], main_oxyg_temp_df["main_S2_percent_air_sat_Trend"],
              label='S2', color='blue', linestyle='-', linewidth=1)
lns8 = ax.plot(main_oxyg_temp_df["index"], main_oxyg_temp_df["main_S3_percent_air_sat_Trend"],
              label='S3', color='deepskyblue', linestyle='-', linewidth=1)
ax.set_xlabel('Cumulative time (' + str(oxyg_data_collection_frequency) + ' min)')
ax.set_ylabel('Diss. O2 (% air sat.)')
ax1 = fig.add_subplot(111)
ax1 = ax.twinx()
lns9 = ax1.plot(main_oxyg_temp_df["index"], main_oxyg_temp_df["Temp_C"],
              label='Temperature', color='darkred', linestyle='-', linewidth=1)
ax1.set_ylabel("Temperature (°C)")
ax1.set_yticks(np.arange(min_temp, max_temp, 3))
ax1.set_ylim(bottom=min_temp-1)
lns = lns5+lns6+lns7+lns8
labs = [l.get_label() for l in lns]
leg = plt.legend(lns, labs, ncol=4, loc='upper center', prop={'size': legend_font_size},
               fancybox=False, frameon=False, bbox_to_anchor=(0.5, 1.2), framealpha=0.7)
# set the linewidth of each legend object
for legobj in leg.legendHandles:
    legobj.set_linewidth(3.0)
ax1.tick_params(axis='y', colors='darkred')
ax1.yaxis.label.set_color('darkred')
plt.savefig(trial_name + '_main_oxyg_raw_vs_trended.pdf',
          bbox_inches='tight')

#####

oxyg_temp_resp_df = main_oxyg_temp_df

```

```

''' The average difference between measurements of Path_Sn and Path_C sensors\
over the 'pre-trial stable-period' is added to the main-trial data of the \

```



```

# Define the hypothetical feeding rate and SFG (in J_per_h) based on filtration at\
# a hypothetical concentration assuming assimilation Efficiency of 80%.
filt_S1_cols = [i for i in list(main_df) if 'filt_ml_per_min_S1' in i]
for i in food_conc:
    for j in filt_S1_cols:
        main_df.loc[:, 'feed_hyp_J_per_h_' + str(i) + '_cells_' + j[-2:]] = (
            (main_df[j]*float(i)*60*coef_cells_to_microJ)/(10**6))
        main_df.loc[:, 'SFG_hypo_J_per_h_' + str(i) + '_cells_' + j[-2:]] = (
            (main_df.loc[:, 'feed_hyp_J_per_h_' + str(i) + '_cells_' + j[-2:]] *
             assimilation_efficiency) - main_df['resp_J_per_h_S1'])
filt_S2_cols = [i for i in list(main_df) if 'filt_ml_per_min_S2' in i]
for i in food_conc:
    for j in filt_S2_cols:
        main_df.loc[:, 'feed_hyp_J_per_h_' + str(i) + '_cells_' + j[-2:]] = (
            (main_df[j]*float(i)*60*coef_cells_to_microJ)/(10**6))
        main_df.loc[:, 'SFG_hypo_J_per_h_' + str(i) + '_cells_' + j[-2:]] = (
            (main_df.loc[:, 'feed_hyp_J_per_h_' + str(i) + '_cells_' + j[-2:]] *
             assimilation_efficiency) - main_df['resp_J_per_h_S2'])
filt_S3_cols = [i for i in list(main_df) if 'filt_ml_per_min_S3' in i]
for i in food_conc:
    for j in filt_S3_cols:
        main_df.loc[:, 'feed_hyp_J_per_h_' + str(i) + '_cells_' + j[-2:]] = (
            (main_df[j]*float(i)*60*coef_cells_to_microJ)/(10**6))
        main_df.loc[:, 'SFG_hypo_J_per_h_' + str(i) + '_cells_' + j[-2:]] = (
            (main_df.loc[:, 'feed_hyp_J_per_h_' + str(i) + '_cells_' + j[-2:]] *
             assimilation_efficiency) - main_df['resp_J_per_h_S3'])

main_df = main_df.iloc[50:-50] # delete marginal rows

### Save the complete trial dataframe
if not os.path.isdir(output_path + "/main_trial_dfs"):
    os.mkdir(output_path + "/main_trial_dfs")
    os.chdir(output_path + "/main_trial_dfs")
else:
    os.chdir(output_path + "/main_trial_dfs")

writer = ExcelWriter(trial_name + '.xlsx')
main_df.to_excel(writer, 'Sheet1')
writer.save()

### Change the path for saving the next plots
if not os.path.isdir(output_path + "/all_plots/time_series/" + trial_name):
    os.mkdir(output_path + "/all_plots/time_series/" + trial_name)
    os.chdir(output_path + "/all_plots/time_series/" + trial_name)
else:
    os.chdir(output_path + "/all_plots/time_series/" + trial_name)

mpl.rcParams["font.size"] = font_size
sns.set_style("white")

# Plot the food concentration (cells_per_ml; NOT dampening-corrected)
fig = plt.figure(figsize=(fig_width, fig_height))
ax = fig.add_subplot(111)
lns0 = ax.plot_date(main_df["DateTime"], main_df["cells_per_ml_C"],
                    label='C', color='limegreen', linestyle='-', linewidth=1, ms=0.01)
lns1 = ax.plot_date(main_df["DateTime"], main_df["cells_per_ml_S1"],
                    label='S1', color='steelblue', linestyle='-', linewidth=1, ms=0.01)
lns2 = ax.plot_date(main_df["DateTime"], main_df["cells_per_ml_S2"],
                    label='S2', color='blue', linestyle='-', linewidth=1, ms=0.01)
lns3 = ax.plot_date(main_df["DateTime"], main_df["cells_per_ml_S3"],
                    label='S3', color='deepskyblue', linestyle='-', linewidth=1, ms=0.01)
ax.set_xlabel('Date & time (MM-dd HH)')
ax.set_ylim(min_cells_per_mL, max_cells_per_mL)
ax.set_ylabel("Food (cells mL$^{-1}$)")
ax1 = fig.add_subplot(111)
fig.autofmt_xdate()
ax1 = ax.twinx()
lns4 = ax1.plot_date(main_df["DateTime"], main_df["Temp_C_x"],
                    label='temperature', color='darkred', linestyle='-',

```

```

        linewidth=1, ms=0.01)
ax1.set_ylabel("Temperature (°C)")
lns = lns0+lns1+lns2+lns3
labs = [l.get_label() for l in lns]
leg = plt.legend(lns, labs, ncol=4, loc='upper center',
                prop={'size': legend_font_size}, fancybox=False,
                frameon=False, bbox_to_anchor=(0.5, 1.2), framealpha=0.7)
# set the linewidth of each legend object
for legobj in leg.legendHandles:
    legobj.set_linewidth(3.0)
ax1.set_yticks(np.arange(min_temp, max_temp, 3))
ax1.set_ylim(bottom=min_temp-1)
ax1.tick_params(axis='y', colors='darkred')
ax1.yaxis.label.set_color('darkred')
plt.savefig(trial_name + '_NOTDampeningEffectCorrected_food_cells_per_ml' +
            '.pdf', bbox_inches='tight')

# Plot Secondary-Trended Dampening-effect-Corrected food-concentration
# (ST_DC_cells_per_ml_C)
fig = plt.figure(figsize=(fig_width, fig_height))
ax = fig.add_subplot(111)
lns0 = ax.plot_date(main_df["DateTime"], main_df["ST_DC_cells_per_ml_C"],
                    label='C', color='limegreen', linestyle='-', linewidth=1, ms=0.01)
lns1 = ax.plot_date(main_df["DateTime"], main_df["ST_DC_cells_per_ml_S1"],
                    label='S1', color='steelblue', linestyle='-', linewidth=1, ms=0.01)
lns2 = ax.plot_date(main_df["DateTime"], main_df["ST_DC_cells_per_ml_S2"],
                    label='S2', color='blue', linestyle='-', linewidth=1, ms=0.01)
lns3 = ax.plot_date(main_df["DateTime"], main_df["ST_DC_cells_per_ml_S3"],
                    label='S3', color='deepskyblue', linestyle='-', linewidth=1, ms=0.01)
ax.set_xlabel('Date & time (MM-dd HH)')
ax.set_ylim(min_cells_per_mL, max_cells_per_mL)
ax.set_ylabel(r"Food (cells mL-1)")
ax1 = fig.add_subplot(111)
fig.autofmt_xdate()
ax1 = ax.twinx()
lns4 = ax1.plot_date(main_df["DateTime"], main_df["Temp_C_x"],
                    label='temperature', color='darkred', linestyle='-',
                    linewidth=1, ms=0.01)
ax1.set_ylabel("Temperature (°C)")
lns = lns0+lns1+lns2+lns3
labs = [l.get_label() for l in lns]
leg = plt.legend(lns, labs, ncol=4, loc='upper center',
                prop={'size': legend_font_size}, fancybox=False,
                frameon=False, bbox_to_anchor=(0.5, 1.2), framealpha=0.7)
# set the linewidth of each legend object
for legobj in leg.legendHandles:
    legobj.set_linewidth(3.0)
ax1.set_yticks(np.arange(min_temp, max_temp, 3))
ax1.set_ylim(bottom=min_temp-1)
ax1.tick_params(axis='y', colors='darkred')
ax1.yaxis.label.set_color('darkred')
plt.savefig(trial_name +
            '_SecondaryTrended_DampeningEffectCorrected_food_cells_per_ml_C' +
            '.pdf', bbox_inches='tight')

# Plot dissolved-oxygen concentration (percent_air_sat)
fig = plt.figure(figsize=(fig_width, fig_height))
ax = fig.add_subplot(111)
lns0 = ax.plot_date(main_df["DateTime"], main_df["control_percent_air_sat_C"],
                    label='C', color='limegreen', linestyle='-', linewidth=1, ms=0.01)
lns1 = ax.plot_date(main_df["DateTime"], main_df["corrected_percent_air_sat_S1"],
                    label='S1', color='steelblue', linestyle='-', linewidth=1, ms=0.01)
lns2 = ax.plot_date(main_df["DateTime"], main_df["corrected_percent_air_sat_S2"],
                    label='S2', color='blue', linestyle='-', linewidth=1, ms=0.01)
lns3 = ax.plot_date(main_df["DateTime"], main_df["corrected_percent_air_sat_S3"],
                    label='S3', color='deepskyblue', linestyle='-', linewidth=1, ms=0.01)
ax.set_xlabel('Date & time (MM-dd HH)')
ax.set_ylim(min_percent_air_sat, max_percent_air_sat)
ax.set_ylabel("Diss. O2 (% air sat.)")

```

```

ax1 = fig.add_subplot(111)
fig.autofmt_xdate()
ax1 = ax.twinx()
lns4 = ax1.plot_date(main_df["DateTime"], main_df["Temp_C_x"],
                    label='temperature', color='darkred', linestyle='-',
                    linewidth=1, ms=0.01)
ax1.set_ylabel("Temperature (°C)")
lns = lns0+lns1+lns2+lns3
labs = [l.get_label() for l in lns]
leg = plt.legend(lns, labs, ncol=4, loc='upper center', prop={'size': legend_font_size},
                fancybox=False, frameon=False, bbox_to_anchor=(0.5, 1.2), framealpha=0.7)
# set the linewidth of each legend object
for legobj in leg.legendHandles:
    legobj.set_linewidth(3.0)
ax1.set_yticks(np.arange(min_temp, max_temp, 3))
ax1.set_ylim(bottom=min_temp-1)
ax1.tick_params(axis='y', colors='darkred')
ax1.yaxis.label.set_color('darkred')
plt.savefig(
    trial_name + '_trended_corrected_oxyg_percent_air_sat' +
    '.pdf', bbox_inches='tight')

# Plot dissolved-oxygen concentration (ymol_per_l)
fig = plt.figure(figsize=(fig_width, fig_height))
ax = fig.add_subplot(111)
lns0 = ax.plot_date(main_df["DateTime"], main_df["control_ymol_per_l_C"],
                    label='C', color='limegreen', linestyle='-', linewidth=1, ms=0.01)
lns1 = ax.plot_date(main_df["DateTime"], main_df["corrected_ymol_per_l_S1"],
                    label='S1', color='steelblue', linestyle='-', linewidth=1, ms=0.01)
lns2 = ax.plot_date(main_df["DateTime"], main_df["corrected_ymol_per_l_S2"],
                    label='S2', color='blue', linestyle='-', linewidth=1, ms=0.01)
lns3 = ax.plot_date(main_df["DateTime"], main_df["corrected_ymol_per_l_S3"],
                    label='S3', color='deepskyblue', linestyle='-', linewidth=1, ms=0.01)
ax.set_xlabel('Date & time (MM-dd HH)')
ax.set_ylim(min_micromol_per_L, max_micromol_per_L)
ax.set_ylabel('Diss. O2 (μmol L-1)')
ax1 = fig.add_subplot(111)
fig.autofmt_xdate()
ax1 = ax.twinx()
lns4 = ax1.plot_date(main_df["DateTime"], main_df["Temp_C_x"],
                    label='temperature', color='darkred', linestyle='-',
                    linewidth=1, ms=0.01)
ax1.set_ylabel("Temperature (°C)")
lns = lns0+lns1+lns2+lns3
labs = [l.get_label() for l in lns]
leg = plt.legend(lns, labs, ncol=4, loc='upper center', prop={'size': legend_font_size},
                fancybox=False, frameon=False, bbox_to_anchor=(0.5, 1.2), framealpha=0.7)
# set the linewidth of each legend object
for legobj in leg.legendHandles:
    legobj.set_linewidth(3.0)
ax1.set_yticks(np.arange(min_temp, max_temp, 3))
ax1.set_ylim(bottom=min_temp-1)
ax1.tick_params(axis='y', colors='darkred')
ax1.yaxis.label.set_color('darkred')
plt.savefig(trial_name + '_trended_corrected_oxyg_ymol_per_l' +
    '.pdf', bbox_inches='tight')

### Plot filtration rate (ml_per_min) and respiration rate (ymolO2_per_min)
fig = plt.figure(figsize=(fig_width, 1.94 * fig_height))
ax = fig.add_subplot(211)
lns1 = ax.plot_date(main_df["DateTime"], main_df["filt_ml_per_min_S1"],
                    label='S1', color='steelblue', linestyle='-', linewidth=1, ms=0.01)
lns2 = ax.plot_date(main_df["DateTime"], main_df["filt_ml_per_min_S2"],
                    label='S2', color='blue', linestyle='-', linewidth=1, ms=0.01)
lns3 = ax.plot_date(main_df["DateTime"], main_df["filt_ml_per_min_S3"],
                    label='S3', color='deepskyblue', linestyle='-', linewidth=1, ms=0.01)
ax.set_xlabel('Date & time (MM-dd HH)')
ax.set_ylabel(r'Filt. (ml min-1)')
ax.set_ylim(min_filt, max_filt)

```

```

ax1 = fig.add_subplot(211)
fig.autofmt_xdate()
ax1 = ax.twinx()
lns4 = ax1.plot_date(main_df["DateTime"], main_df["Temp_C_x"],
                    label='temperature', color='darkred', linestyle='-',
                    linewidth=1, ms=0.01)
ax1.set_ylabel("Temperature (°C)")
ax1.set_yticks(np.arange(min_temp, max_temp, 3))
ax1.set_ylim(bottom=min_temp-1)
lns = lns1+lns2+lns3
labs = [l.get_label() for l in lns]
leg = plt.legend(lns, labs, ncol=3, loc='upper center', prop={'size': legend_font_size},
                fancybox=False, frameon=False, bbox_to_anchor=(0.5, 1.2),
                framealpha=0.7)
# set the linewidth of each legend object
for legobj in leg.legendHandles:
    legobj.set_linewidth(3.0)
ax3 = fig.add_subplot(212)
lns5 = ax3.plot_date(main_df["DateTime"], main_df['resp_ymolO2_per_min_S1'],
                    label='S1', color='steelblue', linestyle='-', linewidth=1, ms=0.01)
lns6 = ax3.plot_date(main_df["DateTime"], main_df['resp_ymolO2_per_min_S2'],
                    label='S2', color='blue', linestyle='-', linewidth=1, ms=0.01)
lns7 = ax3.plot_date(main_df["DateTime"], main_df['resp_ymolO2_per_min_S3'],
                    label='S3', color='deepskyblue', linestyle='-', linewidth=1, ms=0.01)
ax3.set_xlabel('Date & time (MM-dd HH)')
ax3.set_ylabel('Resp. (μmolO2 min-1)')
ax3.set_ylim(min_resp, max_resp)
ax4 = fig.add_subplot(212)
fig.autofmt_xdate()
ax4 = ax3.twinx()
lns8 = ax4.plot_date(main_df["DateTime"], main_df["Temp_C_x"],
                    label='temperature', color='darkred', linestyle='-',
                    linewidth=1, ms=0.01)
ax4.set_ylabel("Temperature (°C)")
ax4.set_yticks(np.arange(min_temp, max_temp, 3))
ax4.set_ylim(bottom=min_temp-1)
ax1.tick_params(axis='y', colors='darkred')
ax1.yaxis.label.set_color('darkred')
ax4.tick_params(axis='y', colors='darkred')
ax4.yaxis.label.set_color('darkred')
fig.subplots_adjust(hspace=0.07)
plt.savefig(
    trial_name + '_filtration (ml_per_min) and respiration (ymolO2_per_min)' +
    '.pdf', bbox_inches='tight')

# Plot the (experimental) feeding (cells_per_min and J_per_h)
fig = plt.figure(figsize=(fig_width, 1.94 * fig_height))
ax = fig.add_subplot(211)
lns1 = ax.plot_date(main_df["DateTime"], main_df["feed_cells_per_min_S1"],
                    label='S1', color='steelblue', linestyle='-', linewidth=1, ms=0.01)
lns2 = ax.plot_date(main_df["DateTime"], main_df["feed_cells_per_min_S2"],
                    label='S2', color='blue', linestyle='-', linewidth=1, ms=0.01)
lns3 = ax.plot_date(main_df["DateTime"], main_df["feed_cells_per_min_S3"],
                    label='S3', color='deepskyblue', linestyle='-', linewidth=1, ms=0.01)
ax.set_xlabel('Date & time (MM-dd HH)')
ax.set_ylabel(r"Feed. (cells min-1)")
ax1 = fig.add_subplot(211)
fig.autofmt_xdate()
ax1 = ax.twinx()
lns4 = ax1.plot_date(main_df["DateTime"], main_df["Temp_C_x"],
                    label='temperature', color='darkred', linestyle='-',
                    linewidth=1, ms=0.01)
ax1.set_ylabel("Temperature (°C)")
lns = lns1+lns2+lns3
labs = [l.get_label() for l in lns]
leg = plt.legend(lns, labs, ncol=3, loc='upper center',
                prop={'size': legend_font_size}, fancybox=False,
                frameon=False, bbox_to_anchor=(0.5, 1.2), framealpha=0.7)
# set the linewidth of each legend object

```

```

for legobj in leg.legendHandles:
    legobj.set_linewidth(3.0)
ax3 = fig.add_subplot(212)
lns5 = ax3.plot_date(main_df["DateTime"], main_df["feed_J_per_h_S1"],
                    label='S1', color='steelblue', linestyle='-', linewidth=1, ms=0.01)
lns6 = ax3.plot_date(main_df["DateTime"], main_df["feed_J_per_h_S2"],
                    label='S2', color='blue', linestyle='-', linewidth=1, ms=0.01)
lns7 = ax3.plot_date(main_df["DateTime"], main_df["feed_J_per_h_S3"],
                    label='S3', color='deepskyblue', linestyle='-', linewidth=1, ms=0.01)
ax3.set_xlabel("Date & time (MM-dd HH)")
ax3.set_ylabel("Feed. (J h$^{-1}$)")
ax4 = fig.add_subplot(212)
fig.autofmt_xdate()
ax4 = ax3.twinx()
lns8 = ax4.plot_date(main_df["DateTime"], main_df["Temp_C_x"],
                    label='temperature', color='darkred', linestyle='-',
                    linewidth=1, ms=0.01)
ax4.set_ylabel("Temperature (°C)")
ax1.set_yticks(np.arange(min_temp, max_temp, 3))
ax1.set_ylim(bottom=min_temp-1)
ax4.set_yticks(np.arange(min_temp, max_temp, 3))
ax4.set_ylim(bottom=min_temp-1)
ax1.tick_params(axis='y', colors='darkred')
ax1.yaxis.label.set_color('darkred')
ax4.tick_params(axis='y', colors='darkred')
ax4.yaxis.label.set_color('darkred')
fig.subplots_adjust(hspace=0.07)
plt.savefig(
    trial_name + '_experimental feeding (cells_per_min and J_per_h)' +
    '.pdf', bbox_inches='tight')

# Plot the respiration rate (J_per_h)
fig = plt.figure(figsize=(fig_width, fig_height))
ax = fig.add_subplot(111)
lns1 = ax.plot_date(main_df["DateTime"], main_df["resp_J_per_h_S1"],
                    label='S1', color='steelblue', linestyle='-', linewidth=1, ms=0.01)
lns2 = ax.plot_date(main_df["DateTime"], main_df["resp_J_per_h_S2"],
                    label='S2', color='blue', linestyle='-', linewidth=1, ms=0.01)
lns3 = ax.plot_date(main_df["DateTime"], main_df["resp_J_per_h_S3"],
                    label='S3', color='deepskyblue', linestyle='-', linewidth=1, ms=0.01)
ax.set_xlabel("Date & time (MM-dd HH)")
ax.set_ylabel(r"Resp. (J h$^{-1}$)")
ax1 = fig.add_subplot(111)
fig.autofmt_xdate()
ax1 = ax.twinx()
lns4 = ax1.plot_date(main_df["DateTime"], main_df["Temp_C_x"],
                    label='temperature', color='darkred', linestyle='-',
                    linewidth=1, ms=0.01)
ax1.set_ylabel("Temperature (°C)")
lns = lns1+lns2+lns3
labs = [l.get_label() for l in lns]
leg = plt.legend(lns, labs, ncol=3, loc='upper center',
                prop={'size': legend_font_size}, fancybox=False,
                frameon=False, bbox_to_anchor=(0.5, 1.2), framealpha=0.7)
# set the linewidth of each legend object
for legobj in leg.legendHandles:
    legobj.set_linewidth(3.0)
ax1.set_yticks(np.arange(min_temp, max_temp, 3))
ax1.set_ylim(bottom=min_temp-1)
ax1.tick_params(axis='y', colors='darkred')
ax1.yaxis.label.set_color('darkred')
plt.savefig(trial_name + '_respiration (J_per_h)' + '.pdf', bbox_inches='tight')

# Plot the (hypothetical) SFG (J_per_h)
for i in food_conc:
    fig = plt.figure(figsize=(fig_width, fig_height))
    ax = fig.add_subplot(111)
    lns1 = ax.plot_date(main_df["DateTime"], main_df["SFG_hypo_J_per_h_" + str(
        i) + "_cells_S1"], label='S1', color='steelblue', linestyle='-', linewidth=1, ms=0.01)

```



```

    Chl_df['Date'].apply(str)+' '+Chl_df['Time'])
Chl_df = Chl_df.reset_index()
# producing robust estimated trends
flatten_lc1, trend_lc1 = flatten(Chl_df['index'],
                                Chl_df[filename[:-4]+'_mV_Ch'],
                                method=robust_estimator,
                                window_length=60, cval=5,
                                return_trend=True)
Chl_df[filename[:-4] + '_mV_Ch' +
        '_Trend'] = pd.Series(trend_lc1)
Chl_df = Chl_df.set_index('DateTime').resample('30S').last()
Chl_df.reset_index(inplace=True)
Chl_temp_df = pd.merge(
    Chl_df, temp_df, on='DateTime', how='inner')
Chl_temp_df['Temp_C'] = Chl_temp_df['Temp_C'].apply(
    pd.to_numeric, errors='coerce') # changes Temp_Ch from object to float64
# temperature compensation (TC)
Chl_temp_df[filename[:-4] + '_mV_Ch' + '_Trend_TC'] = (
    Chl_temp_df[filename[:-4] + '_mV_Ch' + '_Trend']/
    (1 + ((Chl_temp_df['Temp_C'] - reference_temperature)*
        TS_coef)))

if counter == 0:
    Chl_temp_df = pd.DataFrame(
        Chl_temp_df, columns=[
            'DateTime', 'Temp_C', filename[:-4]+'_mV_Ch',
            filename[:-4] + '_mV_Ch' + '_Trend',
            filename[:-4] + '_mV_Ch' + '_Trend_TC'])
else:
    Chl_temp_df = pd.DataFrame(
        Chl_temp_df, columns=[
            filename[:-4]+'_mV_Ch',
            filename[:-4] + '_mV_Ch' + '_Trend',
            filename[:-4] + '_mV_Ch' + '_Trend_TC'])
    appended_data.append(Chl_temp_df)
    counter = counter + 1
appended_data = pd.concat(appended_data, axis=1)
post_Ch temp_df = appended_data.reset_index()

# checking post_Ch temp_df
with pd.option_context('display.max_rows', 10, 'display.max_columns', None):
    print(post_Ch temp_df)

# the trend plot
if not os.path.isdir(output_path + "/all_plots/time_series/" + trial_name):
    os.mkdir(output_path + "/all_plots/time_series/" + trial_name)
    os.chdir(output_path + "/all_plots/time_series/" + trial_name)
else:
    os.chdir(output_path + "/all_plots/time_series/" + trial_name)

mpl.rcParams["font.size"] = font_size
sns.set_style("white")
sns.set_style("ticks", {"xtick.major.size": 8, "ytick.major.size": 8})
fig = plt.figure(figsize=(fig_width, fig_height))
ax = fig.add_subplot(111)
lns1 = ax.plot(post_Ch temp_df["index"], post_Ch temp_df["post_C_mV_Ch"],
               label='C', color='limegreen', linestyle='-', linewidth=1, alpha=0.5)
lns2 = ax.plot(post_Ch temp_df["index"], post_Ch temp_df["post_S1_mV_Ch"],
               label='S1', color='steelblue', linestyle='-', linewidth=1, alpha=0.5)
lns3 = ax.plot(post_Ch temp_df["index"], post_Ch temp_df["post_S2_mV_Ch"],
               label='S2', color='blue', linestyle='-', linewidth=1, alpha=0.5)
lns4 = ax.plot(post_Ch temp_df["index"], post_Ch temp_df["post_S3_mV_Ch"],
               label='S3', color='deepskyblue', linestyle='-', linewidth=1, alpha=0.5)
lns5 = ax.plot(post_Ch temp_df["index"], post_Ch temp_df["post_C_mV_Ch_Trend"],
               label='C', color='limegreen', linestyle='-', linewidth=2)
lns6 = ax.plot(post_Ch temp_df["index"], post_Ch temp_df["post_S1_mV_Ch_Trend"],
               label='S1', color='steelblue', linestyle='-', linewidth=2)
lns7 = ax.plot(post_Ch temp_df["index"], post_Ch temp_df["post_S2_mV_Ch_Trend"],
               label='S2', color='blue', linestyle='-', linewidth=2)

```

```

Ins8 = ax.plot(post_Ch1_temp_df["index"], post_Ch1_temp_df["post_S3_mV_Ch1_Trend"],
              label='S3', color='deepskyblue', linestyle='-', linewidth=2)
Ins9 = ax.plot(post_Ch1_temp_df["index"], post_Ch1_temp_df["post_C_mV_Ch1_Trend_TC"],
              label='C', color='black', linestyle=':', linewidth=1)
Ins10 = ax.plot(post_Ch1_temp_df["index"], post_Ch1_temp_df["post_S1_mV_Ch1_Trend_TC"],
              label='S1', color='black', linestyle=':', linewidth=1)
Ins11 = ax.plot(post_Ch1_temp_df["index"], post_Ch1_temp_df["post_S2_mV_Ch1_Trend_TC"],
              label='S2', color='black', linestyle=':', linewidth=1)
Ins12 = ax.plot(post_Ch1_temp_df["index"], post_Ch1_temp_df["post_S3_mV_Ch1_Trend_TC"],
              label='S3', color='black', linestyle=':', linewidth=1)
ax.set_xlabel('Cumulative time (' + str(flou_data_collection_frequency) + ' min)')
ax.set_ylabel('Ch1 (mV)')
ax1 = fig.add_subplot(111)
ax1 = ax.twinx()
Ins13 = ax1.plot(post_Ch1_temp_df["index"], post_Ch1_temp_df["Temp_C"],
                label='Temperature', color='darkred', linestyle='-',
                linewidth=1)
ax1.set_yticks(np.arange(min_temp, max_temp, 3))
ax1.set_ylim(bottom=min_temp-1)
ax1.set_ylabel("Temperature (°C)")
Ins = Ins5+Ins6+Ins7+Ins8
labs = [l.get_label() for l in Ins]
leg = plt.legend(Ins, labs, ncol=4, loc='upper center',
                prop={'size': legend_font_size}, fancybox=False,
                frameon=False, bbox_to_anchor=(0.5, 1.2),
                framealpha=0.7)
# set the linewidth of each legend object
for legobj in leg.legendHandles:
    legobj.set_linewidth(3.0)
ax1.tick_params(axis='y', colors='darkred')
ax1.yaxis.label.set_color('darkred')
plt.savefig(trial_name + '_post_Ch1_raw_vs_trended.pdf',
            bbox_inches='tight')
plt.show()
plt.pause(0.001)
#input("postss [enter] to continue.")

# choose the stable interval based on the plot and the data frame
# postsented in the Console
while True:
    try:
        start_stable_data = int(input(
            'Please provide start_stable_data as an integer based on the\
            plot and the data frame presented in the Console (the stable\
            data interval usually include the last 10-50 data points): ')
        if start_stable_data < 5 or start_stable_data > \
            (max(post_Ch1_temp_df["index"])-2):
            raise ValueError # this will send it to the print message and back to the input option
        break
    except ValueError:
        print("Invalid integer. The input is out of range or not an integer!")

while True:
    try:
        end_stable_data = int(input(
            'Please provide end_stable_data as an integer (based on the\
            plot and the data frame postsented in the Console): ')
        if end_stable_data < start_stable_data or end_stable_data > \
            max(post_Ch1_temp_df["index"]):
            raise ValueError # this will send it to the print message and back to the input option
        break
    except ValueError:
        print("Invalid integer. The input is out of range or not an integer!")

#####

# Crop the the 'post-trial stable-period'

```

```

mask = (post_Ch1_temp_df["index"] > start_stable_data) & (
    post_Ch1_temp_df["index"] <= end_stable_data)
post_Ch1_temp_filt_df = post_Ch1_temp_df.loc[mask]

if not os.path.isdir(output_path + "/pre_stat_post_drift_tables/post/food"):
    os.mkdir(output_path + "/pre_stat_post_drift_tables/post/food")
    os.chdir(output_path + "/pre_stat_post_drift_tables/post/food")
else:
    os.chdir(output_path + "/pre_stat_post_drift_tables/post/food")

""" Similar to the main-trial processing, calculate percent_Ch1 with \
respect to mV_Ch1_Trend_TC of the 'pre-trial stable-period' (to account \
for inherent differences in the absolute sensors' readouts) and, then, \
convert main-trial food-concentration data from percentage to \
cells_per_ml using the 'initial concentration' (the mean concentration \
recorded by sensor_C over 'pre-trial stable-period')."""
post_Ch1_temp_filt_df.loc[:, 'percent_C'] = (
    post_Ch1_temp_filt_df['post_C_mV_Ch1_Trend_TC']/
    statistics_Ch1_pre.at["mean", "pre_C_mV_Ch1_Trend_TC"])*100
post_Ch1_temp_filt_df.loc[:, 'percent_S1'] = (
    post_Ch1_temp_filt_df['post_S1_mV_Ch1_Trend_TC']/
    statistics_Ch1_pre.at["mean", "pre_S1_mV_Ch1_Trend_TC"])*100
post_Ch1_temp_filt_df.loc[:, 'percent_S2'] = (
    post_Ch1_temp_filt_df['post_S2_mV_Ch1_Trend_TC']/
    statistics_Ch1_pre.at["mean", "pre_S2_mV_Ch1_Trend_TC"])*100
post_Ch1_temp_filt_df.loc[:, 'percent_S3'] = (
    post_Ch1_temp_filt_df['post_S3_mV_Ch1_Trend_TC']/
    statistics_Ch1_pre.at["mean", "pre_S3_mV_Ch1_Trend_TC"])*100

post_Ch1_temp_filt_df.loc[:, 'cells_per_ml_C'] = (
    post_Ch1_temp_filt_df['percent_C']*initial_concentration_cells_per_ml)/100
post_Ch1_temp_filt_df.loc[:, 'cells_per_ml_S1'] = (
    post_Ch1_temp_filt_df['percent_S1']*initial_concentration_cells_per_ml)/100
post_Ch1_temp_filt_df.loc[:, 'cells_per_ml_S2'] = (
    post_Ch1_temp_filt_df['percent_S2']*initial_concentration_cells_per_ml)/100
post_Ch1_temp_filt_df.loc[:, 'cells_per_ml_S3'] = (
    post_Ch1_temp_filt_df['percent_S3']*initial_concentration_cells_per_ml)/100

# to prevent an error related to D&T
post_Ch1_temp_filt_df = post_Ch1_temp_filt_df[(
    post_Ch1_temp_filt_df['DateTime'] > '2018-01-01')]

# Define post_filt columns
post_Ch1_temp_filt_df.loc[:, 'post_filt_S1'] = (
    ((post_Ch1_temp_filt_df["cells_per_ml_C"] -
    post_Ch1_temp_filt_df["cells_per_ml_S1"])/
    post_Ch1_temp_filt_df["cells_per_ml_S1"]) * flow_rate)
post_Ch1_temp_filt_df.loc[:, 'post_filt_S2'] = (
    ((post_Ch1_temp_filt_df["cells_per_ml_C"] -
    post_Ch1_temp_filt_df["cells_per_ml_S2"])/
    post_Ch1_temp_filt_df["cells_per_ml_S2"]) * flow_rate)
post_Ch1_temp_filt_df.loc[:, 'post_filt_S3'] = (
    ((post_Ch1_temp_filt_df["cells_per_ml_C"] -
    post_Ch1_temp_filt_df["cells_per_ml_S3"])/
    post_Ch1_temp_filt_df["cells_per_ml_S3"]) * flow_rate)

""" Calculate the cumulative_random_effects (ratio of the post_trial
to the main_trial_baseline filtration rates."""
post_Ch1_temp_filt_df.loc[:, 'filt_%_cumulative_random_effects_S1'] = (
    post_Ch1_temp_filt_df["post_filt_S1"])/(
    statistics_main_baseline.at["mean", "filt_ml_per_min_S1"])*100
post_Ch1_temp_filt_df.loc[:, 'filt_%_cumulative_random_effects_S2'] = (
    post_Ch1_temp_filt_df["post_filt_S2"])/(
    statistics_main_baseline.at["mean", "filt_ml_per_min_S2"])*100
post_Ch1_temp_filt_df.loc[:, 'filt_%_cumulative_random_effects_S3'] = (
    post_Ch1_temp_filt_df["post_filt_S3"])/(
    statistics_main_baseline.at["mean", "filt_ml_per_min_S3"])*100

```

```

statistics_Ch1_post = post_Ch1_temp_filt_df.describe()
statistics_Ch1_post = statistics_Ch1_post.iloc[[1], :]
statistics_Ch1_post

writer = ExcelWriter('statistics_post_stable_period_' + trial_name + '.xlsx')
statistics_Ch1_post.to_excel(writer, 'Sheet1')
writer.save()

```

Estimate the post-trial respiration rate

```

if os.path.isdir(raw_data_path + "/raw_data_Oxygen/" + trial_name + "/post"):
    os.chdir(raw_data_path + "/raw_data_Oxygen/" + trial_name + "/post")
    filename = glob("*.xlsx")
    post_oxyg_temp_df = pd.ExcelFile(filename[0])
    post_oxyg_temp_df.sheet_names
    [u'Sheet1']
    post_oxyg_temp_df = post_oxyg_temp_df.parse("Sheet1")

post_oxyg_temp_df = post_oxyg_temp_df.reset_index()

oxyg_cols = [i for i in list(post_oxyg_temp_df) if 'post_' in i]
for i in oxyg_cols:
    # producing robust time-series models using robust_estimators
    flatten_lc1, trend_lc1 = flatten(post_oxyg_temp_df[i],
                                   post_oxyg_temp_df[i],
                                   method=robust_estimator,
                                   window_length=60, cval=5,
                                   return_trend=True)
    post_oxyg_temp_df[i + '_Trend'] = pd.Series(trend_lc1)

with pd.option_context('display.max_rows', 20, 'display.max_columns', None):
    print(post_oxyg_temp_df)

# the trend plot
if not os.path.isdir(output_path + "/all_plots/time_series/" + trial_name):
    os.mkdir(output_path + "/all_plots/time_series/" + trial_name)
    os.chdir(output_path + "/all_plots/time_series/" + trial_name)
else:
    os.chdir(output_path + "/all_plots/time_series/" + trial_name)

mpl.rcParams["font.size"] = font_size
sns.set_style("white")
sns.set_style("ticks", {"xtick.major.size": 8, "ytick.major.size": 8})
fig = plt.figure(figsize=(fig_width, fig_height))
ax = fig.add_subplot(111)
lns1 = ax.plot(post_oxyg_temp_df["index"], post_oxyg_temp_df["post_C_percent_air_sat"],
               label='C', color='limegreen', linestyle='-', linewidth=1, alpha=0.5)
lns2 = ax.plot(post_oxyg_temp_df["index"], post_oxyg_temp_df["post_S1_percent_air_sat"],
               label='S1', color='steelblue', linestyle='-', linewidth=1, alpha=0.5)
lns3 = ax.plot(post_oxyg_temp_df["index"], post_oxyg_temp_df["post_S2_percent_air_sat"],
               label='S2', color='blue', linestyle='-', linewidth=1, alpha=0.5)
lns4 = ax.plot(post_oxyg_temp_df["index"], post_oxyg_temp_df["post_S3_percent_air_sat"],
               label='S3', color='deepskyblue', linestyle='-', linewidth=1, alpha=0.5)
lns5 = ax.plot(post_oxyg_temp_df["index"], post_oxyg_temp_df["post_C_percent_air_sat_Trend"],
               label='C', color='limegreen', linestyle='-', linewidth=2)
lns6 = ax.plot(post_oxyg_temp_df["index"], post_oxyg_temp_df["post_S1_percent_air_sat_Trend"],
               label='S1', color='steelblue', linestyle='-', linewidth=2)
lns7 = ax.plot(post_oxyg_temp_df["index"], post_oxyg_temp_df["post_S2_percent_air_sat_Trend"],
               label='S2', color='blue', linestyle='-', linewidth=2)
lns8 = ax.plot(post_oxyg_temp_df["index"], post_oxyg_temp_df["post_S3_percent_air_sat_Trend"],
               label='S3', color='deepskyblue', linestyle='-', linewidth=2)
ax.set_xlabel('Cumulative time (' + str(oxyg_data_collection_frequency) + ' min)')
ax.set_ylabel('Diss. $O_2$ (% air sat.)')
ax1 = fig.add_subplot(111)
ax1 = ax.twinx()
lns9 = ax1.plot(post_oxyg_temp_df["index"], post_oxyg_temp_df["Temp_C"],
                label='Temperature', color='darkred', linestyle='-', linewidth=1)
ax1.set_ylabel("Temperature (°C)")
ax1.set_yticks(np.arange(min_temp, max_temp, 3))

```

```

ax1.set_ylim(bottom=min_temp-1)
lns = lns5+lns6+lns7+lns8
labs = [l.get_label() for l in lns]
leg = plt.legend(lns, labs, ncol=4, loc='upper center',
                prop={'size': legend_font_size}, fancybox=False,
                frameon=False, bbox_to_anchor=(0.5, 1.2),
                framealpha=0.7)
# set the linewidth of each legend object
for legobj in leg.legendHandles:
    legobj.set_linewidth(3.0)
ax1.tick_params(axis='y', colors='darkred')
ax1.yaxis.label.set_color('darkred')
plt.savefig(trial_name + '_post_oxyg_raw_vs_trended.pdf',
            bbox_inches='tight')
plt.show()
plt.pause(0.001)

while True:
    try:
        start_stable_data = int(input(
            'Please provide start_stable_data as an integer based on the\
            plot and the data frame presented in the Console (the stable\
            data interval usually include the last 100 or more data points): ')
        if start_stable_data < 0 or start_stable_data > \
            (max(post_oxyg_temp_df["index"])-2)):
            raise ValueError
        break
    except ValueError:
        print("Invalid integer. The input is out of range or not an integer!")

while True:
    try:
        end_stable_data = int(
            input('Please provide end_stable_data as an integer: ')
        if end_stable_data < start_stable_data or end_stable_data > \
            max(post_oxyg_temp_df["index"]):
            raise ValueError
        break
    except ValueError:
        print("Invalid integer. The input is out of range or not an integer!")

#####
# Crop the 'post-trial stable-interval'
mask = (post_oxyg_temp_df["index"] >= start_stable_data) & (
    post_oxyg_temp_df["index"] <= end_stable_data)
post_oxyg_temp_resp_df = post_oxyg_temp_df.loc[mask]

if not os.path.isdir(output_path + "/pre_stat_post_drift_tables/post/oxyg"):
    os.mkdir(output_path + "/pre_stat_post_drift_tables/post/oxyg")
    os.chdir(output_path + "/pre_stat_post_drift_tables/post/oxyg")
else:
    os.chdir(output_path + "/pre_stat_post_drift_tables/post/oxyg")

""" The average difference between measurements of Path_Sn and Path_C sensors
over the 'pre-trial stable-period' is added to the post-trial data of the
corresponding sensor_Sn."""

post_oxyg_temp_resp_df.loc[:, 'control_ymol_per_1_C'] = (
    post_oxyg_temp_resp_df['post_C_ymol_per_1_Trend'])
post_oxyg_temp_resp_df.loc[:, 'corrected_ymol_per_1_S1'] = (
    post_oxyg_temp_resp_df['post_S1_ymol_per_1_Trend'] +
    statistics_oxyg_pre.at["mean", 'pre_C_minus_S1_ymol_per_1_Trend'])
post_oxyg_temp_resp_df.loc[:, 'corrected_ymol_per_1_S2'] = (
    post_oxyg_temp_resp_df['post_S2_ymol_per_1_Trend'] +
    statistics_oxyg_pre.at["mean", 'pre_C_minus_S2_ymol_per_1_Trend'])
post_oxyg_temp_resp_df.loc[:, 'corrected_ymol_per_1_S3'] = (
    post_oxyg_temp_resp_df['post_S3_ymol_per_1_Trend'] +
    statistics_oxyg_pre.at["mean", 'pre_C_minus_S3_ymol_per_1_Trend'])

```

```

post_oxyg_temp_resp_df.loc[:, 'control_percent_air_sat_C'] = (
    post_oxyg_temp_resp_df['post_C_percent_air_sat_Trend'])
post_oxyg_temp_resp_df.loc[:, 'corrected_percent_air_sat_S1'] = (
    post_oxyg_temp_resp_df['post_S1_percent_air_sat_Trend'] +
    statistics_oxyg_pre.at["mean", 'pre_C_minus_S1_percent_air_sat'])
post_oxyg_temp_resp_df.loc[:, 'corrected_percent_air_sat_S2'] = (
    post_oxyg_temp_resp_df['post_S2_percent_air_sat_Trend'] +
    statistics_oxyg_pre.at["mean", 'pre_C_minus_S2_percent_air_sat'])
post_oxyg_temp_resp_df.loc[:, 'corrected_percent_air_sat_S3'] = (
    post_oxyg_temp_resp_df['post_S3_percent_air_sat_Trend'] +
    statistics_oxyg_pre.at["mean", 'pre_C_minus_S3_percent_air_sat'])

# to prevent an error related to D&T
post_oxyg_temp_resp_df = post_oxyg_temp_resp_df[(
    post_oxyg_temp_resp_df['DateTime'] > '2018-01-01')]

# Add "resp_μmolO2/min_ch" columns to the post_oxyg_temp_resp_df
post_oxyg_temp_resp_df.loc[:, 'post_resp_ymolO2_per_min_S1'] = (
    post_oxyg_temp_resp_df['control_ymol_per_1_C'] -
    post_oxyg_temp_resp_df['corrected_ymol_per_1_S1']) * (flow_rate * 0.001)
post_oxyg_temp_resp_df.loc[:, 'post_resp_ymolO2_per_min_S2'] = (
    post_oxyg_temp_resp_df['control_ymol_per_1_C'] -
    post_oxyg_temp_resp_df['corrected_ymol_per_1_S2']) * (flow_rate * 0.001)
post_oxyg_temp_resp_df.loc[:, 'post_resp_ymolO2_per_min_S3'] = (
    post_oxyg_temp_resp_df['control_ymol_per_1_C'] -
    post_oxyg_temp_resp_df['corrected_ymol_per_1_S3']) * (flow_rate * 0.001)

""" Calculate the cumulative_random_effects (i.e., ratio of the post_trial
to 'main_trial_baseline' respiration rates."""
post_oxyg_temp_resp_df.loc[:, 'resp_%_cumulative_random_effects_S1'] = (
    post_oxyg_temp_resp_df['post_resp_ymolO2_per_min_S1'] / (
        statistics_main_baseline.at["mean", "resp_ymolO2_per_min_S1"])) * 100
post_oxyg_temp_resp_df.loc[:, 'resp_%_cumulative_random_effects_S2'] = (
    post_oxyg_temp_resp_df['post_resp_ymolO2_per_min_S2'] / (
        statistics_main_baseline.at["mean", "resp_ymolO2_per_min_S2"])) * 100
post_oxyg_temp_resp_df.loc[:, 'resp_%_cumulative_random_effects_S3'] = (
    post_oxyg_temp_resp_df['post_resp_ymolO2_per_min_S3'] / (
        statistics_main_baseline.at["mean", "resp_ymolO2_per_min_S3"])) * 100

statistics_oxyg_post_10_Dec = post_oxyg_temp_resp_df.describe()
statistics_oxyg_post_10_Dec = statistics_oxyg_post_10_Dec.iloc[[1], :]

writer = ExcelWriter('statistics_post_stable_period_' + trial_name + '.xlsx')
statistics_oxyg_post_10_Dec.to_excel(writer, 'Sheet1')
writer.save()

```

Script S3: 'FOFS_integrative_processing.py'

```

#!/usr/bin/env python3
# -*- coding: utf-8 -*-
"""
@author: Jahangir Vajedsamiei (last test data: August 26, 2020)

```

Notes:

- This script continues data analysis for 2018-experiment.
- Before using the second script, an excel-sheet including the dry-weights and shell-lengths of the studied bivalves must be made.

```

# The modules used in this script
import os
from glob import glob as glob
import pandas as pd
import numpy as np
import datetime

```

```

import matplotlib.pyplot as plt
from pandas import ExcelWriter
import seaborn as sns
from pygam import LinearGAM, s, f
from matplotlib.lines import Line2D
from matplotlib.pylab import rcParams
import matplotlib as mpl
import matplotlib.dates as mdates
import time

answer = input("Did you already revise the absolute path to the experimental \
folder (experiment_path) and the variables. Enter y or n: ")
if answer == "n":
    print("Please push control+c, manually revise the '###experiment_path' \
and '###variables' below, and then rerun the script.")
    print("Push control+c")
    print("Push control+c")
    time.sleep(30)
elif answer == "y":
    print("OK. continued...")

# Input path definition

experiment_path = "/Users/jahangir/Desktop/FOFS_new_test_/mussel_trials"

main_trial_dfs_path = experiment_path + \
"/trial_by_trial_processing_outputs/main_trial_dfs"
percent_drifts_path = experiment_path + \
"/trial_by_trial_processing_outputs/pre_stat_post_drift_tables/post"

# Input path definition end

# Variables definition (please provide the variables)

""" specifications for the lineplots: provide your values of interest."""
min_temp = 16
max_temp = 29
max_filt = 1.7 # ml/min
min_filt = 0 # ml/min
max_resp = 0.7 # micromolO2/min
min_resp = 0 # micromolO2/min
max_feed = 1200 # cells/min
min_feed = 0 # cells/min

min_percent_air_sat = 75
max_percent_air_sat = 100
min_micromol_per_L = 170
max_micromol_per_L = 260
min_cells_per_mL = 0
max_cells_per_mL = 5000
font_size = 13
fig_width = 6
fig_height = 3

"""will be used for making the hypothetical datetime-column, i.e., similar for
all replicates, allowing selection of specific intervals in iteration (and will
also be used as the x-axis in integrative plots)."""
hypothetical_trial_start_date = '2019-11-01'

# Variables definition end

#Output-path definition

if not os.path.isdir(experiment_path + "/integrative_processing_outputs"):
    os.mkdir(experiment_path + "/integrative_processing_outputs")
output_path = experiment_path + "/integrative_processing_outputs"

```



```

if not os.path.isdir(output_path + "/drift_all_trials"):
    os.mkdir(output_path + "/drift_all_trials")
    os.mkdir(output_path + "/experiment_df")
    os.mkdir(output_path + "/mean_error_lineplots")

#Output-path definition end

#####(1)#####(1)#####(1)#####(1)#####(1)#####(1)
##### Step 1 (integrate %drift dataframes of all trials)
### for Chl and filtration rates
os.chdir(percent_drifts_path + "/food")
trial_names = glob("*.xlsx")
appended_data = []
for trial_name in trial_names:
    df = pd.ExcelFile(trial_name)
    df.sheet_names
    [u'Sheet1']
    df = df.parse("Sheet1")
    df = df.assign(trial = trial_name[
        trial_name.find("post_")+5:trial_name.find(".xlsx")])
    appended_data.append(df)
df1 = pd.concat(appended_data)
df1.index = range(len(df1['trial']))

### for DO and respiration rates
os.chdir(percent_drifts_path + "/oxygen")
trial_names = glob("*.xlsx")
appended_data = []
for trial_name in trial_names:
    df = pd.ExcelFile(trial_name)
    df.sheet_names
    [u'Sheet1']
    df = df.parse("Sheet1")
    df = df.assign(trial = trial_name[
        trial_name.find("post_")+5:trial_name.find(".xlsx")])
    appended_data.append(df)
df2 = pd.concat(appended_data)
df2.index = range(len(df2['trial']))

if not os.path.isdir(output_path + "/drift_all_trials"):
    os.mkdir(output_path + "/drift_all_trials")
    os.chdir(output_path + "/drift_all_trials")
else:
    os.chdir(output_path + "/drift_all_trials")
    writer = ExcelWriter('filt_drift_all_trials.xlsx')
    df1.to_excel(writer, 'Sheet')
    writer.save()
    writer = ExcelWriter('resp_drift_all_trials.xlsx')
    df2.to_excel(writer, 'Sheet')
    writer.save()

#####(2)#####(2)#####(2)#####(2)#####(2)#####(2)
##### Step 2 (integration of trials' outcomes)
start = time.time()

# Read in the size-trait dataframe
os.chdir(experiment_path)
size_traits_df = pd.ExcelFile('size_traits.xlsx')
size_traits_df.sheet_names
[u'Sheet1']
size_traits_df = size_traits_df.parse("Sheet1")
size_traits_df = size_traits_df.set_index(size_traits_df['trial_name'])

# Integrative processing of the trials' dataframes
os.chdir(main_trial_dfs_path)
trial_names = glob("*.xlsx")
trial_names

```

```

appended_data = []
counter = 0
for trial_name in trial_names:
    df = pd.ExcelFile(trial_name)
    df.sheet_names
    [u'Sheet1']
    df = df.parse("Sheet1")

    """Define the hypothetical datetime-column, i.e., similar for all replicates,
    allowing selection of specific intervals in iteration (and will also be
    used as the x-axis in integrative plots)."""
    df.loc[:, 'dates'] = pd.to_datetime(df['DateTime']).dt.date
    df.loc[:, 'time'] = pd.to_datetime(df['DateTime']).dt.time
    df.loc[:, 'date_delta'] = (df['dates'] - (df['dates'].iloc[0]))
    x = datetime.datetime.strptime(hypothetical_trial_start_date, '%Y-%m-%d')
    df.loc[:, 'hypthetical_date'] = x
    df.loc[:, 'hypthetical_date_plus_date_delta'] = df['hypthetical_date'] + df['date_delta']
    df.loc[:, 'final_hypo_datetime'] = pd.to_datetime(df
        'hypthetical_date_plus_date_delta'].apply(str)+' '+df['time'].apply(str))

    df_a = df
    response_cols = [i for i in list(df_a) if 'S1' in i]
    response_cols = [i for i in response_cols if 'feed' in
        i or 'filt' in i or 'resp' in i or 'SFG' in i]
    for i in response_cols:
        df_a.loc[:, 'LS_' + i] = df_a[i]/(
            size_traits_df.loc[trial_name[: -5], 'S1_l']) # l is shell-length
        df_a.loc[:, 'WS_' + i] = df_a[i]/(
            size_traits_df.loc[trial_name[: -5], 'S1_w']) # w is tissue dry weight
    df_a = df_a.assign(path = 'S1')
    df_a = df_a.assign(replicate = 'r' + str(counter + 1))
    #df_a = df_a.assign(grouping_variable_level = df['S1_level'].values[0])
    df_a = df_a.assign(trial_name = trial_name[: -5])
    df_a.columns = [col.replace('S1', 'S') for col in df_a.columns]
    delete_cols = [i for i in list(df_a) if 'S2' in i or 'S3' in i]
    df_a.drop(df_a[delete_cols], axis = 1, inplace = True)

    df_b = df
    response_cols = [i for i in list(df_b) if 'S2' in i]
    response_cols = [i for i in response_cols if 'feed' in
        i or 'filt' in i or 'resp' in i or 'SFG' in i]
    for i in response_cols:
        df_b.loc[:, 'LS_' + i] = df_b[i]/(
            size_traits_df.loc[trial_name[: -5], 'S2_l']) # l is shell-length
        df_b.loc[:, 'WS_' + i] = df_b[i]/(
            size_traits_df.loc[trial_name[: -5], 'S2_w']) # w is tissue dry weight
    df_b = df_b.assign(path = 'S2')
    df_b = df_b.assign(replicate = 'r' + str(counter + 2))
    #df_b = df_b.assign(grouping_variable_level = df['S2_level'].values[0])
    df_b = df_b.assign(trial_name = trial_name[: -5])
    df_b.columns = [col.replace('S2', 'S') for col in df_b.columns]
    delete_cols = [i for i in list(df_b) if 'S1' in i or 'S3' in i]
    df_b.drop(df_b[delete_cols], axis = 1, inplace = True)

    df_c = df
    response_cols = [i for i in list(df_c) if 'S3' in i]
    response_cols = [i for i in response_cols if 'feed' in
        i or 'filt' in i or 'resp' in i or 'SFG' in i]
    for i in response_cols:
        df_c.loc[:, 'LS_' + i] = df_c[i]/(
            size_traits_df.loc[trial_name[: -5], 'S3_l']) # l is shell-length
        df_c.loc[:, 'WS_' + i] = df_c[i]/(
            size_traits_df.loc[trial_name[: -5], 'S3_w']) # w is tissue dry weight
    df_c = df_c.assign(path = 'S3')
    df_c = df_c.assign(replicate = 'r' + str(counter + 3))
    #df_c = df_c.assign(grouping_variable_level = df['S3_level'].values[0])
    df_c = df_c.assign(trial_name = trial_name[: -5])
    df_c.columns = [col.replace('S3', 'S') for col in df_c.columns]
    delete_cols = [i for i in list(df_c) if 'S1' in i or 'S2' in i]

```

```

df_c.drop(df_c[delete_cols], axis = 1, inplace = True)

trial_name = pd.concat([df_a, df_b, df_c])
appended_data.append(trial_name)
counter = int(counter+3)

appended_data = pd.concat(appended_data)
with pd.option_context('display.max_rows', 3, 'display.max_columns', None):
    print(appended_data)

#Slicing an experimental period of interest
answer = input("Do you want to keep or taylor out some parts of the integrated\
dataset. e.g., a\ broken interval). Enter y or n: ")
if answer == "y":
    print("Please push control+c, manually define the conditions below, and\
then continue the processing.")
    print("Push control+c")
    print("Push control+c")
    time.sleep(30)

elif answer == "n":
    print("OK. No change is needed.")

##### Manual imposition of changes
#eg:

# Revise the experimental data frame based on the conditions
mask = (appended_data['final_hypo_datetime'] > '2019-11-01 20:00:00') & (appended_data[
'final_hypo_datetime'] <= '2019-11-03 08:00:00')
appended_data = appended_data.loc[mask]

# exclude the broken replicate data based on the datetime interval and the path-name
appended_data = appended_data.loc[
    (appended_data["trial_name"] != '26_oct') | (appended_data["path"] != 'S3')]
appended_data = appended_data.loc[
    (appended_data["trial_name"] != '30_oct') | (appended_data["path"] != 'S3')]
experiment_df = appended_data

# split the complete experiment_df to the dataframes based on experimental periods of interest
# (here, for example, the warming and cooling phases of the daily thermal cycle)
mask_warming_phase = (experiment_df['final_hypo_datetime'] > '2019-11-02 05:30:00') & (
    experiment_df['final_hypo_datetime'] <= '2019-11-02 16:30:00')
mask_cooling_phase = (experiment_df['final_hypo_datetime'] > '2019-11-02 17:30:00') & (
    experiment_df['final_hypo_datetime'] <= '2019-11-03 05:30:00')
warming_phase_df = experiment_df.loc[mask_warming_phase]
cooling_phase_df = experiment_df.loc[mask_cooling_phase]
'''

# based on a response variable
appended_data = appended_data[
    appended_data["Respiration rate ( $\mu\text{molO}_2\text{.g}^{-1}\text{.min}^{-1}$ )"] < 6]
## based on a replicate name
appended_data = appended_data[
    appended_data["replicate"] != 'r12'] # excluding the replicate r12
'''

###Manual imposition of changes end

#####
### save dataframes
if not os.path.isdir(output_path + "/" + experiment_df):
    os.mkdir(output_path + "/" + experiment_df)
    os.chdir(output_path + "/" + experiment_df)
else:
    os.chdir(output_path + "/" + experiment_df)
writer = ExcelWriter('experiment_df.xlsx')
experiment_df.to_excel(writer, 'Sheet')
writer.save()

writer = ExcelWriter('cooling_phase_df.xlsx')
cooling_phase_df.to_excel(writer, 'Sheet')

```

```

writer.save()

writer = ExcelWriter('warming_phase_df.xlsx')
warming_phase_df.to_excel(writer, 'Sheet')
writer.save()

#####
#### Make lineplots for the response variables
start = time.time()

variable_cols = ['WS_resp_ymolO2_per_min_S', 'LS_filt_ml_per_min_S',
                 'LS_feed_cells_per_min_S']
mpl.rcParams["font.size"] = font_size
sns.set_style("white")
for variable in variable_cols:
    fig, ax = plt.subplots(sharex=True, sharey=True, figsize=(fig_width, fig_height))
    sns.lineplot(x="final_hypo_datetime", y=variable, data=experiment_df, ax=ax,
                 color="darkblue")
    ax.set_ylabel(variable)
    ax2 = ax.twinx()
    sns.lineplot(x="final_hypo_datetime", y="Temp_C_x", data=experiment_df,
                 ax=ax2, color="darkred", label="Temperature")
    ax2.set_ylabel("Temperature (°C)")
    ax2.set_yticks(np.arange(min_temp, max_temp, 3))
    ax2.lines[0].set_linestyle("-")
    ax2.get_legend().remove()
    ax.tick_params(axis='y', colors='darkblue')
    ax.yaxis.label.set_color('darkblue')
    ax2.tick_params(axis='y', colors='darkred')
    ax2.yaxis.label.set_color('darkred')
    ax.set_xlabel("Time (HH)")
    ax.grid(linestyle=':', linewidth=0.2, which='major', axis='y', color='lightgrey')
    plt.gcf().autofmt_xdate()
    myFmt = mdates.DateFormatter("%H")
    plt.gca().xaxis.set_major_formatter(myFmt)
    plt.gca().xaxis.set_major_locator(mdates.HourLocator(byhour=range(0, 24, 4)))
    if 'resp' in variable:
        ax.set_ylabel('Resp. (µmolO2 g-1 min-1)')
        ax.set_ylim(min_resp, max_resp)
    if 'filt' in variable:
        ax.set_ylabel(r'Filt. (mL mm-1 min-1)')
        ax.set_ylim(min_filt, max_filt)
    if 'feed' in variable:
        ax.set_ylabel(r'Feed. (cells mm-1 min-1)')
        ax.set_ylim(min_feed, max_feed)
    if not os.path.isdir(output_path + "/mean_error_lineplots"):
        os.mkdir(output_path + "/mean_error_lineplots")
        os.chdir(output_path + "/mean_error_lineplots")
    else:
        os.chdir(output_path + "/mean_error_lineplots")

    plt.savefig(variable + '.pdf', bbox_inches='tight')

#####
#### Make lineplots for the processed food concentrations
mpl.rcParams["font.size"] = font_size
sns.set_style("white")
sns.set_style("ticks", {"xtick.major.size": 8, "ytick.major.size": 8})
fig, ax = plt.subplots(sharex=True, sharey=True, figsize=(fig_width, fig_height))
sns.lineplot(x="final_hypo_datetime", y='ST_DC_cells_per_ml_S',
             data=experiment_df, ax=ax, color="darkblue")
sns.lineplot(x="final_hypo_datetime", y='ST_DC_cells_per_ml_C',
             data=experiment_df, ax=ax, color="darkgreen")
ax2 = ax.twinx()
sns.lineplot(x="final_hypo_datetime", y="Temp_C_x", data=experiment_df,
             ax=ax2, color="darkred", label="Temperature")
ax2.set_ylabel("Temperature (°C)")
ax2.set_yticks(np.arange(min_temp, max_temp, 3))

```

```

ax2.lines[0].set_linestyle("-")
ax2.get_legend().remove()
ax.tick_params(axis='y', colors='black')
ax.yaxis.label.set_color('black')
ax2.tick_params(axis='y', colors='darkred')
ax2.yaxis.label.set_color('darkred')
ax.set_xlabel("Time (HH)")
ax.grid(linestyle=':', linewidth=0.2, which='major', axis='y', color='lightgrey')
plt.gcf().autofmt_xdate()
myFmt = mdates.DateFormatter("%H")
plt.gca().xaxis.set_major_formatter(myFmt)
plt.gca().xaxis.set_major_locator(mdates.HourLocator(byhour=range(0, 24, 4)))
ax.set_ylabel("Food (cells mL-1 S)")
ax.set_ylim(min_cells_per_mL, max_cells_per_mL)

legend_elements = [
    Line2D([0], [0], color='darkgreen', lw=3, linestyle='-', label='Conc. in Path$_{C}$'),
    Line2D([0], [0], color='darkblue', lw=3, linestyle='-', label='Conc. in Path$_{S}$')
]
legend = ax.legend(handles=legend_elements, ncol=2, handlelength=0.5,
                  prop={'size': 13}, loc='upper center', fancybox=False, frameon=False,
                  bbox_to_anchor=(0.5, 1.2), framealpha=0.7)
if not os.path.isdir(output_path + "/mean_error_lineplots"):
    os.mkdir(output_path + "/mean_error_lineplots")
    os.chdir(output_path + "/mean_error_lineplots")
else:
    os.chdir(output_path + "/mean_error_lineplots")

plt.savefig("food_" + 'ST_DC_cells_per_mL' + '.pdf', bbox_inches='tight')

#####
#### Make lineplots for the processed dissolved oxygen concentrations
variable_cols = ['percent_air_sat', 'ymol_per_l']
for variable in variable_cols:
    mpl.rcParams["font.size"] = font_size
    sns.set_style("white")
    sns.set_style("ticks", {"xtick.major.size": 8, "ytick.major.size": 8})
    fig, ax = plt.subplots(sharex=True, sharey=True, figsize=(fig_width, fig_height))
    sns.lineplot(x="final_hypo_datetime", y="corrected_" + variable + "_S",
                data=experiment_df, ax=ax, color="darkblue")
    sns.lineplot(x="final_hypo_datetime", y="control_" + variable + "_C",
                data=experiment_df, ax=ax, color="darkgreen")
    ax2 = ax.twinx()
    sns.lineplot(x="final_hypo_datetime", y="Temp_C_x", data=experiment_df,
                ax=ax2, color="darkred", label="Temperature")
    ax2.set_ylabel("Temperature (°C)")
    ax2.set_yticks(np.arange(min_temp, max_temp, 3))
    ax2.lines[0].set_linestyle("-")
    ax2.get_legend().remove()
    ax.tick_params(axis='y', colors='black')
    ax.yaxis.label.set_color('black')
    ax2.tick_params(axis='y', colors='darkred')
    ax2.yaxis.label.set_color('darkred')
    ax.set_xlabel("Time (HH)")
    ax.grid(linestyle=':', linewidth=0.2, which='major', axis='y', color='lightgrey')
    plt.gcf().autofmt_xdate()
    myFmt = mdates.DateFormatter("%H")
    plt.gca().xaxis.set_major_formatter(myFmt)
    plt.gca().xaxis.set_major_locator(mdates.HourLocator(byhour=range(0, 24, 4)))
    if 'percent_air' in variable:
        ax.set_ylabel("Diss. O2 (% air sat.)")
        ax.set_ylim(min_percent_air_sat, max_percent_air_sat)
    if 'ymol_per_l' in variable:
        ax.set_ylabel("Diss. O2 (μmol L-1 S)")
        ax.set_ylim(min_micromol_per_L, max_micromol_per_L)
    legend_elements = [
        Line2D([0], [0], color='darkgreen', lw=3, linestyle='-', label='Conc. in Path$_{C}$'),
        Line2D([0], [0], color='darkblue', lw=3, linestyle='-', label='Conc. in Path$_{S}$')
    ]
    legend = ax.legend(handles=legend_elements, ncol=2, handlelength=0.5,

```

```

        prop={'size': 13}, loc='upper center', fancybox=False,
        frameon=False, bbox_to_anchor=(0.5, 1.2), framealpha=0.7)
if not os.path.isdir(output_path + "/mean_error_lineplots"):
    os.mkdir(output_path + "/mean_error_lineplots")
    os.chdir(output_path + "/mean_error_lineplots")
else:
    os.chdir(output_path + "/mean_error_lineplots")
plt.savefig("oxyg_" + variable + '.pdf', bbox_inches='tight')

#####
### Define dataframe and response variable lists for modeling of the thermal response curves
df_list = [warming_phase_df, cooling_phase_df]
df_names = ['warming_phase_df', 'cooling_phase_df']
response_variable_list = ['WS_resp_ymolO2_per_min_S', 'LS_filt_ml_per_min_S',
                          'LS_feed_cells_per_min_S']

## All the processing will be repeated for each dataframe and response variable
counter_ = 0
for df in df_list:
    for res in response_variable_list:
        "" If masking is needed:
        mask = (df["Temp_C_x"] >= 16.8)
        df = df.loc[mask]
        ""

        ### GAM
        # variables of GAM
        x = df[["Temp_C_x"]]
        y = df[res]

        ## lam, short for lambda, controls the strength of the regularization
        # penalty on each spline term. Terms can have multiple penalties, and
        # therefore multiple lam.
        lams = np.random.rand(50, 1) # random points on [0, 1], with shape (100, 1)
        lams = lams * 8 - 3 # shift values to -3, 3
        lams = np.exp(lams) # transforms values to 1e-3, 1e3

        ## A grid-search over multiple lam and n-splines values to see if we can
        # improve our model.
        # We will seek the model with the lowest generalized cross-validation (GCV) score.
        gam = LinearGAM(s(0)).gridsearch(x.values, y.values, lam=lams,
                                         n_splines=np.arange(5,10))

        ## Save statistics of the selected GAM
        d = gam.statistics_
        gam_statistics_df = pd.DataFrame.from_dict(d, orient='index')

        ### save GAM statistics
        if not os.path.isdir(experiment_path + "/GAM_POLY_dfs_plots"):
            os.mkdir(experiment_path + "/GAM_POLY_dfs_plots")
            os.chdir(experiment_path + "/GAM_POLY_dfs_plots")
        else:
            os.chdir(experiment_path + "/GAM_POLY_dfs_plots")

        writer = ExcelWriter('gam_statistics_df_' + df_names[counter_] + '_' +
                             res + '_' + '.xlsx')
        gam_statistics_df.to_excel(writer, 'Sheet')
        writer.save()

        ## Define the x-axis limits of GAM
        m = x.min() # real min temp of the fluctuation treatment
        M = x.max() # real max temp of the fluctuation treatment
        # define the hypothetical x-values for GAM
        XX = np.linspace(m - 0, M + 0, 1000) # GAM prediction temp interval
        Xl = np.linspace(m - 0, m, 50) # m-2 is the min temp of GAM prediction interval
        Xr = np.linspace(M, M + 0, 50) # M+2 is the max temp of GAM prediction interval

        # Make df of GAM predicts

```

```

GAM_response_predict = pd.DataFrame(gam.predict(XX), columns=[res+'_GAM'])
GAM_temp = pd.DataFrame(XX, columns=['temp'])
GAM_df = pd.concat([GAM_temp, GAM_response_predict], axis=1)

# GAM_POLY comparison plots
mpl.rcParams["font.size"] = font_size
sns.set_style("white")
sns.set_style("ticks", {"xtick.major.size": 8, "ytick.major.size": 8})
fig, ax = plt.subplots(figsize=(4,2.5))
ax.plot(XX, gam.predict(XX), color='darkblue', ls='-', linewidth=2)
## XX[:, i] is the ith 'one dimensional slice' of the X_grid matrix of
confi = gam.confidence_intervals(XX, width=0.95)
ax.fill_between(XX.ravel(), y1=confi[:,0], y2=confi[:,1],
                color='darkblue', alpha=0.2)
plt.scatter(df['Temp_C_x'], df[res], s=0.5, c='lightgrey', alpha=0.5)
ax.set_xlabel('Temperature (°C)')
ax.set_xticks(np.arange(18, 28, 1))
if 'resp' in res:
    ax.set_ylabel('Resp. ( $\mu\text{molO}_2\text{ g}^{-1}\text{ s}^{-1}\text{ min}^{-1}\text{ g}^{-1}\text{ s}^{-1}$ )')
    ax.set_ylim(0, 1)
if 'filt' in res:
    ax.set_ylabel(r"Filt. ( $\text{mL mm}^{-1}\text{ s}^{-1}\text{ min}^{-1}\text{ g}^{-1}\text{ s}^{-1}$ )")
    ax.set_ylim(0, 2.5)
if 'feed' in res:
    ax.set_ylabel(r"Feed. ( $\text{cells mm}^{-1}\text{ s}^{-1}\text{ min}^{-1}\text{ g}^{-1}\text{ s}^{-1}$ )")
    ax.set_ylim(0, 1500)
ax.grid(linestyle=':', linewidth='0.2', which='both', axis='both',
        color='lightgrey')

plt.savefig("GAM_Poly_" + df_names[counter_] + '_' + res + '_' + '.pdf',
            bbox_inches='tight') #
counter_ += 1

end = time.time()
print(end - start)

```

SI for Chapter 2 “Burden or relief? Impact of cyclic thermal variability on ectotherms capable of metabolic suppression”

Contents:

Supporting Tables

Supporting Figures

Supporting R and Python Scripts

Supporting Tables

Table S1 Generalized Additive Mixed-effect Model (GAMM) outcome for growth of mussel shell length and shell and tissue dry weights under thermal averages and daily fluctuations (crossed design) of the long-term (5-weeks) experiment. Twelve temperature scenarios, at four thermal averages (18.5, 21.0, 23.5, and 26.0 °C), were applied at three daily fluctuation amplitudes (± 0 , 2, and 4 °C). The group was defined as a random-effect factor (see Fig. S1).

<u>Shell length growth</u>	e.d.f.	d.f.	F-value	p-value
Thermal Average (T)	2.104	2.496	68.563	<0.001***
Fluctuation (F)	1.001	1.002	0.293	0.589
T x F	2.929	4.000	7.568	<0.001***
Group	1.415	33.000	0.045	0.347
<u>Shell dry weight growth</u>				
Thermal Average (T)	1.925	2.331	45.501	<0.001***
Fluctuation (F)	1.000	1.000	0.132	0.717
T x F	2.847	4.000	7.267	<0.001***
Group	0.001	33.000	0.000	0.570
<u>Tissue dry weight growth</u>				
Thermal Average (T)	2.403	2.657	30.631	<0.001***
Fluctuation (F)	1.001	1.001	0.089	0.766
T x F	2.800	4.000	6.431	0.001***
Group	8.320	33.000	0.347	0.075

Table S2 Analyses of variance (ANOVA) outcome for growth of mussel shell length and shell and tissue dry weights under thermal averages and daily fluctuations (crossed design) of the long-term (5-weeks) experiment. Twelve temperature scenarios, at four thermal averages (18.5, 21.0, 23.5, and 26.0 °C), were applied at three daily fluctuation amplitudes (± 0 , 2, and 4 °C). ANOVA was applied to data of each thermal average, separately. Daily fluctuations were considered as the predictor in all models.

Thermal Average	Growth response	d.f.	Sum Sq	Average Sq	F-value	p-value
18.5 (°C)	Shell length	2	0.0023	0.00114	1.231	0.297
	Shell dry weight	2	0.0463	0.02313	1.977	0.145
	Tissue dry weight	2	0.0002	0.00008	0.196	0.823
21 (°C)	Shell length	2	0.0009	0.00045	0.500	0.608
	Shell dry weight	2	0.0055	0.00277	0.193	0.825
	Tissue dry weight	2	0.0007	0.00036	0.902	0.409
23.5 (°C)	Shell length	2	0.0317	0.01586	15.24	<0.001***
	Shell dry weight	2	0.3401	0.17006	12.56	<0.001***
	Tissue dry weight	2	0.0064	0.00320	10.87	<0.001***
26 (°C)	Shell length	2	0.0046	0.00233	3.173	0.047*
	Shell dry weight	2	0.0342	0.01711	3.806	0.026*
	Tissue dry weight	2	0.0047	0.00235	16.82	<0.001***

Supporting figures

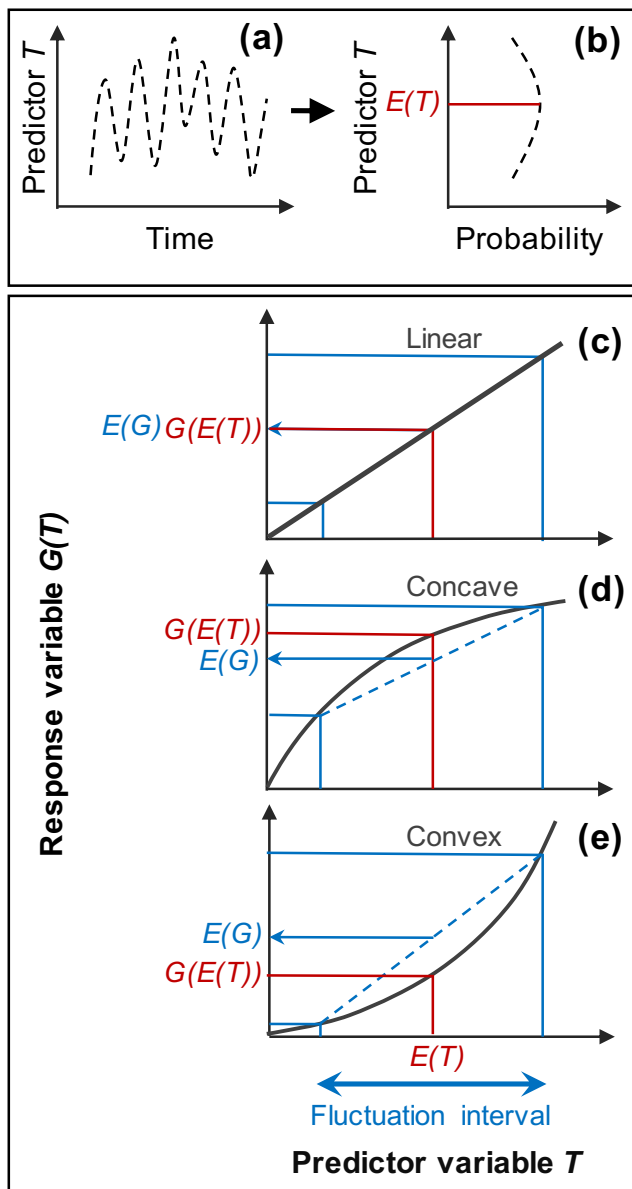


Figure S1 Schematic representation of the general statement of *Jensen's Inequality* (nonlinear averaging) in the context of Probability Theory. A predictor random variable (temperature T) fluctuates in time (a) following a specific probability density (b). Suppose the ecological response (growth G) is a function of the predictor T with a linear (c), a concave (d), or a convex (e) relationship on the predictor's fluctuation interval. In that case, nonlinear averaging predicts that the average (expected) value of the response, $E(G)$, is equal to, higher or lower than the response to the expected value of the predictor, $G(E(T))$, respectively. Subplots c–e are modified after Ruel & Ayres 1999 (see the main text's reference section).

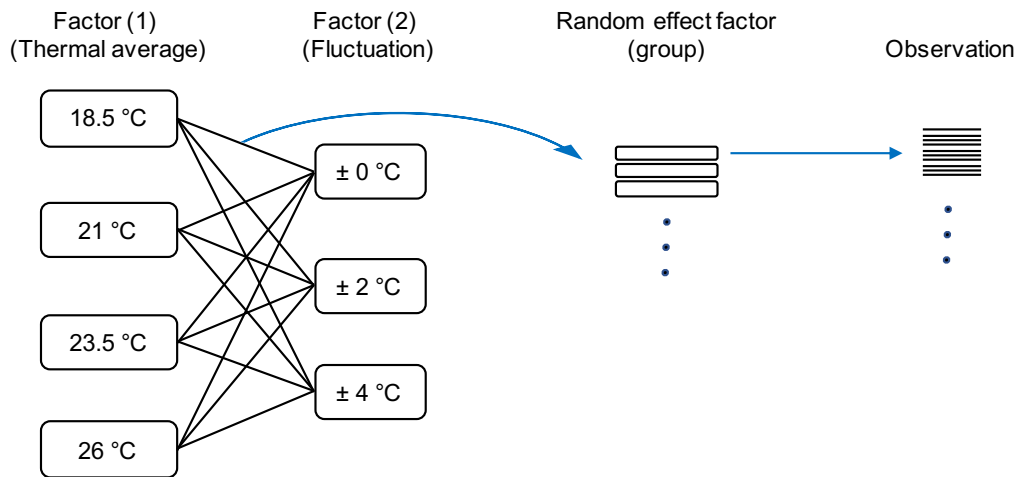


Figure S2 Experimental design applied in the long-term (5-weeks) experiment. Twelve temperature scenarios, at four thermal averages (18.5, 21.0, 23.5, and 26.0 °C), were applied at three daily fluctuation amplitudes (± 0 , 2, and 4 °C). Main-effect factors (thermal average and daily fluctuation with 3 and 4 levels, respectively) were fully crossed. The random effect factor (group) was nested to the main treatments, and each group (3 groups per treatment) included 10 observations (single mussels).

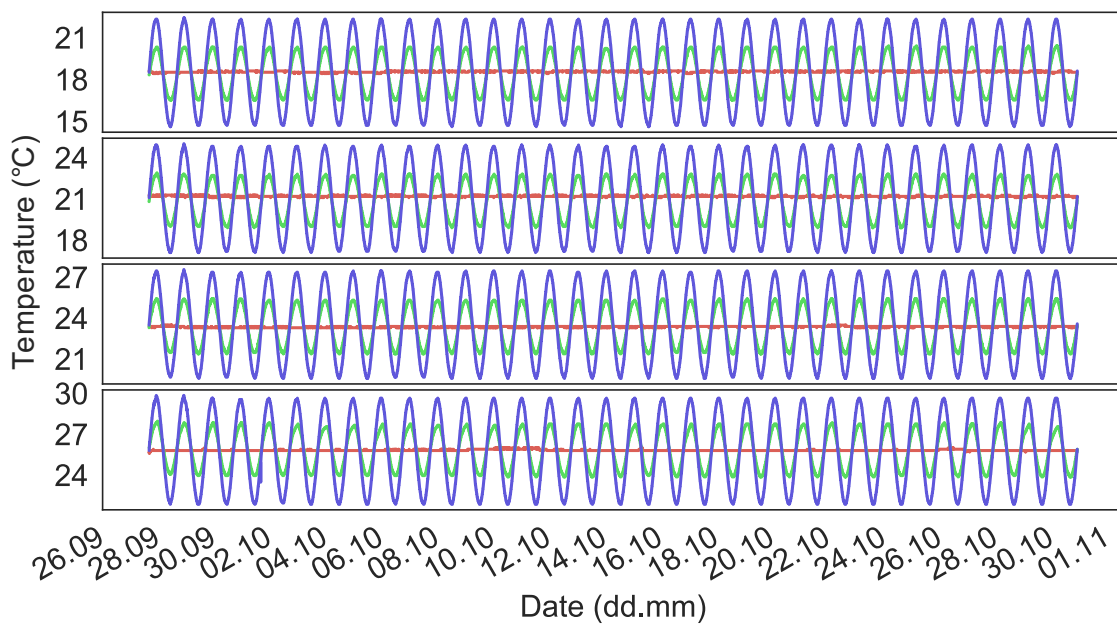


Figure S3 Treatments applied in the long-term (5-weeks) experiment. Twelve temperature scenarios, at four thermal averages (18.5, 21.0, 23.5, and 26.0 °C), were applied at three daily fluctuation amplitudes (± 0 , 2, and 4 °C). Data were logged every 5 min over the five weeks.

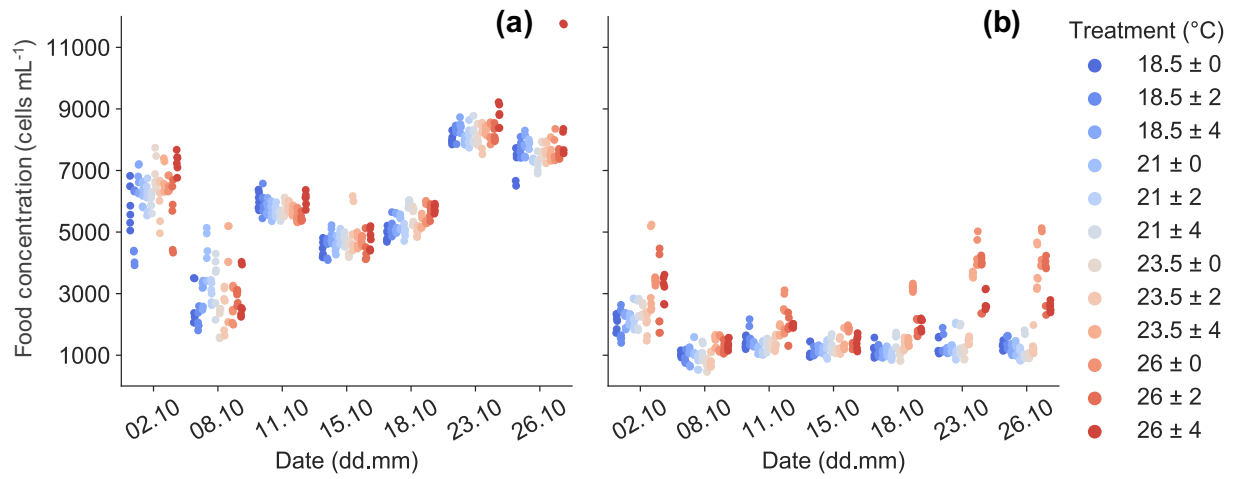


Figure S4 Food concentrations in the source and experimental containers (**a** and **b**, respectively) during the long-term (5-weeks) experiment. Twelve temperature scenarios, at four thermal averages (18.5, 21.0, 23.5, and 26.0 °C), were applied at three daily fluctuation amplitudes (± 0 , 2, and 4 °C). Food concentration was measured every five days in each of the 12 experimental treatments. Deviations between treatments in **b** arise from mussel's activities in response to the different thermal treatments.

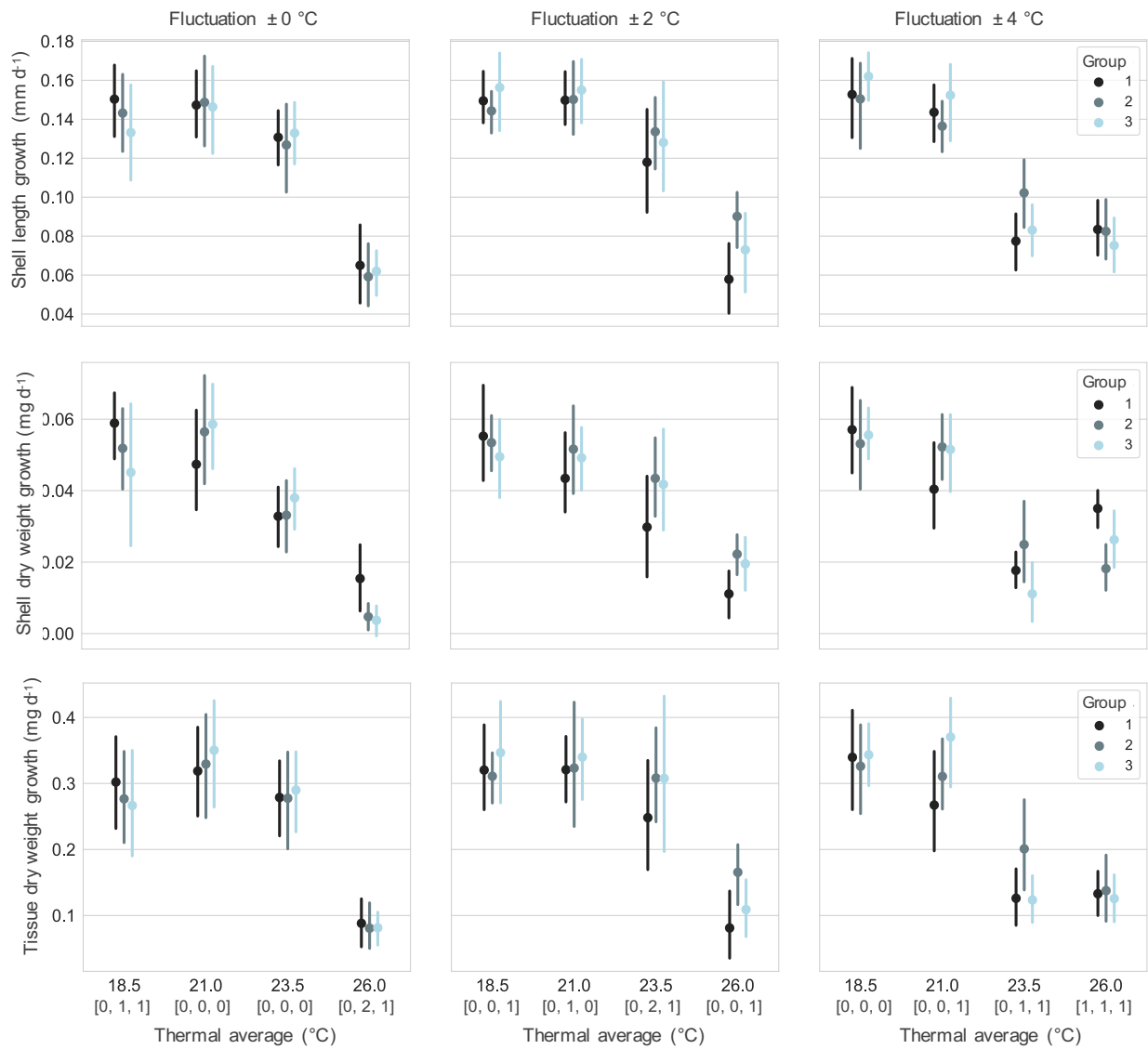


Figure S5 Growth of mussel shell length and shell and tissue dry weights under thermal averages and daily fluctuations (crossed design) of the long-term (5-weeks) experiment. Presented are 5-weeks-integrated changes. Twelve temperature scenarios, at four thermal averages (18.5, 21.0, 23.5, and 26.0 °C), were applied at three daily fluctuation amplitudes (± 0 , 2, and 4 °C). Data are presented as averages with 95 % confidence intervals for the 10-mussel-groups (discerned by different colors). The numbers in parentheses (lower x-title row) indicate the numbers of dead mussels in each group of 10 by the end of the experiment.

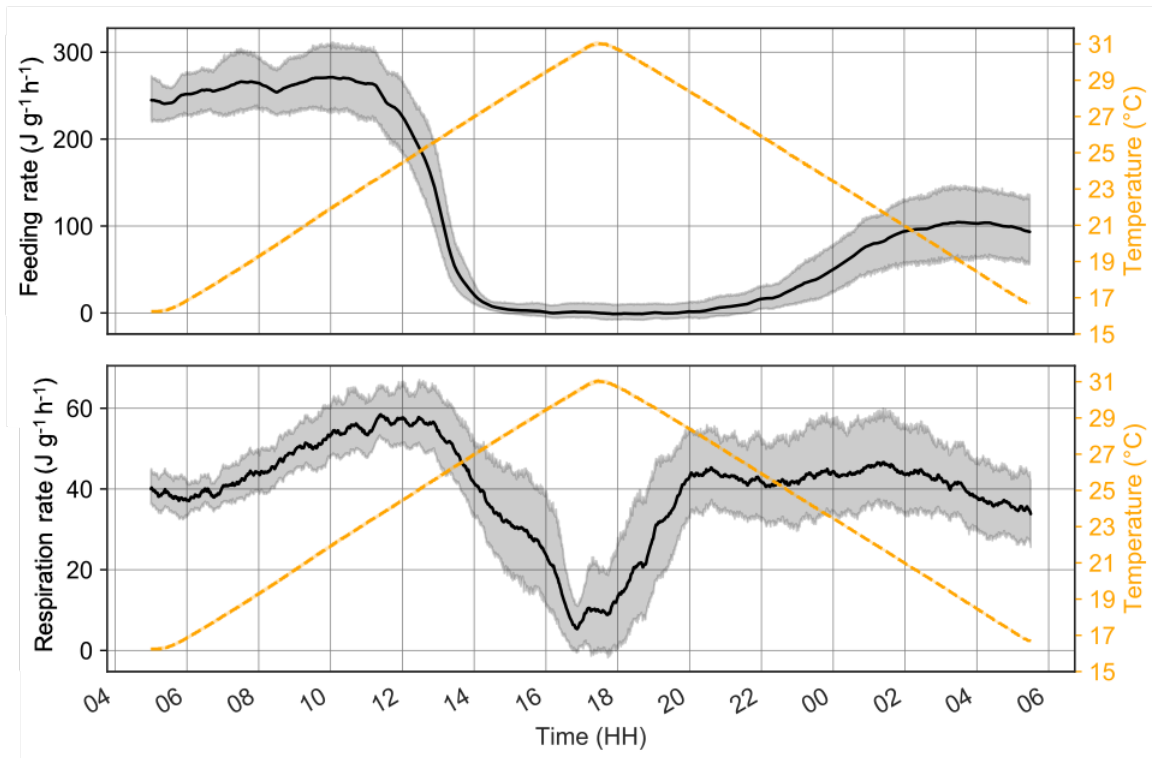


Figure S6 Temporal variation in rates of metabolic processes retrieved from the short-term (one-day) assay. Weight-specific feeding and respiration ($N = 11$) along the applied daily thermal fluctuation cycle (orange dashed lines) are provided using the method developed by Vajedsamiei *et al.* (under review). Values are averaged at each time point, presented with 95 % confidence intervals. The rate of energy ingestion (feeding) was estimated, assuming the constancy of filtration rate at a constant food concentration ($4000 \text{ cells mL}^{-1}$).

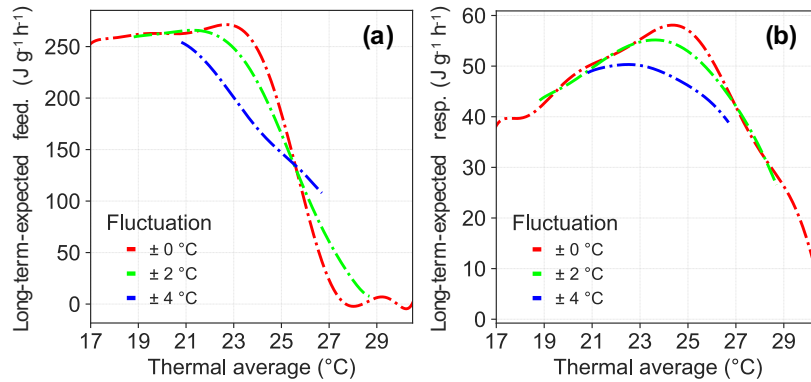


Figure S7 Predictions of temporally-upscaled thermal metabolic-response relations (feeding, **a**; respiration, **b**) retrieved from the short-term (one-day) assay. Upscaled models (dashed lines) presenting the expected rates of metabolic processes (y-axes) as functions of the thermal average (x-axes) and daily fluctuations (note the legends; see Equation 3 in the Method). The red dashed lines are the same best-fit Polynomials which described the short-term responses to temperature. The thermal fluctuation sets used for the predictions (named ± 0 , 2, and 4 °C) are the same as were applied in the long-term (5-weeks) experiment. Subplots are based on data from the warming-phase of the fluctuation. Here, the absolute values of predicted responses are presented. For the relative values, see Fig. 5a–b. The analytical procedure is described in the Method section of this paper.

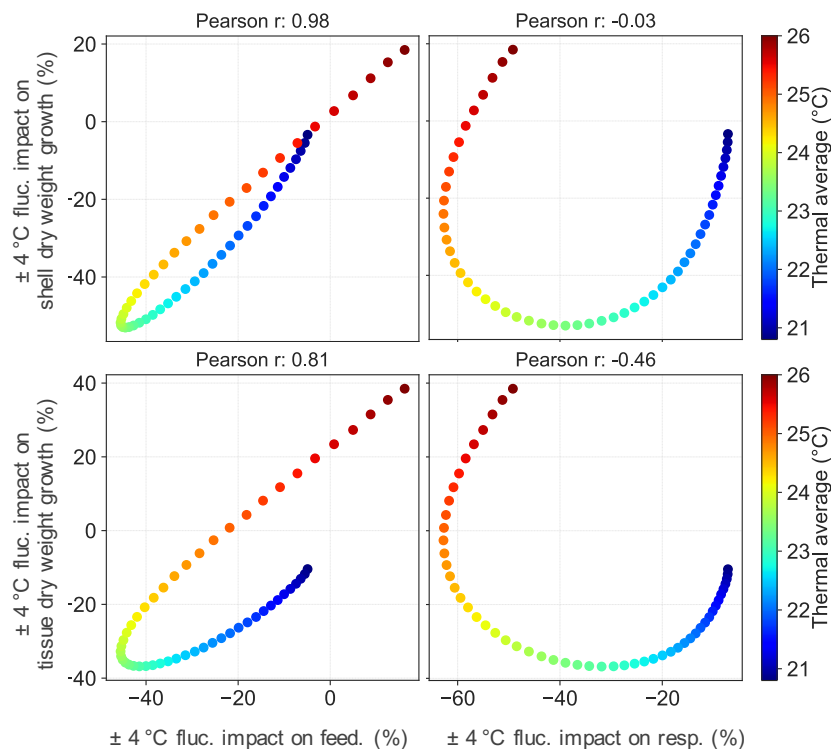


Figure S8 The impacts from ± 4 °C daily fluctuations on the 5-weeks-integrated growth of mussel shell (upper) and tissue (lower) dry weights in correlation to the upscaling-predicted impacts of the same fluctuations on long-term-expected feeding (left) and respiration (right) rates (based on data from the short-term assay), over thermal averages from 21 to 26°C (heat chart to the right). Pearson's correlation of > 0.7 (or < -0.7) indicates a strong linear correlation.

Supporting R and Python scripts

The following R and Python scripts were used to process the experimental data that will be published in PANGEA.

Script S1

```
# This R script applies the dataframe of the long-term thermal performance experiment
to test the significance of the main and interactive (fixed) effects of the thermal
average and fluctuation treatments and the random effect of the group using
Generalized Additive Mixed-effect Model.
# Besides, this script performs the pairwise comparison of the average responses
between different fluctuation-levels.

@author: Jahangir Vajedsamiei (last checked in Dec. 2020)
""
# needed packages
install.packages("nlme")
install.packages("mgcv")
install.packages("data.table")
library("nlme")
library("mgcv")
library(data.table)
library(ggplot2)
install.packages("stargazer")
library(stargazer)

## Inspecting and revising the data frame
df <- Performance_data
head(df)
str(df)

# Set colnames
setnames(df, old = c('Mean temperature (°C)'), new = c('Mean_temperature'))
setnames(df, old = c('Fluctuation scenario'), new = c('Fluctuation'))
setnames(df, old = c('temp_SD'), new = c('SD_temperature'))
setnames(df, old = c('group'), new = c('Group'))
setnames(df, old = c('Length growth (mm/day)'), new = c('Length_growth'))
setnames(df, old = c('Shell dry weight growth (mg/day)'), new = c('Shell_DW_growth'))
setnames(df, old = c('Tissue dry weight growth (mg/day)'), new = c('Tissue_DW_growth'))

df$Fluctuation <- as.factor(df$Fluctuation)
df$SD_temperature <- as.numeric(df$SD_temperature)
df$Mean_temperature <- as.numeric(df$Mean_temperature)
df$Group <- as.factor(df$Group)

## GAM definition, test of significance, and model comparison
lapply(df[,c(names(df)[15:17])], function(y) {
  GAMM <- gam(y ~ s(Mean_temperature, k=4) + s(SD_temperature, k=3) +
    te(Mean_temperature, SD_temperature, k=3) +
    s(Group, bs = 're'),
    data=df, method = 'ML')
  #summary(GAMM)
  GAM_simple <- gam(y ~ s(Mean_temperature, k=4, by=Fluctuation) +
    Fluctuation,
    data=df, method = 'ML')
  #summary(GAM_simple)
  AIC(GAMM, GAM_simple)
  #anova(GAM_1, GAM_2)
})

## ANOVA on the effect of the fluctuation at each thermal average
# and, pairwise comparison of the average responses
df$Mean_temperature <- as.factor(df$Mean_temperature)
thermal_mean_list = list("18.5", "21", "23.5", "26")
for (thermal_mean in thermal_mean_list) {
```

```

# Compute anova with TukeyHSD
print(thermal_mean)
res <- aov(Tissue_DW_growth ~ Fluctuation, data = df[df$Mean_temperature == thermal_mean,])
print(summary(res))
#print(res)
print(TukeyHSD(res))
}

```

Script S2

```

#!/usr/bin/env python3
# -*- coding: utf-8 -*-
"""
# This Python script processes temperature data of the long-term thermal performance
experiment. It produces Figure S2 of the paper. Besides, it calculates first 10
central moments for each of the 12 temperature sets.
Odd moments are nearly equal to zero since the variability around the mean
was balanced. Average values of the even number moments (2d to 10th moment) are
applied later to define upscaled models in Script_S4 (also generally presented as
Equation 3 in the method section of the paper).

@author: Jahangir Vajedsamiei (last checked in Dec. 2020)
"""

import os
from glob import glob as glob
import pandas as pd
from pandas import ExcelWriter
import numpy as np
from scipy.stats import moment
import datetime as dt
import seaborn as sns
import matplotlib.pyplot as plt
import matplotlib as mpl
import matplotlib.dates as mdates
from matplotlib.pylab import rcParams
import matplotlib.ticker as ticker
import math
import time

start = time.time()

# Define the path for the folder containing raw data
os.chdir("/Users/jahangir/Desktop/fluctuation_plasticity_2018/Long_term_exp/Data/" +
"Long_term_thermal_performance/Temperature_csv_xlsx")
filelist = glob("*.csv") # Make the list of files

appended_temp_data = []
moments_df = []
counter = 0

# Loop over the files in the filelist
for filename in filelist:
    temp_df = pd.read_csv(filename, encoding='utf-8', sep=",", names = [
        'datetime', 'Temperature (°C)'], header = 0, usecols = [1,2])
    temp_df = temp_df.drop([0])
    temp_df = temp_df.dropna()
    temp_df['datetime'] = pd.to_datetime(temp_df['datetime'])
    temp_df['Temperature (°C)'] = temp_df['Temperature (°C)'].apply(
        pd.to_numeric, errors='coerce')
    mask = (temp_df['datetime'] > '2018-09-27 10:30:00') & (temp_df[
        'datetime'] < '2018-10-30 16:10:00')
    temp_df = temp_df.loc[mask]

    temp_df = temp_df.assign(Thermal_mean = str(filename[:filename.find("_")]))
    temp_df = temp_df.assign(Thermal_fluctuation = str(filename[
        filename.find("_")+1:filename.find(".csv")]))

```

```

# Calculate i-th central moment for each of the 12 temperature sets
index = [np.arange(1, 11)]
columns = ["i_moment_" + str(filename[:filename.find(".csv")]), "i_moment/i_factorial_" +
str(filename[:filename.find(".csv")])]
moments = pd.DataFrame(index=index, columns=columns)
for i in np.arange(1, 11, 1):
    moments["i_moment_" + str(filename[:filename.find(".csv")])].values[i - 1] = moment(temp_df["Temperature (°C)"],
moment=i)
    moments["i_moment/i_factorial_" + str(filename[:filename.find(".csv")])].values[i - 1] =
moment(temp_df["Temperature (°C)"], moment=i)/math.factorial(i)

    appended_temp_data.append(temp_df)
    moments_df.append(moments)

appended_temp_df = pd.concat(appended_temp_data)
appended_temp_df["Temperature (°C)"] = appended_temp_df["Temperature (°C)"].apply(pd.to_numeric, errors='coerce')
appended_temp_df["Thermal_mean"] = appended_temp_df["Thermal_mean"].apply(pd.to_numeric, errors='coerce')
appended_temp_df["Thermal_fluctuation"] = appended_temp_df["Thermal_fluctuation"].apply(pd.to_numeric, errors='coerce')
df = appended_temp_df.sort_values(by=["Thermal_mean", "Thermal_fluctuation"], ascending=True)

moments_df = pd.concat(moments_df, axis = 1)
moments_df["i"] = np.arange(1, 11)

with pd.option_context('display.max_rows', 10, 'display.max_columns', None):
    print(moments_df)

## Save Moments dataframe
os.chdir("/Users/jahangir/Desktop/fluctuation_plasticity_2018/Long_term_exp/Data/" +
"Long_term_thermal_performance/Temperature_csv_xlsx")
writer = ExcelWriter('Moments_df1.xlsx')
moments_df.to_excel(writer, 'Sheet')
writer.save()

## Save the complete temperature dataframe
writer = ExcelWriter('Complete_temperature_df.xlsx')
df.to_excel(writer, 'Sheet')
writer.save()

## Plot temperature data
grouped = df.groupby('Thermal_mean')

mpl.rcParams["font.size"] = 15
sns.set_style("white")
fig, axes = plt.subplots(ncols=1, nrows=4, sharex=True, sharey=False, figsize=(9,5))
for ax, (n,grp) in zip(axes, grouped):
    sns.lineplot(x="datetime", y='Temperature (°C)', hue='Thermal_fluctuation', data=grp, ax=ax,
palette=sns.color_palette("hls", 3))
    ax.yaxis.set_major_locator(ticker.MultipleLocator(3))
    ax.set_ylabel(' ')
    ax.get_legend().remove()
    ax.set_xlabel("Date (dd.mm)")
plt.gcf().autofmt_xdate()
myFmt = mdates.DateFormatter("%d.%m")
plt.gca().xaxis.set_major_formatter(myFmt)
plt.gca().xaxis.set_major_locator(mdates.DayLocator(interval=2))
fig.subplots_adjust(hspace=0.05, wspace = 2)

os.chdir("/Users/jahangir/Desktop/fluctuation_plasticity_2018/Long_term_exp/Plots/" +
"Long_term_thermal_performance/Temperature")
plt.savefig('Figure_S2_raw' + '.pdf', bbox_inches='tight')

```

Script S3

```

#!/usr/bin/env python3
# -*- coding: utf-8 -*-
"""
# This Python script calculates the means with 95 % confidence intervals for each

```

response variable (growth trait) and plot them combined with the predictions of the simple GAMs (with 95 % confidence intervals), creating Figure 4a-c of the paper.

@author: Jahangir Vajedsamiei (last checked in Dec. 2020)

```

"""
import os
import pandas as pd
import numpy as np
import matplotlib.pyplot as plt
import seaborn as sns
from pygam import LinearGAM, s, f
from numpy import exp, loadtxt, pi, sqrt
from matplotlib.lines import Line2D
import scipy.stats
import matplotlib as mpl
from pandas import ExcelWriter

## Read in the experimental performance data
Performance_data = pd.ExcelFile("/Users/jahangir/Desktop/fluctuation_plasticity_2018/Long_term_exp/Data/" +
                                "Long_term_thermal_performance/" +
                                "Performance_xlsx/Performance_data.xlsx")
Performance_data.sheet_names
[u'Sheet1']
Performance_data = Performance_data.parse("Sheet1")
df = Performance_data.dropna()

## Mean and error and GAM for all treatments
response_list = ['Length growth (mm/day)', 'Shell dry weight growth (mg/day)',
                'Tissue dry weight growth (mg/day)']
mean_temp_grouped = df.groupby('Mean temperature (°C)')
for response in response_list:
    mpl.rcParams["font.size"] = 14
    sns.set_style("white")
    sns.set_style("ticks", {"xtick.major.size": 8, "ytick.major.size": 8})
    color = ['red', 'lime', 'blue']
    fig, ax = plt.subplots(sharex=True, sharey=True, figsize=(4.5,4))
    grouped = df.groupby('temp_SD')
    counter=0
    for i, (n,grp) in enumerate(grouped):
        # mean ± CI
        sub_df = grp.reset_index()
        sub_grouped = sub_df.groupby('Mean temperature (°C)')
        ssms = sub_grouped[response].agg(
            ['size','sum','mean','std']).reset_index()
        ssms['CI'] = (scipy.stats.t.ppf((1 + 0.95) / 2., ssms['size']-1))*
            (ssms['std']/sqrt(ssms['size']))
        x = ssms['Mean temperature (°C)']
        y = ssms['mean']
        e = ssms['CI']
        if counter ==0:
            ax.errorbar(x, y, yerr = e, fmt = 'o', color = color[i], alpha=0.8,
                        capsize=3, capthick=2, elinewidth=0.6)
        elif counter ==1:
            ax.errorbar(x + 0.05, y, yerr = e, fmt = 'o', color = color[i],
                        alpha=0.8, capsize=3, capthick=2, elinewidth=0.6)
        else:
            ax.errorbar(x - 0.05, y, yerr = e, fmt = 'o', color = color[i],
                        alpha=0.8, capsize=3, capthick=2, elinewidth=0.6)

    # GAM
    x = grp['Mean temperature (°C)']
    y = grp[response]

    gam = LinearGAM(s(0)).fit(x, y)

# Save statistics of the simple GAMs
os.chdir("/Users/jahangir/Desktop/fluctuation_plasticity_2018/Long_term_exp/output_dfs/" +
        "Long_term_thermal_performance/GAM_statistics")

```

```

d = gam.statistics_
gam_statistics_df = pd.DataFrame.from_dict(d, orient='index')
writer = ExcelWriter('SimpleGAM_statistics_df_' + str(n) + '_' +
                    response[:response.find(" ")] + '_'.xlsx')
gam_statistics_df.to_excel(writer, 'Sheet')
writer.save()

m = x.min()
M = x.max()
XX = np.linspace(m - 0, M + 0, 500)
Xl = np.linspace(m - 0, m, 50)
Xr = np.linspace(M, M + 0, 50)

ax.plot(XX, gam.predict(XX), color=color[i], ls='-', linewidth=2)
confi = gam.confidence_intervals(XX)
ax.fill_between(XX.ravel(), y1=confi[:,0], y2=confi[:,1],
               color=color[i], alpha=0.2)
ax.plot(Xl, gam.confidence_intervals(Xl), color=color[i], ls='--')
ax.plot(Xr, gam.confidence_intervals(Xr), color=color[i], ls='--')
ax.set_ylabel(response)

GAM_response_predict = pd.DataFrame(gam.predict(XX), columns=[str(n) +
                    '_' + response + '_GAM'])
GAM_temp = pd.DataFrame(XX, columns=['temp_Passay'])
GAM_df = pd.concat([GAM_temp, GAM_response_predict], axis=1)

# Save predictions of the simple GAMs
os.chdir("/Users/jahangir/Desktop/fluctuation_plasticity_2018/Long_term_exp/output_dfs/" +
"Long_term_thermal_performance/GAM_dfs")
writer = ExcelWriter('GAM_df_' + str(n) + '_' + response[
    :response.find(" ")] + '_'.xlsx')
GAM_df.to_excel(writer, 'Sheet')
writer.save()

counter += 1

ax.set_xticks(np.arange(18, 26.5, 1))
ax.set_xlabel("Thermal average (°C)")
ax.grid(linestyle=':', linewidth=0.2, which='both', color='lightgrey')
if response == 'Length growth (mm/day)':
    legend_elements = [Line2D([0], [0], color=color[0], lw=3,
                              label='± 0 °C'),
                      Line2D([0], [0], color=color[1], lw=3,
                              label='± 2 °C'),
                      Line2D([0], [0], color=color[2], lw=3,
                              label='± 4 °C')]
    legend = ax.legend(handles=legend_elements, ncol=1, handlelength=0.5,
                      prop={'size': 13}, fancybox=False, frameon=False,
                      title="Fluctuation ", loc="lower left", framealpha=0.7)
    ax.set_ylabel('Shell length growth (mm d$^{-1}$)')
if response == 'Shell dry weight growth (mg/day)':
    ax.set_ylabel('Shell dry weight growth (mg d$^{-1}$)')
if response == 'Tissue dry weight growth (mg/day)':
    ax.set_ylabel('Tissue dry weight growth (mg d$^{-1}$)')

counter=1
plt.tight_layout()
os.chdir("/Users/jahangir/Desktop/fluctuation_plasticity_2018/Long_term_exp/Plots/" +
"Long_term_thermal_performance/Performance")
plt.savefig('GAM_mean&error_' + response[0:6] + '.pdf',
           bbox_inches='tight')

```

Script S4

```

#!/usr/bin/env python3
# -*- coding: utf-8 -*-
"""
# This script processes data collected in the short-term assay.

```

- Data of the warming and cooling phases (thermal feeding and respiration responses) are read in separately.
- Thermal variation in the traits are described by the best-fit Polynomials with maximum possible order of 10 (i.e., $g_p(T)$ in the paper) versus Generalized Additive Models (GAMs). The best-fit GAMs are only used to visually check the goodness of the polynomial fits (see Figure 4d-g of the paper).
- The expectation of the Taylor expansion of each Polynomial function at the average temperature μ_T , or $E(g(T))$, is defined (Jensen's Inequality; here, JI).

Output dfs and the figure subplots are saved.

@author: Jahangir Vajedsamiei (last checked in Dec. 2020)

"""

```

import os
import pandas as pd
import numpy as np
import datetime
import matplotlib.pyplot as plt
import matplotlib as mpl
from matplotlib.lines import Line2D
from pandas import ExcelWriter
from pygam import LinearGAM, s, f
from RegscorePy import * # For Polynomial model selection based on BIC
import seaborn as sns
import time

start = time.time()

# Input path definition

experiment_path = "/Users/jahangir/Desktop/fluctuation_plasticity_2018/Short_term_exp/Dec_2018_exp"
integrated_dfs_path = experiment_path + "/integrative_processing_outputs/experiment_df"

# Input path definition end

## Data of the warming and cooling-phase of the short-term thermal energetics
# experiment are read in separately.
os.chdir(integrated_dfs_path)
cooling_phase_df = pd.ExcelFile('cooling_phase_df.xlsx')
cooling_phase_df.sheet_names
[u'Sheet']
cooling_phase_df = cooling_phase_df.parse("Sheet")

warming_phase_df = pd.ExcelFile('warming_phase_df.xlsx')
warming_phase_df.sheet_names
[u'Sheet']
warming_phase_df = warming_phase_df.parse("Sheet")

# Define dataframe and response variable lists
df_list = [warming_phase_df, cooling_phase_df]
df_names = ['warming_phase_df', 'cooling_phase_df']
response_variable_list = ['WS_resp_J_per_h_S', 'WS_feed_hyp_J_per_h_4000_cells_S']

start = time.time()

## All the processing will be repeated for each dataframe and response variable
counter_ = 0
for df in df_list:
    for res in response_variable_list:
        # mask
        mask = (df['Temp_C_x'] >= 16.8) #####
        df = df.loc[mask]

        ### GAM
        # variables of GAM

```

```

x = df[["Temp_C_x"]]          #####
y = df[res]

## lam, short for lambda, controls the strength of the regularization
# penalty on each spline term. Terms can have multiple penalties, and
# therefore multiple lam.
lams = np.random.rand(100, 1) # random points on [0, 1], with shape (100, 1)
lams = lams * 8 - 3 # shift values to -3, 3
lams = np.exp(lams) # transforms values to 1e-3, 1e3

## A grid-search over multiple lam and n-splines values to see if we can
# improve our model.
# We will seek the model with the lowest generalized cross-validation (GCV) score.
gam = LinearGAM(s(0)).gridsearch(x.values, y.values, lam=lams,
                                n_splines=np.arange(4,11))

## Save statistics of the selected GAM
d = gam.statistics_
gam_statistics_df = pd.DataFrame.from_dict(d, orient='index')

### save GAM statistics
if not os.path.isdir(experiment_path + "/GAM_POLY_dfs_plots"):
    os.mkdir(experiment_path + "/GAM_POLY_dfs_plots")
    os.chdir(experiment_path + "/GAM_POLY_dfs_plots")
else:
    os.chdir(experiment_path + "/GAM_POLY_dfs_plots/GAM_statistics")

writer = ExcelWriter('gam_statistics_df_' + df_names[counter_] + '_' +
                    res + '_' + '.xlsx')
gam_statistics_df.to_excel(writer, 'Sheet')
writer.save()

## Define the x-axis limits of GAM
m = x.min() # real min temp of the fluctuation treatment
M = x.max() # real max temp of the fluctuation treatment
# define the hypothetical x-values for GAM
XX = np.linspace(m - 0, M + 0, 1000) # GAM prediction temp interval
Xl = np.linspace(m - 0, m, 50) # m-2 is the min temp of GAM prediction interval
Xr = np.linspace(M, M + 0, 50) # M+2 is the max temp of GAM prediction interval

# Make df of GAM predicts
GAM_response_predict = pd.DataFrame(gam.predict(XX), columns=[res+'_GAM'])
GAM_temp = pd.DataFrame(XX, columns=['temp'])
GAM_df = pd.concat([GAM_temp, GAM_response_predict], axis=1)

# GAM_POLY comparison plots
mpl.rcParams["font.size"] = 15
sns.set_style("whitegrid")
sns.set_style("ticks", {"xtick.major.size": 8, "ytick.major.size": 8})
fig, ax = plt.subplots(figsize=(4,4))

ax.plot(XX, gam.predict(XX), color='black', ls='-', linewidth=2)
## XX[:, i] is the ith 'one dimensional slice' of the X_grid matrix of
#the GAM
confi = gam.confidence_intervals(XX)
ax.fill_between(XX.ravel(), y1=confi[:,0], y2=confi[:,1],
               color='black', alpha=0.2)
ax.plot(Xl, gam.confidence_intervals(Xl), color='black', ls='--')
ax.plot(Xr, gam.confidence_intervals(Xr), color='black', ls='--')

## Find the best-fit polynomial based on BIC and include its
# predictions in the graph
x = df[["Temp_C_x"]]
y = df[res]

degrees = np.arange(2, 11)
counter = 0
for deg in degrees:
    p =int(deg + 1)

```

```

fit = np.polyfit(x, y, deg)
yp = np.poly1d(fit)
from RegscorePy import *
bic = bic.bic(y, yp(x), p)
#aic = aic.aic(y, yp(x), p)
if counter==0:
    min_bic = bic
    best_deg = deg
else:
    if bic < min_bic:
        min_bic = bic
        best_deg = deg
    print('degree {} with BIC {}'.format(deg, bic))
    counter += 1
print('Best degree {} with BIC {}'.format(best_deg, min_bic))

# define the best-fit polynomial
fit = np.polyfit(x, y, best_deg)
yp = np.poly1d(fit)

# r-squared
# fit values, and mean
yhat = yp(x) # or [p(z) for z in x]
ybar = np.sum(y)/len(y) # or sum(y)/len(y)
ssreg = np.sum((yhat-ybar)**2) # or sum([(yihat - ybar)**2 for yihat in yhat])
sstot = np.sum((y - ybar)**2) # or sum([(yi - ybar)**2 for yi in y])
r_squared = ssreg / sstot
print(round(r_squared, 2))

# add the axe to the plot
Xp = np.linspace(m - 0, M + 0, 1000)
ax.plot(Xp, yp(Xp), color='red', ls='-', lw=2)
plt.scatter(df["Temp_C_x"], df[res], s=0.5, c='grey', alpha=0.5)
ax.set_xlabel("Temperature (°C)")
ax.set_ylabel(res[:res.find("J")-1])
#the forecast is not accountable for >31
ax.set_xlim(left=17, right=30.5)
ax.set_xticks(np.arange(16, 31, 2))
ax.grid(linestyle='-', linewidth=0.2, which='both', color='lightgrey')
legend_elements = [Line2D([0], [0], color='black', lw=3, linestyle='-',
    label='GAM '(n-sp: '+str(gam.n_splines[0])+')'),
    Line2D([0], [0], color='red', lw=3, linestyle='-',
    label='PM (ord.: ' + str(best_deg) +
    ', r^{2}$: ' + str(round(r_squared, 1)) +')')]
legend = ax.legend(handles=legend_elements, ncol=1, handlelength=0.5,
    prop={'size': 13}, fancybox=False, frameon=False,
    title=None, loc="best", framealpha=0.7)

## Save the plots
os.chdir(experiment_path + "/GAM_POLY_dfs_plots/Plots")

plt.savefig("GAM_Poly_" + df_names[counter] + '_' + res + '_' + '.pdf',
    bbox_inches='tight') #

## Define Taylor expansions of the polynomial functions around
# numerous hypothetical-mean temperatures, based on moments of the
# temperature sets used in the long-term experiment.
y_SD_0_ = yp(Xp)

deriv_dic={}
for i in range(1,11):
    #print(i)
    deriv_dic["derivative{0}"].format(i) = np.polyder(yp, i)

## The numbers (e.g., 0.910) are calculated via the following command in
# Script_S2: moment(temp_df["Temperature (°C)"], moment=i)/math.factorial(i)
y_SD_1_35_ = (yp(Xp) + (deriv_dic["derivative2"](Xp) * 0.910) +
    (deriv_dic["derivative4"](Xp) * 0.208) + (deriv_dic["derivative6"](Xp) * 0.021) +

```



```

        (deriv_dic["derivative8"](Xp) *0.001) + (deriv_dic["derivative10"](Xp) *0.00005))

y_SD_2_7_ = (yp(Xp) + (deriv_dic["derivative2"](Xp) * 3.698) +
(deriv_dic["derivative4"](Xp) *3.416) + (deriv_dic["derivative6"](Xp) *1.403) +
(deriv_dic["derivative8"](Xp) *0.325) + (deriv_dic["derivative10"](Xp) *0.048))

pd.Series(y_SD_1_35_.flatten())

poly_JI_df = pd.concat([pd.Series(y_SD_0_.flatten()),
                        pd.Series(y_SD_1_35_.flatten()),
                        pd.Series(y_SD_2_7_.flatten())], axis=1)
poly_JI_df.columns = ['y_SD_0_'+JI_+'res', 'y_SD_1_35_'+JI_+'res', 'y_SD_2_7_'+JI_+'res']
GAM_Poly_JI_df = pd.concat([GAM_df, poly_JI_df], axis=1)

### save the complete data frame
if df is df_list[1]:
    os.chdir(experiment_path + "/GAM_POLY_dfs_plots/GAM_Poly_JI_dfs/Cooling_phase")
if df is df_list[0]:
    os.chdir(experiment_path + "/GAM_POLY_dfs_plots/GAM_Poly_JI_dfs/Warming_phase")

writer = ExcelWriter('GAM_Poly_JI_df_' + df_names[counter_] + '_' + res +
                    '_' + '.xlsx')
GAM_Poly_JI_df.to_excel(writer, 'Sheet')
writer.save()

# masking
mask = (GAM_Poly_JI_df['temp'] >= 16.8 + 2) & (GAM_Poly_JI_df['temp'] <= 30.7 - 2) # since the JI
prediction+forecast (x-)interval is (17.5, 30.3)
GAM_Poly_JI_df1_ = GAM_Poly_JI_df.loc[mask]

mask = (GAM_Poly_JI_df['temp'] >= 16.8 + 4) & (GAM_Poly_JI_df['temp'] <= 30.7 - 4) # since the JI
prediction+forecast (x-)interval is (17.5, 30.3)
GAM_Poly_JI_df2_ = GAM_Poly_JI_df.loc[mask]

# Figure with subplots
mpl.rcParams["font.size"] = 15
sns.set_style("whitegrid")
sns.set_style("ticks", {'xtick.major.size': 8, "ytick.major.size": 8})
fig, ax = plt.subplots(sharex=True, sharey=True, figsize=(4,4))

#ax.plot(GAM_Poly_JI_df['temp'], GAM_Poly_JI_df[res+'_GAM'], color='black', ls='-', lw=2)
ax.plot(GAM_Poly_JI_df['temp'], GAM_Poly_JI_df['y_SD_0_'+JI_+'res'],
        color='red', ls='-', lw=2)
ax.plot(GAM_Poly_JI_df1_['temp'], GAM_Poly_JI_df1_['y_SD_1_35_'+JI_+'res'],
        color='lime', ls='-', lw=2)
ax.plot(GAM_Poly_JI_df2_['temp'], GAM_Poly_JI_df2_['y_SD_2_7_'+JI_+'res'],
        color='blue', ls='-', lw=2)

ax.set_xlabel("Thermal average (°C)")
ax.set_ylabel(res[:res.find("J")-1])
ax.set_xlim(left=17, right=30.5)
#ax.set_ylim(-50, 100)
ax.set_xticks(np.arange(17, 30.5, 2))
ax.grid(linestyle='-', linewidth=0.2, which='both', color='lightgrey')
color = ['red', 'lime', 'blue']
legend_elements = [Line2D([0], [0], color=color[0], lw=3,
                          linestyle='-', label='± 0 °C'),
                   Line2D([0], [0], color=color[1], lw=3,
                          linestyle='-', label='± 2 °C'),
                   Line2D([0], [0], color=color[2], lw=3,
                          linestyle='-', label='± 4 °C')]
legend = ax.legend(handles=legend_elements, ncol=1, handlelength=0.5,
                  prop={'size': 12}, fancybox=False, frameon=False,
                  title="Fluctuation ", loc="lower left", framealpha=0.7)

# save the plots
os.chdir(experiment_path + "/GAM_POLY_dfs_plots/Plots")

plt.savefig("JI-predicts_" + df_names[counter_] + '_' + res + '_' + '.pdf',

```

```

        bbox_inches='tight')

    counter_ += 1

end = time.time()
print(end - start)

```

Script S5

```

#!/usr/bin/env python3
# -*- coding: utf-8 -*-
"""
This Script enables the comparison of thermal performance curves (shell-length growth
versus feeding and respiration).
The observed (GAM fits of) growth and upscaling-predicted metabolic responses
are converted to relative values (considering the maximum and minimum values of
each response under 18.5 and 26 °C at the constant thermal setting as 0 and 100,
respectively).

```

This script prepares subplots of Figure 5 of the paper.

```

@author: Jahangir Vajedsamiei (last checked in Dec. 2020)
"""

```

```

import os
import pandas as pd
from glob import glob as glob
import numpy as np
import matplotlib.pyplot as plt
import seaborn as sns
import matplotlib as mpl
from pandas import ExcelWriter
from matplotlib.lines import Line2D

```

```

# Input path definition
experiment_path = "/Users/jahangir/Desktop/fluctuation_plasticity_2018"

```

```

## Merge all GAM-outputs of the long-term thermal performance experiment
os.chdir(experiment_path + "/Long_term_exp/output_dfs/" +
         "Long_term_thermal_performance/GAM_dfs")
files = glob("*.xlsx")
thermal_performance_df = []
for file in files:
    df = pd.ExcelFile(file)
    df.sheet_names
    [u'Sheet']
    df = df.parse("Sheet")
    thermal_performance_df.append(df)
thermal_performance_df = pd.concat(thermal_performance_df, axis=1)
thermal_performance_df = thermal_performance_df.loc[
    :,~thermal_performance_df.columns.duplicated()]
with pd.option_context('display.max_rows', 10, 'display.max_columns', None):
    print(thermal_performance_df)

```

```

## Merge all Polynomial-predicts (including Jensen's Inequality predicts) of
# the warming-phase of the short-term thermal metabolic experiment.
os.chdir(experiment_path + "/Short_term_exp/Dec_2018_exp" +
         "/GAM_POLY_dfs_plots/GAM_Poly_JI_dfs/Warming_phase")
files = glob("*.xlsx")
thermal_metabolic_df = []
for file in files:
    df = pd.ExcelFile(file)

```

```

df.sheet_names
[u'Sheet']
df = df.parse("Sheet")
thermal_metabolic_df.append(df)
thermal_metabolic_df = pd.concat(thermal_metabolic_df, axis=1)
thermal_metabolic_df = thermal_metabolic_df.loc[
    :,~thermal_metabolic_df.columns.duplicated()]
with pd.option_context('display.max_rows', 10, 'display.max_columns', None):
    print(thermal_metabolic_df)

## Make sub_dfs of thermal_metabolic_df, will be used later in the processing
mask = (thermal_metabolic_df['temp'] >= 18.5) & (
    thermal_metabolic_df['temp'] <= 26)
thermal_metabolic_df_cropped_ref_ = thermal_metabolic_df.loc[mask]

mask = (thermal_metabolic_df['temp'] >= 16.8) & (
    thermal_metabolic_df['temp'] <= 30.7)
thermal_metabolic_df_cropped_0_ = thermal_metabolic_df.loc[mask]

mask = (thermal_metabolic_df['temp'] >= 16.8 + 2) & (
    thermal_metabolic_df['temp'] <= 30.7 - 2)
thermal_metabolic_df_cropped_2_ = thermal_metabolic_df.loc[mask]

mask = (thermal_metabolic_df['temp'] >= 16.8 + 4) & (
    thermal_metabolic_df['temp'] <= 30.7 - 4)
thermal_metabolic_df_cropped_4_ = thermal_metabolic_df.loc[mask]

## Plot the relative rates of performances at different thermal means and
# fluctuations (such as, Figure 6).
performance_responses = ['Length growth (mm/day)_GAM',
    'Shell dry weight growth (mg/day)_GAM',
    'Tissue dry weight growth (mg/day)_GAM']
mpl.rcParams["font.size"] = 15
sns.set_style("whitegrid")
sns.set_style("ticks", {"xtick.major.size": 8, "ytick.major.size": 8})
for performance_response in performance_responses:
    ## The rates are converted to relative values considering the max and min
    # at the constant-temperature treatment as 0 and 100, respectively
    maximum = thermal_performance_df['0.0_' + performance_response].max()
    minimum = thermal_performance_df['0.0_' + performance_response].min()
    max_min_range = maximum - minimum
    target_cols = [i for i in list(thermal_performance_df) if
        performance_response in i]
    for i in target_cols:
        thermal_performance_df.loc[:, 'percent_' + i] = (
            (thermal_performance_df[i] - minimum)/max_min_range)*100
    fig, ax = plt.subplots(sharex=True, sharey=True, figsize=(4,4))
    ax.plot(thermal_performance_df['temp_Passay'],
        thermal_performance_df['percent_' + '0.0_' + performance_response],
        color='red', ls='-', lw=2)
    ax.plot(thermal_performance_df['temp_Passay'],
        thermal_performance_df['percent_' + '1.35_' + performance_response],
        color='lime', ls='-', lw=2)
    ax.plot(thermal_performance_df['temp_Passay'],
        thermal_performance_df['percent_' + '2.7_' + performance_response],
        color='blue', ls='-', lw=2)
    ax.set_xlabel("Thermal average (°C)")
    ax.set_ylabel(performance_response[:performance_response.find('(')] + ' (%)')
    ax.set_xlim(left=18, right=27)
    ax.set_ylim(-20, 120)
    ax.set_xticks(np.arange(18, 27, 1))
    ax.grid(linestyle='-', linewidth=0.2, which='both', color='lightgrey')
    color = ['red', 'lime', 'blue']
    legend_elements = [Line2D([0], [0], color=color[0], lw=2, linestyle='-'),
        label='Obse., ± 0 °C'),
        Line2D([0], [0], color=color[1], lw=2, linestyle='-'),
        label='Obse., ± 2 °C'),
        Line2D([0], [0], color=color[2], lw=2, linestyle='-'),

```

```

        label='Obse., ± 4 °C')]
legend = ax.legend(handles=legend_elements, ncol=1, handlelength=0.5,
                  prop={'size': 13}, fancybox=False, frameon=False,
                  title="Mod., Fluc. ", loc="best", framealpha=0.7)
os.chdir(experiment_path + "/Long_term_exp/Plots/" +
        "Long_term_thermal_performance/Performance")
plt.savefig('percent_' + performance_response[
        :performance_response.find('(')] + '.pdf', bbox_inches='tight')

## Plot the relative rates metabolic (JI-predictions) at different thermal
# means and fluctuations.
metabolic_responses = ['WS_feed_hyp_J_per_h_4000_cells_S', 'WS_resp_J_per_h_S']
mpl.rcParams["font.size"] = 15
sns.set_style("whitegrid")
sns.set_style("ticks", {"xtick.major.size": 8, "ytick.major.size": 8})
for metabolic_response in metabolic_responses:
    ## JI-predicts are converted to relative values considering the max and min
    # of the best-fit Polynomials (the red dashed lines in Figures S6 and S7)
    # over the mean temperatures 18.5-26 °C as 0 and 100.
    maximum = thermal_metabolic_df_cropped_ref['y_SD_0_JI_' +
        metabolic_response].max()
    minimum = thermal_metabolic_df_cropped_ref['y_SD_0_JI_' +
        metabolic_response].min()
    max_min_range = maximum - minimum
    target_cols = [i for i in list(thermal_metabolic_df_cropped_0_) if 'JI_' +
        metabolic_response in i]
    for i in target_cols:
        thermal_metabolic_df_cropped_0_.loc[:, 'percent_' + i] = ((
            thermal_metabolic_df_cropped_0_[i] - minimum)/max_min_range)*100
    target_cols = [i for i in list(thermal_metabolic_df_cropped_2_) if 'JI_' +
        metabolic_response in i]
    for i in target_cols:
        thermal_metabolic_df_cropped_2_.loc[:, 'percent_' + i] = ((
            thermal_metabolic_df_cropped_2_[i] - minimum)/max_min_range)*100
    target_cols = [i for i in list(thermal_metabolic_df_cropped_4_) if 'JI_' +
        metabolic_response in i]
    for i in target_cols:
        thermal_metabolic_df_cropped_4_.loc[:, 'percent_' + i] = ((
            thermal_metabolic_df_cropped_4_[i] - minimum)/max_min_range)*100
fig, ax = plt.subplots(sharex=True, sharey=True, figsize=(4,4))
ax.plot(thermal_metabolic_df_cropped_0_['temp'],
        thermal_metabolic_df_cropped_0_['percent_' + 'y_SD_0_' + 'JI_' + metabolic_response],
        color='red', ls='-', lw=2)
ax.plot(thermal_metabolic_df_cropped_2_['temp'],
        thermal_metabolic_df_cropped_2_['percent_' + 'y_SD_1_35_' + 'JI_' + metabolic_response],
        color='lime', ls='-', lw=2)
ax.plot(thermal_metabolic_df_cropped_4_['temp'],
        thermal_metabolic_df_cropped_4_['percent_' + 'y_SD_2_7_' + 'JI_' + metabolic_response],
        color='blue', ls='-', lw=2)
ax.set_xlabel('Thermal average (°C)')
ax.set_xlim(left=18, right=27)
ax.set_ylim(-20, 120)
ax.set_xticks(np.arange(18, 27, 1))
ax.grid(linestyle='-', linewidth=0.2, which='both', color='lightgrey')
color = ['red', 'lime', 'blue']
legend_elements = [Line2D([0], [0], color=color[0], lw=2, linestyle='-',
        label='Upssc., ± 0 °C'),
        Line2D([0], [0], color=color[1], lw=2, linestyle='-',
        label='Upssc., ± 2 °C'),
        Line2D([0], [0], color=color[2], lw=2, linestyle='-',
        label='Upssc., ± 4 °C')]
if metabolic_response == 'WS_feed_hyp_J_per_h_4000_cells_S':
    ax.set_ylabel('Feeding rate (%)')
    legend = ax.legend(handles=legend_elements, ncol=1, handlelength=0.5,
                    prop={'size': 13}, fancybox=False, frameon=False,
                    title="Type, Fluc. ", loc="lower left", framealpha=0.7)
if metabolic_response == 'WS_resp_J_per_h_S':
    ax.set_ylabel('Respiration rate (%)')

```

```

legend = ax.legend(handles=legend_elements, ncol=1, handlelength=0.5,
                  prop={'size': 13}, fancybox=False, frameon=False,
                  title="Type, Fluc. ", loc="upper left", framealpha=0.7)
if metabolic_response == 'WS_SFG_hypo_J_per_h_4000_cells_S':
    ax.set_ylabel('SFG (%)')
    legend = ax.legend(handles=legend_elements, ncol=1, handlelength=0.5,
                    prop={'size': 13}, fancybox=False, frameon=False,
                    title="Type, Fluc. ", loc="best", framealpha=0.7)
os.chdir(experiment_path + "/Short_term_exp/Dec_2018_exp/GAM_POLY_dfs_plots/Plots")
plt.savefig("Relative-JI-predict_" + metabolic_response + ".pdf",
          bbox_inches='tight')

## Plot the relationship between the fluctuation effects on the length growth
# and each metabolic trait based on the mean temperature.
## First, make round the temperatures to one decimal and calculate the mean
# values of the response at each temperature.
thermal_performance_df['temp'] = thermal_performance_df['temp_Passay'].round(1)
thermal_metabolic_df_cropped_0['temp'] = thermal_metabolic_df_cropped_0['temp'].round(1)
thermal_metabolic_df_cropped_2['temp'] = thermal_metabolic_df_cropped_2['temp'].round(1)
thermal_metabolic_df_cropped_4['temp'] = thermal_metabolic_df_cropped_4['temp'].round(1)
thermal_performance_df_grouped = thermal_performance_df.groupby(['temp']).mean()
thermal_metabolic_df_cropped_0_grouped = thermal_metabolic_df_cropped_0.groupby(['temp']).mean()
thermal_metabolic_df_cropped_2_grouped = thermal_metabolic_df_cropped_2.groupby(['temp']).mean()
thermal_metabolic_df_cropped_4_grouped = thermal_metabolic_df_cropped_4.groupby(['temp']).mean()
## Second, merge the thermal performance and metabolic dataframes based on the
# their temperature indices.
complete_df = pd.concat([thermal_performance_df_grouped,
                        thermal_metabolic_df_cropped_4_grouped], axis=1, sort=False)

## Third, add the fluctuation effect columns
for performance_response in performance_responses:
    complete_df[performance_response[:performance_response.find('(')] + '2-0 %diff'] = complete_df[
        'percent_' + '1.35_' + performance_response] - complete_df['percent_' + '0.0_' + performance_response]
    complete_df[performance_response[:performance_response.find('(')] + '4-0 %diff'] = complete_df[
        'percent_' + '2.7_' + performance_response] - complete_df['percent_' + '0.0_' + performance_response]
for metabolic_response in metabolic_responses:
    complete_df[metabolic_response[:metabolic_response.find('J')] + '2-0 %diff'] = complete_df[
        'percent_' + 'y_SD_1_35_' + 'JI_' + metabolic_response] - complete_df['percent_' + 'y_SD_0_' + 'JI_' + metabolic_response]
    complete_df[metabolic_response[:metabolic_response.find('J')] + '4-0 %diff'] = complete_df[
        'percent_' + 'y_SD_2_7_' + 'JI_' + metabolic_response] - complete_df['percent_' + 'y_SD_0_' + 'JI_' + metabolic_response]
with pd.option_context('display.max_rows', 5, 'display.max_columns', None):
    print(complete_df)

## Plot the three dimensional relationships
for performance_response in performance_responses:
    for metabolic_response in metabolic_responses:
        mpl.rcParams["font.size"] = 15
        sns.set_style("whitegrid")
        sns.set_style("ticks", {'xtick.major.size': 8, 'ytick.major.size': 8})
        os.chdir(experiment_path + "/Short_term_exp/Dec_2018_exp/GAM_POLY_dfs_plots/Plots")
        ### (0-2)
        mini, maxi = 18.8, 26 # or use different method to determine the minimum and maximum to use
        norm = plt.Normalize(mini, maxi)
        pair_df = pd.concat([complete_df[metabolic_response[:metabolic_response.find('J')] + '2-0 %diff'],
                            complete_df[performance_response[:performance_response.find('(')] + '2-0 %diff']], axis=1, sort=False)
        pair_df = pair_df.dropna()
        x = pair_df[metabolic_response[:metabolic_response.find('J')] + '2-0 %diff']
        y = pair_df[performance_response[:performance_response.find('(')] + '2-0 %diff']
        fig = plt.figure(figsize=(5, 4))
        plt.scatter(x, y, c=pair_df.index, cmap='jet', norm=norm)
        plt.xlabel(metabolic_response[:metabolic_response.find('J')] + '2-0 %diff')
        plt.ylabel(performance_response[:performance_response.find('(')] + '2-0 %diff')
        plt.grid(linestyle=':', linewidth=0.2, which='both', color='lightgrey')
        cor_coef_df = np.corrcoef(x, y)
        plt.title('Pearson r: ' + str(cor_coef_df[0,1].round(2)), fontsize=14)
        plt.colorbar().set_label("Thermal average (°C)", labelpad=1.1)
        plt.savefig('2-0_diff_corr_' + metabolic_response + '_VERSUS_' +
                    performance_response[:performance_response.find('(')] +

```

```

        '.pdf', bbox_inches='tight')
### (0-4)
mini, maxi = 20.8, 26 # or use different method to determine the minimum and maximum to use
norm = plt.Normalize(mini, maxi)
pair_df = pd.concat([complete_df[metabolic_response[:metabolic_response.find('J')]+ '4-0 %diff'],
                    complete_df[performance_response[:performance_response.find('(')] + '4-0 %diff']], axis=1, sort=False)
pair_df = pair_df.dropna()
x = pair_df[metabolic_response[:metabolic_response.find('J')]+ '4-0 %diff']
y = pair_df[performance_response[:performance_response.find('(')] + '4-0 %diff']
fig = plt.figure(figsize=(5, 4))
plt.scatter(x, y, c=pair_df.index, cmap='jet', norm=norm)
plt.xlabel(metabolic_response[:metabolic_response.find('J')]+ '4-0 %diff')
plt.ylabel(performance_response[:performance_response.find('(')] + '4-0 %diff')
plt.grid(linestyle=':', linewidth=0.2, which='both', color='lightgrey')
cor_coef_df = np.corrcoef(x, y)
plt.title('Pearson r: ' + str(cor_coef_df[0,1].round(2)), fontsize=14)
plt.colorbar().set_label('Thermal average (°C)', labelpad=1.1)
plt.savefig('4-0_diff_corr_' + metabolic_response + '_VERSUS_' +
           performance_response[:performance_response.find('(')] +
           '.pdf', bbox_inches='tight')

```

SI for Chapter 3 “The higher the needs, the lower the tolerance: Extreme events may select ectotherm recruits with lower metabolic demand and heat sensitivity”

Content:

Supplementary Figure

Supplementary Tables

Supplementary Python and R Scripts

Supplementary figures

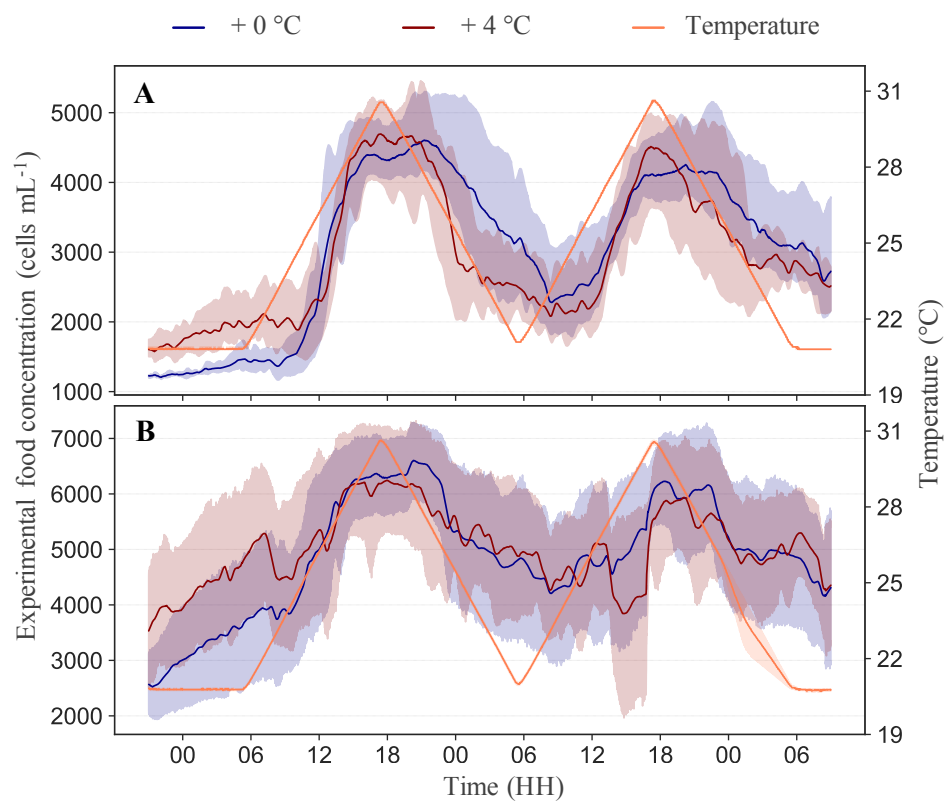


Figure S1. Variation in the food (*Rhodomonas salina*) concentration in the surrounding solution of recruited (A) and transplanted (B) mussels along the applied daily temperature fluctuation cycles (orange lines) during the short-term assays. The replicated values were averaged at each time point, presented with 95 % confidence intervals.

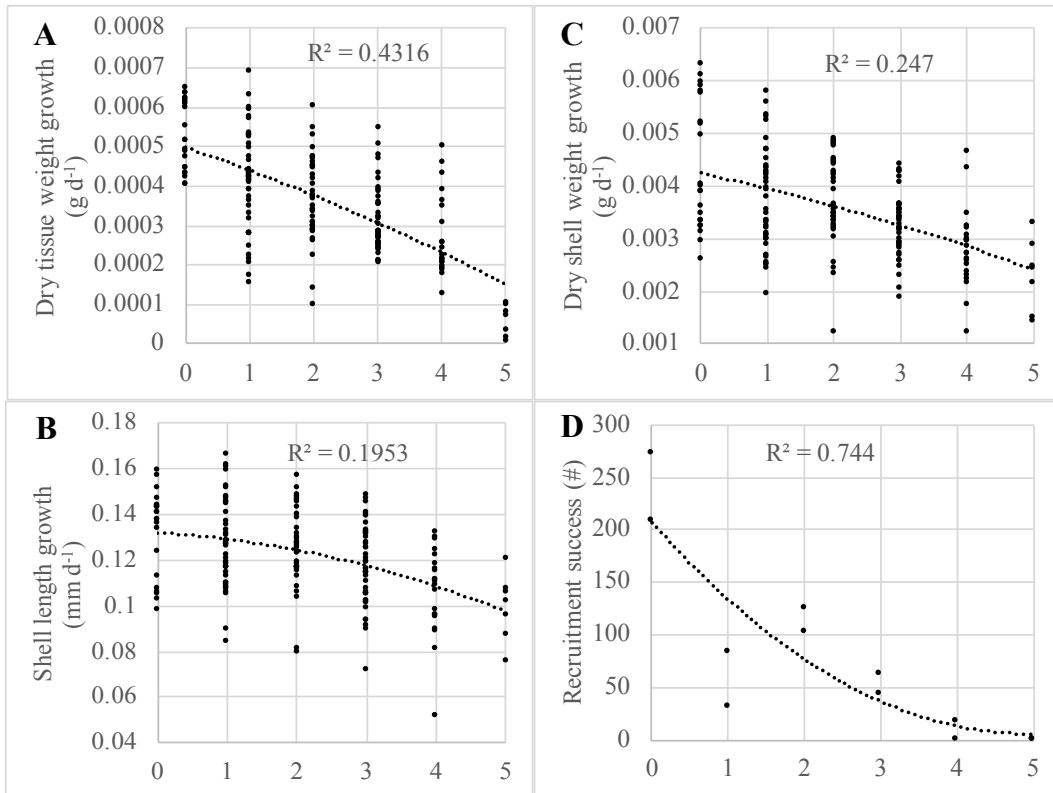


Figure S2. Mussel growth (A–C) and recruitment success (D) in response to all, +0, +1, +2, +3, +4, +5 °C (X-axes), incubation levels of the four-months long community-level study conducted in summer 2018 (Pansch et al. in prep.). Second-order polynomial curves fitted to data and the R-square values are presented. See Material and methods in the main text of the present paper for details.

Supplementary Tables

Table S1. Dry tissue weights ('W' in g) and shell-lengths ('L' in mm) for each transplanted mussel or batch of recruited mussels (S1–3) used in the trials of the short-term assays (darkest grey boxes). The replicates from two thermal history (TH) treatment levels (current and future extreme summer conditions denoted by + 0 °C and + 4 °C, respectively) were randomly assigned to the trials (intermediate grey boxes). The number of mussels (n) assigned as one replicate is presented (lightest grey boxes).

Transplants	Trial name	S1 W	S1 L	S2 W	S2 L	S3 W	S3 L	S1 TH	S2 TH	S3 TH	S1 N	S2 N	S3 N
	29_aug	0.0469	20.43	0.0634	23.10	0.0751	23.50	+ 0 °C	+ 4 °C	+ 0 °C	1	1	1
	01_sep	0.0478	23.65	0.0396	17.35	0.0677	24.04	+ 4 °C	+ 4 °C	+ 0 °C	1	1	1
	04_sep	0.0722	25.17	0.0395	23.32	0.0581	25.73	+ 0 °C	+ 4 °C	+ 0 °C	1	1	1
	07_sep	0.0399	23.50	0.0401	20.52	0.0567	22.61	+ 4 °C	+ 4 °C	+ 0 °C	1	1	1
	10_sep	-	-	0.0752	26.33	0.0604	24.50	+ 4 °C	+ 0 °C	+ 0 °C	1	1	1
	13_sep	0.0313	20.30	0.0327	21.60	0.0443	20.14	+ 4 °C	+ 4 °C	+ 0 °C	1	1	1
Recruits	Trial name	B1 W	B1 L	B2 W	B2 L	B3 W	B3 L	B1 TH	B2 TH	B3 TH	B1 N	B2 N	B3 N
	17_sep	0.0259	57.40	0.0256	64.20	0.0345	69.40	+ 0 °C	+ 4 °C	+ 4 °C	5	6	6
	21_sep	0.0187	58.33	0.0268	59.95	0.0165	51.15	+ 0 °C	+ 0 °C	+ 4 °C	5	5	5

Table S2. Tests on the significance of *thermal history* (with two levels: current and future) as a source of variation in the scaled filtration (potential for feeding) and respiration rates observed during the entire assay. Thermal history was defined as an ordered factor in the Generalized Additive Mixed-effect Models (GAMMs), and the intercept (or the average) and smooth terms of the reference level smoother (current or + 0 °C) were compared to zero and the respective terms of the heat-treated level smoother (future or + 4 °C). Parametric coefficients' estimates and the effective degrees of freedom (*edf*) represents each smoother's intercept and nonlinearity. Parametric coefficients' estimates and the effective degrees of freedom (*edf*) represent each smoother's intercept and nonlinearity, respectively. As measurements were replicated time series, and *replicate* was included as the random (intercept) factor. The predictors with a *p-value* < 0.05 had significant effects. See Material and Methods for more details on how residual autocorrelation was considered in GAMMs.

		Recruited mussels				Transplanted mussels			
		Estimate	Std. Error	t-value	p-value	Estimate	Std. Error	t-value	p-value
Scaled potential for feeding	A. parametric coefficients								
	current	0.2691	0.0194	13.8767	< 0.0001	0.2920	0.0620	4.7060	< 0.0001
	future – current	0.1608	0.0274	5.8647	< 0.0001	0.1043	0.0929	1.1233	0.2613
	B. smooth terms	edf	Ref.df	F-value	p-value	edf	Ref.df	F-value	p-value
	s(time):current	11.2988	11.8777	62.0867	< 0.0001	8.4106	8.9222	25.2412	< 0.0001
	s(time):future	10.9640	11.7895	8.5746	< 0.0001	1.2706	1.4973	0.0811	0.8856
	s(replicate)	0.0130	4.0000	0.0025	0.5537	7.2451	14.0000	1.0726	0.0105
Scaled respiration rate	A. parametric coefficients								
	current	0.5981	0.0507	11.8031	< 0.0001	0.7419	0.0768	9.6667	< 0.0001
	future – current	0.3360	0.0717	4.6887	< 0.0001	-0.0058	0.1159	-0.0503	0.9599
	B. smooth terms	edf	Ref.df	F-value	p-value	edf	Ref.df	F-value	p-value
	s(time):current	17.2592	19.6052	24.2018	< 0.0001	15.5938	16.7618	20.1044	< 0.0001
	s(time):future	5.3690	6.7357	22.1215	< 0.0001	1.0005	1.0010	0.0539	0.8172
	s(replicate)	3.7258	4.0000	13.5864	< 0.0001	12.6693	14.0000	9.5210	< 0.0001

Table S3. Growth rates of transplanted mussels' shell length, dry shell weight, and dry tissue weight under the current (+ 0 °C) and future (+ 4 °C) extreme summer regimes (thermal history levels) of the long-term incubation.

Thermal history	Statistics	Shell length growth (mm d ⁻¹)	Dry shell weight growth (g d ⁻¹)	Dry tissue weight growth (g d ⁻¹)
+ 0 °C	Mean	0.13292	0.004379	0.00053
+ 0 °C	Standard deviation	0.01866	0.00122	0.00009
+ 4 °C	Mean	0.10682	0.002821	0.00027
+ 4 °C	Standard deviation	0.01907	0.00077	0.00010

Table S4. Tests on the significance of *thermal history* (+ 0 °C versus + 4 °C) explain the variation in the scaled filtration (potential for feeding) and respiration rates during the before-fluctuation phase. Thermal history was defined as an ordered factor in the Generalized Additive Mixed-effect Models (GAMMs). Accordingly, the intercept (or the average) and smooth terms of the reference level smoothers (+ 0 °C) were compared to zero and the other smoothers' respective terms (+ 4 °C). Besides *time*, dry tissue weight (*TDW*) and real-time feeding rate (*RF*) were included as smooth-effect factors in the GAMMs. Parametric coefficients' estimates and the effective degrees of freedom (*edf*) represent each smoother's intercept and nonlinearity, respectively. As measurements were replicated time series, *replicate* was included as the random (intercept) factor. The predictors with a *p-value* < 0.05 had significant effects. See Material and Methods for more details on how residual autocorrelation was considered in GAMMs.

		Recruited mussels				Transplanted mussels			
Potential for feeding	A. parametric coefficients	Estimate	Std. Error	t-value	p-value	Estimate	Std. Error	t-value	p-value
	current	2.4103	0.1320	18.2550	< 0.0001	5.9865	1.5011	3.9881	0.0001
	future – current	-0.9963	0.1925	-5.1743	< 0.0001	-1.6633	2.6741	-0.6220	0.5341
	B. smooth terms	edf	Ref.df	F-value	p-value	edf	Ref.df	F-value	p-value
	s(TDW)	1.6193	1.6288	0.7352	0.3121	1.0001	1.0001	0.9299	0.3351
	s(time):current	1.5854	1.8065	54.8413	< 0.0001	1.4111	1.6530	77.7932	< 0.0001
	s(time):future	1.8366	1.9517	3.2410	0.0276	1.0019	1.0035	1.3053	0.2540
	s(replicate)	2.2850	3.0000	16.1139	< 0.0001	12.9445	13.0000	233.6223	< 0.0001
	R ²	0.9600				0.9700			
	Respiration rate	A. parametric coefficients	Estimate	Std. Error	t-value	p-value	Estimate	Std. Error	t-value
current		0.4027	0.0194	20.7236	< 0.0001	1.7567	0.0840	20.9247	< 0.0001
future – current		-0.1400	0.0295	-4.7477	< 0.0001	-0.1869	0.1514	-1.2346	0.2172
B. smooth terms		edf	Ref.df	F-value	p-value	edf	Ref.df	F-value	p-value
s(TDW)		1.0000	1.0000	0.0037	0.9514	1.3571	1.3643	8.9104	0.0007
s(RF)		1.0001	1.0002	2.7690	0.0968	1.9235	1.9901	12.6097	< 0.0001
s(time):current		1.0003	1.0006	4.2485	0.0399	1.0001	1.0002	0.3741	0.5409
s(time):future		1.0003	1.0005	1.5849	0.2088	1.0001	1.0002	0.7141	0.3983
s(replicate)		2.6615	3.0000	5.4562	0.0005	12.0767	13.0000	27.7578	< 0.0001
R ²		0.9500				0.9400			

Supplementary Python and R scripts

Script S1

The following Python script (in combination to the Python scripts and the protocol described in Vajedsamiei et al., 2021) were used to conduct the initial processing of the raw experimental data (will be published in PANGEA). See Materials and Methods and References in the main text of the current study for more details.

Variables definition

```
flow_rate = 15 ## The flow rate of the pump1 (ml/min)
Volume = 350 # fluorometry-chamber volume in ml
fluo_data_collection_frequency = 0.5 # in min
oxyg_data_collection_frequency = 0.5 # in min
"""The robust m-estimator used for modelling the trend of time-series can \
# include 'biweight' or 'welsch' or another robust m-estimator"""
robust_estimator = 'welsch'
"""Other variables needed for calculation of the dampening_effect (time-lag) correction \
coefficient"""
dt = 5 # the time-window (min) for differencing of food-concentration series
diff_window = dt/fluo_data_collection_frequency
""" The coefficients for converting the food (Rhodomonas salina) concentration \
from mV_Ch1 to cells/ml. The conversion coefficient should be empirically-\
established at a specific reference-temperature for the control sensor of \
FOFS (ideally before each experiment)"""
FC_conversion_coef = 2100/764 # (cells/ml/mV)
reference_temperature = 20.5 # (°C)
""" Temperature-specific coefficient for Cyclops 7f fluorometers, i.e., \
the change in Chl or food concentration (in percentage) per °C deviation from \
the reference temperature."""
TS_coef = (-2.2/100)
""" The coefficients for converting the respired molO2 and ingested R. salina \
cells to energy (J), and the assimilation efficiency and the hypothetical food \
(Rhodomonas) concentrations used for estimation of SFG"""
coef_molO2_to_kJ = 450 # 450 kJ/mol O2 (Widdows and Hawkins 1989)
coef_cells_to_microJ = 1.75 # 1.75 µJ per (R. salina) cell (Kiørboe et al. 1985)
assimilation_efficiency = 0.8
```

Script S2

The following R scripts were used to analyze data of the short-term experiments. The integrated experimental data frames used in the analyses will be published in PANGEA. See also the Material and methods in the main text of the current study for more details.

(1) Modelling before-fluctuation phase data

```
### define ordered factor
df$OFGGroup <- as.ordered(df$thermal_history)
contrasts(df$OFGGroup) <- "contr.treatment"
contrasts(df$OFGGroup)
### Generalized Additive Mixed Model (GAMM) definition "RI" (random intercept) and "AC" (auto-correlation corrected).
### GAMM for the potential for feeding (feed_hyp_J_per_h_3000_cells_S_ind)
k_ = 3
simp_bam_RI = bam(feed_hyp_J_per_h_3000_cells_S_ind ~ OFGroup +
  s(dry_weigth_g_ind, k=k_) + s(total_min, k=k_) +
  s(total_min, by=OFGGroup, k=k_) + s(replicate, bs='re'),
  family=gaussian, data=df, method = "REML")
summary(simp_bam_RI)
# NOTE: The dependency of replicate data along time was better modeled via AR1 than the random slope! It was checked thoroughly by comparing RIS versus RI_AC residuals and AIC values.
### consider auto-correlation of residuals
r1 <- start_value_rho(simp_bam_RI, plot=T)
simp_bam_RI_AC <- bam(feed_hyp_J_per_h_3000_cells_S_ind ~ OFGroup +
  s(dry_weigth_g_ind, k=k_) + s(total_min, k=k_) +
  s(total_min, by=OFGGroup, k=k_) + s(replicate, bs='re'),
  family=gaussian, data=df, method = "REML",
  rho=r1, AR.start=df$start.event)

#### GAMM for respiration (resp_J_per_h_S_ind)
simp_bam_RI = bam(resp_J_per_h_S_ind ~ OFGroup +
  s(dry_weigth_g_ind, k=k_) + s(feed_J_per_h_S_ind, k=k_) +
  s(total_min, k=k_) + s(total_min, by=OFGGroup, k=k_) +
  s(replicate, bs='re'), family=gaussian, data=df, method = "REML")
### consider auto-correlation of residuals
r1 <- start_value_rho(simp_bam_RI, plot=T)
simp_bam_RI_AC <- bam(resp_J_per_h_S_ind ~ OFGroup +
  s(dry_weigth_g_ind, k=k_) + s(feed_J_per_h_S_ind, k=k_) +
  s(total_min, k=k_) + s(total_min, by=OFGGroup, k=k_) +
  s(replicate, bs='re'), family=gaussian, data=df, method = "REML",
  rho=r1, AR.start=df$start.event)
```

(2) Modelling fluctuation-phase data

```
### scaled response variables
i = "resp_ymolO2_per_min_S_RefSca"
i = "filt_ml_per_min_S_RefSca"
### GAMM definition
k_ = ? # For the exact number, see the effective degree of freedom (edf) in Table 1 of the main text.
simp_bam_RI = bam(df[,i] ~ OFGroup + s(total_min, k=k_) + s(total_min, by=OFGGroup, k=k_) +
  s(replicate, bs='re'), family=gaussian, data=df, method = "REML")
### consider auto-correlation of residuals
r1 <- start_value_rho(simp_bam_RI, plot=T)
simp_bam_RI_AC <- bam(df[,i] ~ OFGroup + s(total_min, k=k_) + s(total_min, by=OFGGroup, k=k_) +
  s(replicate, bs='re'), family=gaussian, data=df, method = "REML", rho=r1, AR.start=df$start.event)
```

Acknowledgement

This work and my position were funded through the **Deutsche Forschungsgemeinschaft (DFG)** project: The neglected role of environmental fluctuations as a modulator of stress and driver of rapid evolution (Grant Number: PA 2643/2/348431475) and through **GEOMAR Helmholtz Centre for Ocean Research Kiel**.

I acknowledge the supervisors and advisors **Prof. Dr. Martin Wahl, Dr. Christian Pansch, Dr. Frank Melzner, Dr. Michael Raatz** for their effective guidance, critical discussion, and collaboration during the last four years. Especial thanks to **Christian Pansch** for being open to new ideas and investments (for example, for developing FOFS) as well as being supportive and always available as a supervisor and friend.

I also thank **Hadi Bordbar** for checking the mathematical overview presented in the General Introduction of this thesis.

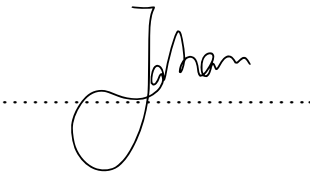
Thank you to all colleagues in the **Benthic Ecology** department at GEOMAR (Hohenbergstr. 2) for their support and for the happy time. Especial thanks to **Maral Khosravi** and **Dakeishla Diaz-Morales** for their supports. During these four years together, in this friendly environment of **HBS**, the conditions were right for me to practice how to do high quality research and also to be a correct researcher. Cheers.

I dedicate this research to my family and friends, and I hope they percept the environmental and political fluctuations as forces of progress.

Declaration

I, Jahangir Vajedsamiei, hereby declare that the dissertation submitted, entitled “**The neglected role of environmental fluctuations as modulator of stress**” was written independently by me and only using the sources listed. The content and design of this thesis, apart from the supervisor’s guidance, is my own work. The thesis has not been submitted either partially or wholly as a part of a doctoral degree to another examining body and is my first and only doctoral procedure. In time of defense, Chapter 1 of this thesis is published in *Limnology & Oceanography: Methods*, Chapter 2 of this thesis is resubmitted to *Functional Ecology*, and its state is under review, and Chapter 3 of this thesis is submitted to *Frontiers in Marine Science*. The authors' share of the manuscripts is explained in the subsection "Chapters and contributions of authors" (pages 20–21). This work has been prepared respecting the Rules of Good Scientific Practice of the German Research Foundation. I have not been deprived of an academic degree.

Kiel, January 27, 2021

A handwritten signature in black ink, appearing to read 'Jahan', is written above a horizontal dotted line. The signature is stylized and cursive.

Jahangir Vajedsamiei